

Increased estrogen receptor expression leads to a novel DNA binding signature which
differentiates luminal A and luminal B breast cancers

by

Lacey Samantha Jean Haddon

A thesis submitted in partial fulfillment of the requirements for the degree of

Doctor of Philosophy

in

Molecular Pathology

Department of Laboratory Medicine and Pathology

University of Alberta

© Lacey Samantha Jean Haddon, 2018

Abstract

Eighty percent of all breast cancers are estrogen receptor positive (ER+) and molecular profiling has identified two ER+ subtypes: luminal A and luminal B. The accurate diagnosis of these luminal subtypes is one of the greatest clinical challenges with current gene assays obtaining only 75% accuracy at best. The need for an improved diagnostic arises from clinical evidence that luminal subtypes have a differential response to the anti-estrogen tamoxifen, which has been the standard of care for all ER+ patients. While luminal A patients have an excellent response to tamoxifen alone, luminal B patients often respond poorly and require additional chemotherapy. Luminal A tumors have the highest levels of ER expression and clinical studies have shown the response to tamoxifen increases as the level of ER expression increases. These tumors occur predominantly in postmenopausal women after the levels of serum estrogen (E2) decreases suggesting that premenopausal levels of E2 may help prevent luminal A cancers. Tamoxifen has well-documented estrogenic properties and there is strong clinical evidence that E2 is growth suppressive for some ER+ patients. This would suggest that the anti-proliferative effect of tamoxifen in tumors with high levels of ER expression is a response to E2.

All *in vitro* ER+ cell lines have the luminal B molecular profile and a marked proliferative response to E2 thereby impeding the study of a potential growth suppressive effect of E2 in luminal A tumors. This has led to the current dogma that E2 is growth promoting for all ER+ tumors. However, *in vitro* studies have shown that cells with increased ER expression become growth suppressed by E2. These findings led to the hypothesis that the two biological subtypes of ER+ breast cancers represent a differential response to E2 that is regulated by the level of ER. A stable MCF-7 transfectant with an inducible ER plasmid (MCF7-ER) was generated to study the effect of increased ER

expression on proliferation, gene regulation, ER-DNA binding and chromatin reconfiguration in the absence and presence of E2.

Increased ER expression led to an anti-proliferative response to E2 which was mediated through inhibition of cell cycle progression. The cell cycle block detected after E2 treatment correlated with an increase in p21 expression that may be directly regulated through ER binding at the p21 (*CDKN1A*) gene. A significant decrease in E2F1 expression was also detected and correlated with the down-regulation of several E2F regulated cell cycle genes in MCF7-ER cells after E2 treatment. These results suggest that increased ER expression mediates an anti-proliferative response to E2 through regulation of the E2F1 pathway.

Investigation of the differential response to E2 using full transcriptome analysis (RNA-Seq) was done to determine the effect of increased ER expression on gene regulation. There were 72 basally up-regulated genes in the MCF7-ER cells in the absence of E2 which became down-regulated after E2 treatment. Chromatin immunoprecipitation followed by full genome sequencing (ChIP-Seq) experiments in chapter 4 showed ER binding at previously mapped anchor regions for long-range loops for five of the differentially expressed genes in the presence and absence of E2. Fluorescence *in situ* hybridization (FISH) experiments confirmed the presence of a long-range loop near the *TFF1* gene in the MCF7-ER cells in the absence of E2 which was maintained after E2 treatment. These results suggest that ER-mediated DNA reconfiguration may serve as a biological mechanism that regulates the differential response to E2. Further investigation of E2-regulated genes with a unique DNA loop formation may enable the development of a new clinical assay that can predict an ER⁺ patient's response to E2.

Preface

This thesis is an original work by Lacey Haddon. No part of this thesis has been previously published.

This thesis is dedicated to my inspiring parents,

Bonnie Chaffey-Haddon and Stan Haddon.

Thank you for your unconditional love and unwavering support.

Acknowledgements

I would like to thank my supervisor, Dr. Judith Hugh, for her constant support and guidance throughout my graduate studies. Thank you for sharing your incredible passion for research and brilliant approach to problem solving with me. Your mentorship has taught me to think critically and pushed me to challenge myself. I have become a better researcher and person because of our time together.

Thank you to the members of my Supervisory committee, Dr. Nadia Giannakopoulos, Dr. Lynne Postovit and Dr. James (Jim) Davie, for their ongoing support of this research and the many relevant and exceptional suggestions and comments throughout this project.

My heartfelt thanks go to Sunny (Xiuying) Hu, who taught me so much in my first few years in the Hugh lab. Your patience, thoughtfulness and integrity will be something I strive to carry forward in every experiment I do. I would also like to thank Dr. Hosna Jabbari for her support throughout this project, both personally and professionally, and for her constant encouragement for my success. Thank you to the previous members of the Hugh lab, Brittney Loney and Kirsten Arnold, who made the lab an engaging place to do research.

I would like to extend my sincerest thanks to Kim Formenti, for making so much of the work possible on this project. Thank you for taking so much of your time to train me on new techniques and for your determination to help me succeed.

Thank you to Dr. Xuejun Sun for generously giving countless hours of his time to help me with the confocal imaging and analysis. Thank you to Geraldine (Gerry) Barron whose enthusiasm to help students with all aspects of confocal imaging makes the most daunting tasks achievable. Thank you to John Hanson for his help and advice on the statistical analyses throughout this project.

I would like to personally thank Dr. Deborah Tsuyuki for providing her knowledge and expertise for our next generation sequencing (NGS) experiments. Thank you for your clear and concise answers to so many of my troubleshooting and experimental questions.

Thank you to all the members of the department of Laboratory Medicine and Pathology who have given me feedback and encouragement throughout my graduate studies. I would like to personally thank Cheryl Titus for being such a strong support for LMP graduate students. I would also like to thank Dr. Monika Keelan for her ongoing support and understanding throughout my graduate program.

To my fellow LMP students, Hadeel Alyenbaawi, Luciana Da Silveira Cavalcante and Gurnit Kaur, thank you for being a constant support and for always taking the time to listen when I needed a friend. To my dearest friend, Jennifer Travis, thank you for being one of my biggest cheerleaders and for making the great distance between us seem nonexistent.

I am forever grateful to my parents, Bonnie Chaffey-Haddon and Stan Haddon. Without you I would not have the courage or determination to pursue my dreams. Thank you for teaching me integrity, work ethic, and the value of an education. Everything I accomplish is because of the never-ending support you've given me.

To Wassim Daoud, thank you for understanding and supporting my hectic schedule. Your drive and determination have inspired me to be better and try harder. You have been my best friend and confidant and I appreciate all the support you've given me over the last 6 years.

I am grateful for the funding received from the Lilian McCullough Breast Cancer Chair and the Canadian Breast Cancer Foundation, which made all of this research possible.

<u>Table of Contents</u>	Page
Chapter 1: Introduction	1
1.1. Mammary gland development	2
1.1.1. Hormonal regulation of breast development	2
1.2. Breast cancer progression	4
1.2.1. Diagnosing breast cancer	5
1.2.1.1. Histological grade, TNM staging and receptor status	5
1.2.1.2. Molecular subtypes of breast cancer	6
1.3. Breast cancer treatment strategies	7
1.3.1. Local treatment: Surgery	7
1.3.2. Systemic therapies	8
1.3.2.1. Chemotherapy	8
1.3.2.2. Trastuzumab (Herceptin)	9
1.3.2.3. Hormone therapies	9
1.3.2.3.1. Selective estrogen receptor modulators (SERMs)	9
1.3.2.3.2. Selective estrogen receptor down-regulators (SERDs)	10
1.3.2.3.3. Aromatase Inhibitors (AIs)	11
1.3.2.3.4. Combination therapy	11
1.3.2.3.5. Estrogens as a therapeutic strategy	11
1.3.3. ER+ breast cancers	13
1.3.4. ER+ tumors have a differential response to hormones	14
1.3.4.1. Clinical evidence	14
1.3.4.2. <i>In vitro</i> evidence	15

2.2.1. Reagents	70
2.2.2. Development of stable MCF7-EM and MCF7-ER transfectants	71
2.2.3. Cell culture and E2 treatment	71
2.2.4. Western Blot Analysis	72
2.2.5. Densitometry analysis	73
2.2.6. Flow Cytometry Analysis	74
2.2.7. Cell Viability Assay (MTT)	74
2.2.8. Quantitative reverse-transcription PCR (RT-qPCR)	75
2.2.9. Chromatin Immunoprecipitation (ChIP)	75
2.2.10. ChIP Quality Checks (QC)	76
2.2.11. ChIP-Seq library build	77
2.2.12. ER peak calling	78
2.2.13. DiffBind analysis of ChIP-Seq datasets	78
2.2.14. ChIP-String Analysis	79
2.2.15. Statistical analysis	80
2.3. Results	82
2.3.1. Increased ER expression promotes an anti-proliferative response to E2	82
2.3.2. ER-DNA binding regulates the proliferative and anti-proliferative response to E2	84
2.3.3. E2 induces G1 and G2 cell cycle arrest but not apoptosis in MCF7-ER cells	86
2.3.4. MCF7-ER cells correlate with ER+ patients that respond to	

hormone therapy	89
2.4. Conclusion	90
2.5. References	114
Chapter 3: Increased ER expression mediates differential gene regulation by binding to high and low affinity DNA regions	120
3.1. Introduction	121
3.2. Methods	122
3.2.1. RNA-Seq	122
3.2.2. Differential gene expression analysis	123
3.2.3. ChIP-Seq analysis	123
3.2.4. Motif analysis for ChIP-Seq peaks	124
3.2.5. ChIP-String analysis	125
3.2.6. Statistical analysis	125
3.3. Results	125
3.3.1. Increased ER expression mediates differential gene expression in response to E2	125
3.4. Conclusions	131
3.5. References	157
Chapter 4: Increased ER expression regulates the formation of long-range DNA loops in the presence and absence of E2	160
4.1. Introduction	161
4.2. Methods	162
4.2.1. Cross-referencing ER binding with ER anchors from a published ChIA-PET dataset	163

4.2.2. ChIP-String validation	163
4.2.3. Fluorescence in situ hybridization (FISH)	163
4.2.4. Confocal imaging and Imaris image analysis	165
4.2.5. Calculations and statistics	166
4.3. Results	167
4.3.1. Differentially expressed genes are associated with ER-mediated DNA loops	167
4.3.2. Increased ER expression promotes ER-mediated DNA loops	169
4.4. Conclusions	171
4.5. References	191
Chapter 5: Discussion and future directions	192
5.1. Discussion	193
5.1.1. Increased ER expression leads to an anti-proliferative response to E2	193
5.1.2. Increased ER expression leads to differential gene regulation upon E2 treatment	197
5.1.3. A theoretical model for ER-mediated gene regulation	201
5.1.4. Comparison of experimental results against previously published ER+ cell line models	203
5.1.5. Clinical significance	207
5.2. Limitations	208
5.3. Future directions	213
5.4. References	218

Bibliography	229
Appendix A	269
Appendix B	273
Appendix C	284

<u>List of Tables</u>		Page
Table 1.1	Descriptions for the Tumor, Node, and Metastasis staging system.	29
Table 1.2	American Joint Committee on Cancer (AJCC) Breast cancer staging guidelines.	30
Table 2.1	Antibody list.	92
Table 2.2	Primer sequences.	93
Table 2.3	Experimental conditions for the differential response to E2.	93
Table 3.1	Summary of differential expression (DE) analysis results.	134
Table 3.2	Summary of up-regulated genes that overlap with the PAM50 gene list.	135
Table 3.3	Two-way comparison of DE datasets.	137
Table 3.4	72 genes with a differential response to E2.	138
Table 3.5	PANTHER Overrepresentation results.	142
Table 3.6	HOMER motif analysis of ChIP-Seq peaks.	143
Table 3.7	Summary of ChIP-Seq ER binding for five genes with a differential response to E2.	144
Table 4.1	Summary of ER binding associated with ChIA-PET anchors for five genes with a differential response to E2.	173
Table 4.2	FISH validation data for <i>ADORA1</i> .	174
Table 4.3	FISH validation data for <i>TFF1</i> .	175
Table B1	RIN scores for RNA-Seq libraries.	273
Table C1	Mean Geometric % Change by Group.	285

<u>List of Figures</u>	Page	
Figure 1.1	Structure of the normal mammary gland.	31
Figure 1.2	Hormonal regulation of mammary gland development.	32
Figure 1.3	Progression of breast cancer.	33
Figure 1.4	The molecular subtypes of breast cancer.	34
Figure 1.5	Structure of ER α and ER β .	35
Figure 1.6	ER-mediated gene activation.	36
Figure 1.7	ER-mediated DNA loops.	37
Figure 2.1	Cell cycle regulation.	94
Figure 2.2	p21 regulation of E2F transcription.	95
Figure 2.3	Doxycycline titrations for MCF7-EM and MCF7-ER transfectants.	96
Figure 2.4	MCF7-EM and MCF7-ER cell lines show a differential proliferative response to increased E2 concentrations.	97
Figure 2.5	Increased ER expression leads to an anti-proliferative response to E2.	98
Figure 2.6	Increased ER expression promotes a basal increase in proliferation.	99
Figure 2.7	Transcriptional inhibition prevents the proliferative and anti-proliferative effects of E2.	100
Figure 2.8	Increased ER mediates the anti-proliferative effect through DNA binding.	101
Figure 2.9	MCF7-ER cells treated with E2 do not show evidence of apoptotic markers.	102

Figure 2.10	E2 induces accumulation of MCF7-ER cells in the G1 and G2 phases of the cell cycle.	103
Figure 2.11	The expression of cell cycle proteins indicate MCF7-ER cells treated with E2 encounter a G1/S and G2/M cell cycle arrest.	104
Figure 2.12	E2 induces <i>E2F1</i> repression in MCF7-ER cells.	105
Figure 2.13	Novel region of <i>CDKN1A</i> is bound by ER in MCF7-ER cells treated with E2.	106
Figure 2.14	The intragenic region of <i>CDKN1A</i> bound by ER contains AP1 and half ERE motifs.	107
Figure 2.15	ER binding at <i>CDKN1A</i> only occurs in MCF7-ER cells treated with E2.	108
Figure 2.16	ChIP-Seq data from MCF7-EM and MCF7-ER cells at the <i>E2F1</i> gene.	109
Figure 2.17	E2 induces the differential regulation of 10 cell cycle genes in MCF7-EM and MCF7-ER cells.	110
Figure 2.18	ER binding patterns in MCF7-EM cells do not correspond with tamoxifen response.	111
Figure 2.19	The MCF7-ER cell line correlates with ER+ patients that respond to tamoxifen.	112
Figure 2.20	The intragenic region of <i>CDKN1A</i> is bound by ER in tamoxifen nonresponsive and responsive tumors.	113
Figure 3.1	Venn diagrams for genes that are up-regulated and down-regulated by E2 in the MCF7-EM and MCF7-ER	

	cell lines.	145
Figure 3.2	Differentially regulated genes that are up-regulated in the MCF7-ER cell line are enriched for cell communication.	146
Figure 3.3	Differentially regulated genes that are up-regulated in the MCF7-EM cell line are enriched for cell cycle function.	147
Figure 3.4	Selection process for selecting five differentially regulated genes for validation.	148
Figure 3.5	Increased ER expression leads to novel ER peaks associated with half ERE motifs.	149
Figure 3.6	ER peaks are located near genes that show a differential response to E2.	150
Figure 3.7	Increased ER mediates differential gene expression in response to E2.	151
Figure 3.8	ER binds a common region upstream of <i>ADORA1</i> in the MCF7-EM and MCF7-ER cells.	152
Figure 3.9	ER binds two regions near the <i>TFF1</i> TSS in the MCF7-EM and MCF7-ER cells.	153
Figure 3.10	ER binds a region downstream from the <i>XBPI</i> gene in the MCF7-EM and MCF7-ER cells.	154
Figure 3.11	ER binds an intragenic region of <i>IGFBP4</i> in the MCF7-EM and MCF7-ER cells.	155
Figure 3.12	ER binds a region >100 kb away from <i>AURKB</i> in only MCF7-ER cells.	156
Figure 4.1	ER binding at anchor regions of a long-range DNA loop	

	near <i>TFF1</i> .	176
Figure 4.2	ER binding at anchor regions of a long-range DNA loop near <i>ADORA1</i> .	178
Figure 4.3	ER binding at anchor regions of a long-range DNA loop near <i>XBPI</i> .	180
Figure 4.4	ER binding at anchor regions of a long-range DNA loop near <i>IGFBP4</i> .	182
Figure 4.5	ER binding at anchor regions of a long-range DNA loop near <i>AURKB</i> .	184
Figure 4.6	ER binding at proximal and distal anchor regions confirmed by ChIP-String.	186
Figure 4.7	FISH analysis of the long-range loop for <i>ADORA1</i> in MCF7-EM cells.	187
Figure 4.8	FISH analysis of the long-range loop for <i>ADORA1</i> in MCF7-ER cells.	188
Figure 4.9	FISH analysis of the long-range loop for <i>TFF1</i> in MCF7-EM cells.	189
Figure 4.10	FISH analysis of the long-range loop for <i>TFF1</i> in MCF7-ER cells.	190
Figure 5.1	Theoretical mechanism for unliganded ER mediated DNA loop formation.	216
Figure 5.2	Theoretical mechanism for ER mediated repression at DNA loops.	217
Figure A1	ER lentiviral doxycycline inducible constructs.	272

Figure B1	Representative Bioanalyzer trace for DNA shearing.	274
Figure B2	Quality check confirming the presence of ER binding at the <i>pS2</i> promoter region.	275
Figure B3	Representative Bioanalyzer trace for ChIP-Seq library.	276
Figure B4	Quality check confirming pattern of ER binding at the <i>pS2</i> promoter region in a ChIP-Seq library.	277
Figure B5	Representative FastQC result obtained from the sequencing of ChIP-Seq library.	278
Figure B6	Principle component analysis (PCA) plot for ChIP peak sets.	279
Figure B7	Representative Bioanalyzer traces for RNA-Seq experiments.	280
Figure B8	Representative FastQC result obtained from the sequencing of RNA-Seq library	281
Figure B9	Illustration of the Imaris split by seed points function.	282
Figure B10	Illustration of paired FISH signals included for analysis.	283
Figure C1	Ki67 Index in CNB and SS.	284
Figure C2	Median Change in Ki67.	284
Figure C3	Staining for p21 on the core and surgical tissues from a patient from PRESTO clinical trial.	287

List of Abbreviations

3C	Chromatin conformation capture
4C	Circular chromosome conformation capture
AC	Anthracycline Adriamycin
Act. D	Actinomycin D
AF	Activation function
AJCC	American Joint Committee on Cancer
AI	Aromatase inhibitors
ANOVA	Analysis of variance
AP-1	Activating protein
APD	Avalanche photodiode detectors
APS	Ammonium persulfate
AR	Androgen receptor
Areg	Amphiregulin
ATCC	American Type Culture Collection
BAC	Bacterial artificial chromosome
BM	basement membrane
BSA	bovine serum albumin
CBP	CREB binding protein
CDK	Cyclin dependent kinase
CDKI	Cyclin dependent kinase inhibitor
ChIA-PET	Chromatin interaction analysis with paired-end tag sequencing
ChIP	Chromatin immunoprecipitation
CHO	Chinese hamster ovary

CMF	Cyclophosphamide, methotrexate, and 5- fluorouracil
CoRNR	Corepressor/nuclear receptor
CtBP	Carboxyl-terminal binding protein
CTCF	CCCTC-binding factor
DBD	DNA binding domain
DC	Cyclophosphamide combined with the taxane doxorubicin
DCIS	Ductal carcinoma in situ
DES	Diethylstilbestrol
DMEM	Dulbecco's modified eagle medium
Dox	Doxycycline
DREAM	DP, RB-like, E2F4 and MuvB
E2	Estrogen, estradiol
EGF	Epidermal growth factor
EGFR	Epidermal growth factor receptor
EM	mEmerald fluorescent tag
ER	Estrogen receptor
ER+	Estrogen receptor positive
ERE	Estrogen response element
ER-mDBD	<i>ESR1</i> DNA binding domain mutant
FBS	Fetal bovine serum
FDA	Food and Drug Administration
FISH	Fluorescence in situ hybridization
FITC	5-fluorescein dUTP
FRET	Fluorescence resonance energy transfer

G1	Gap 1
G2	Gap 2
G418	Geneticin
GEO	Gene Expression Omnibus
GOI	Gene of interest
GPCR	G-protein coupled receptor
GR	Glucocorticoid receptor
GRO-Seq	Global run-on sequencing
HDAC	Histone deacetylase
HER2	Human epidermal growth factor receptor 2
hERE	Estrogen response element half-site
HMGB1	High-mobility group protein B1
HMR	Human, mouse and rat
Hsp	Heat shock protein
IDC	Invasive ductal carcinoma
IGF	Insulin growth factor
IHC	Immunohistochemistry
INK4	Inhibitor of CDK4
KAT	Lysine acetyltransferase
KMT	Lysine methyltransferases
LBD	Ligand binding domain
LCIS	Lobular carcinoma in situ
LCoR	Ligand-dependent nuclear receptor corepressor
LH-RH	Luteinizing hormone-releasing hormone

MAP	Mitogen activated protein
MAP3K1	Mitogen-activated protein kinase kinase kinase 1
MBSU	Molecular Biology Service Unit
MEM	Minimum essential medium
M phase	Mitotic phase
MR	Mineralocorticoid Receptor
NCB	Needle core biopsy
NCoR	Nuclear receptor corepressor
NF	Normalization factor
NF- κ B	Nuclear factor kappa B
NGS	Next generation sequencing
NLS	Nuclear localization signal
NR	Nuclear receptor
NRQ	Normalized expression level
NuRD	Nucleosome remodeling deacetylase
ORF	Open reading frame
P4	Progesterone
PAM50	Prediction analysis of microarray 50
PANTHER	Protein analysis through evolutionary relationships
PARP	Poly (ADP-ribose) Polymerase
P-Box	Proximal box
PBS	Phosphate buffered saline
pCAF	p300/CBP-associated cofactor
PI	Propidium iodide

PI3K	Phosphatidylinositol-3-kinase
PIC	Protease inhibitor cocktail
PKA	Protein kinase A
Pol II	RNA Polymerase II
PR	Progesterone receptor
PRESTO	PRE-operative ESTradiOl
PRL	Prolactin
Rb1	Retinoblastoma protein
REA	Repressor of estrogen receptor activity
RIN	RNA integrity number
RIP140	Receptor interacting protein 140
RIPA	Radioimmunoprecipitation assay
ROR	Risk of recurrence
RQ	Relative quantity
RT-qPCR	Quantitative reverse-transcription PCR
SAFB1	Scaffold attachment factor B1
SD	Standard deviation
SERD	Selective estrogen receptor down-regulator
SERM	Selective estrogen receptor modulator
SLNB	Sentinel lymph node biopsy
SMRT	Silencing mediator of retinoid and thyroid receptors
SORP	Special order research product
Sp1	Specificity protein 1
S phase	DNA-synthesis phase

SRC-1	Steroid receptor coactivator-1
STR	Short tandem repeat
STS	Staurosporine
SWI/SNF	Switch/sucrose non-fermentable
TAD	Topological associating domains
TBP	TATA box-binding protein
TBS	Tris-buffered saline
TBST	TBS with 0.1% Tween20
TCAG	The Centre for Applied Genomics
TDLU	Terminal duct lobular unit
TEB	Terminal end bud
TEMED	Tetramethylethylenediamine
TF	Transcription factor
TNM	Tumor, lymph node and metastasis
TSA	Trichostatin A
TSS	Transcription start site
UCSC	University of California Santa Cruz
VPA	Valproic acid
WHI	Women's Health Initiative

Chapter 1: Introduction

1.1 Mammary gland development

The formation of the mammary gland begins *in utero* when the epidermal layer thickens bilaterally from the thoracic region to the groin to form the ‘milk lines’ (1). Throughout the first trimester the milk lines regress, except for the pectoral regions, where proliferation of the epithelial cells promotes invasion into the underlying mesenchyme to create the primary mammary buds (2). During the second and third trimesters the invading epithelium branches to form secondary buds. Cell differentiation leads to the organization of the basic ductal structure with a layer of luminal epithelial cells lining a rudimentary lumen that is supported by a basal layer of myoepithelial cells (Figure 1.1) (3-5). Secretion of laminins and collagen IV from the myoepithelial cells generates a basement membrane which separates the epithelium from the underlying stromal tissue (6, 7). Beta-integrins promote the attachment of the epithelial cells to the basement membrane and maintain the highly organized structure of the mammary tissue (8). While the development of the rudimentary ductal system does not require hormonal stimulation, the maturation to a fully functional mammary gland requires a series of tightly regulated hormonal interactions that begin at puberty when the ovaries start secreting the reproductive hormones estrogen (E2) and progesterone (P4) (9).

1.1.1 Hormonal regulation of breast development

E2 and P4 function primarily through their nuclear transcription factors, estrogen receptor (ER) and progesterone receptor (PR). ER and PR are co-expressed in luminal cells throughout the mammary epithelium and E2 and P4 stimulation leads to up-regulation of paracrine factors such as amphiregulin (Areg) which bind to epidermal growth factor receptors (EGFRs) on nearby stromal cells and triggers the release of growth factors to

promote proliferation of neighbouring ER-/PR- negative cells (Figure 1.2) (10-12). ER can also function at the cell membrane through direct interactions with G-protein coupled receptors (GPCRs) which activate non-genomic protein kinase signaling such as the phosphatidylinositol-3-kinase (PI3K) pathway which phosphorylate transcription factors, including ER, and promote additional transcriptional function (13-16). The additional release of growth factors works in synergy with E2 to drive of elongation and branching of the ductal system by promoting the proliferation of the cap cells on the leading edge of the bulb-shaped terminal end buds (TEBs). These cap cells differentiate into myoepithelial cells as the TEB elongates (1, 12, 17, 18). The interior of the TEB is filled with several layers of body cells and as the bud elongates, the body cells at the centre of the bud undergo apoptosis to form the lumen. Those cells closest to the myoepithelial layer differentiate into mature, polarized luminal cells that line the milk duct (12). Luminal cell differentiation is driven by the transcription factor GATA3 which is highly expressed in the body cells within the TEB and maintained in mature luminal cells (19).

Alveolar buds arise from the TEBs and make up the functional structures of the breast known as the terminal duct lobular units (TDLUs) (Figure 1.2) (20). The earliest TDLUs have about 11 alveolar buds and express the highest levels of ER and PR which correlates to a higher rate of proliferation (3). TDLUs mature with each menstrual cycle, and by age 35 they contain about 80 alveolar buds (21). The majority of ductal growth occurs during the luteal phase of the menstrual cycle, when both E2 and P4 are present, indicating a synergistic role for these hormones during ductal growth (10). Interestingly, during the follicular phase of the menstrual cycle when E2 alone is present the endometrium

shows a marked increase in proliferation whereas the breast shows very little mitotic activity (22).

A fully functional mammary gland will only develop during pregnancy, when P4 and prolactin (PRL) take over and stimulate the differentiation of the alveolar cells into acini, which are responsible for milk secretion (5, 9, 17). E2 functions indirectly at this stage by promoting PR expression in luminal epithelium and PRL secretion from the anterior pituitary gland (17, 21). High levels of P4 prevent milk secretion during pregnancy and the decrease in P4 after parturition allows for lactation to commence. High levels of PRL further promote and maintain milk production (17). Secretion of oxytocin from the posterior pituitary gland stimulates the underlying myoepithelial cells to eject the milk from the ducts (17). Lactation is maintained through suckling by the infant and when this stimulus is removed apoptosis and phagocytosis lead to involution of the milk-secreting alveoli, producing TDLUs that closely resemble their pre-pregnancy state (1, 9). The major decline in serum E2 and P4 levels during menopause leads to involution of the lobules, reduction of the milk ducts and the replacement of the dense stroma with adipose tissue (1).

1.2 Breast cancer progression

Breast cancer is the most common cancer in women and remains the second leading cause of cancer related deaths in Western countries (23). The incidence of breast cancer increases with age, with 83% of cancers occurring in women after menopause (24). Breast cancer arises from stem cells located in the TEB which can differentiate into either the ductal or lobular phenotype, with ductal carcinomas accounting for 80% of all breast cancers (25-27). In the early stages of breast cancer, the proliferating tumor is contained within the duct by the basement membrane and the tumors are histologically classified as

either lobular or ductal carcinoma *in situ* (LCIS or DCIS), with DCIS being the most common (Figure 1.3) (28). Early detection of DCIS through mammography screening enables the complete removal of these tumors with complete cure in over 95% of patients (29).

DCIS precedes invasive carcinoma and it is estimated that invasion can be present for up to ten years before being detected as a palpable mass. Once the proliferating cancer cells have begun to invade through a defective basement membrane and into the surrounding tissue they are classified as invasive ductal carcinoma (IDC) and contrary to *in situ* lesions invasive tumors are associated with a significant increase in the risk of breast cancer related deaths (Figure 1.3) (29, 30). Invasion into the surrounding mammary stroma enables cancer cells to gain access to lymph nodes and blood vessels in a process of metastasis of the primary tumor. Breast cancer commonly metastasizes to the lung, liver, bone and brain and these secondary tumors are the major sources of breast cancer related deaths (31). The treatment options for breast cancer patients depends upon the extent of cancer progression and clinicopathologic features of the tumor. The latter include histological grade, stage and hormone receptor status as well as the molecular subtype of the tumor (32, 33).

1.2.1 Diagnosing breast cancer

1.2.1.1 Histological grade, TNM staging and receptor status

The histological grade is determined by staining the tumor tissue with hematoxylin-eosin which enables pathologists to assess the nuclear, architectural and proliferative features that determine the degree of cell differentiation within the tumor sample (34). Tumors can range from well-differentiated (low grade) to poorly-differentiated (high

grade), with the probability of survival decreasing with increased histological grade (35). Tumor, lymph node and metastasis (TNM) staging provides an analysis of a patient's tumor progression (Table 1.1). The stage increases with the size of the primary tumor, the number of lymph nodes with cancer cell involvement and the detection of distant metastases (Table 1.2) (32). Tumor samples are also tested for ER, PR and human epidermal growth factor receptor (HER)2 expression using immunohistochemistry (IHC). Equivocal HER2 IHC results are further assayed for *HER2* gene amplification using fluorescence or chromogenic *in situ* hybridization. The presence of these receptors will trigger selective anti-estrogen or anti-HER2 agents and this personalized treatment approach is a major advance in cancer care. The major implications for the expression of these receptors in relation to patient prognosis was highlighted in the paradigm shifting work of Perou et al. (2000) which showed breast cancer can be divided into four intrinsic subtypes, each with a unique gene expression signature that could predict patient outcomes (36, 37).

1.2.1.2 Molecular subtypes of breast cancer

The initial intrinsic gene subset obtained in Perou's molecular portraits of breast cancer found there was a major separation between breast tumors based on the presence or absence of ER expression; ER+ tissues were enriched for genes of the luminal phenotype while the ER- branch more closely resembled a basal-like gene expression (36). This work also highlighted a major role for proliferation in the clustering of breast tumor samples, as the largest cluster of genes were related to cell proliferation (36). Further work on the intrinsic subset using large patient datasets led to the division of breast cancer into four major subtypes, with the ER- tumors subdivided into the HER2+ amplified and triple-

negative (ER-, PR-, HER2-)/basal-like subtypes and the ER+ branch subdivided into the luminal A and luminal B subtypes (Figure 1.4) (38).

Analysis of patient outcome found that luminal A tumors consistently show the longest overall survival, whereas luminal B tumors trend downward over time toward the poor survival rates seen in the basal-like and untreated HER2+ tumors (Figure 1.4) (37, 39). This finding led to the development of multigene panels such as Oncotype DX, Prosigna, MammaPrint and EndoPredict, each designed using a unique set of genes to predict the likelihood of recurrence (40). The Prosigna gene panel, also known as prediction analysis of microarray 50 (PAM50), utilizes 50 genes derived from the original intrinsic subtypes and is enriched for proliferation markers enabling the diagnosis of the patient's molecular subtype, as well as their risk of recurrence (41, 42).

Currently, gene signatures are only 75% accurate at predicting recurrence in patients with ER+ tumors (43). This has major implications on patient outcome as high-risk cancers (presumed luminal B) require a different treatment strategy (discussed in section 1.3). The inaccuracies found in current gene panels, such as Prosigna and Oncotype DX, may be due to their enrichment in proliferation and cell cycle genes which may confound the true biological differences present in ER+ breast tumors (44). In order to improve the current diagnostic strategies, a better understanding of the biological mechanism(s) which differ between luminal A and luminal B tumors must be obtained.

1.3 Breast cancer treatment strategies

1.3.1 Local treatment: Surgery

Breast masses that are detected by palpation or radiologic examination will have a needle core biopsy (NCB) in order for the pathologist to assess the tumor grade and subtype.

LCIS is considered a risk lesion and if there is no associated invasive disease on subsequent biopsy can be monitored by regular clinical and radiologic follow-up (45). DCIS is considered a precursor for invasive carcinoma and requires complete resection (33). Patients treated with less than mastectomy often have subsequent radiotherapy to prevent recurrence of DCIS or invasive disease (33). Invasive carcinomas are also treated with partial mastectomy followed by radiation or total mastectomy (33). A sentinel lymph node biopsy (SLNB) is taken at the time of surgery to determine the nodal status which is used to determine the likelihood of spread beyond the breast and the need for systemic therapy (46).

1.3.2 Systemic therapies

The goal of systemic therapy is to kill any tumor cells which have already spread beyond the breast. The treatment regimen prescribed is based on the level of risk for systemic dissemination of the tumor (47). This is assessed based on the stage of the tumor and the presence of the following risk factors: high grade (3/3), vascular involvement, hormone receptor status, HER2 expression, age and an unfavourable molecular test result (33).

1.3.2.1 Chemotherapy

Chemotherapy regimens are often combinations of agents such as anthracyclines (daunorubicin, doxorubicin (adriamycin) and epirubicin) and taxanes (paclitaxel and docetaxel). Anthracyclines are antibiotics that damage the DNA whereas taxanes function as mitotic inhibitors and interfere with microtubules (48, 49). Chemotherapy is administered as three-week cycles with patients often receiving six cycles (50). If the chemotherapy is not well tolerated, the doses of each drug can be reduced.

Chemotherapy is offered to patients with intermediate or high-risk tumors. Intermediate risk tumors or elderly patients that are lymph node negative may be offered non-anthracycline containing combinations, such as cyclophosphamide, methotrexate, and 5- fluorouracil (CMF) or cyclophosphamide combined with the anthracycline adriamycin (AC), or cyclophosphamide combined with the taxane doxorubicin (DC) (51). High risk, node negative tumors are treated with either DC or sequential anthracycline-taxane regimens if the tumor is ER- (51). Node positive cancers are considered high risk and receive either a sequential anthracycline-taxane regimen or DC as a non-anthracycline regimen. Tumors that are HER2+ receive chemotherapy in combination with the HER2 targeted therapy, Trastuzumab.

1.3.2.2 Trastuzumab (Herceptin)

Tumors that are HER2+ are treated with the HER2 targeted therapeutic trastuzumab, also known as Herceptin, which is a monoclonal antibody that binds cell surface HER2 receptors and prevents their function (52). Trastuzumab alone is the standard of care for node negative HER2+ tumors <0.5cm and is typically given for one year. HER2+ tumors that are node negative or positive and >1cm should receive adjuvant trastuzumab combined with chemotherapy. Concurrent trastuzumab with a taxane based chemotherapy is the preferred treatment regimen, as anthracycline based chemotherapies increase the risk of cardiotoxicity (51, 53). No matter the size or nodal status, HER2+ tumors that are also ER+ will be considered for additional hormone therapy (51).

1.3.2.3 Hormone therapies

1.3.2.3.1 Selective estrogen receptor modulators (SERMs)

Selective estrogen receptor modulators (SERMs) are synthetic compounds derived from type I and II estrogens which bind ER and regulate its function (54). SERMs have both antagonist and agonist properties depending on the tissue they are located in (55). The two most common SERMs are raloxifene and tamoxifen. Raloxifene functions as an antagonist in the breast and uterus but as an agonist in the bone and is currently approved for the treatment of osteoporosis in postmenopausal women (56). Raloxifene has been studied for its use as a potential preventative therapy in postmenopausal women who are at high risk for developing invasive breast cancer (57).

Tamoxifen is the oldest SERM used to treat ER+ breast cancer and functions as an antagonist in the breast and an agonist in the bone and uterus (56). This agonistic property of tamoxifen leads to an increased risk of endometrial cancer (58). In the breast tamoxifen acts as a competitive-inhibitor that binds ER to prevent E2-ligation and subsequent receptor activation (59). Tamoxifen treatment for 5-10 years used to be the standard of care for pre- and postmenopausal ER+ invasive carcinomas (51). For premenopausal patients with higher risk tumors combining tamoxifen with treatments that decrease E2 production may provide additional therapeutic benefit. Strategies to reduce E2 production include luteinizing hormone-releasing hormone (LH-RH) agonists which suppress ovarian function, or more permanent alternatives which include ovarian irradiation and surgical oophorectomy (51, 60, 61).

1.3.2.3.2 Selective estrogen receptor down-regulators (SERDs)

Fulvestrant is a selective estrogen receptor down-regulator (SERD) that was developed by adding a long alkyl side chain with a reactive sulfide group to the estrogen molecule which generated a compound that functions as a full ER antagonist (54, 62).

Fulvestrant binds ER and prevents ligand binding, similar to SERM function, but also promotes proteasomal degradation of ER leading to decreased ER expression (63). Fulvestrant is currently approved for the treatment of postmenopausal women with hormone receptor positive breast cancer and may be used in advanced breast cancers that have developed resistance to other forms of hormone therapy.

1.3.2.3.3 Aromatase Inhibitors (AIs)

The aromatase inhibitors (AIs), anastrozole and letrozole, have been designed to treat postmenopausal ER+ patients (64). AIs function by inhibiting aromatase activity in the adipose tissues which converts androgens to estrogen resulting in elevated serum E2 levels (65). The current recommendations for AI treatment duration is 3-5 years (51). AIs have also been shown to reduce recurrence in certain high-risk women as well as contralateral breast cancer when used as an adjuvant therapy for up to ten years (66).

1.3.2.3.4 Combination therapy

ER+ patients that have high risk tumors are treated with adjuvant hormone therapies in combination with chemotherapy. However, ER+ tumors that are considered intermediate risk will receive adjuvant endocrine therapies and may or may not receive additional chemotherapy (51). The decision to treat ER+ patients with additional chemotherapy is often based on the recurrence scores obtained from molecular tests such as Oncotype DX or Prosigna.

1.3.2.3.5 Estrogens as a therapeutic strategy

In the normal breast, ER+ cells do not proliferate in response to E2 but regulate proliferation of adjacent ER- cells through paracrine signaling involving growth factors such as Areg (67). Furthermore, the high levels of E2 during the follicular phase of the

menstrual cycle are associated with proliferation in the endometrium, but not the breast (68). Thus, exposure of the breast epithelium to E2 alone is not enough to promote proliferation. This is further evidenced by the proliferation that occurs in the breast epithelium during the luteal phase which is driven by the synergistic effects of both E2 and P4 (68, 69). This synergistic effect was seen in the Women's Health Initiative (WHI) study by the increased incidence of breast cancers in women after short-term treatment with estrogen and progestin (70).

Another important finding from the WHI study was that postmenopausal women who received estrogen-only hormone replacement therapy showed a decrease in breast cancer incidence (71-73). This therapeutic role for E2 has also been shown in clinical studies where low-dose oral estradiol treatment led to tumor regression for 30% of postmenopausal women with advanced breast cancer (74). The synthetic estrogen, diethylstilbestrol (DES), was the standard treatment for ER+ breast cancers before being replaced with the anti-estrogen tamoxifen which had fewer side-effects (75). However, the long-term follow-up study comparing tamoxifen to DES showed that DES was associated with increased survival (76). Interestingly, luminal A tumors show the best response to tamoxifen treatment yet occur predominately in postmenopausal women with extremely limited serum E2 to antagonize (77, 78). This suggests that the primary method of action for tamoxifen may not be through an anti-estrogenic effect. Tamoxifen has well-documented estrogenic activity in the endometrium and bone (58, 79, 80), and a study of postmenopausal women treated with tamoxifen for two years found a 106% increase in serum E2 levels (81). When taken together, these studies indicate there is an important role for E2 in the treatment of ER+ breast cancer.

1.3.3 ER+ breast cancers

Approximately 75% of breast cancers are ER+ with the luminal A subtype accounting for at least half of all breast cancers diagnosed (82, 83). Luminal A tumors occur predominately in postmenopausal women and are characterized by low grade (I and II) and low proliferation rates (84). This subtype has the highest levels of ER expression and is enriched in ER-regulated genes involved in cell differentiation including *GATA3*, *FOXA1*, *XBPI*, *BCL-2*, and *TFF3* (19, 85-88). Luminal A tumors have the fewest overall mutations, but most often harbour significant mutations in *PIK3CA*, *GATA3*, *MAP3K1* and *TP53* (89). *PIK3CA* is a subunit of the PI3K-AKT signaling pathway which has been associated with poor survival for ER+ patients (90), however the mutations found in luminal A tumors did not correlate with increased PI3K-AKT activation (89).

GATA3 mutations were the second most frequent mutation in luminal A tumors and were most frequently associated with “simplex” copy number alterations with the gain of the long arm of chromosome 1 and the loss of the long arm of chromosome 16 (1q/16) (89, 91, 92). The loss of 16q is highly associated with ER+ breast cancers and correlates with increased survival (93, 94). Additionally, translocation of 1q and 16p leads to the derivative chromosome der(1;16)(q10;p10) and is thought to be a marker of early breast cancer progression (95). Preliminary comparisons suggest that this derivative chromosome may occur more frequently in luminal A breast cancer, however this needs to be confirmed on a larger sample size (91).

Inactivating mutations in the mitogen-activated protein kinase kinase kinase 1 (MAP3K1) may also contribute to slow growing nature of luminal A tumors through down-regulation of the ERK and JNK pathways (96). The tumor suppressor TP53 was found to

be mutated in 12% of luminal A tumors, yet this signaling pathway remained largely intact in this subtype (89). The increased levels of MYB protein found in luminal A tumors may enable TP53 function through inhibition of MDM2 down-regulation of TP53 via interactions with Hep27 (97). When taken together, the mutations that accumulate in luminal A tumors promote a lower rate of proliferation and the more indolent nature of this subtype.

Luminal B tumors tend to occur in younger women, have higher grade and increased proliferation index (98). These tumors have decreased ER expression and increased expression of genes related to cell cycle regulation (99). Unlike the simplex 1q/16 pattern found in luminal A tumors, luminal B tumors often show high levels of DNA amplification for genes involved in proliferation such as *CCND1*, *MYC*, *FGFR1*, *MDM2*, *HER2*, *ZNF217*, and *PIK3CA* (89, 100). Increased expression of *CCND1* may promote the reduced expression of the cell-cycle mediator retinoblastoma protein (Rb)1 seen in luminal B tumors and loss of Rb1 would further promote cell cycle progression (89, 101). TP53 mutations are increased in luminal B tumors (32%) further contributing to the more aggressive nature of these tumors (89). High levels of the transcription factor FOXM1 may contribute to the transcriptional hyperactivity seen in luminal B tumors and has been correlated with resistance to endocrine therapies in ER+ tumors (89, 102).

1.3.4 ER+ tumors have a differential response to hormones

1.3.4.1 Clinical evidence

There is growing clinical evidence that measuring the changes in proliferation after short term exposure to hormone therapies can serve as an accurate predictor of long-term patient outcome when treated with these agents (103, 104). Luminal A tumors are

characterized by their increased ER expression and low proliferative index, and patients with the highest levels of ER expression are shown to have the greatest reduction in proliferation after two weeks of tamoxifen (37, 105). This is consistent with trials that include long term follow-up which show luminal A patients have excellent response to tamoxifen, whereas luminal B patients do poorly with tamoxifen alone and require additional chemotherapy (106, 107).

1.3.4.2 *In vitro* evidence

The classic *in vitro* model for ER+ breast cancer is the MCF-7 cell line, which has low to moderate ER expression consistent with its known luminal B phenotype and displays a well-established proliferative response to E2 (108, 109). Exogenous ER expression in cell lines derived from the more aggressive ER negative tumors led to growth suppression in the presence of E2 (110). Interestingly, increased exogenous ER expression in MCF-7 cells also leads to loss of E2-induced proliferation by preventing cell cycle progression (111). The anti-proliferative effects seen in tumors and cell lines expressing high levels of ER suggests that the differential response to hormone therapy seen in luminal A and luminal B tumors maybe regulated by the level of ER expression.

1.4 ER structure and function

1.4.1 The estrogen receptors: ER α and ER β

The nuclear receptor superfamily is made up of three major classes of receptors: the steroid receptors, the thyroid/retinoic receptors and the orphan receptors which have no known ligands. The estrogen receptors, ER α and ER β , belong to the steroid receptor class which includes four other members: PR, Glucocorticoid Receptor (GR), Androgen Receptor (AR) and Mineralocorticoid Receptor (MR) (112). Both ER proteins are

expressed in the mammary gland, uterus, ovary, brain and cardiovascular system (113). Certain organs show dominant expression for a specific ER, with ER α predominately expressed in the liver and ER β in the testis (113, 114). ER α and ER β are both activated by E2 and regulate sexual development and reproductive function. Both receptors also promote bone growth and inhibit osteoclast-mediated bone degradation (115). ER α and ER β also regulate cardioprotective effects of E2 via increased mitochondrial function, protection against cardiac fibrosis and increased cardiac angiogenesis (116).

ER α is transcribed from the *ESR1* gene located on chromosome 6q25.1 which encodes for a 66 kDa protein (117). ER β is encoded by the *ESR2* gene, which is located on a completely separate chromosome (chr14q23.2) and generates a 59 kDa protein (117). Steroid receptors have five major domains: N-terminal region (A/B), DNA binding domain (DBD) (C), hinge region (D), ligand binding domain (LBD) (E), and a variable C-terminal region (F) (Figure 1.5) (112). Steroid receptors mediate transcriptional activation through two activation functions (AF): the ligand-independent activation function (AF-1) located in the A/B domain and the ligand-dependent activation function (AF-2) in the E domain (118). The DBD shows the highest amount of sequence homology between the two ER receptors at 96%, whereas the A/B region of ER β shares only 30% homology with wild-type ER α (Figure 1.5) (119). The decreased homology and shorter length of the A/B region in ER β leads to decreased AF-1 transcriptional function (120). A recent meta-analysis suggested that ER β expression in breast cancers that are negative for ER α correlates to an increase in DFS (121), however the overall role of ER β in breast cancer still remains unclear (122). Thus, ER α continues to be the major target for the diagnosis and treatment of ER+ breast cancers and will be the focus of the remaining sections of this thesis.

1.4.2 ER α structure

1.4.2.1 A/B domain

The N-terminal region of ER α (hereafter called ER) has an intrinsically disordered conformation that becomes stabilized through interactions with target molecules, including members of the transcriptional machinery such as the TATA box-binding protein (TBP) (123). Amino acids 51-149 within the A/B domain are responsible for the ligand-independent AF-1 activity (124). AF-1 can be activated by the cyclin A-cyclin dependent kinase (CDK)2 complex through phosphorylation of serines 104 and 106 (125). Epidermal growth factor (EGF) and insulin growth factor (IGF) can both activate AF-1 via phosphorylation of serine 118 via the mitogen activated protein (MAP) kinase (126). Phosphorylation of serines 104, 106 and 118 promote recruitment of steroid receptor coactivator-1 (SRC-1) and CREB binding protein (CBP), and this enables gene activation in the absence of ligand (127). SRC-1 can also mediate an association between AF-1 and AF-2 in the presence of E2 and leads to enhanced transcriptional activity (128, 129).

1.4.2.2 C domain

The C domain is highly conserved between nuclear receptors and contains two zinc fingers that recognize one half of the palindromic estrogen response element (ERE) sequence GGTCAnnnTGACC (n=any nucleotide) promoting complete DNA binding as a homodimer (130, 131). The proximal box (P-Box) of the first zinc finger of each monomer makes direct contacts with the four central nucleotides on each half of the ERE within the major groove of the DNA and is stabilized by additional contacts between the protein and the phosphate backbone (131). The second zinc finger of both ER monomers interact to form a tight dimerization interface above the minor groove, and the 3 bp spacer region of

the ERE enables this interaction (132). Phosphorylation at serine 236 by protein kinase A (PKA) enables ER dimerization and occurs in the absence of ligand (133). The dimerization interface enables ER interactions with imperfect EREs through cooperative binding, where each monomer stabilizes the other through strong interactions with the consensus base pairs within the sequence and permits non-specific binding between the remaining non-consensus DNA (132). Binding of ER to the ERE causes the DNA to bend toward the major groove (134). This change in DNA structure has been suggested to promote gene activation by enabling interactions between distal enhancers and the basal transcriptional machinery at the gene's promoter via DNA looping (135). The C domain also contains a nuclear localization signal (NLS) that works cooperatively with two additional NLSs in the D domain to promote ER nuclear accumulation (136).

1.4.2.3 D domain

The disordered D domain is known as the hinge region and contains two additional lysine-rich NLSs (136). These NLSs are constitutively active and enable ER nuclear localization in the absence of ligand (137). Post-translational modifications including acetylation, sumoylation, and methylation occur at the ²⁹⁹KRSKK³⁰³ motif within the hinge region and influence ligand-mediated transcriptional regulation (138-140). Lysines 302 and 303 are also targets for ubiquitination and regulate the proteasomal degradation of the receptor (141). The hinge region is also involved in regulating the synergistic association between AF-1 and AF-2 in the presence of SRC-1 (142).

1.4.2.4 E domain

The E domain extends from amino acids 302 to 552 and contains the LBD and AF-2 activity. The LBD is made up of 11 α -helices (H1, H3-H12) which rearrange upon

binding of E2 to form the ligand binding pocket made of three anti-parallel groups of helices with H4, H5, H6, H8 and H9 being flanked by H1 and H3 on one side and H7, H10 and H11 on the other (143). H12 folds on top of the ligand pocket and packs against H3, H5, H6 and H11 but makes no direct contact with the ligand (144). The folding of H12 exposes a hydrophobic coactivator recognition groove which binds to the LXXLL motif of the coactivator's nuclear receptor (NR) box and enables AF-2 activity (144). Anti-estrogens have large side-chains which extrude from the ligand binding pocket and displace H12 so that it lies in the coactivator recognition groove, and this association is promoted by the LXXML motif on H12 (143, 144). This configuration prevents the binding of coactivators and inhibits AF-2 activity (145). The LBD also promotes ligand-specific ER homodimerization which is mediated primarily through H10 and H11 (123, 146).

1.4.2.5 F domain

Deletion of the F domain increased E2-induced reporter activation by two-fold, indicating this region contains an inhibitory signal that mediates the ligand-dependent dimerization activity in the LBD (147). The F domain has also been implicated in enhancing both AF-1 and AF-2 activity and loss of the F domain reduces but does not prevent transcriptional activity (148). Studies have shown that residues within the F domain contribute to the agonist activity of tamoxifen (149). The F domain lies in close proximity to H12 in the LBD and contributes to the conformational changes required to associate with ligands as well as the cofactor SRC-1, thereby regulating the transcriptional activity of the receptor (150).

1.4.3 ER- mediated transcription

IHC staining shows that ER is primarily located in the nucleus and this has been confirmed by confocal imaging (151-153). In the absence of ligand, ER is kept as an inactive monomer in the nucleus through association with a chaperone complex consisting of heat shock protein (Hsp)90, p23, and immunophilin-type protein which keep ER properly folded and compatible for ligand binding (54, 154). Upon ligand binding, ER dissociates from the chaperone complex and forms a homodimer that can bind DNA at the consensus ERE (155). There is increasing evidence that ER frequently binds gene promoter regions at lower affinity sites, such as non-consensus EREs and ERE half-sites (hERE) (156, 157). ER binding and subsequent gene activation at these low affinity sites is enabled through DNA bending (158) and this may be regulated by the high-mobility group protein B1 (HMGB1) which binds non-specifically in the minor groove and bends the DNA (159). Recent studies have shown ER binds DNA in the absence of E2 and mediates basal level of some genes in addition to ‘priming’ the promoter for E2-induced transcription (160, 161).

ER-E2 binding causes conformational changes in the LBD enabling association with coactivators and enables further recruitment of lysine acetyltransferases (KATs) and lysine methyltransferases (KMTs) (162, 163). Alternatively, ER can recruit corepressors such as histone deacetylases (HDACs) through interactions with its DBD which then modify the surrounding chromatin to repress gene transcription (164, 165). ER can also have an indirect role in gene transcription by acting as a coregulatory partner for transcription factors such as the specificity protein (Sp)1, activating protein (AP)-1 and nuclear factor kappa B (NF- κ B) (166, 167). This indirect “tethering” enables ER to mediate transcription at genes that do not have ERE motifs in their promoters. ER regulates gene

activation and repression at equal amounts, with 51.2% of genes being down-regulated after three hours of E2 treatment (157). Though ER has obvious repressive effects, studies remain focused on its role in gene activation. Interestingly, all ER⁺ luminal cell lines currently available have the transcriptional and genomic profiles of the luminal B subtype and show a marked proliferative response to E2 (108, 109, 168). A study investigating DNA binding in ER⁺ patients who were either responsive or nonresponsive to tamoxifen therapy showed that ER-DNA binding patterns in nonresponsive patients correlated more closely with the binding patterns obtained from MCF-7 cells (169). This provides further evidence that the anti-proliferative response to hormones seen in luminal A tumors is not represented in the current *in vitro* ER⁺ breast cancer models.

1.4.3.1 The role of cofactors in ER-mediated transcription

1.4.3.1.1 Coactivators

E2-induced ER DNA binding occurs in a cyclical manner with an initial 20-minute pre-initiation cycle in which ER recruits the SWItch/sucrose non-fermentable (SWI/SNF) nucleosome remodeling complex along with KATs and KMTs which modify the histone tails on surrounding nucleosomes to generate a more accessible chromatin state (170). Subsequent cycles of ER binding last approximately 45 minutes and enable gene activation through the recruitment of several coactivators including the p160/SRC family, CBP/p300, p300/CBP-associated cofactor (pCAF), and Mediator complex which recruits and activates RNA Polymerase II (Pol II) (170-172). The p160/SRC family consists of three SRC proteins: SRC-1, SRC-2 and SRC-3 which interact with nuclear receptors at the LBD via the NR box (173). SRC-1 and SRC-3 have been shown to interact with ER and promote gene transcription by recruiting CBP/p300 (170). CBP and p300 are functional homologs

which acetylate the four histone tails on the nucleosomes promoting an active chromatin state which is more accessible to RNA Pol II (171, 174). Though p300 is required for initial recruitment of Pol II, chromatin immunoprecipitation (ChIP) experiments have shown it does not participate in additional cycles of activation at the same promoter (171). Additional acetyltransferase activity may be achieved in the later transcriptional cycles through binding of pCAF (Figure 1.6) (171). The final step of ER-mediated gene activation involves recruitment of the Mediator complex which phosphorylates Pol II and initiates transcription (Figure 1.6) (170). ER is removed during each transcriptional cycle by the attachment of ubiquitin proteins to lysine residues on ER via ubiquitination enzymes. The formation of polyubiquitin chains targets ER for degradation via the 26S proteasome (170, 175). ER deletion studies have implicated the LBD in the regulation of ligand induced ER degradation (176).

1.4.3.1.2 Corepressors

In the absence of E2, ER continues to associate with the promoter at shorter 20-minute cycles and recruits corepressive complexes (161). The nuclear receptor corepressor (NCoR) and silencing mediator of retinoid and thyroid receptors (SMRT) are well described for their ability to repress nuclear receptors in the absence of ligand (177). These corepressors bind the LBD of unliganded nuclear receptors through a corepressor/nuclear receptor (CoRNR) box that mimics the coactivator LXXLL motif and become displaced in the presence of ligand (178, 179). Interestingly, ER associates with NCoR and SMRT when bound to tamoxifen and promotes gene repression by preventing coactivator association (171, 180, 181). Furthermore, NCoR and SMRT have been shown to mediate gene repression by binding ER's DBD rather than the LBD and this may support their ability to

function as repressors in the presence of tamoxifen which binds the LBD (164). Clinical studies have shown increased levels of NCoR1 expression correlate with increased relapse-free survival in patients treated with tamoxifen (182), and decreased NCoR1 expression has been implicated in endocrine resistance in luminal A tumors (92).

Corepressors involved in E2-induced repression via ER include scaffold attachment factor B1 (SAFB1), NCoR, ligand-dependent nuclear receptor corepressor (LCoR), carboxyl-terminal binding protein (CtBP), receptor interacting protein (RIP)140 and repressor of estrogen receptor activity (REA) (summarized in (183)). SAFB1 and NCoR were shown to repress the activation of a transient E-Cadherin promoter in the presence of E2 (184). LCoR binds ER at the LBD through a LXXLL motif and functions as an E2-induced repressor by recruiting HDACs to the gene promoter (185). LCoR and RIP140 both interact with corepressor CtBP, which can suppress gene activation through histone deacetylase- dependent and independent pathways (185-187). REA does not have intrinsic repressor activity but serves as corepressor by competing with coactivators for the hydrophobic pocket in the LBD and recruiting HDACs (188, 189). ChIP experiments for the *pS2* promoter have shown that after Pol II phosphorylation, ER is removed via proteasomal degradation and HDACs along with the nucleosome remodeling deacetylase (NuRD) complex remove the acetyl groups from the histone tails and remodel the chromatin to a closed, repressed state (170).

1.4.3.1.3 Histone deacetylase (HDAC) activity in breast cancer

The role for HDAC activity in breast cancer has gained attention over the past decade. Though there is conflicting experimental and clinical results from several research

groups for the roles of HDACs in breast cancer, it has become evident that HDACs are important mediators of ER expression and function.

1.4.3.1.3.1 Experimental evidence

Kawai et al. (2006) found that MCF-7 cells overexpressing HDAC1 had increased proliferation which correlated with a decrease in ER expression and transcriptional activity (190). Treatment of these HDAC1 overexpressing MCF-7 cells with the HDAC inhibitor trichostatin A (TSA) enabled ER re-expression (190). This effect has also been shown in ER negative MDA-MB-231 cells which show re-expression on ER upon treatment with TSA (191). HDAC inhibitor induced ER expression in MDA-MB-231 cells correlates with response to tamoxifen that promotes the recruitment of repressive complexes (192). These finding suggested that increased HDAC1 activity could promote suppression of ER expression and activity which promotes breast cancer progression. Further *in vitro* work found the HDAC inhibitor valproic acid (VPA) could enhance the anti-proliferative effect of tamoxifen in MCF-7 cells (193). MCF-7 cells with experimentally induced tamoxifen resistance were shown to have increased ER expression which is thought to promote their proliferative ability and when these cells were treated with HDAC inhibitors ER expression was reduced and the cells regained their anti-proliferative response to tamoxifen (194). Conversely, *in vivo* mouse models found the combination of a HDAC inhibitor with tamoxifen increased tumor suppression and correlated with increased ER expression (195). Despite conflicting results these studies highlighted a potential role for the use of HDAC inhibitors in reversing endocrine resistance in ER+ breast cancers.

1.4.3.1.3.2 Clinical evidence

Studies for the use of HDAC inhibitors in the treatment of breast cancer are limited. In 2011, Munster et al. found a combination of tamoxifen with the Food and Drug Administration (FDA) approved HDAC inhibitor Vorinostat lead to tumor regression or prolonged disease stabilization in ~40% of ER+ patients who progressed on prior hormone therapy (196). The response seen in this study was correlated to inhibition of HDAC2 and suggests that down-regulation of HDACs could improve the response to tamoxifen (196). This is consistent with other clinical findings that increased HDAC2 expression correlates with more aggressive tumors, interestingly this study also found HDAC1 expression correlated strongly with hormone receptor positive tumors (197). This association between HDAC1 and hormone receptor status has also been shown by Krusche et al. (2005) and increased HDAC1 expression correlated with improved survival in patients with small and well differentiated tumors (198). Seo et al. (2014) found that a subset of luminal A tumors which have increased levels of HDAC1 also had an increase in overall survival (199). This correlation was supported by Eom et al. (2012) who showed decreased HDAC1 expression in IDC was associated with higher histologic grade and decreased ER expression (200). When taken together, the experimental and clinical studies highlight a key role for HDACs in the regulation of ER and provide evidence that some tumors may benefit from combined treatment of endocrine therapy and HDAC inhibitors. Since *in vitro* studies of HDAC inhibitor function have been conducted primarily in luminal B cell lines like the MCF-7s it is likely that the clinical benefits of HDAC inhibitors is most pronounced in luminal B tumors. Furthermore, the beneficial effects for HDAC1 in luminal A tumors highlights a critical role for chromatin remodeling which enables transcriptional repression in these tumors.

1.4.3.2 ER-mediated chromosomal reconfiguration

Advanced molecular techniques combined with next generation sequencing (NGS) have provided new insights into the mechanisms involved in long-range gene regulation. These experiments have shown that chromatin is organized into topological associating domains (TADs) which have boundaries marked by the insulator protein CCCTC-binding factor (CTCF) (201). TADs are dynamic structures that form throughout the cell cycle and regulate specific interactions between gene promoters and enhancer regions by limiting their association with regions outside of the CTCF boundaries (202). TAD formation has been described as a dynamic loop extrusion model in which the binding and orientation of CTCF proteins serves as the support for further binding of ring-shaped cohesin molecules which extrude the DNA between the two CTCF anchors as a loop (202). Genes within sub-megabase TAD regions show coordinated transcriptional responses and this may be mediated through smaller-scale DNA looping between enhancers and gene promoters within the TAD (203).

Fullwood et al. (2009) mapped ER-mediated DNA loops in MCF-7 cells treated with E2 using chromatin interaction analysis with paired-end tag sequencing (ChIA-PET) (204). These experiments showed ER-DNA binding serves as the anchor for small (<100Kb) and large (>1Mb) scale DNA-loops which are centred around the transcriptional machinery enabling the simultaneous activation of multiple genes upon E2 treatment (204). ChIP experiments for ER have shown the majority of binding occurs at distal regions and requires the pioneer factor FOXA1 (205). A more in-depth look at ER enriched-enhancers revealed the MegaTrans complex which consists of transcription factors such as GATA3, AP2 γ , FOXA1, STAT1, RAR α/γ , AP1 and c-Fos which bind ER and recruit coactivators required

for transcription (206). FOXA1, GATA3, AP2 γ and cohesin have all been implicated in maintaining ER-mediated loops (Figure 1.7) (207). CTCF has been shown to colocalize with ER and FOXA1 peaks in MCF-7 cells and may provide further support for ER-mediated looping (208).

Unliganded ER has been shown to bind DNA and enable cofactor recruitment in order to ‘prime’ the promoter for E2-induced transcription (161). Consistent with this ER-mediated loops containing ‘paused’ Pol II are formed in the absence of E2 (209). For ER-activated genes treatment with E2 is thought to recruit additional coactivators which initiate elongation (209). For ER-repressed genes, E2 treatment was shown to disrupt the loop formation, moving the gene away from the transcriptional machinery (209). In this way, genes become repressed by being sequestered in the loop region and away from the transcriptional machinery (204, 209). The ability of unliganded ER to mediate DNA looping is significant as increased ER expression leads to increased basal proliferation in the absence of E2 (210). This led to the hypothesis that increased ER expression may enable low affinity binding of distal enhancer regions and promote a novel chromatin reconfiguration which alters the pattern of gene activation and repression in the presence of E2. Luminal A tumors, with their increased ER content may therefore have a unique chromatin structure which promotes their anti-proliferative response to hormone therapy.

1.5 Hypothesis and objectives

The aim of this thesis is to investigate the underlying mechanism(s) that regulate the differential response to hormones seen in luminal A and luminal B tumors. Luminal A tumors have been shown to have increased ER expression and an improved response to hormone therapy (105). The estrogenic properties of tamoxifen along with the clinical

evidence from the WHI study support a therapeutic role for E2 in ER+ breast cancers. This assumption is furthered by *in vitro* models which have shown increased ER expression leads to an anti-proliferative response to E2 (111). Therefore, throughout this work the therapeutic response of ER+ breast cancers to tamoxifen is assumed to be an estrogenic effect that is mediated by ER. Investigation into a potential anti-proliferative response to E2 in luminal A tumors is limited by the absence of a luminal A cell line (108, 168). To address this limitation, the first part of this thesis will focus on the development of a stable MCF-7 transfectant with increased ER expression and a potential anti-proliferative response to E2.

This model will be used in subsequent experiments to investigate the differences in ER-DNA binding and gene transcription when the level of ER expression is increased. Finally, changes in chromatin reconfiguration at previously mapped ER-mediated DNA loops will be investigated. These *in vitro* studies will serve as a proof of principle for chromatin reconfiguration as a potential diagnostic tool to accurately differentiate those ER+ patients with hormone responsive tumors from those who will require additional chemotherapy.

Main hypothesis: The level of estrogen receptor expression regulates a differential proliferative response to estrogen via altered DNA loop configuration.

This hypothesis will be tested using the following main objectives:

1. Determine if the level of ER mediates an opposite proliferative response to E2.
2. Determine how the level of ER mediates an opposite transcriptional response to E2.
3. Establish a diagnostic assay to differentiate estrogen responsive and nonresponsive breast cancer cells.

Table 1.1 Descriptions for the Tumor, lymph Node, and Metastasis staging system.

Adapted from (211).

Tumors	T0/Tis	T1	T2	T3	T4
Tumor size	T0: No primary tumor. Tis: <i>In situ</i> carcinoma	0-2 cm	2-5 cm	>5 cm	Tumor of any size with extension to the chest wall/skin or ulceration
Nodes	N0	N1mi	N1	N2	N3
	No lymph node involvement	Lymph node tumor between 0.2-2 mm	Cancer cells present in at least 1-3 axillary lymph nodes	Cancer cells present in 4-9 axillary lymph nodes	Cancer cells in infra or supraclavicular lymph nodes, or in >10 axillary lymph nodes
Metastasis	M0	M1			
	No evidence of cancer metastasis	Cancer found in other areas of the body			

Table 1.2 American Joint Committee on Cancer (AJCC) Breast cancer staging guidelines. Adapted from (211).

Stage	Tumor	Node	Metastasis
0	T0	N0	M0
IA	T1	N0	M0
IB	T0-T1	N1mi	M0
IIA	T0-T1	N1	M0
	T2	N0	M0
IIB	T2	N1	M0
	T3	N0	M0
IIIA	T0-T2	N2	M0
	T3	N1-N2	M0
IIIB	T4	N0-N2	M0
IIIC	Tis-T4	N3	M0
IV	Tis-T4	N0-N4	M1

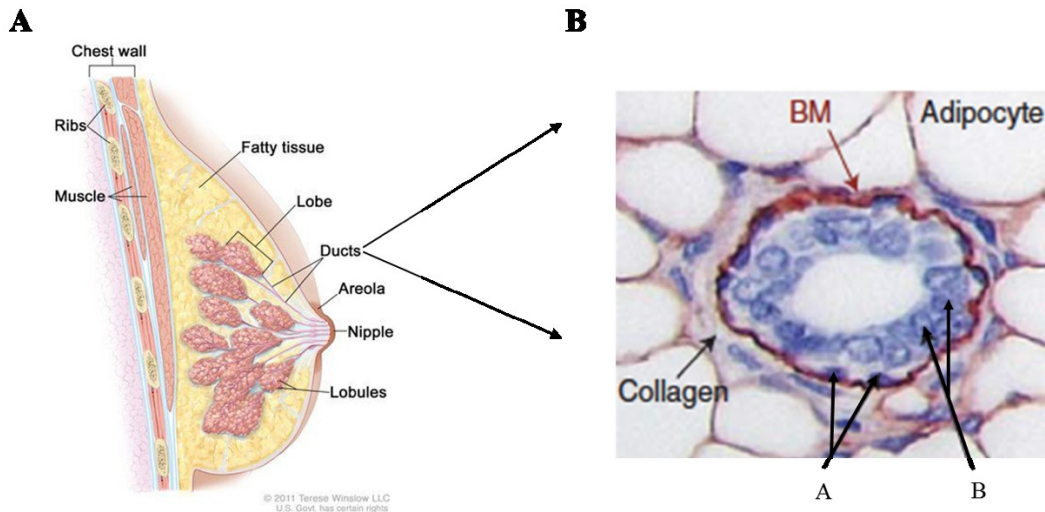


Figure 1.1. Structure of the normal mammary gland. **A.** Cross-section of the female breast showing the ducts, lobes, lobules, areola, nipple and fatty tissues. Adapted from (212). **B.** Mammary duct structure showing the laminin-rich basement membrane (BM), myoepithelial cells (A) and luminal epithelial cells (B) lining the lumen. Adapted from (9) with permission from the publisher ©Cold Spring Harbor Laboratory Press.

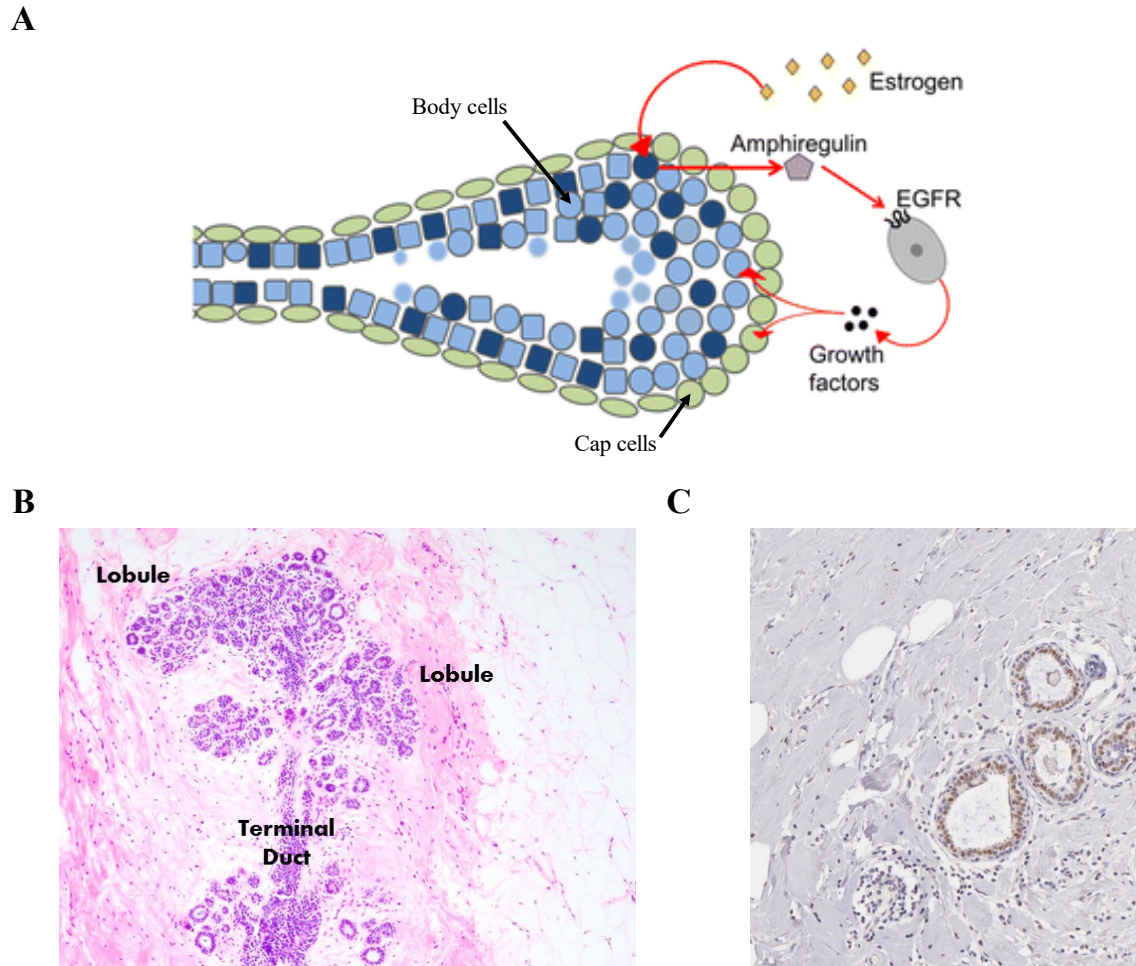
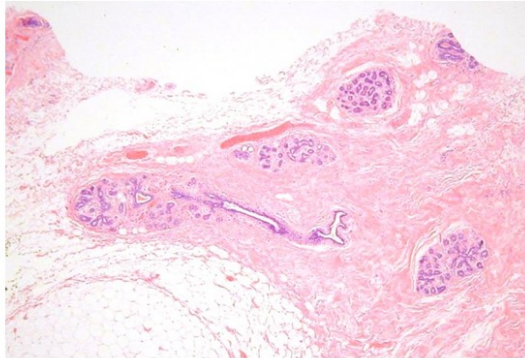
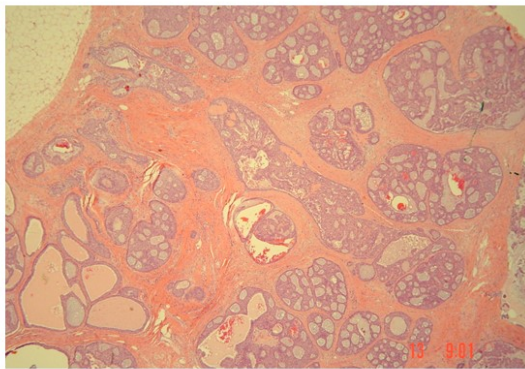


Figure 1.2 Hormonal regulation of mammary gland development. **A.** Estrogen induced paracrine signaling in the elongating terminal end bud (TEB). Cap cells (green), ER- (light blue) and ER+ (dark blue) body cells shown. Adapted from (12) with permission from the publisher. **B.** Histological view of the adult mammary gland showing the terminal duct and lobules. Images obtained from (213). **C.** The epithelial cells of the duct show staining for ER. Image obtained from (214).

A



B



C

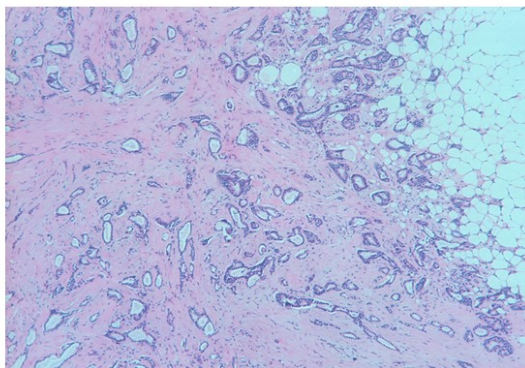


Figure 1.3. Progression of breast cancer. A. Normal Breast B. Ductal carcinoma in situ (DCIS) C. Invasive ductal carcinoma (IDC). Images provided by Dr. Judith Hugh.

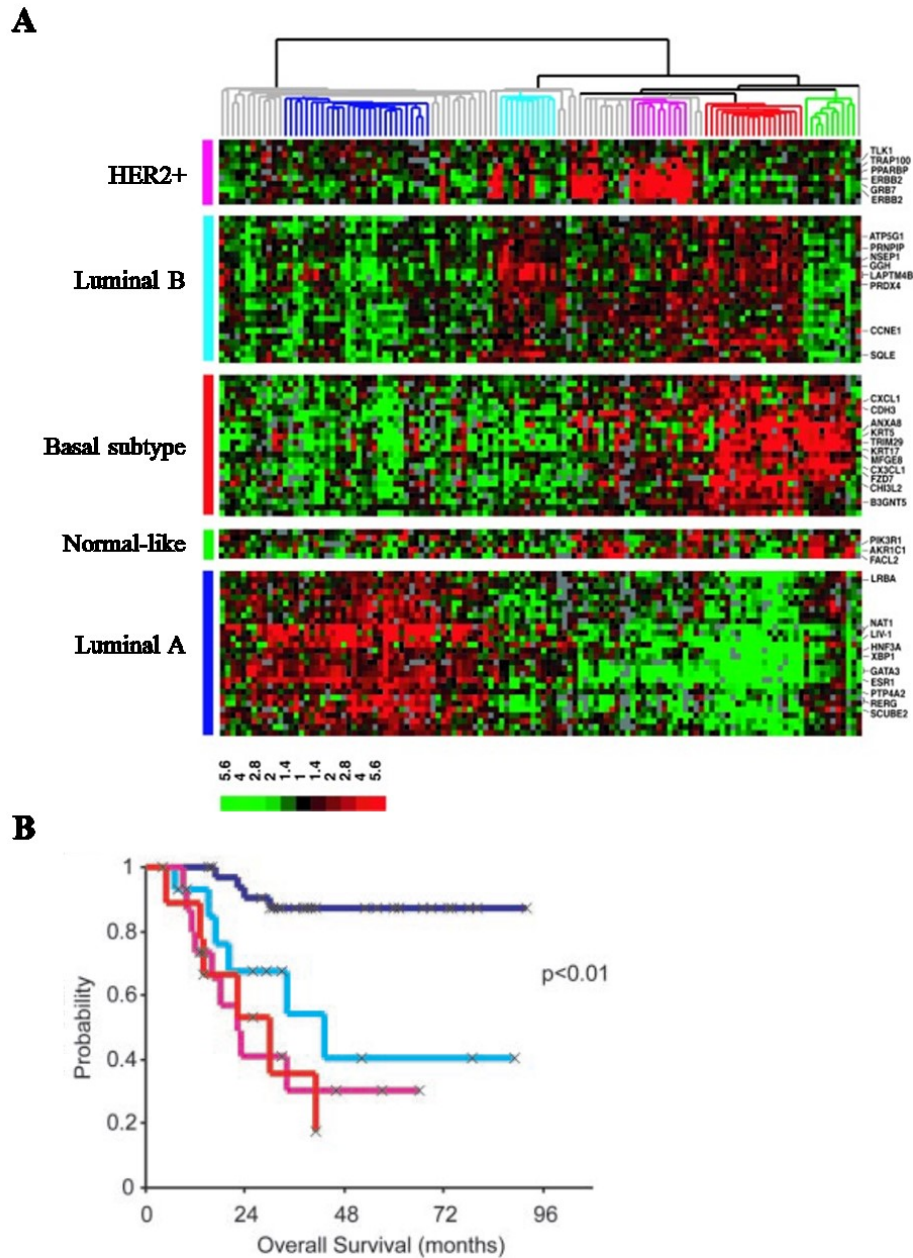


Figure 1.4. The molecular subtypes of breast cancer. **A.** Hierarchical clustering showing the four intrinsic breast cancer subtypes: luminal A, luminal B, HER2+, and Basal-like. The corresponding hierarchical clustering profiles are shown. **B.** Kaplan-Meier curves showing the overall survival for the four intrinsic subtypes. Figures A and B were adapted from (37) with permission from the publisher. Copyright (2003) National Academy of Sciences.

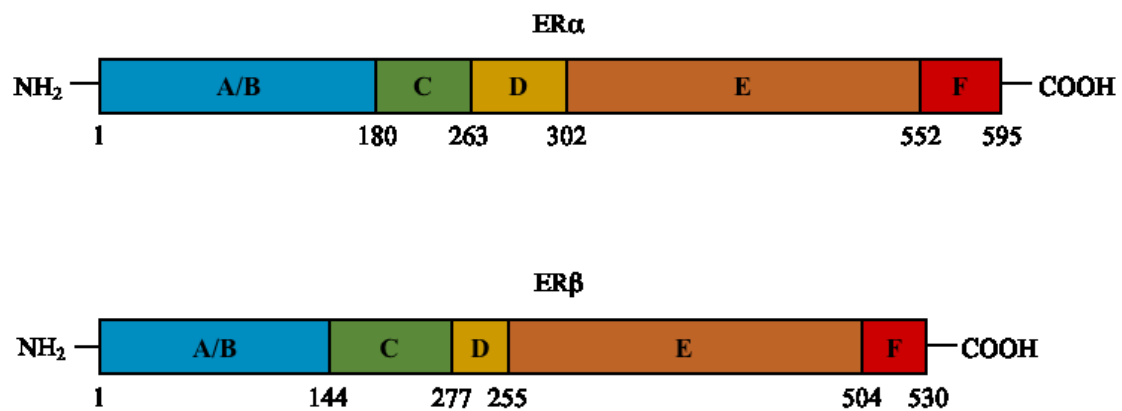


Figure 1.5 Structure of ER α and ER β . Schematic showing the A/B, C, D, E and F domains of the ERs. Adapted from (123).

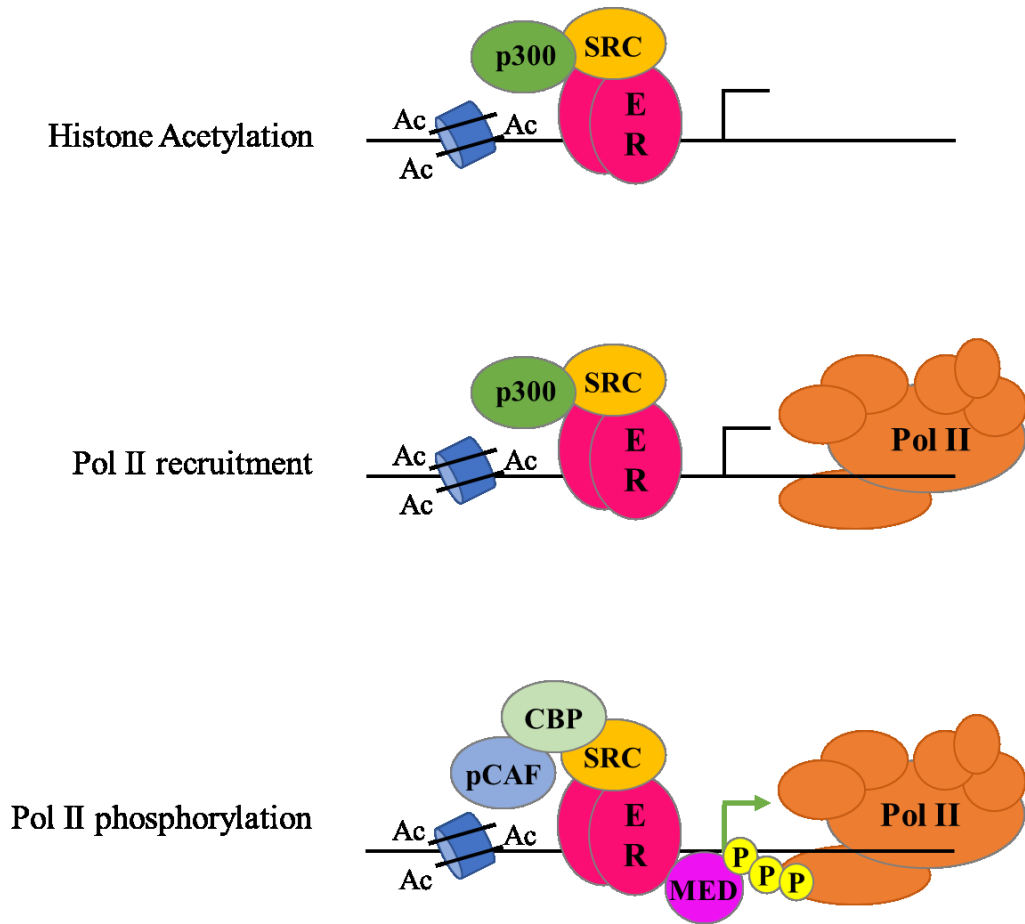


Figure 1.6 ER-mediated gene activation. Coactivator recruitment leads to histone acetylation, followed by Pol II recruitment and phosphorylation. Adapted from (171).

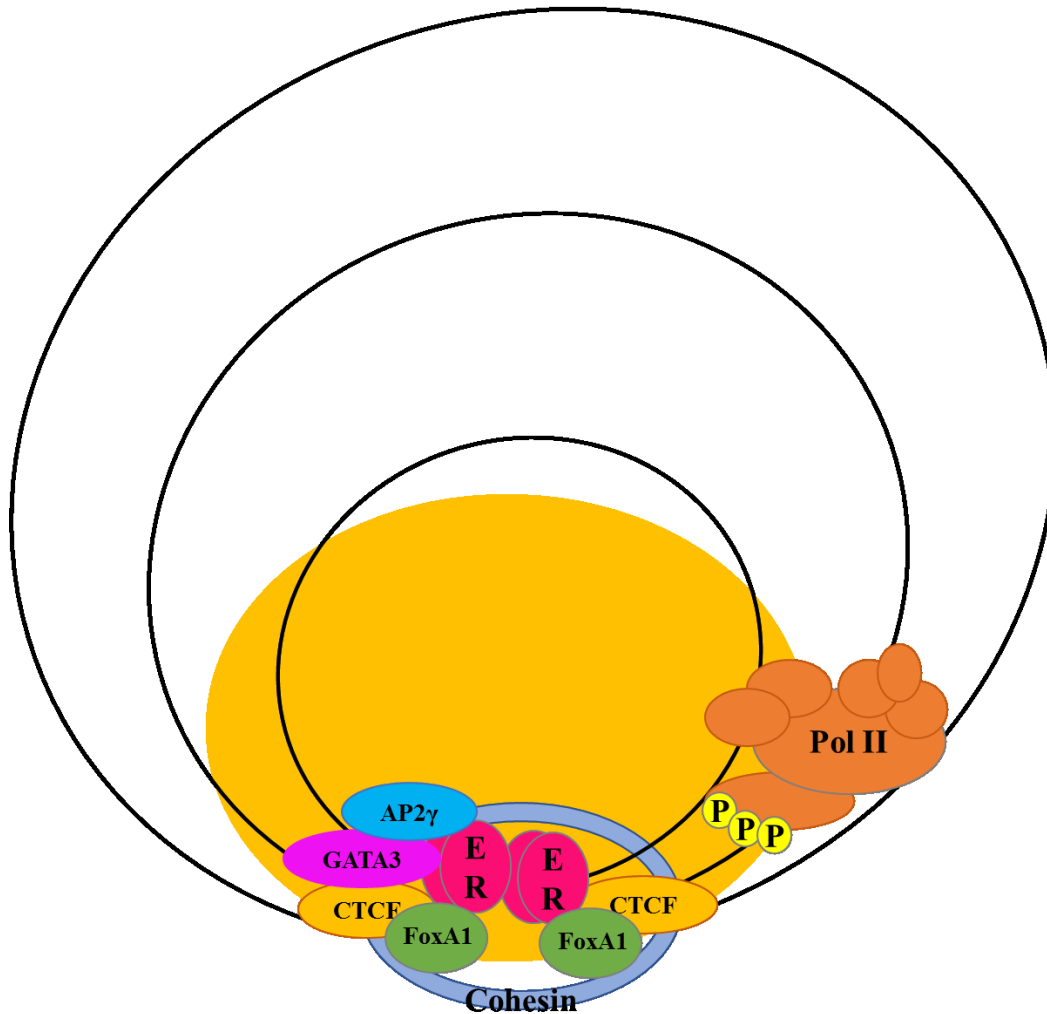


Figure 1.7 ER-mediated DNA loops. ER binding at enhancer and promoter regions serves as the anchors for DNA loops which are further supported by associations with transcription factors including FOXA1, GATA3, AP2 γ and CTCF. The looped DNA is threaded through the ring-like structure of the cohesin complex which stabilizes the 3D structure. The formation of ER-mediated DNA loops enables the poised RNA Pol II (Pol II) to initiate gene transcription. Figure adapted from (204, 207).

1.6 References

1. Howard B, Gusterson B. Human breast development. *J Mammary Gland Biol Neoplasia*. 2000;5(2):119-37.
2. Javed A, Lteif A. Development of the Human Breast. *Seminars in Plastic Surgery*. 2013;27(1):5-12.
3. Hovey R, Trott J, Vonderhaar B. Establishing a framework for the functional mammary gland: From endocrinology to morphology. *J Mammary Gland Biol Neoplasia*. 2002;7(1):17-38.
4. Russo J, Russo IH. Development of the human breast. *Maturitas*. 2004;49(1):2-15.
5. Oakes SR, Hilton HN, Ormandy CJ. Key stages in mammary gland development: The alveolar switch: Coordinating the proliferative cues and cell fate decisions that drive the formation of lobuloalveoli from ductal epithelium. *Breast Cancer Res*. 2006;8(2).
6. Gudjonsson T, Adriance MC, Sternlicht MD, Petersen OW, Bissell MJ. Myoepithelial cells: Their origin and function in breast morphogenesis and neoplasia. *J Mammary Gland Biol Neoplasia*. 2005;10(3):261-72.
7. Albrechtsen R, Nielsen M, Wewer U, Engvall E, Ruoslahti E. Basement-Membrane Changes in Breast-Cancer Detected by Immunohistochemical Staining for Laminin. *Cancer Res*. 1981;41(12):5076-81.
8. Wu X, Chen G, Qiu J, Lu J, Zhu W, Chen J, et al. Visualization of basement membranes in normal breast and breast cancer tissues using multiphoton microscopy. *Oncology Letters*. 2016;11(6):3785-9.
9. Muschler J, Streuli CH. Cell-Matrix Interactions in Mammary Gland Development and Breast Cancer. *Cold Spring Harbor Perspectives in Biology*. 2010;2(10):a003202.

10. Arendt LM, Kuperwasser C. Form and Function: how Estrogen and Progesterone Regulate the Mammary Epithelial Hierarchy. *J Mammary Gland Biol Neoplasia*. 2015;20(1-2):9-25.
11. Mallepell S, Krust A, Chambon P, Briskin C. Paracrine signaling through the epithelial estrogen receptor alpha is required for proliferation and morphogenesis in the mammary gland. *Proc Natl Acad Sci U S A*. 2006;103(7):2196-201.
12. Paine IS, Lewis MT. The Terminal End Bud: the Little Engine that Could. *J Mammary Gland Biol Neoplasia*. 2017;22(2):93-108.
13. Kumar P, Wu Q, Chambliss KL, Yuhanna IS, Mumby SM, Mineo C, et al. Direct interactions with G alpha i and G beta gamma mediate nongenomic signaling by estrogen receptor alpha. *Molecular Endocrinology*. 2007;21(6):1370-80.
14. Filardo EJ, Thomas P. Minireview: G Protein-Coupled Estrogen Receptor-1, GPER-1: Its Mechanism of Action and Role in Female Reproductive Cancer, Renal and Vascular Physiology. *Endocrinology*. 2012;153(7):2953-62.
15. Pedram A, Razandi M, Lewis M, Hammes S, Levin ER. Membrane-Localized Estrogen Receptor alpha Is Required for Normal Organ Development and Function. *Developmental Cell*. 2014;29(4):482-90.
16. Bjornstrom L, Sjoberg M. Mechanisms of estrogen receptor signaling: Convergence of genomic and nongenomic actions on target genes. *Molecular Endocrinology*. 2005;19(4):833-42.
17. Neville M, McFadden T, Forsyth I. Hormonal regulation of mammary differentiation and milk secretion. *J Mammary Gland Biol Neoplasia*. 2002;7(1):49-66.

18. Inman JL, Robertson C, Mott JD, Bissell MJ. Mammary gland development: cell fate specification, stem cells and the microenvironment. *Development*. 2015;142(6):1028-42.
19. Kouros-Mehr H, Slorach EM, Sternlicht MD, Werb Z. GATA-3 maintains the differentiation of the luminal cell fate in the mammary gland. *Cell*. 2006;127(5):1041-55.
20. Neville MC, Daniel CW. *The Mammary gland : development, regulation, and function*. New York: Plenum Press; 1987.
21. Brisken C. Hormonal control of alveolar development and its implications for breast carcinogenesis. *J Mammary Gland Biol Neoplasia*. 2002;7(1):39-48.
22. Longacre TA, Bartow SA. A Correlative Morphological-Study of Human-Breast and Endometrium in the Menstrual-Cycle. *Am J Surg Pathol*. 1986;10(6):382-93.
23. Ferlay J, Soerjomataram I, Dikshit R, Eser S, Mathers C, Rebelo M, et al. Cancer incidence and mortality worldwide: Sources, methods and major patterns in GLOBOCAN 2012. *International Journal of Cancer*. 2015;136(5):E359-86.
24. *Canadian Cancer Statistics 2017*. Toronto, ON: Canadian Cancer Society: Canadian Cancer Society's Advisory Committee on Cancer Statistics; 2017.
25. Smith GH. Experimental mammary epithelial morphogenesis in an in vivo model: Evidence for distinct cellular progenitors of the ductal and lobular phenotype. *Breast Cancer Res Treat*. 1996;39(1):21-31.
26. Smalley M, Ashworth A. Stem cells and breast cancer: A field in transit. *Nat Rev Cancer*. 2003;3(11):832-44.

27. Bombonati A, Sgroi DC. The molecular pathology of breast cancer progression. *J Pathol.* 2011;223(2):307-17.
28. Allred DC. Ductal carcinoma in situ: terminology, classification, and natural history. *Journal of the National Cancer Institute. Monographs.* 2010;2010(41):134-8.
29. Narod SA, Iqbal J, Giannakeas V, Sopik V, Sun P. Breast Cancer Mortality After a Diagnosis of Ductal Carcinoma In Situ. *Jama Oncology.* 2015;1(7):888-96.
30. Erbas B, Provenzan E, Armes J, Gertig D. The natural history of ductal carcinoma in situ of the breast: a review. *Breast Cancer Res Treat.* 2006;97(2):135-44.
31. Weigelt B, Peterse JL, Van't Veer LJ. Breast cancer metastasis: Markers and models. *Nat Rev Cancer.* 2005;5(8):591-602.
32. Cserni G, Chmielik E, Cserni B, Tot T. The new TNM-based staging of breast cancer. *Virchows Archiv : an international journal of pathology.* 2018.
33. National Comprehensive Cancer Network. NCCN Clinical Practice Guidelines in Oncology: Breast Cancer. National Comprehensive Cancer Network; 2016.
34. Elston C, Ellis I. Pathological Prognostic Factors in Breast-Cancer .1. the Value of Histological Grade in Breast-Cancer - Experience from a Large Study with Long-Term Follow-Up. *Histopathology.* 1991;19(5):403-10.
35. Rakha EA, Reis-Filho JS, Baehner F, Dabbs DJ, Decker T, Eusebi V, et al. Breast cancer prognostic classification in the molecular era: The role of histological grade. *Breast Cancer Res.* 2010;12(4).
36. Perou CM, Sørile T, Eisen MB, Van De Rijn M, Jeffrey SS, Renshaw CA, et al. Molecular portraits of human breast tumours. *Nature.* 2000;406(6797):747-52.

37. Sørlie T, Perou CM, Tibshirani R, Aas T, Geisler S, Johnsen H, et al. Gene expression patterns of breast carcinomas distinguish tumor subclasses with clinical implications. *Proc Natl Acad Sci U S A*. 2001;98(19):10869-74.
38. Carey LA, Perou CM, Livasy CA, Dressler LG, Cowan D, Conway K, et al. Race, breast cancer subtypes, and survival in the Carolina Breast Cancer Study. *J Am Med Assoc*. 2006;295(21):2492-502.
39. Hu Z, Fan C, Oh DS, Marron JS, He X, Qaqish BF, et al. The molecular portraits of breast tumors are conserved across microarray platforms. *BMC Genomics*. 2006;7:96.
40. Chang MC, Souter LH, Kamel-Reid S, Rutherford M, Bedard P, Trudeau M, et al. Clinical utility of multigene profiling assays in early-stage breast cancer. *Current Oncology*. 2017;24(5):E403-22.
41. Parker JS, Mullins M, Cheang MCU, Leung S, Voduc D, Vickery T, et al. Supervised Risk Predictor of Breast Cancer Based on Intrinsic Subtypes. *Journal of Clinical Oncology*. 2009;27(8):1160-7.
42. Wallden B, Storhoff J, Nielsen T, Dowidar N, Schaper C, Ferree S, et al. Development and verification of the PAM50-based Prosigna breast cancer gene signature assay. *Bmc Medical Genomics*. 2015;8:54.
43. Prat A, Parker JS, Fan C, Cheang MCU, Miller LD, Bergh J, et al. Concordance among gene expression-based predictors for ER-positive breast cancer treated with adjuvant tamoxifen. *Ann Oncol*. 2012;23(11):2866-73.
44. Venet D, Dumont JE, Detours V. Most Random Gene Expression Signatures Are Significantly Associated with Breast Cancer Outcome. *Plos Computational Biology*. 2011;7(10):e1002240.

45. Lester J. Local Treatment of Breast Cancer. *Semin Oncol Nurs.* 2015;31(2):122-33.
46. Lyman G, Giuliano A, Somerfield M, Benson A, Bodurka D, Burstein H, et al. American Society of Clinical Oncology guideline recommendations for sentinel lymph node biopsy in early-stage breast cancer. *Journal of Clinical Oncology.* 2005;23(30):7703-20.
47. Chew H. Adjuvant therapy for breast cancer: who should get what? *West J Med.* 2001;174(4):284-7.
48. Gewirtz D. A critical evaluation of the mechanisms of action proposed for the antitumor effects of the anthracycline antibiotics Adriamycin and daunorubicin. *Biochem Pharmacol.* 1999;57(7):727-41.
49. Rowinsky E. The development and clinical utility of the taxane class of antimicrotubule chemotherapy agents. *Annu Rev Med.* 1997;48:353-74.
50. National Breast and Ovarian Cancer Centre. Recommendations for use of chemotherapy for the treatment of advanced breast cancer. Surry Hills, NSW: National Breast and Ovarian Cancer Centre; 2010.
51. Alberta Health Services. Adjuvant Systemic Therapy for Early Stage (Lymph Node Negative and Lymph Node Positive) Breast Cancer. Alberta Health Services; 2016.
52. Hudis CA. Drug therapy: Trastuzumab - Mechanism of action and use in clinical practice. *N Engl J Med.* 2007;357(1):39-51.
53. National Breast and Ovarian Cancer Centre. Recommendations for use of Trastuzumab (Herceptin®) for the treatment of HER2 positive breast cancer. Camperdown, NSW: National Breast and Ovarian Cancer Centre; 2011.

54. Leclercq G, Lacroix M, Laios L, Laurent G. Estrogen receptor alpha: Impact of ligands on intracellular shuttling and turnover rate in breast cancer cells. *Current Cancer Drug Targets*. 2006;6(1):39-64.
55. Jordan V. Antiestrogens and selective estrogen receptor modulators as multifunctional medicines. 1. Receptor interactions. *J Med Chem*. 2003;46(6):883-908.
56. Lewis J, Jordan V. Selective estrogen receptor modulators (SERMs): Mechanisms of anticarcinogenesis and drug resistance. *Mutat Res -Fundam Mol Mech Mutag*. 2005;591(1-2):247-63.
57. Vogel VG. Effects of tamoxifen vs raloxifene on the risk of developing invasive breast cancer and other disease outcomes: The NSABP study of tamoxifen and raloxifene (STAR) P-2 trial (vol 295, pg 2727, 2006). *Jama-Journal of the American Medical Association*. 2007;298(9):973-.
58. Fisher B, Costantino J, Redmond C, Fisher E, Wickerham D, Cronin W, et al. Endometrial Cancer in Tamoxifen-Treated Breast-Cancer Patients - Findings from the National Surgical Adjuvant Breast and Bowel Project (Nsabp) B-14. *J Natl Cancer Inst*. 1994;86(7):527-37.
59. Jordan VC. The Role of Tamoxifen in the Treatment and Prevention of Breast-Cancer. *Curr Probl Cancer*. 1992;16(3):134-76.
60. Boccardo F, Rubagotti A, Amoroso D, Mesiti M, Romeo D, Sismondi P, et al. Cyclophosphamide, methotrexate, and fluorouracil versus tamoxifen plus ovarian suppression as adjuvant treatment of estrogen receptor-positive pre-/perimenopausal breast cancer patients: Results of the Italian Breast Cancer Adjuvant Study Group 02 Randomized Trial. *Journal of Clinical Oncology*. 2000;18(14):2718-27.

61. National Breast and Ovarian Cancer Centre. Recommendations for use of endocrine therapy for the treatment of hormone receptor-positive advanced breast cancer. Surry Hills, NSW: National Breast and Ovarian Cancer Centre; 2010.
62. Wakeling A, Dukes M, Bowler J. A Potent Specific Pure Antiestrogen with Clinical Potential. *Cancer Res.* 1991;51(15):3867-73.
63. Howell A. Pure oestrogen antagonists for the treatment of advanced breast cancer. *Endocr Relat Cancer.* 2006;13(3):689-706.
64. Smith IE, Dowsett M. Aromatase inhibitors in breast cancer. *New Engl J Med.* 2003;348(24):2431-42.
65. Folkard E, Dowsett M. Sex hormones and breast cancer risk and prognosis. *Breast.* 2013;22(Suppl 2):S38-43.
66. Goss PE, Ingle JN, Pritchard KI, Robert NJ, Muss H, Galow J, et al. Extending Aromatase-Inhibitor Adjuvant Therapy to 10 Years. *N Engl J Med.* 2016;375(3):209-19.
67. Clarke R. Human breast cell proliferation and its relationship to steroid receptor expression. *Climacteric.* 2004;7(2):129-37.
68. Anderson T, Battersby S, King R, McPherson K, Going J. Oral-Contraceptive use Influences Resting Breast Proliferation. *Hum Pathol.* 1989;20(12):1139-44.
69. McCarty K. Proliferative Stimuli in the Normal Breast - Estrogens Or Progestins. *Hum Pathol.* 1989;20(12):1137-8.
70. Chlebowski RT, Hendrix SL, Langer RD, Stefanick ML, Gass M, Lane D, et al. Influence of estrogen plus progestin on breast, cancer and mammography in healthy

- postmenopausal women - The Women's Health Initiative Randomized trial. *Jama-Journal of the American Medical Association*. 2003;289(24):3243-53.
71. LaCroix AZ, Chlebowski RT, Manson JE, Aragaki AK, Johnson KC, Martin L, et al. Health Outcomes After Stopping Conjugated Equine Estrogens Among Postmenopausal Women With Prior Hysterectomy A Randomized Controlled Trial. *Jama-Journal of the American Medical Association*. 2011;305(13):1305-14.
72. Anderson GL, Chlebowski RT, Aragaki AK, Kuller LH, Manson JE, Gass M, et al. Conjugated equine oestrogen and breast cancer incidence and mortality in postmenopausal women with hysterectomy: extended follow-up of the Women's Health Initiative randomised placebo-controlled trial. *Lancet Oncology*. 2012;13(5):476-86.
73. Manson JE, Chlebowski RT, Stefanick ML, Aragaki AK, Rossouw JE, Prentice RL, et al. Menopausal Hormone Therapy and Health Outcomes During the Intervention and Extended Poststopping Phases of the Women's Health Initiative Randomized Trials. *Obstet Gynecol Surv*. 2014;69(2):83-5.
74. Ellis MJ, Gao F, Dehdashti F, Jeffe DB, Marcom PK, Carey LA, et al. Lower-Dose vs High-Dose Oral Estradiol Therapy of Hormone Receptor-Positive, Aromatase Inhibitor-Resistant Advanced Breast Cancer A Phase 2 Randomized Study. *Jama-Journal of the American Medical Association*. 2009;302(7):774-80.
75. Ingle JN, Ahmann DL, Green SJ, Edmonson JH, Bisel HF, Kvols LK, et al. Randomized Clinical-Trial of Diethylstilbestrol Versus Tamoxifen in Post-Menopausal Women with Advanced Breast-Cancer. *N Engl J Med*. 1981;304(1):16-21.

76. Peethambaram P, Ingle J, Suman V, Hartmann L, Loprinzi C. Randomized trial of diethylstilbestrol vs. tamoxifen in postmenopausal women with metastatic breast cancer. An updated analysis. *Breast Cancer Res Treat.* 1999;54(2):117-22.
77. Jenkins EO, Deal AM, Anders CK, Prat A, Perou CM, Carey LA, et al. Age-specific changes in intrinsic breast cancer subtypes: A focus on older women. *Oncologist.* 2014;19(10):1076-83.
78. Verkasalo PK, Thomas HV, Appleby PN, Davey GK, Key TJ. Circulating levels of sex hormones and their relation to risk factors for breast cancer: A cross-sectional study in 1092 pre- and postmenopausal women (United Kingdom). *Cancer Causes Control.* 2001;12(1):47-59.
79. Kedar RP, Bourne TH, Powles TJ, Collins WP, Ashley SE, Cosgrove DO, et al. Effects of Tamoxifen on Uterus and Ovaries of Postmenopausal Women in a Randomized Breast-Cancer Prevention Trial. *Lancet.* 1994;343(8909):1318-21.
80. Love RR, Mazess RB, Barden HS, Epstein S, Newcomb PA, Jordan VC, et al. Effects of Tamoxifen on Bone-Mineral Density in Postmenopausal Women with Breast-Cancer. *N Engl J Med.* 1992;326(13):852-6.
81. Lum S, Woltering E, Fletcher W, Pommier R. Changes in serum estrogen levels in women during tamoxifen therapy. *Am J Surg.* 1997;173(5):399-402.
82. Anderson WF, Chatterjee N, Ershler WB, Brawley OW. Estrogen receptor breast cancer phenotypes in the surveillance, epidemiology, and end results database. *Breast Cancer Res Treat.* 2002;76(1):27-36.
83. Yersal O, Barutca S. Biological subtypes of breast cancer: Prognostic and therapeutic implications. *World J Clin Oncol.* 2014;5(3):412-24.

84. Geyer FC, Rodrigues DN, Weigelt B, Reis-Filho JS. Molecular Classification of Estrogen Receptor-positive/Luminal Breast Cancers. *Adv Anat Pathol.* 2012;19(1):39-53.
85. Bernardo GM, Lozada KL, Miedler JD, Harburg G, Hewitt SC, Mosley JD, et al. FOXA1 is an essential determinant of ER alpha expression and mammary ductal morphogenesis. *Development.* 2010;137(12):2045-54.
86. Silvestrini R, Veneroni S, Daidone MG, Benini E, Boracchi P, Mezzetti M, et al. The Bcl-2 protein: A prognostic indicator strongly related to p53 protein in lymph node-negative breast cancer patients. *J Natl Cancer Inst.* 1994;86(7):499-504.
87. Hasegawa D, Calvo V, Avivar-Valderas A, Lade A, Chou H, Lee YA, et al. Epithelial Xbp1 Is Required for Cellular Proliferation and Differentiation during Mammary Gland Development. *Mol Cell Biol.* 2015;35(9):1543-56.
88. Ahmed ARH, Griffiths AB, Tilby MT, Westley BR, May FEB. TFF3 is a normal breast epithelial protein and is associated with differentiated phenotype in early breast cancer but predisposes to invasion and metastasis in advanced disease. *Am J Pathol.* 2012;180(3):904-16.
89. Koboldt DC, Fulton RS, McLellan MD, Schmidt H, Kalicki-Veizer J, McMichael JF, et al. Comprehensive molecular portraits of human breast tumours. *Nature.* 2012;490(7418):61-70.
90. Li S, Rong M, Grier F, Iacopetta B. PIK3CA mutations in breast cancer are associated with poor outcome. *Breast Cancer Res Treat.* 2006;96(1):91-5.

91. Rye IH, Lundin P, Månér S, Fjelldal R, Naume B, Wigler M, et al. Quantitative multigene FISH on breast carcinomas identifies der(1;16)(q10;p10) as an early event in luminal A tumors. *Genes Chromosomes Cancer*. 2015;54(4):235-48.
92. Ciriello G, Sinha R, Hoadley KA, Jacobsen AS, Reva B, Perou CM, et al. The molecular diversity of Luminal A breast tumors. *Breast Cancer Res Treat*. 2013;141(3):409-20.
93. Nordgard SH, Johansen FE, Alnæs GIG, Bucher E, Syvänen A-, Naume B, et al. Genome-wide analysis identifies 16q deletion associated with survival, molecular subtypes, mRNA expression, and germline haplotypes in breast cancer patients. *Genes Chromosomes Cancer*. 2008;47(8):680-96.
94. Natrajan R, Lambros MBK, Geyer FC, Marchio C, Tan DSP, Vatcheva R, et al. Loss of 16q in High Grade Breast Cancer is Associated with Estrogen Receptor Status: Evidence for Progression in Tumors with a Luminal Phenotype? *Genes Chromosomes & Cancer*. 2009;48(4):351-65.
95. Tsarouha H, Pandis N, Bardi G, Teixeira M, Andersen J, Heim S. Karyotypic evolution in breast carcinomas with i(1)(q10) and der(1;16)(q10;p10) as the primary chromosome abnormality. *Cancer Genet Cytogenet*. 1999;113(2):156-61.
96. Ellis MJ, Ding L, Shen D, Luo J, Suman VJ, Wallis JW, et al. Whole-genome analysis informs breast cancer response to aromatase inhibition. *Nature*. 2012;486(7403):353-60.
97. Deisenroth C, Thorner AR, Enomoto T, Perou CM, Zhang Y. Mitochondrial HEP27 Is a c-Myb Target Gene That Inhibits Mdm2 and Stabilizes p53. *Mol Cell Biol*. 2010;30(16):3981-93.

98. Cheang MCU, Chia SK, Voduc D, Gao D, Leung S, Snider J, et al. Ki67 Index, HER2 Status, and Prognosis of Patients With Luminal B Breast Cancer. *Jnci-Journal of the National Cancer Institute*. 2009;101(10):736-50.
99. Ades F, Zardavas D, Bozovic-Spasojevic I, Pugliano L, Fumagalli D, de Azambuja E, et al. Luminal B Breast Cancer: Molecular Characterization, Clinical Management, and Future Perspectives. *Journal of Clinical Oncology*. 2014;32(25):2794.
100. Vargas-Rondón N, Villegas VE, Rondón-Lagos M. The role of chromosomal instability in cancer and therapeutic responses. *Cancers*. 2018;10(1).
101. Herschkowitz JI, He X, Fan C, Perou CM. The functional loss of the retinoblastoma tumour suppressor is a common event in basal-like and luminal B breast carcinomas. *Breast Cancer Research*. 2008;10(5):R75.
102. Millour J, Lam EW. FOXM1 is a transcriptional target of ERα and has a critical role in breast cancer endocrine sensitivity and resistance. *Breast Cancer Research*. 2010;12:S3-.
103. Goncalves R, Ma C, Luo J, Suman V, Ellis MJ. Use of neoadjuvant data to design adjuvant endocrine therapy trials for breast cancer. *Nature Reviews Clinical Oncology*. 2012;9(4):223-9.
104. Dowsett M, Smith IE, Ebbs SR, Dixon JM, Skene A, A'Hern R, et al. Prognostic value of Ki67 expression after short-term presurgical endocrine therapy for primary breast cancer. *J Natl Cancer Inst*. 2007;99(2):167-70.
105. Dowsett M, Ebbs SR, Dixon JM, Skene A, Griffith C, Boeddinghaus I, et al. Biomarker changes during neoadjuvant anastrozole, tamoxifen, or the combination:

- Influence of hormonal status and HER-2 in breast cancer - A study from the IMPACT trialists. *Journal of Clinical Oncology*. 2005;23(11):2477-92.
106. Hugh J, Hanson J, Cheang MCU, Nielsen TO, Perou CM, Dumontet C, et al. Breast Cancer Subtypes and Response to Docetaxel in Node-Positive Breast Cancer: Use of an Immunohistochemical Definition in the BCIRG 001 Trial. *J Clin Oncol*. 2009;27(8):1168-76.
107. Lonning PE. Poor-prognosis estrogen receptorpositive disease: present and future clinical solutions. *Therapeutic Advances in Medical Oncology*. 2012;4(3):127-37.
108. Prat A, Karginova O, Parker JS, Fan C, He X, Bixby L, et al. Characterization of cell lines derived from breast cancers and normal mammary tissues for the study of the intrinsic molecular subtypes. *Breast Cancer Res Treat*. 2013;142(2):237-55.
109. Liao X, Lu D, Wang N, Liu L, Wang Y, Li Y, et al. Estrogen receptor alpha mediates proliferation of breast cancer MCF-7 cells via a p21/PCNA/E2F1-dependent pathway. *Febs Journal*. 2014;281(3):927-42.
110. Moggs J, Murphy T, Lim F, Moore D, Stuckey R, Antrobus K, et al. Anti-proliferative effect of estrogen in breast cancer cells that re-express ER alpha is mediated by aberrant regulation of cell cycle genes. *J Mol Endocrinol*. 2005;34(2):535-51.
111. Zhao H, Yu J, Peltier CP, Davie JR. Elevated expression of the estrogen receptor prevents the down-regulation of p21(Waf1/Cip1) in hormone dependent breast cancer cells. *J Cell Biochem*. 2004;93(3):619-28.
112. Mangelsdorf DJ, Thummel C, Beato M, Herrlich P, Schutz G, Umesono K, et al. The Nuclear Receptor Superfamily - the 2nd Decade. *Cell*. 1995;83(6):835-9.

113. Pearce S, Jordan V. The biological role of estrogen receptors alpha and beta in cancer. *Critical Reviews in Oncology Hematology*. 2004;50(1):3-22.
114. Bondesson M, Hao R, Lin C, Williams C, Gustafsson J. Estrogen receptor signaling during vertebrate development. *Biochimica Et Biophysica Acta- Gene Regulatory Mechanisms*. 2015;1849(2):142-51.
115. Khalid AB, Krum SA. Estrogen receptors alpha and beta in bone. *Bone*. 2016;87:130-5.
116. Iorga A, Cunningham CM, Moazeni S, Ruffenach G, Umar S, Eghbali M. The protective role of estrogen and estrogen receptors in cardiovascular disease and the controversial use of estrogen therapy. *Biology of Sex Differences*. 2017;8:33.
117. National Center for Biotechnology Information [Internet]. 8600 Rockville Pike, Bethesda MD, 20894 USA: U.S. National Library of Medicine; 2018. Available from: <https://www.ncbi.nlm.nih.gov/>.
118. Warnmark A, Treuter E, Wright A, Gustafsson J. Activation functions 1 and 2 of nuclear receptors: Molecular strategies for transcriptional activation. *Molecular Endocrinology*. 2003;17(10):1901-9.
119. Ogawa S, Inoue S, Watanabe T, Hiroi H, Orimo A, Hosoi T, et al. The complete primary structure of human estrogen receptor β (hER β) and its heterodimerization with ER α in vivo and in vitro. *Biochem Biophys Res Commun*. 1998;243(1):122-6.
120. Hall J.M MDP. The Estrogen Receptor β -Isoform (ER β) of the Human Estrogen Receptor Modulates ER α Transcriptional Activity and Is a Key Regulator of the Cellular Response to Estrogens and Antiestrogens. *Endocrinology*. 1999;140:5566-5578.

121. Tan W, Li Q, Chen K, Su F, Song E, Gong C. Estrogen receptor beta as a prognostic factor in breast cancer patients: A systematic review and meta-analysis. *Oncotarget*. 2016;7(9):10373-85.
122. Iwase H, Zhang ZH, Omoto Y, Sugiura H, Yamashita H, Toyama T, et al. Clinical significance of the expression of estrogen receptors alpha and beta for endocrine therapy of breast cancer. *Cancer Chemother Pharmacol*. 2003;52:S34-8.
123. Kumar R, Zakharov MN, Khan SH, Miki R, Jang H, Toraldo G, et al. The dynamic structure of the estrogen receptor. *Journal of amino acids*. 2011;2011:812540-.
124. Metzger D, Ali S, Bornert JM, Chambon P. Characterization of the Amino-Terminal Transcriptional Activation Function of the Human Estrogen-Receptor in Animal and Yeast-Cells. *J Biol Chem*. 1995;270(16):9535-42.
125. Rogatsky I, Trowbridge JM, Garabedian MJ. Potentiation of human estrogen receptor alpha transcriptional activation through phosphorylation of serines 104 and 106 by the cyclin A-CDK2 complex. *J Biol Chem*. 1999;274(32):22296-302.
126. Kato S, Endoh H, Masuhiro Y, Kitamoto T, Uchiyama S, Sasaki H, et al. Activation of the Estrogen-Receptor through Phosphorylation by Mitogen-Activated Protein-Kinase. *Science*. 1995;270(5241):1491-4.
127. Dutertre M, Smith CL. Ligand-independent interactions of p160/steroid receptor coactivators and CREB-binding protein (CBP) with estrogen receptor-alpha: Regulation by phosphorylation sites in the A/B region depends on other receptor domains. *Molecular Endocrinology*. 2003;17(7):1296-314.

128. Kraus WL, McInerney EM, Katzenellenbogen BS. Ligand-dependent, transcriptionally productive association of the amino- and carboxyl-terminal regions of a steroid hormone nuclear receptor. *Proc Natl Acad Sci U S A.* 1995;92(26):12314-8.
129. Metivier R, Penot G, Flouriot G, Pakdel F. Synergism between ER alpha transactivation function 1 (AF-1) and AF-2 mediated by steroid receptor coactivator protein-1: Requirement for the AF-1 alpha-helical core and for a direct interaction between the N- and C-terminal domains. *Molecular Endocrinology.* 2001;15(11):1953-70.
130. Green S, Kumar V, Theulaz I, Wahli W, Chambon P. The N-terminal DNA-binding 'zinc finger' of the oestrogen and glucocorticoid receptors determines target gene specificity. *EMBO J.* 1988;7(10):3037-44.
131. Schwabe J, Chapman L, Finch J, Rhodes D. The Crystal-Structure of the Estrogen-Receptor Dna-Binding Domain Bound to Dna - how Receptors Discriminate between their Response Elements. *Cell.* 1993;75(3):567-78.
132. Schwabe JWR, Chapman L, Rhodes D. The Estrogen-Receptor Recognizes an Imperfectly Palindromic Response Element through an Alternative Side-Chain Conformation. *Structure.* 1995;3(2):201-13.
133. Chen DS, Pace PE, Coombes RC, Ali S. Phosphorylation of human estrogen receptor alpha by protein kinase A regulates dimerization. *Mol Cell Biol.* 1999;19(2):1002-15.

134. Nardulli AM, Grobner C, Cotter D. Estrogen Receptor-Induced Dna Bending - Orientation of the Bend and Replacement of an Estrogen Response Element with an Intrinsic Dna Bending Sequence. *Molecular Endocrinology*. 1995;9(8):1064-76.
135. Kim J, deHaan G, Nardulli AM, Shapiro DJ. Prebending the estrogen response element destabilizes binding of the estrogen receptor DNA binding domain. *Mol Cell Biol*. 1997;17(6):3173-80.
136. Ylikomi T, Bocquel MT, Berry M, Gronemeyer H, Chambon P. Cooperation of proto-signals for nuclear accumulation of estrogen and progesterone receptors. *EMBO J*. 1992;11(10):3681-94.
137. Picard D, Kumar V, Chambon P, Yamamoto KR. Signal transduction by steroid hormones: Nuclear localization is differentially regulated in estrogen and glucocorticoid receptors. *Mol Biol Cell*. 1990;1(3):291-9.
138. Wang C, Fu M, Angeletti RH, Siconolfi-Baez L, Reutens AT, Albanese C, et al. Direct Acetylation of the Estrogen Receptor a Hinge Region by p300 Regulates Transactivation and Hormone Sensitivity. *J Biol Chem*. 2001;276(21):18375-83.
139. Sentis S, Le Romancer M, Bianchin C, Rostan M-, Corbo L. Sumoylation of the estrogen receptor β hinge region regulates its transcriptional activity. *Mol Endocrinol*. 2005;19(11):2671-84.
140. Subramanian K, Jia D, Kapoor-Vazirani P, Powell DR, Collins RE, Sharma D, et al. Regulation of Estrogen Receptor a by the SET7 Lysine Methyltransferase. *Mol Cell*. 2008;30(3):336-47.

141. Berry NB, Fan M, Nephew KP. Estrogen receptor-alpha hinge-region lysines 302 and 303 regulate receptor degradation by the proteasome. *Molecular Endocrinology*. 2008;22(7):1535-51.
142. Zwart W, De Leeuw R, Rondaij M, Neefjes J, Mancini MA, Michalides R. The hinge region of the human estrogen receptor determines functional synergy between AF-1 and AF-2 in the quantitative response to estradiol and tamoxifen. *J Cell Sci*. 2010;123(8):1253-61.
143. Ruff M, Gangloff M, Wurtz JM, Moras D. Estrogen receptor transcription and transactivation Structure-function relationship in DNA- and ligand-binding domains of estrogen receptors. *Breast Cancer Research*. 2000;2(5):353-9.
144. Brzozowski AM, Pike ACW, Dauter Z, Hubbard RE, Bonn T, Engstrom O, et al. Molecular basis of agonism and antagonism in the oestrogen receptor. *Nature*. 1997;389(6652):753-8.
145. Shiau AK, Barstad D, Loria PM, Cheng L, Kushner PJ, Agard DA, et al. The structural basis of estrogen receptor/coactivator recognition and the antagonism of this interaction by tamoxifen. *Cell*. 1998;95(7):927-37.
146. Kumar V, Chambon P. The estrogen receptor binds tightly to its responsive element as a ligand-induced homodimer. *Cell*. 1988;55(1):145-56.
147. Peters GA, Khan SA. Estrogen receptor domains E and F: Role in dimerization and interaction with coactivator RIP-140. *Mol Endocrinol*. 1999;13(2):286-96.
148. Montano MM, Muller V, Trobaugh A, Katzenellenbogen BS. The Carboxy-Terminal F-Domain of the Human Estrogen-Receptor - Role in the Transcriptional

- Activity of the Receptor and the Effectiveness of Antiestrogens as Estrogen Antagonists. *Molecular Endocrinology*. 1995;9(7):814-25.
149. Schwartz JA, Zhong L, Deighton-Collins S, Zhao CQ, Skafar DF. Mutations targeted to a predicted helix in the extreme carboxyl-terminal region of the human estrogen receptor-alpha alter its response to estradiol and 4-hydroxytamoxifen. *J Biol Chem*. 2002;277(15):13202-9.
150. Koide A, Zhao C, Naganuma M, Abrams J, Deighton-Collins S, Skafar DF, et al. Identification of regions within the F domain of the human estrogen receptor alpha that are important for modulating transactivation and protein-protein interactions. *Molecular Endocrinology*. 2007;21(4):829-42.
151. King WJ, Greene GL. Monoclonal-Antibodies Localize Estrogen-Receptor in the Nuclei of Target-Cells. *Nature*. 1984;307(5953):745-7.
152. Welshons WV, Lieberman ME, Gorski J. Nuclear localization of unoccupied oestrogen receptors. *Nature*. 1984;307(5953):747-9.
153. Htun H, Holth LT, Walker D, Davie JR, Hager GL. Direct visualization of the human estrogen receptor alpha reveals a role for ligand in the nuclear distribution of the receptor. *Mol Biol Cell*. 1999;10(2):471-86.
154. Knoblauch R, Garabedian MJ. Role for Hsp90-associated cochaperone p23 in estrogen receptor signal transduction. *Mol Cell Biol*. 1999;19(5):3748-59.
155. Pratt W. The hsp90-based chaperone system: Involvement in signal transduction from a variety of hormone and growth factor receptors. *Proceedings of the Society for Experimental Biology and Medicine*. 1998;217(4):420-34.

156. Gruber CJ, Gruber DM, Gruber IML, Wieser F, Huber JC. Anatomy of the estrogen response element. *Trends in Endocrinology and Metabolism*. 2004;15(2):73-8.
157. Carroll JS, Meyer CA, Song J, Li W, Geistlinger TR, Eeckhoute J, et al. Genome-wide analysis of estrogen receptor binding sites. *Nat Genet*. 2006;38(11):1289-97.
158. Li XM, Onishi Y, Kuwabara K, Rho JY, Wada-Kiyama Y, Sakuma Y, et al. Ligand-dependent transcriptional enhancement by DNA curvature between two half motifs of the estrogen response element in the human estrogen receptor alpha gene. *Gene*. 2002;294(1-2):279-90.
159. Joshi SR, Ghattamaneni RB, Scovell WM. Expanding the Paradigm for Estrogen Receptor Binding and Transcriptional Activation. *Molecular Endocrinology*. 2011;25(6):980-94.
160. Caizzi L, Ferrero G, Cutrupi S, Cordero F, Ballare C, Miano V, et al. Genome-wide activity of unliganded estrogen receptor-alpha in breast cancer cells. *Proc Natl Acad Sci U S A*. 2014;111(13):4892-7.
161. Metivier R, Penot G, Carmouche RP, Hubner MR, Reid G, Denger S, et al. Transcriptional complexes engaged by apo-estrogen receptor-alpha isoforms have divergent outcomes. *EMBO J*. 2004;23(18):3653-66.
162. Mak HY, Hoare S, Henttu PMA, Parker MG. Molecular determinants of the estrogen receptor-coactivator interface. *Mol Cell Biol*. 1999;19(5):3895-903.
163. Yi P, Wang Z, Feng Q, Pintilie GD, Foulds CE, Lanz RB, et al. Structure of a Biologically Active Estrogen Receptor-Coactivator Complex on DNA. *Mol Cell*. 2015;57(6):1047-58.

164. Varlakhanova N, Snyder C, Jose S, Hahm JB, Privalsky ML. Estrogen receptors recruit SMRT and N-CoR corepressors through newly recognized contacts between the corepressor N terminus and the receptor DNA binding domain. *Mol Cell Biol.* 2010;30(6):1434-45.
165. Eberharter A, Becker PB. Histone acetylation: A switch between repressive and permissive chromatin. Second in review on chromatin dynamics. *EMBO Rep.* 2002;3(3):224-9.
166. Kalaitzidis D, Gilmore TD. Transcription factor cross-talk: the estrogen receptor and NF-kappa B. *Trends in Endocrinology and Metabolism.* 2005;16(2):46-52.
167. Safe S, Kim K. Non-classical genomic estrogen receptor (ER)/specificity protein and ER/activating protein-1 signaling pathways. *J Mol Endocrinol.* 2008;41(5-6):263-75.
168. Kao J, Salari K, Bocanegra M, Choi Y, Girard L, Gandhi J, et al. Molecular Profiling of Breast Cancer Cell Lines Defines Relevant Tumor Models and Provides a Resource for Cancer Gene Discovery. *Plos One.* 2009;4(7):e6146.
169. Ross-Innes CS, Stark R, Teschendorff AE, Holmes KA, Ali HR, Dunning MJ, et al. Differential oestrogen receptor binding is associated with clinical outcome in breast cancer. *Nature.* 2012;481(7381):389-93.
170. Metivier R, Penot G, Hubner MR, Reid G, Brand H, Kos M, et al. Estrogen receptor-alpha directs ordered, cyclical, and combinatorial recruitment of cofactors on a natural target promoter. *Cell.* 2003;115(6):751-63.
171. Shang Y, Hu X, DiRenzo J, Lazar MA, Brown M. Cofactor dynamics and sufficiency in estrogen receptor-regulated transcription. *Cell.* 2000;103(6):843-52.

172. Foulds CE, Feng Q, Ding C, Bailey S, Hunsaker TL, Malovannaya A, et al. Proteomic Analysis of Coregulators Bound to ER alpha on DNA and Nucleosomes Reveals Coregulator Dynamics. *Mol Cell*. 2013;51(2):185-99.
173. Xu J, Wu R-, O'Malley BW. Normal and cancer-related functions of the p160 steroid receptor co-activator (SRC) family. *Nat Rev Cancer*. 2009;9(9):615-30.
174. Ogryzko VV, Schiltz RL, Russanova V, Howard BH, Nakatani Y. The transcriptional coactivators p300 and CBP are histone acetyltransferases. *Cell*. 1996;87(5):953-9.
175. Nawaz Z, Lonard D, Dennis A, Smith C, O'Malley B. Proteasome-dependent degradation of the human estrogen receptor. *Proc Natl Acad Sci U S A*. 1999;96(5):1858-62.
176. Lonard D, Nawaz Z, Smith C, O'Malley B. The 26S proteasome is required for estrogen receptor-alpha and coactivator turnover and for efficient estrogen receptor-alpha transactivation. *Mol Cell*. 2000;5(6):939-48.
177. Klinge CM. Estrogen receptor interaction with co-activators and co-repressors. *Steroids*. 2000;65(5):227-51.
178. Glass CK, Rosenfeld MG. The coregulator exchange in transcriptional functions of nuclear receptors. *Genes Dev*. 2000;14(2):121-41.
179. Hu X, Lazar MA. The CoRNR motif controls the recruitment of corepressors by nuclear hormone receptors. *Nature*. 1999;402(6757):93-6.
180. Smith CL, Nawaz Z, O'Malley BW. Coactivator and corepressor regulation of the agonist/antagonist activity of the mixed antiestrogen, 4-hydroxytamoxifen. *Mol Endocrinol*. 1997;11(6):657-66.

181. Lavinsky RM, Jepsen K, Heinzl T, Torchia J, Mullen TM, Schiff R, et al. Diverse signaling pathways modulate nuclear receptor recruitment of N-CoR and SMRT complexes. *Proc Natl Acad Sci U S A*. 1998;95(6):2920-5.
182. Girault I, Lerebours F, Amarir S, Tozlu S, Tubiana-Hulin M, Lidereau R, et al. Expression analysis of estrogen receptor alpha coregulators in breast carcinoma: Evidence that NCOR1 expression is predictive of the response to tamoxifen. *Clinical Cancer Research*. 2003;9(4):1259-66.
183. Heldring N, Pike A, Andersson S, Matthews J, Cheng G, Hartman J, et al. Estrogen receptors: How do they signal and what are their targets. *Physiol Rev*. 2007;87(3):905-31.
184. Oesterreich S, Deng W, Jiang S, Cui X, Ivanova M, Schiff R, et al. Estrogen-mediated down-regulation of E-cadherin in breast cancer cells. *Cancer Res*. 2003;63(17):5203-8.
185. Fernandes I, Bastien Y, Wai T, Nygard K, Lin R, Cormier O, et al. Ligand-dependent nuclear receptor corepressor LCoR functions by histone deacetylase-dependent and -independent mechanisms. *Mol Cell*. 2003;11(1):139-50.
186. Vo N, Fjeld C, Goodman RH. Acetylation of nuclear hormone receptor-interacting protein RIP140 regulates binding of the transcriptional corepressor CtBP. *Mol Cell Biol*. 2001;21(18):6181-8.
187. Chinnadurai G. CtBP, an unconventional transcriptional corepressor in development and oncogenesis. *Mol Cell*. 2002;9(2):213-24.
188. Montano MM, Ekena K, Delage-Mourroux R, Chang WR, Martini P, Katzenellenbogen BS. An estrogen receptor-selective coregulator that potentiates the

- effectiveness of antiestrogens and represses the activity of estrogens. *Proc Natl Acad Sci U S A*. 1999;96(12):6947-52.
189. Kurtev V, Margueron R, Kroboth K, Ogris E, Cavailles V, Seiser C. Transcriptional regulation by the repressor of estrogen receptor activity via recruitment of histone deacetylases. *J Biol Chem*. 2004;279(23):24834-43.
190. Kawai H, Li H, Avraham S, Jiang S, Avraham H. Overexpression of histone deacetylase HDAC1 modulates breast cancer progression by negative regulation of estrogen receptor alpha. *International Journal of Cancer*. 2003;107(3):353-8.
191. Yang X, Ferguson A, Nass S, Phillips D, Butash K, Wang S, et al. Transcriptional activation of estrogen receptor alpha in human breast cancer cells by histone deacetylase inhibition. *Cancer Res*. 2000;60(24):6890-4.
192. Sharma D, Saxena N, Davidson N, Vertino P. Restoration of tamoxifen sensitivity in estrogen receptor-negative breast cancer cells: Tamoxifen-bound reactivated ER recruits distinctive corepressor complexes. *Cancer Res*. 2006;66(12):6370-8.
193. Hodges-Gallagher L, Valentine CD, El Bader S, Kushner PJ. Inhibition of histone deacetylase enhances the anti-proliferative action of antiestrogens on breast cancer cells and blocks tamoxifen-induced proliferation of uterine cells. *Breast Cancer Res Treat*. 2007;105(3):297-309.
194. Raha P, Thomas S, Thurn KT, Park J, Munster PN. Combined histone deacetylase inhibition and tamoxifen induces apoptosis in tamoxifen-resistant breast cancer models, by reversing Bcl-2 overexpression. *Breast Cancer Research*. 2015;17:26.

195. Restall C, Doherty J, Bin Liu H, Genovese R, Paiman L, Byron KA, et al. A novel histone deacetylase inhibitor augments tamoxifen-mediated attenuation of breast carcinoma growth. *International Journal of Cancer*. 2009;125(2):483-7.
196. Munster PN, Thurn KT, Thomas S, Raha P, Lacevic M, Miller A, et al. A phase II study of the histone deacetylase inhibitor vorinostat combined with tamoxifen for the treatment of patients with hormone therapy-resistant breast cancer. *Br J Cancer*. 2011;104(12):1828-35.
197. Mueller BM, Jana L, Kasajima A, Lehmann A, Prinzler J, Budczies J, et al. Differential expression of histone deacetylases HDAC1, 2 and 3 in human breast cancer - overexpression of HDAC2 and HDAC3 is associated with clinicopathological indicators of disease progression. *BMC Cancer*. 2013;13:215.
198. Krusche C, Wulfing P, Kersting C, Vloet A, Bocker W, Kiesel L, et al. Histone deacetylase-1 and-3 protein expression in human breast cancer: a tissue microarray analysis. *Breast Cancer Res Treat*. 2005;90(1):15-23.
199. Seo J, Min SK, Park H, Kim DH, Kwon MJ, Kim LS, et al. Expression of Histone Deacetylases HDAC1, HDAC2, HDAC3, and HDAC6 in Invasive Ductal Carcinomas of the Breast. *Journal of Breast Cancer*. 2014;17(4):323-31.
200. Eom M, Oh SS, Lkhagvadorj S, Han A, Park KH. HDAC1 Expression in Invasive Ductal Carcinoma of the Breast and Its Value as a Good Prognostic Factor. *Korean Journal of Pathology*. 2012;46(4):311-7.
201. Dixon JR, Selvaraj S, Yue F, Kim A, Li Y, Shen Y, et al. Topological domains in mammalian genomes identified by analysis of chromatin interactions. *Nature*. 2012;485(7398):376-80.

202. Hansen AS, Cattoglio C, Darzacq X, Tjian R. Recent evidence that TADs and chromatin loops are dynamic structures. *Nucleus*. 2018;9(1):20-32.
203. Le Dily F, Bau D, Pohl A, Vicent GP, Serra F, Soronellas D, et al. Distinct structural transitions of chromatin topological domains correlate with coordinated hormone-induced gene regulation. *Genes Dev*. 2014;28(19):2151-62.
204. Fullwood MJ, Liu MH, Pan YF, Liu J, Xu H, Bin Mohamed Y, et al. An oestrogen-receptor-alpha-bound human chromatin interactome. *Nature*. 2009;462(7269):58-64.
205. Carroll JS, Liu XS, Brodsky AS, Li W, Meyer CA, Szary AJ, et al. Chromosome-wide mapping of estrogen receptor binding reveals long-range regulation requiring the forkhead protein FoxA1. *Cell*. 2005;122(1):33-43.
206. Liu Z, Merkurjev D, Yang F, Li W, Oh S, Friedman MJ, et al. Enhancer Activation Requires trans-Recruitment of a Mega Transcription Factor Complex. *Cell*. 2014;159(2):358-73.
207. Liu MH, Cheung E. Estrogen receptor-mediated long-range chromatin interactions and transcription in breast cancer. *Mol Cell Endocrinol*. 2014;382(1):624-32.
208. Ross-Innes CS, Brown GD, Carroll JS. A co-ordinated interaction between CTCF and ER in breast cancer cells. *BMC Genomics*. 2011;12.
209. Osmanbeyoglu HU, Lu KN, Oesterreich S, Day RS, Benos PV, Coronello C, et al. Estrogen represses gene expression through reconfiguring chromatin structures. *Nucleic Acids Res*. 2013;41(17):8061-71.
210. Fowler A, Solodin N, Preisler-Mashey M, Zhang P, Lee A, Alarid E. Increases in estrogen receptor-alpha concentration in breast cancer cells promote serine

- 118/104/106-independent AF-1 transactivation and growth in the absence of estrogen.
Faseb Journal. 2004;18(1):81-93.
211. Cancer Genetics [Internet]: MIT; 2016. Available from:
<http://www.cubocube.com/dashboard.php?a=1643&c=1>.
212. Breast anatomy and how breast cancer starts [Internet]. Available from:
<https://nbcf.org.au/about-national-breast-cancer-foundation/about-breast-cancer/what-you-need-to-know/breast-anatomy-cancer-starts/>.
213. Normal Histology [Internet]. Available from:
<http://www.ezpath.org/gallery/#/new-gallery-50/>.
214. ESR1 [Internet].; 2017. Available from:
<https://www.proteinatlas.org/ENSG00000091831-ESR1/tissue/breast#img>.

**Chapter 2: Increased ER expression regulates an anti-proliferative response to
estrogen**

2.1 Introduction

The differential hormonal response is a key clinical difference between the luminal subtypes. As described in chapter 1, luminal A patients have the highest levels of ER expression and an excellent response to tamoxifen, whereas luminal B patients do poorly with tamoxifen alone and require additional chemotherapy (1, 2). There is growing clinical evidence that E2 is growth suppressive for some ER+ breast cancers (3, 4) and that tamoxifen itself has estrogenic properties (5, 6). This raises the possibility that the differential response to tamoxifen between the luminal subtypes may actually represent a differential response to E2 that is mediated by ER. Currently, the study of the pro- and anti-proliferative effects of E2 on the two luminal subtypes is hindered by the available ER+ *in vitro* models.

Recent work by Prat et al. (2013) compared microarrays of 93 cell lines including MCF-7 against 320 breast tumors and determined that all ER+ breast cancer cell lines represent the luminal B subtype (7). MCF-7 cells are the most commonly used model for ER+ breast cancer and consistently mark as luminal B (8, 9). MCF-7 cells have a well-established proliferative response to E2 which is mediated by ER through its regulation of proliferation and cell cycle proteins (10-12). This pro-proliferative effect of E2 promoted the use of anti-estrogen therapies, such as tamoxifen, as the main strategy for treating all ER+ patients. However, the absence of luminal A cell lines means that the effects of estrogens as well as anti-estrogens on proliferation and the cell cycle has not been explored *in vitro* in luminal A tumors.

Progression through the cell cycle lasts from 10-48 hours and requires passage through four major phases: an initial Gap 1 (G1) phase, the DNA-synthesis phase (S phase), a Gap

2 (G2) phase, and then the final mitotic phase (M phase) (Figure 2.1) (13). A cell's progression into each phase is mediated by checkpoints which monitor the DNA integrity and ensure the current phase was successfully completed prior to progression to subsequent phases. Cells with DNA damage, unreplicated DNA or issues with the cell cycle machinery will be arrested at these checkpoints until the cell can be repaired or the cell undergoes apoptosis (14). The cell cycle checkpoints are tightly regulated by specific cyclin proteins which function through interactions with cyclin dependent kinases (CDKs) (Figure 2.1) (13). The G1 checkpoint is regulated by the D and E cyclins (Figure 2.1). Cyclin D/CDK4/6 complexes are present in the early G1 phase and phosphorylate the retinoblastoma protein (Rb), a tumor suppressor which binds the E2F transcription factors and prevents their regulation of cell cycle and proliferation genes (15, 16). In the later part of G1 Cyclin E/CDK2 complexes will further phosphorylate Rb and this hyperphosphorylated form of Rb releases E2F (16). The release of E2F allows this transcription factor to bind the promoter regions of proliferation and cell cycle associated genes and the translation of the corresponding proteins enables the cell to progress into S phase (17). Cyclin A/CDK2 complexes are abundant during early S phase and then cyclin A complexes with CDK1 in late S phase and enables progression through the S/G2 checkpoint (Figure 2.1). The cyclin A/CDK1 complexes are also present throughout the G2 phase and may be involved in regulation of the G2/M checkpoint along with the major regulators of the G2/M checkpoint, the cyclin B/CDK1 complexes (Figure 2.1) (15, 18). Both the cyclin A/CDK and cyclin B/CDK complexes function throughout the cell cycle by maintaining Rb in its hyperphosphorylated state thereby enabling E2F mediated transcription (15).

The activity of cyclin/CDK complexes is regulated throughout the cell cycle by interactions with two families of cyclin dependent kinase inhibitors (CKDIs) (Figure 2.1) (15). The inhibitor of CDK4 (INK4) CDKI family contains the p15, p16, p18 and p19 proteins which specifically inactivate CDK4 and 6 (15). Whereas the Cip/Kip family of CDKIs which includes the p21, p27 and p57 proteins can act as broad inhibitors and inactivate both cyclins and CDKs (15). Throughout the cell cycle p21 inactivates cyclin E/CDK2 complexes and prevents Rb phosphorylation. At increased levels p21 can also inactivate the cyclin D/CDK4/6 complexes in early G1 phase (Figure 2.2) (12). Cyclin D/CDK4/6 complexes can sequester p21 away from the cyclin E/CDK2 complexes, enabling cyclin E/CDK2 phosphorylation of Rb and progression into S phase (12). This mechanism of p21-sequestering has been shown to regulate the E2 induced proliferation in MCF-7 cells (19). More recent studies have shown that the proliferative effect of E2 in MCF-7 cells is regulated by a direct, ER-mediated down-regulation of p21 expression which promotes increased activity through a cyclin D/CDK/Rb/E2F1 pathway (Figure 2.2) (11, 19). Interestingly, increased ER expression in breast cancer cell lines leads to a G1 phase arrest in the presence of E2 which is mediated through up-regulation of p21 and its downstream effect on E2F (Figure 2.2) (20-23). Thus, the level of ER expression can mediate a differential proliferative response to E2 in a luminal cell line.

Luminal A tumors show the highest level of ER expression (24), and clinical data have shown patients with the highest levels of ER have the greatest anti-proliferative response to tamoxifen (25). Luminal A tumors occur most frequently after the menopause when there is minimal serum E2 available for tamoxifen to antagonize (26, 27). When the therapeutic role for E2 discussed in section 1.3.2.3.5 is considered the clinical data suggest that the

anti-proliferative effect of tamoxifen may be regulated by its weak estrogenic properties rather than its antagonistic function. For this work, the anti-proliferative effects of tamoxifen seen in patients is assumed to be mediated through its weak estrogenic properties. Therefore, E2 rather than tamoxifen will be used to simulate the response to hormone therapies seen in ER+ breast cancer patients. In this chapter, ER expression will be increased and the consequences for the proliferative response to E2 will be examined. The hypothesis that increased ER expression will promote an anti-proliferative response to E2 that is mediated through direct regulation of p21 will be examined. Correlation of these findings with published clinical data will enable validation of the usefulness of this model for further study of the mechanism(s) which regulate hormone response in ER+ tumors.

2.2 Materials and methods

2.2.1 Reagents

Dulbecco's Modified Eagle Medium (DMEM), Minimum Essential Medium (MEM), fetal bovine serum (FBS), Geneticin (G418), MEM-no phenol red, and radioimmunoprecipitation assay (RIPA) buffer, 100X Halt™ Protease Inhibitor Cocktail (PIC), Qubit™ protein assay kit, Qubit™ high sensitivity RNA assay kit, Qubit™ dsDNA high sensitivity assay kit, and protein A Dynabeads were purchased from Thermo Fisher Scientific (Waltham, MA). Bovine insulin, puromycin, charcoal-stripped FBS, β -estradiol (E2), actinomycin D, bovine serum albumin (BSA), ammonium persulfate (APS), tetramethylethylenediamine (TEMED) and propidium iodide (PI) were purchased from Sigma-Aldrich Canada Co. (Oakville, ON). The TACS® MTT cell proliferation assay kit was purchased from Trevigen (Gaithersburg, MD). Phosphate buffered saline (PBS) and tris-buffered saline (TBS) were purchased from the Department of Experimental Oncology

(University of Alberta). Lenti-X HTX packaging system, Lenti-X 293T cells, Lenti-X GoStix, Tet-System approved FBS and doxycycline were purchased from Clontech Laboratories, Inc (Mountain View, CA). The 1.5 M Tris-HCl pH 8.8, 0.5 M Tris-HCl pH 6.8 and 30% acrylamide/Bis (37.5:1) were purchased from Bio-rad Laboratories (Hercules, CA). The antibodies used for western blot and ChIP experiments are listed in Table 2.1.

2.2.2 Development of stable MCF7-EM and MCF7-ER transfectants

The MCF7-EM and MCF7-ER stable transfectants used in this study were generated previously in the Hugh lab by Xiuying Hu. The methods for this work are outlined in Appendix A.

2.2.3 Cell culture and E2 treatment

The Lenti-X 293T cells were maintained in DMEM supplemented with 10% Tet-free FBS. MCF-7 parental cells were obtained from American Type Culture Collection (ATCC) and were maintained in MEM containing 10% FBS and 10 µg/ml bovine insulin. Stably transduced MCF-7 transfectants were maintained in selection media containing 10% Tet-system approved FBS, 10 µg/ml bovine insulin, 500 µg/ml G418 and 1µg/ml puromycin. Cell line authentication was confirmed by The Centre for Applied Genomics (TCAG) Genetic Analysis Facility through short tandem repeat (STR) profiling using Promega's GenePrint® 10 System.

The standard experimental treatment conditions were determined through collaborations between Judith Hugh, Lacey Haddon and Xiuying Hu. For all experiments the cells were first rinsed with PBS then adapted in phenol red-free MEM containing 10% charcoal-stripped FBS, 10 µg/ml bovine insulin, 500 µg/ml G418 and 1µg/ml puromycin for three days. On day four the adaptation media was removed, and the MCF7-EM and

MCF7-ER cells were induced with 0.5 µg/ml doxycycline for 24 hours. After this incubation, the doxycycline media was removed, and the cells were treated with adaptation media containing either 10 nM E2 dissolved in 100% ethanol or vehicle control (100% ethanol) for the times indicated. The four major experimental conditions are outline in Table 2.3. For transcriptional inhibitor experiments after 24 hours of doxycycline cells were pretreated with 1 µg/µl of actinomycin D for 1 hour and then treated with 10 nM E2 or ethanol control containing 1 µg/µl of actinomycin D for 24 hours.

2.2.4 Western Blot Analysis

Western blot experiments for cell cycle proteins were designed through collaborations between Judith Hugh, Lacey Haddon, Xiuying Hu and Brittney Loney and experiments were carried out by Brittney Loney. Western blot experiments for MCF7-ERmDBD doxycycline titration, PARP cleavage and cytochrome C protein were designed through collaborations between Judith Hugh, Lacey Haddon and Xiuying Hu and were carried out by Xiuying Hu in the Hugh lab. Western blot experiments for ER protein were designed by Judith Hugh and Lacey Haddon and were carried out by Lacey Haddon. For these experiments, cells were placed on ice and rinsed once with cold PBS then lysed in RIPA buffer supplemented with fresh 1X PIC. Protein concentration was determined using the Qubit 3.0 protein analysis kit. For mitochondrial fractionation experiments cells were lysed in digitonin lysis buffer (75 mM NaCl, 1 mM NaH₂PO₄, 8 mM Na₂HPO₄, 250 mM sucrose, 0.2 mg/ml digitonin) and centrifuged at 14,000 rpm for 5 minutes. The supernatant was kept as a cytosolic fraction and the pellet was resuspended in Triton X-100 lysis buffer (0.1% Triton X-100, 25 mM Tris PH 8.0) and kept as the mitochondrial fraction. For all Western blot experiments 2X sample buffer (4% SDS, 10% β-mercaptoethanol, 20%

glycerol, 0.125 M Tris-HCl pH 6.8, and 0.004% bromophenol blue) was added to the protein lysate at a 1X final concentration and samples were denatured by boiling at 95°C for 10 minutes. Equal concentrations of denatured lysates were loaded onto a 10% SDS-polyacrylamide separation gel (375 mM Tris-HCl pH 8.8, 10% acrylamide/Bis (37.5:1), 0.1% SDS, 0.05% APS, 0.05% TEMED) with a 4% stacking layer (125 mM Tris-HCl pH 6.8, 4% acrylamide/Bis (37.5:1), 0.1% SDS, 0.05% APS, and 0.2% TEMED). Proteins were separated at 150V for 1 hour by SDS-PAGE and then transferred to 0.45 µm nitrocellulose membranes. Membranes were blocked in 1% BSA dissolved in 1X TBS with 0.1% Tween20 (TBST) for 1 hour at room temperature. Membranes were incubated at 4°C overnight with primary antibodies diluted to the recommended concentrations in 1X TBST. The next day membranes were rinsed four times with 1X TBST followed by 1-hour incubation with fluorescently labelled secondary antibody diluted 1:20,000 in TBST. Membranes were scanned with Odyssey Infrared Imaging System (LI-COR Bioscience).

2.2.5 Densitometry analysis

Densitometry analysis for estrogen receptor protein was done by Lacey Haddon and measurements for cell cycle proteins were done by Brittney Loney. Files obtained from the Odyssey Infrared Imaging System were analyzed using Image Studio Lite (version 5.2). The fluorescent tags on the secondary antibodies enabled simultaneous measurements of membranes in the red and green fluorescent channels. Fluorescence intensity values were obtained from each channel by using the shape tool to draw a rectangle around the protein bands with the appropriate molecular weight. These fluorescence values were exported to Excel for further analysis. The relative protein expression for each sample was calculated

by dividing the intensity values for the protein of interest to the actin loading control associated with that sample.

2.2.6 Flow Cytometry Analysis

All flow cytometry experiments were designed through collaborations between Judith Hugh, Lacey Haddon and Xiuying Hu and were conducted by Xiuying Hu in the Hugh lab. MCF7-EM and MCF7-ER cells were prepared as described in section 2.2.5 and treated with 10 nM E2 or ethanol control for 24 hours. After treatment, cells were washed with 1X PBS, then trypsinized and centrifuged at 1,400 rpm for 5 minutes at room temperature. The cell pellets were washed once with PBS then resuspended in 500 μ l PBS. Cells were fixed with 70% ethanol and stained with propidium iodide (10 μ g/ml) for 30 minutes at room temperature. Cell cycle profiles were measured with BD LSR Fortessa Special Order Research Product (SORP) (BD Biosciences) and analyzed using ModFit LT software. Flow cytometry experiments were done in triplicate.

2.2.7 Cell Viability Assay (MTT)

The cell viability experiments were designed and performed by Lacey Haddon. MCF7-EM, MCF7-ER, and MCF7-ERmDBD cells were plated at 5×10^3 cells/ml in a 96-well plate and adapted in estrogen-free media as described in section 2.2.5. MCF7-EM and MCF7-ER cells were induced with 0.5 μ g/ml doxycycline and MCF7-ERmDBD cells were induced with 2 μ g/ml doxycycline. After 24 hours, each MCF-7 transfectant had three technical replicates treated with 10 nM E2 or ethanol control and incubated at 37°C and 5% CO₂ for five days. Cell viability was assessed with TACS MTT assay (Trevigen) as per manufacturer's protocol. Absorbance values were measured with the FLUOStar Omega microplate reader (BMG Labtech). All MTT experiments were done in triplicate

2.2.8 Quantitative reverse-transcription PCR (RT-qPCR)

The RT-qPCR experiments were designed and performed by Lacey Haddon. Total RNA was extracted from MCF7-EM and MCF7-ER cells treated with vehicle control or 10 nM E2 for 24 hours using the NucleoSpin RNA extraction kit, which included a DNase digestion step to remove potential contaminating DNA (Macherey-Negel). Reverse transcription followed by direct SYBR-green qPCR amplification was facilitated by the Power SYBR Green RNA-to-CT 1-Step Kit (Applied Biosystems). Commercially designed Taqman gene expression assays (Applied Biosystems) were purchased to measure the expression of genes of interest as well as three housekeeping genes: *PUM1*, *TBP*, and *RPL13A*. Two technical replicates were run for each experimental condition. Three biological replicates were done for each experiment.

2.2.9 Chromatin Immunoprecipitation (ChIP)

ChIP experiments were designed by Dr. Judith Hugh and Lacey Haddon and performed by Lacey Haddon in the Hugh lab. ChIP was performed on MCF7-EM and MCF7-ER cells treated with ethanol control or 10 nM E2 for 1 hour. Cell monolayers were crosslinked with 1% formaldehyde for 10 minutes at room temperature and then quenched with 0.125 M glycine. Cells were rinsed twice with ice cold PBS + PIC and then scraped into 15 ml tubes and centrifuged at 3,000 rpm for 5 minutes at room temperature. The PBS was aspirated, and the cell pellets were lysed in ChIP lysis buffer (5 mM PIPES, 85 mM KCl, 0.5% IGEPAL + PIC) followed by centrifugation at 3,000 rpm for 5 minutes at 4°C. The cell pellet was resuspended in nuclei lysis buffer (50 mM Tris-HCl pH 8.0, 10 mM EDTA pH 8.0, 1% SDS + PIC), then sonicated on ice 30X at 40% amplitude for 20 seconds on/30 seconds rest followed by centrifugation at 14,000 rpm for 10 minutes at 4°C.

Supernatants were diluted 1:10 in ChIP dilution buffer (0.01% SDS, 1.1% Triton X-100, 1.2 mM EDTA pH 8.0, 16.7 mM Tris-HCl pH 8.0, 167 mM NaCl + PIC) and a 1% volume was saved as input. Diluted lysates were pre-cleared with 1.5 mg protein A Dynabeads then incubated with 10 µg ER polyclonal antibody (HC-20-discontinued) on rotation at 4°C overnight. Immunoprecipitates were incubated with 1.5 mg protein A Dynabeads on rotation for 2 hours at 4°C, then washed twice with the following buffers: ChIP low salt buffer (0.1% SDS, 1% Triton X-100, 2 mM EDTA pH 8.0, 150 mM NaCl and 20 mM Tris-HCl pH 8.0), ChIP high salt buffer (0.1% SDS, 1% Triton X-100, 2 mM EDTA pH 8.0, 500 mM NaCl and 20 mM Tris-HCl pH 8.0), ChIP LiCl wash buffer (0.25 M LiCl, 1% IGEPAL, 1% sodium deoxycholate, 10 mM Tris-HCl pH 8.0 and 1 mM EDTA pH 8.0), and ChIP TE buffer (1 mM EDTA pH 8.0 and 10 mM Tris-HCl pH 8.0). Antibody-protein complexes were eluted in ChIP elution buffer (1% SDS and 100 mM NaHCO₃) at 65°C for 40 minutes, then 0.3 M NaCl was added and samples (including the input) were incubated at 65°C overnight (<18 hours) to reverse the formaldehyde crosslinks. The next day a 1:5 volume of 5x proteinase K buffer (50 mM Tris-HCl pH 7.5, 25 mM EDTA, and 1.25% SDS) along with 40 µg/ml proteinase K was added and the samples were incubated at 45°C for 2 hours, followed by incubation with 20 µg/ml RNase A at 37°C for 30 minutes. DNA was purified with the ThermoFisher PCR purification Kit (K0702) and then quantified using the Qubit™ high sensitivity dsDNA reagents.

2.2.10 ChIP Quality Checks (QC)

The ChIP QCs were performed by Lacey Haddon. An initial check of DNA shearing was done by loading 10 µl of the supernatant obtained after sonication on a 1.5% agarose gel. This step showed consistent smear between 100-600 bp and indicated successful

sonication for the majority of the sample. A more sensitive measurement for the overall fragment size range in each ChIP sample was done using the Agilent Bioanalyzer 2100 High sensitivity DNA assay. These experiments show that >70% of the ChIP-Seq sample had a fragment size between 100-500 bp (see Figure B1 in Appendix B) which is the optimal fragment range for building sequencing libraries. To confirm the success of the ChIP experiment, 1 ng of ChIP material was analyzed by qPCR using commercially available ChIP primers for a well-known ER target: *pS2*. As a negative control, commercial primers for a gene desert on human chromosome 12 were also run. Percent input was calculated for each primer set using the Ct values obtained from input and ER-enriched ChIP material. For these calculations the 1% input is adjusted to 100% by subtracting 6.664 from the raw input Ct value. This calculation accounts for number of cycles needed to make up the 100-fold dilution and is the Log₂ of 100. The Ct value for the ER-enriched ChIP sample is then divided into the adjusted input and given as a percent of input using the following formula: Percent input = $100 * 2^{(Adjusted\ input - Ct\ (IP))}$

The percent input results calculated for the *pS2* primers were divided into those obtained for the negative control to give a final percent input that was normalized to the negative region. This QC test confirmed the assay's ability to detect ER at the *pS2* gene and served as a validation of the ChIP protocol (see Figure B2 in Appendix B).

2.2.11 ChIP-Seq library build

One ChIP-Seq replicate was generated and sequenced by Active Motif on MCF-7-EM and MCF-7-ER cells treated vehicle control or 10 nM E2 for 1 hour using their established ChIP-Seq protocol. Two ChIP-Seq libraries were generated by Lacey Haddon in the Hugh lab with instruction from Dr. Deborah Tsuyuki. Sequencing libraries were

prepared from ChIP and Input DNAs obtained in the Hugh lab using the NEBNext Ultra II DNA Library Prep Kit for Illumina (E7645S) and indexed using the NEBNext Multiplex Oligos for Illumina (E7335S). ChIP-Seq libraries were run on an Agilent Bioanalyzer High Sensitivity DNA chip to assess the fragment size distribution (see Figure B3 in Appendix B). As a QC check, qPCR for the *pS2* and negative control primers was done using 1 ng of ChIP-Seq library DNA (as described in section 2.2.12). These results showed that the pattern of ER binding in the four experimental conditions was maintained after the library build (see Figure B4 in Appendix B). The ChIP-Seq libraries were sequenced on Illumina's NextSeq 500 using the NextSeq 500/550 High Output Kit (1x75 cycles) at the Molecular Biology Service Unit (MBSU) in the Department of Biological Sciences at the University of Alberta (Edmonton, AB).

2.2.12 ER peak calling

ER peak calling was done by Lacey Haddon with instruction from Dr. Hosna Jabbari. Fastq reads obtained from the NextSeq500 were analyzed using the FastQC program designed by the Bioinformatics Group at the Babraham Institute (Cambridge, UK). All Fastq files had sequence quality scores in the 'very good quality' range of 28-36 (see Figure B5 in Appendix B). The Fastq files were aligned to the human reference genome (build hg19) using the Bowtie2 algorithm (28). The aligned reads were filtered to retain only the uniquely mapped reads, which were then sorted, the duplicates were removed, and the remaining reads were indexed using SAMtools (29). The BED files obtained from this analysis were input into the MACS2 program (v1.4.2) which called peaks with a cutoff P value of 0.005 (30).

2.2.13 DiffBind analysis of ChIP-Seq datasets

DiffBind analysis was done by Lacey Haddon in the Hugh lab with guidance from Dr. Hosna Jabbari. Published datasets for tamoxifen-responsive and resistant patients (31) were obtained from the Gene Expression Omnibus (GSE32222) and processed using the same bioinformatics protocol described in section 2.2.10. DiffBind analysis was done using R Studio software and followed the published guidelines for the DiffBind program (32). ChIP peak sets from the MCF7-EM and MCF7-ER cells treated with and without E2 and those obtained from tamoxifen responsive and nonresponsive patients were loaded into the DiffBind program and the reads for each peak set were counted. For the differential binding analysis, the contrast function was used to sort the ChIP peak sets into two groups based on the experimental condition: resistant and responsive. For this the tamoxifen nonresponsive and MCF7-EM +/- E2 peak sets were labelled as resistant and the tamoxifen responsive and MCF7-ER +/- E2 peak sets were labelled as responsive. These data were then analyzed using the differential analysis function and correlation heatmaps were plotted for the significantly differentially bound sites. Principle component analysis of the three biological replicates for the MCF7-EM and MCF7-ER cells +/- E2 was also done using the DiffBind plot PCA function. This analysis confirmed a strong correlation between the replicates (See Figure B6 in Appendix B).

2.2.14 ChIP-String Analysis

The ChIP-String experiments were designed through collaborations between Judith Hugh and Lacey Haddon and performed by Lacey Haddon with technical help from Kim Formenti. ChIP samples were obtained as described in section 2.1.9. An nCounter custom ChIP-String code set was designed by Nanostring Technologies against target sequences which correspond to significant peaks obtained in the ChIP-Seq experiments as well as

regions devoid of ER binding to serve as negative controls. ChIP and input DNA samples (1 ng/ μ l) were denatured at 95°C for 5 minutes and then immediately cooled on ice. Hybridization buffer was added to the Reporter Code Set and 8 μ l of this master mix was added to individual tubes. Ten microliters (total 10 ng) of denatured DNA was added to the Reporter master mix, followed by 2 μ l of Capture Probe Set (Nanostring Technologies). The samples were hybridized at 65°C overnight, then processed in the automatic Nanostring Prep Station. The fluorescent probes were counted the nCounter Digital Analyzer (Nanostring Technologies). All counts obtained from the nCounter were normalized to exogenous positive controls. The counts for the ChIP DNA sample were then normalized to the corresponding input samples for each probe set. To obtain the enrichment over background, each probe was normalized to the values obtained for the negative control regions. A final comparison was done to obtain the amount of ER binding relative to the baseline using the MCF7-EM cells in the absence of estrogen (set to 1). Three biological replicates of ChIP and Input DNA were used for ChIP-String analysis.

2.2.15 Statistical analysis

Statistical analyses were carried out by Lacey Haddon with guidance from John Hanson. All experiments had a least three biological replicates in order to assess statistical significance. For the gene expression data obtained from RT-qPCR, the Ct values of the three biological replicates were used to determine the raw average and standard deviation (SD) for each gene. These values were used to further calculate a relative quantity (RQ) value for each gene. For these calculations, the Ct values obtained for the MCF7-EM cells treated with ethanol (EM0) were considered the control condition for each gene, and the RQ was set to 1 using the following formula:

$$RQ = 2^{(Ct(EM0) - Ct(EM0))}$$

The RQ for the other 3 experimental conditions were calculated for each gene using the following formula: $RQ = 2^{(Ct(EM0) - Ct(biological\ condition))}$

The SD was corrected for this RQ calculation using the following formula:

$$SDRQ = SD * RQ * LN(2)$$

The RQ values for the three housekeeping genes were then used to determine the normalization factor (NF) for each experimental condition using the following formula:

$$NF = GEOMEAN(RQ(PUM1), RQ(TBP), RQ(RPL13A))$$

The normalized SD was calculated for each experimental condition using the following formula:

$$NFSD = NF * \left(\left(\frac{SDRQ}{(3 * RQ)} \right)^2 PUM1 + \left(\frac{SDRQ}{(3 * RQ)} \right)^2 TBP + \left(\frac{SDRQ}{(3 * RQ)} \right)^2 RPL13A \right)^{0.5}$$

The final normalized expression level (NRQ) was calculated for each gene of interest (GOI) using the following formula: $NRQ(GOI) = RQ/NF$

The final NFSD was adjusted using the following formula:

$$NRQSD = \left(\left(\frac{NFSD}{NF} \right)^2 + \left(\frac{SDRQ}{RQ} \right)^2 \right)^{0.5}$$

Statistical analyses were performed using Prism 7 for Mac OS X (version 7.0e) software.

The two-tailed Student's t-test with the assumption of unequal variance was used to assess differences when only two experimental conditions were compared. One-way analysis of variation (ANOVA) followed by Tukey's posthoc analysis was used to assess differences when greater than two treatment conditions were measured. Two-way ANOVA was used

to assess differences between multiple experimental groups. Only P values ≤ 0.05 were considered as significant.

2.3 Results

2.3.1 Increased ER expression promotes an anti-proliferative response to E2

The MCF-7 parental cell line was stably transduced with one of two main lentiviral doxycycline inducible plasmids (see Figure A1 in Appendix A). The first MCF-7 stable transfectant was mock transduced with the lentiviral doxycycline inducible plasmid containing only the mEmerald fluorescent tag. These cells maintain the low ER expression of MCF-7 parental cells when treated with increasing concentrations of doxycycline and will be referred to as MCF7-EM transfectants for the rest of this thesis. The second stable MCF-7 transfectant was transduced with the doxycycline inducible plasmid with the *ESR1* ORF cloned near the mEmerald fluorescent tag (See Figure A1 in Appendix A). This enabled the increase of ER expression by using increasing concentrations of doxycycline and will further be referred to as MCF7-ER.

The MCF7-ER transfectants were used to investigate the effects of increased ER expression on the proliferation in the presence and absence of E2. To determine the concentration of doxycycline needed to generate high ER expression, MCF7-ER cells were adapted for three days in phenol-red free MEM then induced with increasing concentrations of doxycycline for 24 hours and lysed using RIPA buffer. Protein extracts were separated by SDS-PAGE and ER expression was assessed by Western blot analysis (Figure 2.3). The same experiment was also carried out on the MCF7-EM cells to test for any potential effects of doxycycline treatment on endogenous ER expression (Figure 2.3). Densitometry analysis showed that a doxycycline concentration of 0.5 $\mu\text{g/ml}$ gave a >20-fold increase in

ER protein level in the MCF7-ER cells but did not affect the level of endogenous ER expression in the MCF7-EMs (Figure 2.3). Clinical experiments measuring the level of ER protein in tumor samples found tumors with up to 100-fold increases in ER protein were more likely to reach remission when treated with endocrine therapy (33, 34). In these studies, a 20-fold increase in ER protein represented the mid-range of ER levels measured for all the ER⁺ tumors tested (33, 34). Thus, the level of ER expression in the MCF7-ER cells induced with 0.5 µg/ml doxycycline is within a range that should represent a large majority of ER⁺ tumors. This concentration of doxycycline was used as the standard when inducing both the MCF7-ER and MCF7-EM cells for further experiments examining the differential response to E2.

Using this standard doxycycline concentration, the proliferative response to increasing concentrations of E2 was measured using the MTT cell proliferation assay. The results from this experiment show that as the concentration of E2 increases the MCF7-EM cells show a dose-dependent increase in proliferation (Figure 2.4). Alternatively, while the MCF7-ER cells are able to maintain a basal level of proliferation at low levels of E2 as the concentration increases the response becomes anti-proliferative (Figure 2.4). Since 10 nM E2 has been shown to induce the maximal proliferative growth in MCF-7 cells (35) this concentration was used as the standard E2 treatment for subsequent experiments.

To confirm that the anti-proliferative effect of E2 on MCF7-ER cells was related to increased ER expression a doxycycline titration experiment was conducted in the presence and absence of 10 nM E2 and cells were measured for changes in S phase fraction using flow cytometry analysis. The results show that the proliferative response in cells with endogenous low ER expression (0 µg/ml doxycycline) changes to an anti-proliferative

response as the level of ER increases (Figure 2.5). An additional finding for the MCF7-ER cells was that the increased ER expression induced by 0.5 µg/ml doxycycline promotes a basal increase in S phase fraction in the absence of E2 (Figure 2.6). This effect of ER on basal proliferation has been previously described (36). When taken together, these experiments confirmed that the level of ER influences the proliferative versus anti-proliferative response in luminal cells.

The Hugh lab has initiated a clinical trial to examine the use of low-dose estradiol in treatment naïve, newly diagnosed post-menopausal women with ER+ breast cancer prior to definitive breast surgery (PRE-operative ESTrAdiOl (PRESTO) (Registration ID #NCT02238808). Patient eligibility criteria were focused on clinical parameters that are associated with the luminal A subtype and included: ER+, HER2-, low grade, age > 55yrs with no hormone replacement therapy for the preceding 5 years. The Ki67 indices from core samples obtained pre-treatment were compared to those from the surgical excision and showed that 7-14 days of estradiol treatment resulted in a decrease in Ki67 indices in 7 of 10 women (see Figure C1 of interim report in Appendix C). These findings indicate that E2 treatment is growth suppressive for certain ER+ breast cancers.

2.3.2 ER-DNA binding regulates the proliferative and anti-proliferative response to E2

Since ER can function through genomic and non-genomic pathways, the role for the direct transcriptional function of ER on anti-proliferative effect of E2 was examined. To assess the role of transcription MCF7-EM and MCF7-ER cells were treated with or without actinomycin D, an antibiotic which intercalates DNA and prevents RNA polymerase mediated elongation (37). These experiments were conducted with or without E2 treatment

and assessed for changes in proliferation by flow cytometry. The results show that treatment with actinomycin D prevented the proliferative and anti-proliferative effects of E2 in the MCF7-EM and MCF7-ER cells, respectively (Figure 2.7).

Since actinomycin D is a general inhibitor of transcription and does not indicate a direct effect on ER-mediated transcription, the role of ER-DNA binding on proliferation was assessed using a stable MCF-7 transfectant with the doxycycline inducible plasmid cloned with an *ESR1* gene that has three point-mutations (E203G, G204S and A207V) in the first zinc finger of the DBD (see Figure A1 in Appendix A). These point-mutations have been previously described for their ability to prevent ER-DNA binding (38) and these cells are referred to as MCF7-ER-mDBD. In order to directly compare the effect of this ER mutant against the MCF7-ER cells, doxycycline titration experiments were conducted to assess the concentration that would induce a similar level ER expression between the MCF7-ER and MCF7-ER-mDBD cells.

Western blot analysis showed that MCF7-ER-mDBD cells had similar ER expression to MCF7-ER cells when induced with 2.0 $\mu\text{g/ml}$ doxycycline (Figure 2.8). The proliferative effect of E2 on the MCF7-ER-mDBD cells at this concentration of doxycycline was examined using the MTT assay. These experiments showed the significant decrease in cell viability in the MCF7-ER cells treated with E2 ($P=0.0007$) is not present in the MCF7-ER-mDBD cells after E2 treatment ($P=0.1943$) despite their similar levels of ER expression (Figure 2.8). The MCF7-ER-mDBD cells also lacked a significant increase in E2-induced proliferation indicating that the mutant ER may be forming homodimers with the endogenous ER protein and acting as a dominant negative regulator of ER-DNA binding (Figure 2.8). Interestingly, the basal increase in proliferation seen in the MCF7-ER cells

was not present in the MCF7-ER-mDBD cells, suggesting basal proliferation is also mediated through ER-DNA binding (Figure 2.8). When taken together, these results provide further evidence that proliferation in low and high ER expressing luminal cells is a transcriptional response that is regulated by ER-DNA binding.

Lysates were not prepared from MCF7-ERmDBD cells in the absence of doxycycline, therefore the level of endogenous ER was not assessed for this cell line. Additionally, the effects of the ER-mDBD transduction on the endogenous levels of ER are unknown. A previous study of ERE reporter activity in Chinese hamster ovary (CHO) cells transfected with ER containing this DBD mutant found a loss of reporter activity in the presence of E2; however, when wild type ER was co-expressed the ERmDBD transfectant did not negatively affect the activity of the wild type receptor (38). Our current MTT results suggest that expression of the DBD mutant in MCF-7 cells with endogenous ER leads to a dominant negative effect. The discrepancy between the current results and the previous findings may be due to differences in the cell type used as CHO cells do not express endogenous levels of ER (39).

2.3.3 E2 induces G1 and G2 cell cycle arrest but not apoptosis in MCF7-ER cells

Previous investigations of the effect of E2 on MCF-7 cells after long-term hormone depletion concluded the anti-proliferative effect of E2 was due to the induction of apoptosis (40), however this E2-induced apoptotic response is not present in ER negative cells transfected with ER (23). To determine if E2 was inducing apoptosis Poly (ADP-ribose) Polymerase (PARP) cleavage and the release of cytochrome C from the mitochondria was measured using the known apoptotic inducing antibiotic staurosporine (STS) as a positive control. There was no evidence of PARP cleavage or cytosolic cytochrome C after E2

treatment in either the MCF-7-ER or MCF-7-EM cells (Figure 2.9). These results show that the anti-proliferative response in the MCF7-ER cells is not due to an apoptotic response to E2.

Increased ER expression in the ER negative cell line, MDA-MB-231, induced an anti-proliferative response to E2 that was shown to be mediated through the regulation of cell cycle genes resulting in a G1/S phase block (41). The effect of E2 on the different cell cycle phases in the MCF7-EM and MCF7-ER cells was assessed using flow cytometry. E2 is known to promote the transition of MCF-7 cells from the G1 to S-phase of the cell cycle (12, 42). Consistent with previously published results (43) these experiments found that after exposure to E2-free MEM for three days, E2 treatment relieves the G1 arrest of MCF7-EM (Figure 2.10). These results also confirmed the work of Fowler et al. (2004) in that MCF7-ER cells do not show a G1 arrest when kept in E2-free MEM but exhibit a basal increase in proliferation (Figure 2.10) (36).

When treated with E2 for 24 hours, MCF7-EM cells exhibit the characteristic proliferative response with a significant increase in S-phase ($P < 0.0001$) (Figure 2.10), whereas the MCF7-ER cells have a significant reduction in S-phase fraction ($P = 0.0006$) and a significant increase in cells arrested in both the G1 phase ($P = 0.0439$) and G2 phase ($P = 0.0243$) of the cell cycle (Figure 2.10). The G1 arrest in the MCF7-ER cells after E2 treatment was associated with a significant increase in p21 protein levels ($P = 0.0039$) and a significant decrease in the transcription factor E2F1 which mediates S-phase transition ($P = 0.0284$) (Figure 2.11). A significant decrease in *E2F1* mRNA in the MCF7-ER cells treated with E2 was confirmed by RT-qPCR (Figure 2.12). The G2 arrest corresponds with a significant decrease in cyclin B2 in MCF7-ER cells compared to MCF7-EM cells treated

with E2 ($P=0.0028$) which is a known target for E2F transcriptional regulation (Figure 2.11) (44). These results show that the anti-proliferative effect of E2 in MCF7-ER cells is due to cell cycle arrest at both the G1 and G2 phases.

To determine whether ER was directly regulating p21 (*CDKN1A*) and *E2F1* gene transcription ChIP-Seq analysis was conducted in both the MCF7-EM and MCF7-ER cells treated with or without E2 for 1 hour. Analysis of the ER binding patterns using the University of California Santa Cruz (UCSC) genome browser showed a novel ER peak within the intragenic region of *CDKN1A* which was bound in at least 2/3 biological replicates in the MCF7-ER cells after E2 treatment (Figure 2.13). This region contained a conserved AP1 binding site and two half EREs (Figure 2.14). Analysis of ENCODE data for transcription factor binding sites indicated ER, POL2RA, E2F1, E2F6, FOS and NR3C1 had been previously mapped to this region in other cells (Figure 2.14). ER binding at this intragenic region was measured using ChIP-String analysis and confirmed the presence of ER peaks only in the MCF7-ER cells after E2 treatment (Figure 2.15). The ChIP-Seq results did not detect consistent ER-binding near *E2F1* in either of the MCF-7 transfectants with or without E2 (Figure 2.16). These results suggest ER mediates the G1 arrest in MCF7-ER cells treated with E2 through direct transcriptional regulation of p21.

The effect of E2 on ten proliferation and cell cycle associated genes was investigated in the MCF7-EM and MCF7-ER cells by RT-qPCR. Each of these ten genes had E2F binding mapped near their promoter regions in the ENCODE ChIP-Seq datasets. The results show the expression of these proliferation and cell cycle genes becomes increased in MCF7-EM cells when treated with E2 (Figure 2.17). However, in the MCF7-ER cells these genes become down-regulated when treated with E2 (Figure 2.17). Interestingly, the

increased basal proliferation seen in the MCF7-ERs in the absence of E2 corresponds to an increase in these proliferation and cell cycle genes (Figure 2.17). These results show that increased ER expression promotes an anti-proliferative response to E2 through down-regulation of proliferation and cell cycle genes which is likely mediated by the p21-induced repression of E2F.

2.3.4 MCF7-ER cells correlate with ER+ patients that respond to hormone therapy

To further validate that the response to E2 seen in the MCF7-ER cells is more representative of tumors which respond to hormone therapies, peak sets from the MCF7-EM and MCF7-ER ChIP-Seq experiments were compared against a previously published dataset of genome-wide ER-DNA binding profiles from ER+ breast cancer patients that were either responsive or non-responsive to tamoxifen (31). For this published dataset an assumption that patients who were responsive to tamoxifen would represent the luminal A subtype, whereas non-responsive patients would more closely resemble a luminal B subtype was made. This assumption was furthered by the authors previous finding that the MCF-7 binding profiles correlated best (79.8%) with tamoxifen non-responsive ER+ patients (31). However, the results showed that the MCF7-EM cells did not correlate well with either the responsive or non-responsive patients (Figure 2.18). More significantly, the MCF7-ER cells correlated best with the tamoxifen responsive patients, regardless of E2 treatment (Figure 2.19). These results suggest that increased ER expression promotes an ER-DNA binding signature that is more representative of ER+ patients who respond to hormone therapy.

The tamoxifen responsive and nonresponsive peak sets were used to investigate whether there were differences in the ER binding at the intragenic region of the *CDKN1A*

gene in ER+ patient samples. The results showed that the putative ER region of *CDKN1A* that is bound in the MCF7-ER cells in the presence of E2 was also bound in at least 2/5 replicates for both the responsive and nonresponsive patients (Figure 2.20). The presence of significant ER binding at *CDKN1A* for tamoxifen responsive and nonresponsive patients suggests there may be some overlap in the regulation of p21 in these patients.

2.4 Conclusion

The results from these experiments show that increased ER expression promotes an anti-proliferative response to E2 that is mediated through a transcriptional response that requires an intact ER-DNA binding mechanism. These experiments also confirm increased ER expression can promote an increase in basal proliferation in the absence of E2, and this unliganded ER effect is regulated by ER-DNA binding and transcription. Assessment of apoptotic markers gave no evidence for apoptosis in the MCF7-ER cells treated with E2. An accumulation of cells in the G1 phase was detected which correlated with an increase in p21 and a decrease in E2F1 indicating a cell cycle arrest at the G1/S checkpoint. Additionally, a significant accumulation of cells in the G2 phase was detected and this correlated with decreased levels of cyclin B2 indicating an additional cell cycle arrest at the G2/M checkpoint. ChIP experiments uncovered a novel ER peak at an intragenic region of the *CDKN1A* gene which contained a half ERE and was bound only in MCF7-ER cells treated with E2. When taken together, these results show the anti-proliferative effect of E2 in the MCF7-ER cells is due to a cell cycle block that may be mediated by direct ER regulation of p21. Comparison of ChIP-Seq datasets obtained from the MCF7-EM and MCF7-ER cells against those previously published for tamoxifen responsive or nonresponsive patients showed the ER-binding patterns in the MCF7-ER cells correlated

best with those obtained from tamoxifen responsive patients. ER binding was detected at the intragenic region of *CDKN1A* in patients that were responsive and nonresponsive to tamoxifen suggesting there is an overlap in ER regulation at this region. These results provide strong evidence that the anti-proliferative response to E2 in the MCF7-ER cells can serve as an improved model for ER+ tumors that are responsive to hormone therapy. It also provides further support that changes in ER binding patterns may serve as an underlying mechanism which can identify these patients.

Table 2.1 Antibody list.

Antibody	Isotype	Clone	Supplier
ER α	Rabbit IgG	D8H8	Cell Signaling
ER α	Rabbit polyclonal	HC-20	Santa Cruz
PARP	Rabbit	46D11	Cell Signaling
Cytochrome C	Rabbit IgG	D18C7	Cell Signaling
P21 Waf1/Cip1	Rabbit IgG	12D1	Cell Signaling
Cyclin B2	Rabbit IgG	R17985	Abcam
Cyclin D1	Rabbit IgG	EPR2241	Abcam
Cyclin E2	Rabbit	4132	Cell Signaling
β -Actin	Mouse IgG1	A5441	Sigma Aldrich
Alexa Fluor 700	Goat anti-rabbit IgG	A21038	Thermo Fisher Scientific
Alexa Fluor 800	Goat anti-mouse IgG	A32730	Thermo Fisher Scientific

Table 2.2 Primer sequences.

Primer	Sequence 5'-3'
ESR1-F	ATCCGCTAGCGCCACCATGACCATGACCCTCCACACCAAA
ESR1-R	TCCGGAGGCTCGCGACCGTGGCAGGGAAACCCTCTGC
ESR1-EM-F	ATCCGCTAGCGCCACCATGACCATGACCCTCCACACCAAA
ESR1-EM-R	TCCGAGAATTCCGCTTACTTGTACAGCTCGTCCAT
ER-mDBD-F	ATCCGGATCCGCCACCATGACCATGACCCTCCACACCAAA
ER-mDBD-R	CGGTGGATCCCCTCCGGAGCTCGCGACCGTGGCAGGGAA ACCCTCT

F- forward
R-reverse

Table 2.3 Experimental conditions for the differential response to E2.

Cell line	Treatment	
	EtOH control	10nM E2
MCF7-EM	EM0	EM10
MCF7-ER	ER0	ER10

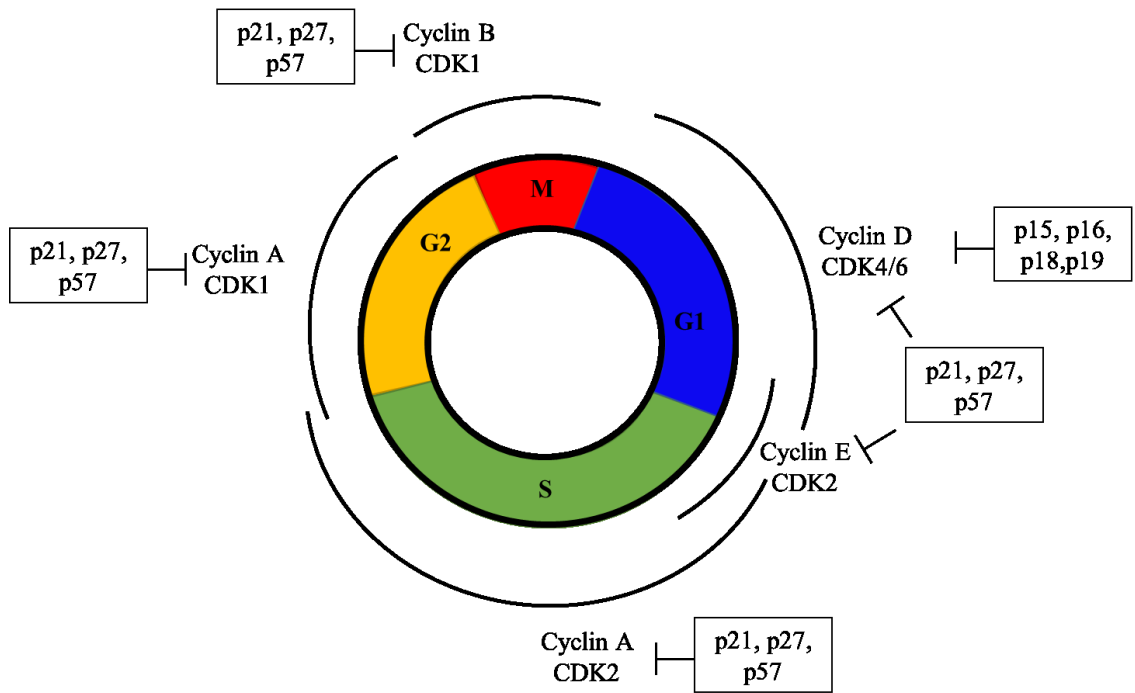


Figure 2.1 Cell cycle regulation. Diagram indicates the four major phases of the cell cycle and the cyclin/CDK complexes which regulate the major checkpoints.

A



B

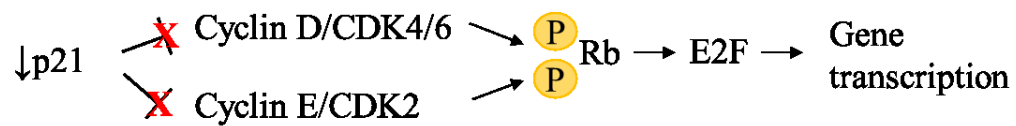


Figure 2.2 p21 regulation of E2F transcription. **A.** Increased p21 expression leads to inhibition of cyclin D/CDK4/6 and cyclin E/CDK2 complexes and prevents the phosphorylation of Rb. Hypophosphorylated Rb remains complexed with E2F and prevents the transcription of E2F target genes. **B.** Decreased p21 expression cannot inhibit the cyclin D/CDK4/6 and cyclin E/CDK2 complexes allowing them to phosphorylate Rb. Hyperphosphorylated Rb releases E2F which binds its target genes and regulates their transcription.

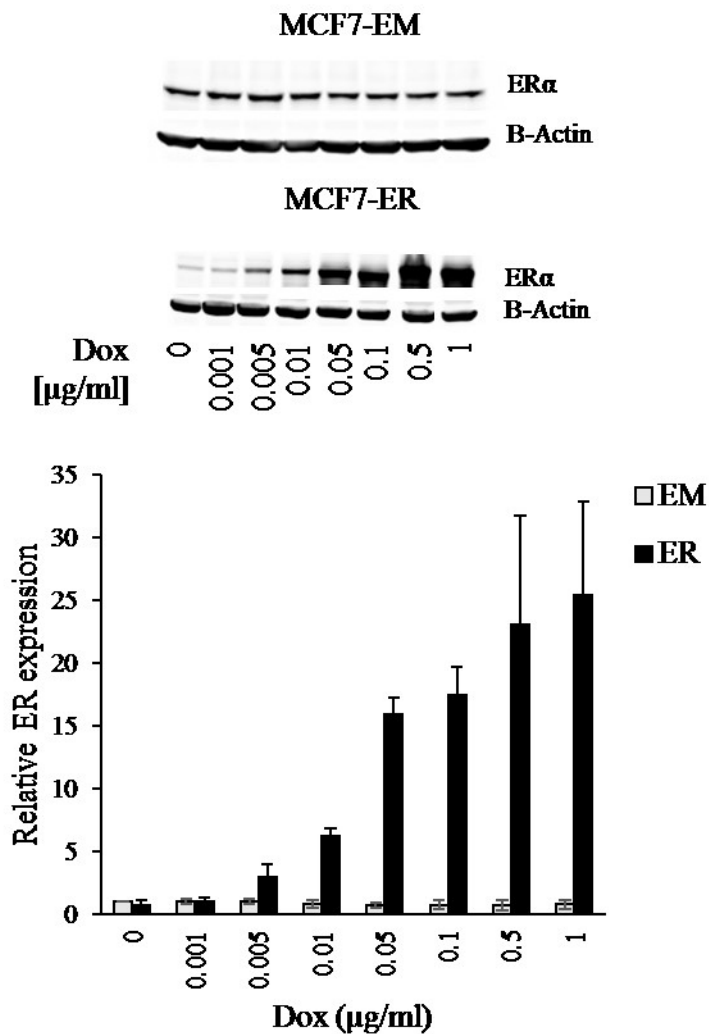


Figure 2.3 Doxycycline titrations for MCF7-EM and MCF7-ER transfectants. Representative western blot for ER protein expression in MCF7-EM (EM) and MCF7-ER (ER) cells induced with varying doses of doxycycline (Dox). Densitometry analysis for relative ER expression was normalized to β -actin. Data are shown as mean \pm SD, n=3.

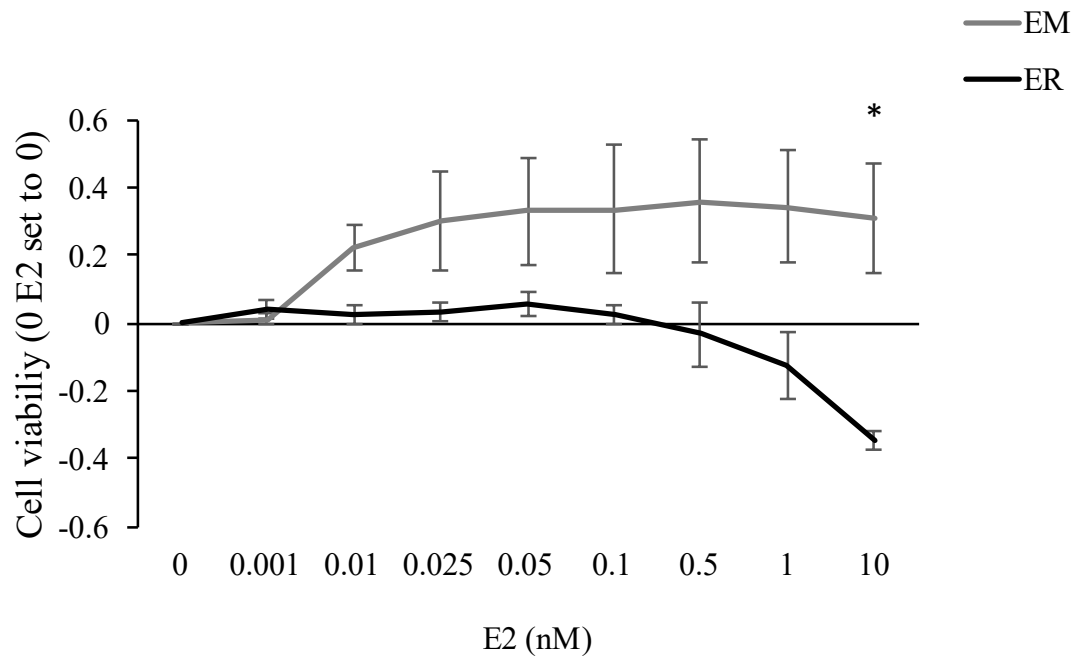


Figure 2.4 MCF7-EM and MCF7-ER cells show a differential proliferative response to increased E2 concentrations. Cell viability assay for MCF7-EM (EM) and MCF7-ER (ER) cells treated with increasing doses of E2. The 0 E2 condition was set to 0 for each MCF-7 transfectant. Data are shown as mean \pm SD. There was a significant decrease in cell viability for the MCF7-ER cells treated with E2 compared to the MCF7-EM cells treated with E2 (Two-way ANOVA with Tukey's posthoc analysis, $n=3$, $*P=0.01$).

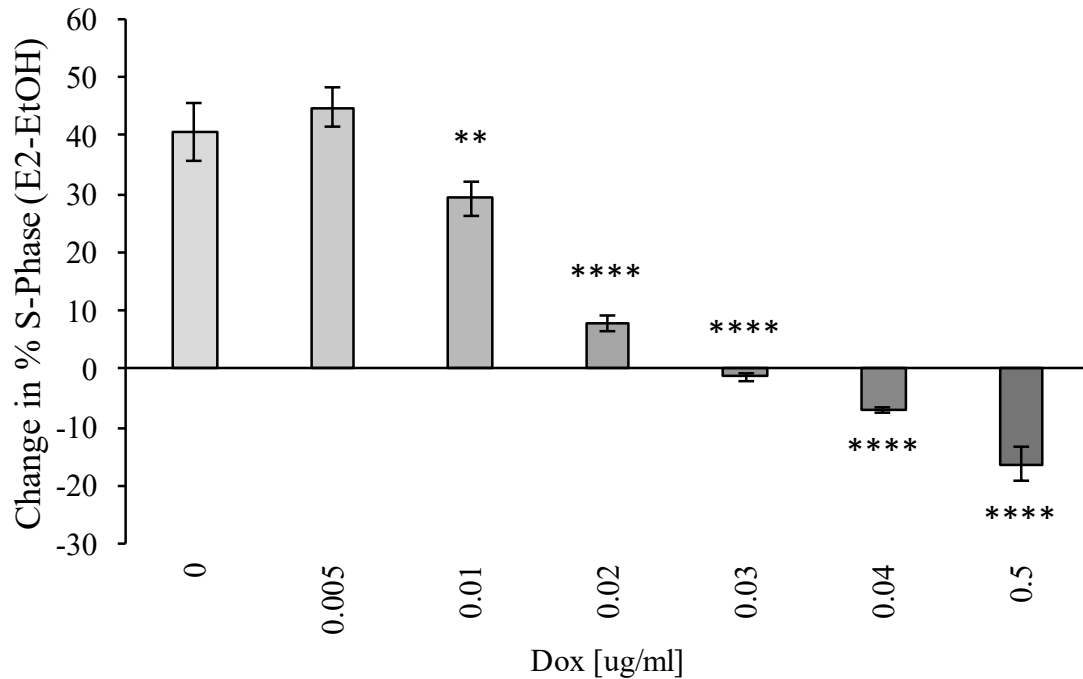


Figure 2.5 Increased ER expression leads to an anti-proliferative response to E2.

Change in % S-Phase in MCF7-ER cells induced with increasing concentrations of doxycycline (Dox) and treated with 10nM E2 for 24 hours. Change in S-phase was calculated as the percentage of cells in S-phase for the E2 treated condition divided by vehicle control for each dose of doxycycline. Data are shown as mean \pm SD. A significant decrease in the percentage of cells in S phase as the concentration of doxycycline increases from 0.005 μ g/ml (One-way ANOVA followed by Tukey's posthoc analysis, $n=3$, $**P=0.003$, $****P<0.0001$ compared against 0 μ g/ml Dox).

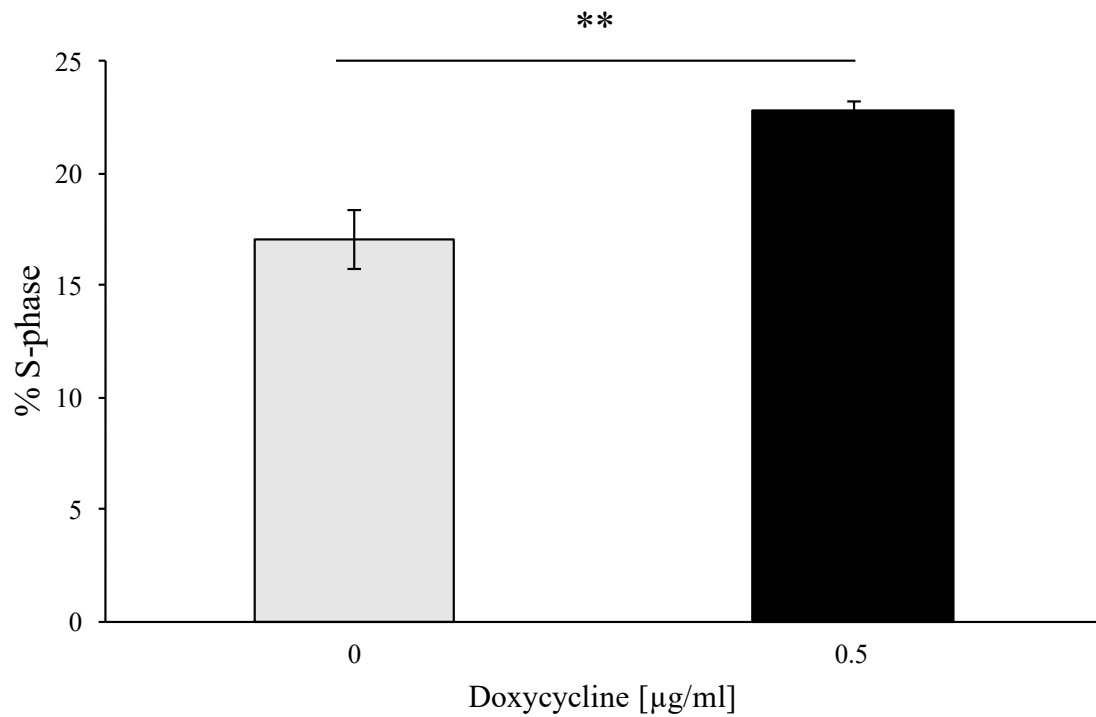


Figure 2.6 Increased ER expression promotes a basal increase in proliferation. Flow cytometry analysis for S phase fraction of MCF7-ER cells induced with 0 or 0.5 µg/ml doxycycline (Dox) for 24 hours and then treated with EtOH. Data are shown as mean ± SD, n=3. A significant increase in S phase fraction was seen in MCF7-ER cells treated with 0.5 µg/ml Dox by Student's t-test, n=3, ** $P=0.002$.

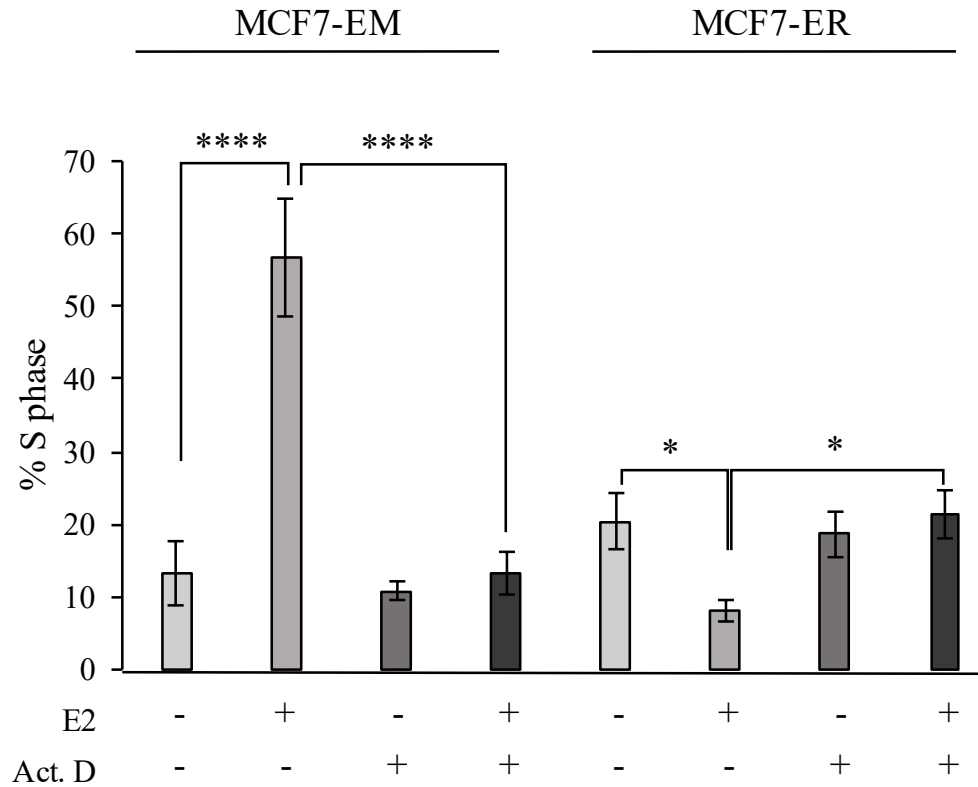


Figure 2.7 Transcriptional inhibition prevents the proliferative and anti-proliferative effects of E2. MCF7-EM and MCF7-ER cells were induced with 0.5 $\mu\text{g/ml}$ doxycycline and the percentage of cells in the S phase of the cell cycle was measured by flow cytometry analysis in the presence of E2, actinomycin D (Act. D) and the combination of Act.D + E2. Data are shown as mean \pm SD. There was a significant increase in the percent of MCF7-EM cells in S phase when treated with E2 compared to no E2 and a significant decrease when Act. D was added. There was a significant decrease in the percentage of MCF7-ER cells in S phase when treated with E2 compared to no E2 and a significant increase when Act. D was added (Two-way ANOVA with Tukey's posthoc analysis, $n=3$, $*P=0.03$, $****P<0.0001$).

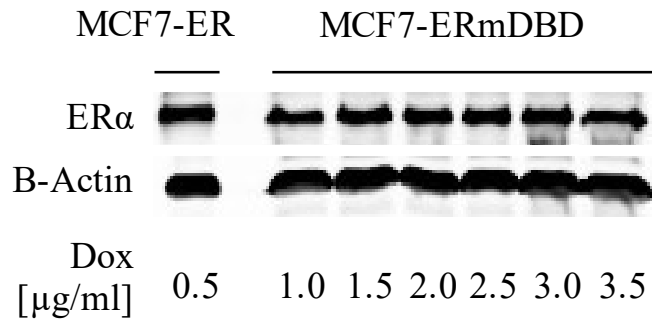
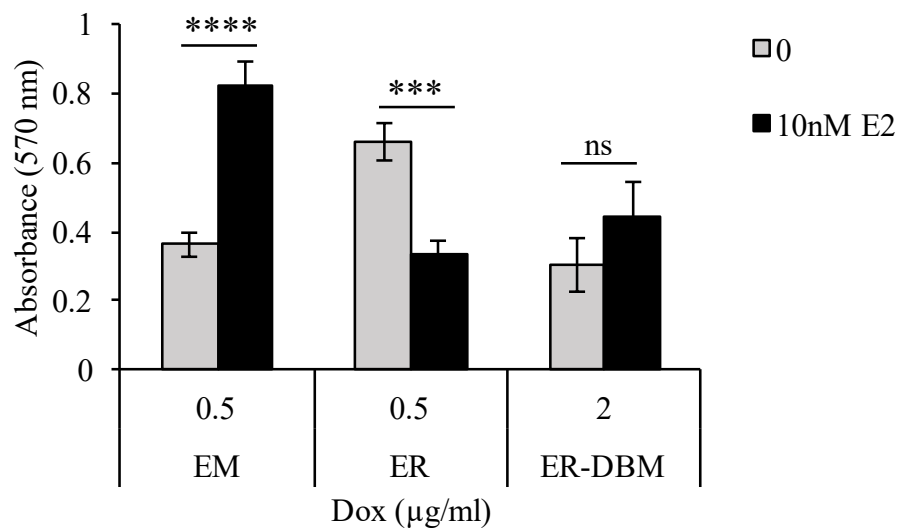
A**B**

Figure 2.8 Increased ER mediates the anti-proliferative effect through DNA binding.

A. Representative western blot for ER protein expression in MCF7-ER and MCF7-ERmDBD cells under varying doses of doxycycline induction. Lysates from MCF7-ERmDBD cells were not harvested in the absence of doxycycline therefore the level of endogenous ER expression cannot be shown. **B.** Cell viability was measured as absorbance (570 nm) in MCF7-EM (EM), MCF7-ER (ER) and MCF7-ER-mDBD (ERmDBM) cells treated with vehicle control (EtOH) or 10 nM E2 after 24 hours of doxycycline induction. Data are shown as mean \pm SD. Absorbance was significantly increased in the MCF7-EM cells after E2 treatment and significantly decreased in the MCF7-ER cells after E2 treatment (Two-way ANOVA with Tukey's posthoc analysis, $n=3$, ns= non significant, *** $P=0.0007$, **** $P<0.0001$).

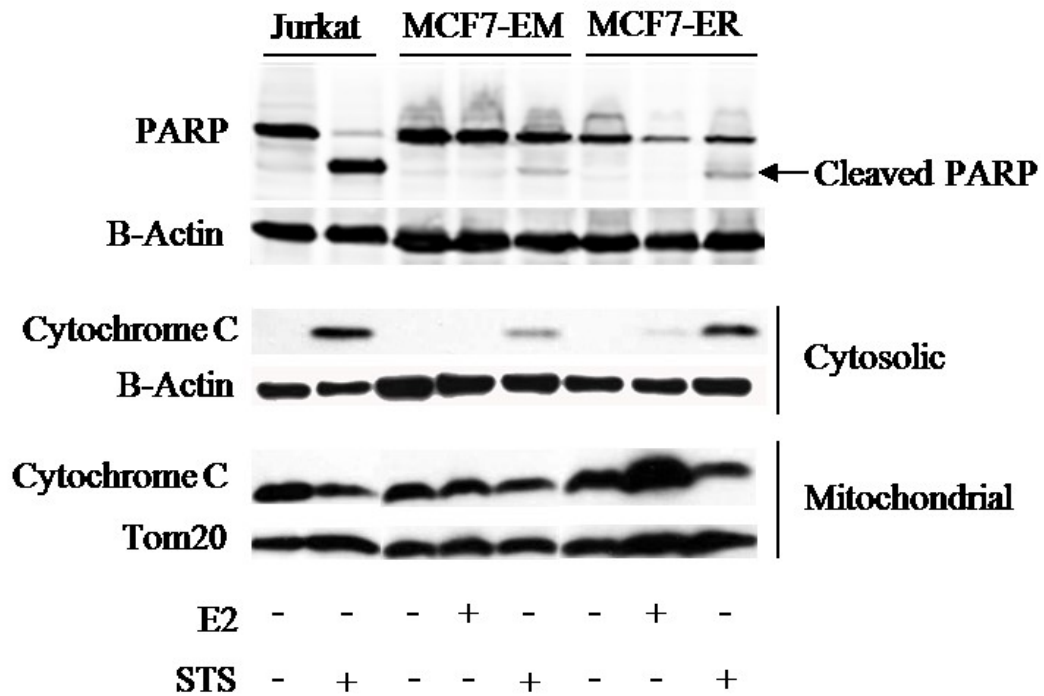


Figure 2.9 MCF7-ER cells treated with E2 do not show evidence of apoptotic markers. Representative Western blot for PARP cleavage and cytochrome C protein expression in MCF7-EM and MCF7-ER cells were treated with E2 or staurosporine (STS) for 24 hours. β -actin and Tom20 served as loading controls. Jurkat cells were treated with STS as a positive marker for apoptosis.

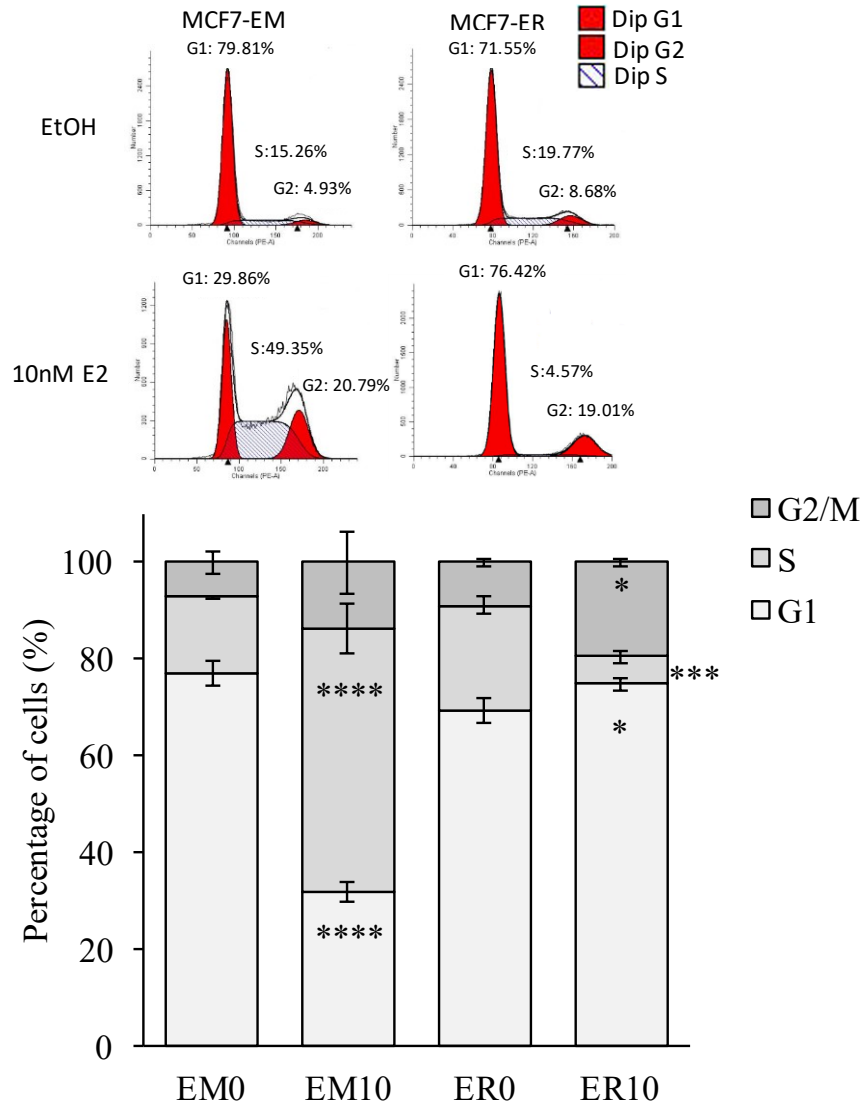


Figure 2.10 E2 induces accumulation of MCF7-ER cells in the G1 and G2 phases of the cell cycle. Cell cycle distribution of MCF7-EM and MCF7-ER cells treated with vehicle control (EM0 and ER0) or 10 nM E2 (EM10 and ER10) for 24 hours was assessed by flow cytometry. Graph depicts the average percentage of cells in the G2/M, S and G1 phases. Data are shown as mean \pm SD. There was a significant decrease in the percentage of MCF7-EM cells in the G1 phase and a significant increase in the S Phase after E2 treatment. There was a significant increase in the percentage of MCF7-ER cells in the G1 and G2/M phases and a significant decrease in the S phase after E2 treatment (Two-way ANOVA with Tukey's posthoc analysis, $n=3$, $*P<0.05$, $***P=0.0006$, $****P<0.0001$. Each cell line was compared against the 0 E2 control).

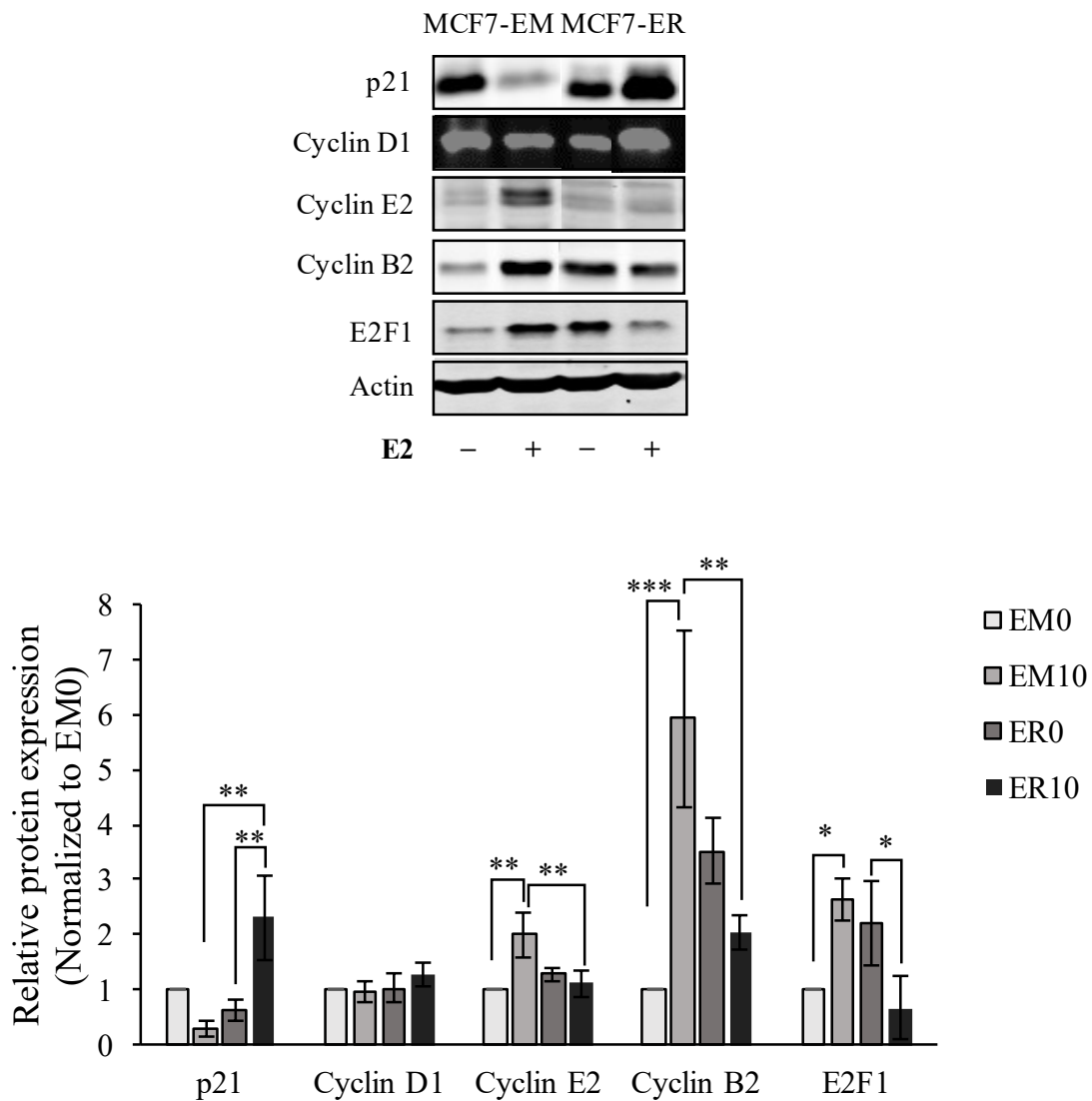


Figure 2.11 The expression of cell cycle proteins indicate MCF7-ER cells treated with E2 encounter a G1/S and G2/M cell cycle arrest. Representative western blot for p21, cyclin D1, cyclin E2, cyclin B2, E2F1 and actin protein expression in MCF7-EM and MCF7-ER cells treated with vehicle control (EM0 and ER0) or 10 nM E2 (EM10 and ER10). Relative protein expression was normalized to actin as loading control. Relative protein expression was calculated with EM0 set as 1. Data are shown as mean \pm SD, n=3. Statistical significance was determined using two-way ANOVA followed by Tukey's posthoc analysis, n=3, * $P < 0.03$, ** $P < 0.01$, *** $P = 0.006$.

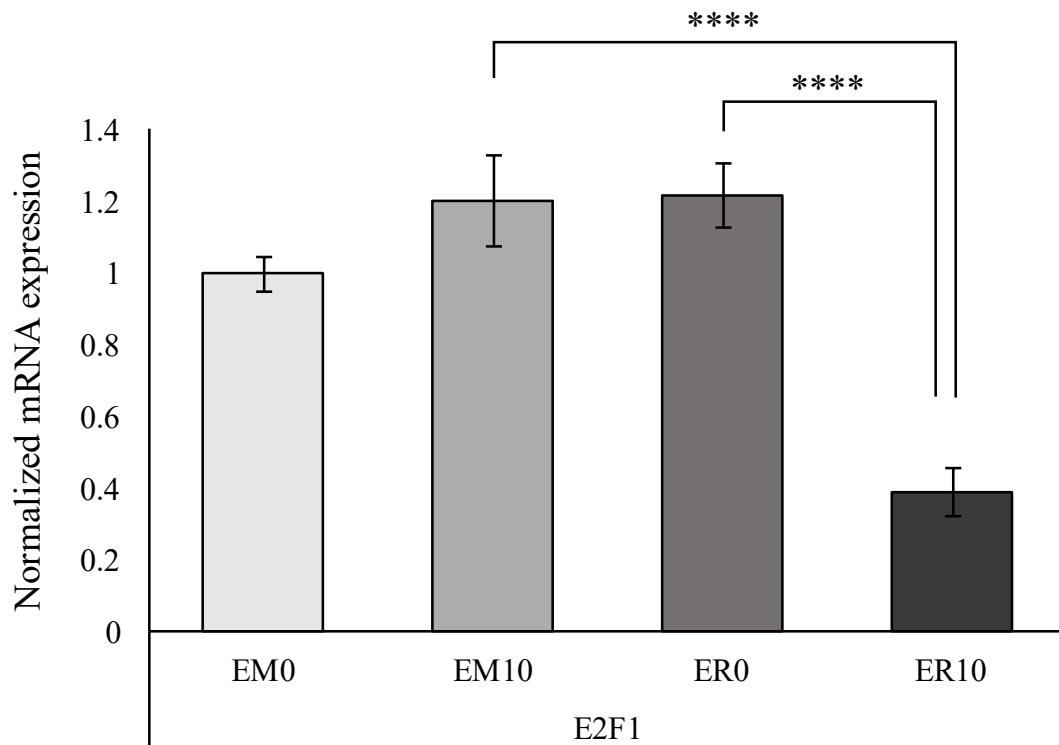


Figure 2.12 E2 induces *E2F1* repression in MCF7-ER cells. RNA was extracted from MCF7-EM and MCF7-ER cells treated with 0 (EM0 and ER0) or 10 nM E2 (EM10 and ER10) for 24 hours and quantified by RT-qPCR. Gene expression was normalized to three house-keeping genes and MCF7-EM 0 E2 control was set to 1. Data are shown as mean \pm SD. There was a significant decrease in *E2F1* mRNA expression in the MCF7-ER cells compared to the MCF7-EM cells when both were treated with E2. There was also a significant decrease in *E2F1* mRNA expression in the MCF7-ER cells after E2 treatment (Two-way ANOVA followed by Tukey's posthoc analysis, $n=3$, **** $P<0.0001$).

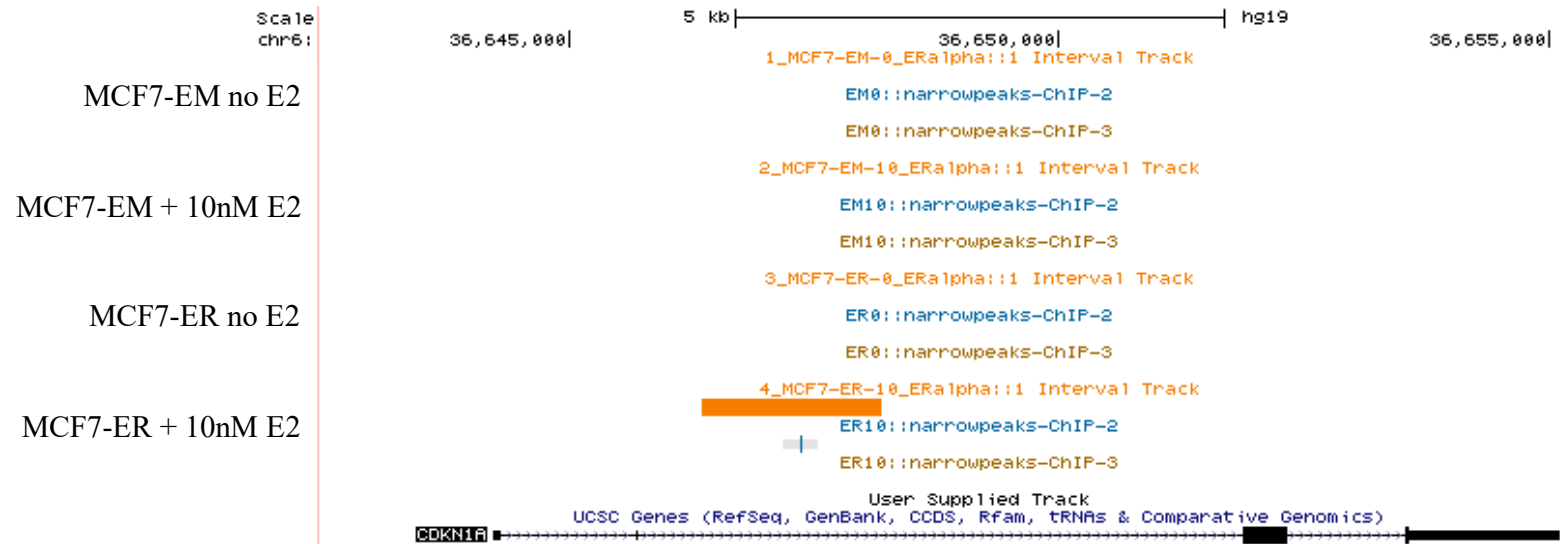


Figure 2.13 Novel region of *CDKN1A* is bound by ER in MCF7-ER cells treated with E2. UCSC genome browser view of *CDKN1A* showing mapped DNA binding from MCF7-EM and MCF7-ER ChIP-Seq data sets. The ER peak at an intragenic region of *CDKN1A* is highlighted in light blue. Orange bars indicate regions bound in the first biological replicate done by Active Motif. The gray bar with blue line represents ER binding from the second biological replicate, n=3.

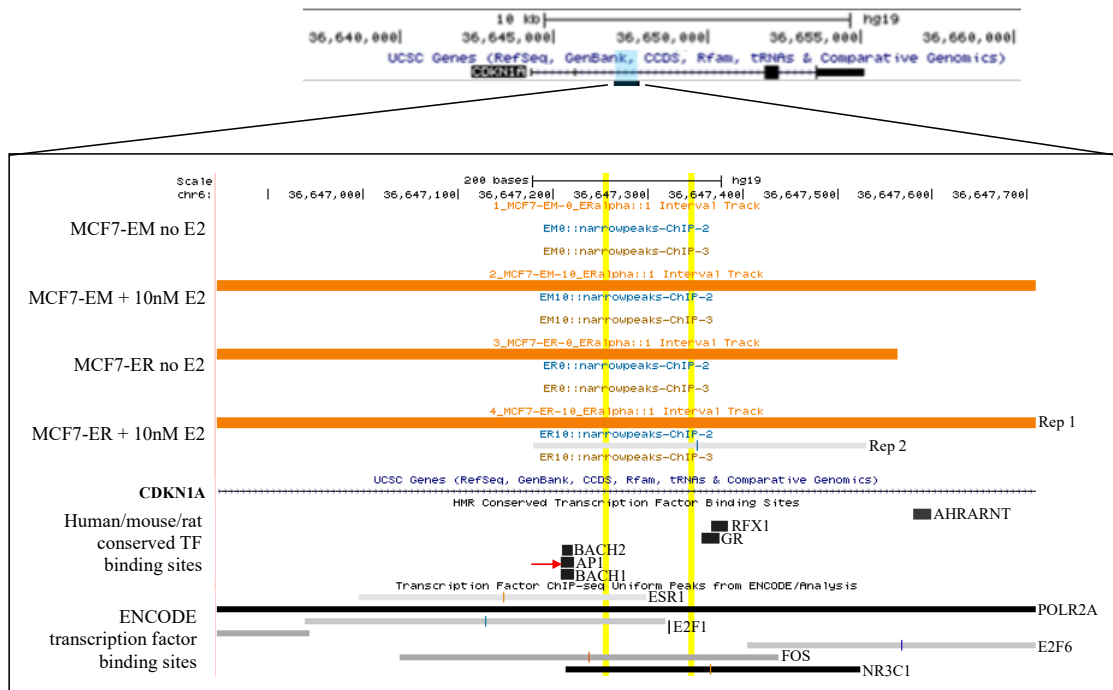


Figure 2.14 The intragenic region of *CDKN1A* bound by ER contains AP1 and half ERE motifs. Zoomed in UCSC genome browser view of the intragenic region of *CDKN1A* (highlighted in blue) showing mapped DNA binding from MCF7-EM and MCF7-ER ChIP-Seq data sets. Orange bars indicate regions bound in the first biological replicate done by Active Motif (Rep 1). The gray bar with blue line represents ER binding from the second biological replicate (Rep 2), n=3. The locations of two half EREs within the ER peak are highlighted in yellow. ENCODE data showing transcription factor (TF) binding sites that are conserved between human, mouse and rat (HMR) genomes are shown as thick black bars. The presence of a conserved AP1 binding site is indicated by a red arrow. ENCODE data showing mapped transcription factor binding sites for ER (ESR1), POLR2A, E2F1, E2F6, FOS and NR3C1 from ChIP-Seq experiments from various cell lines are shown as thin black and gray bars at the bottom of the image.

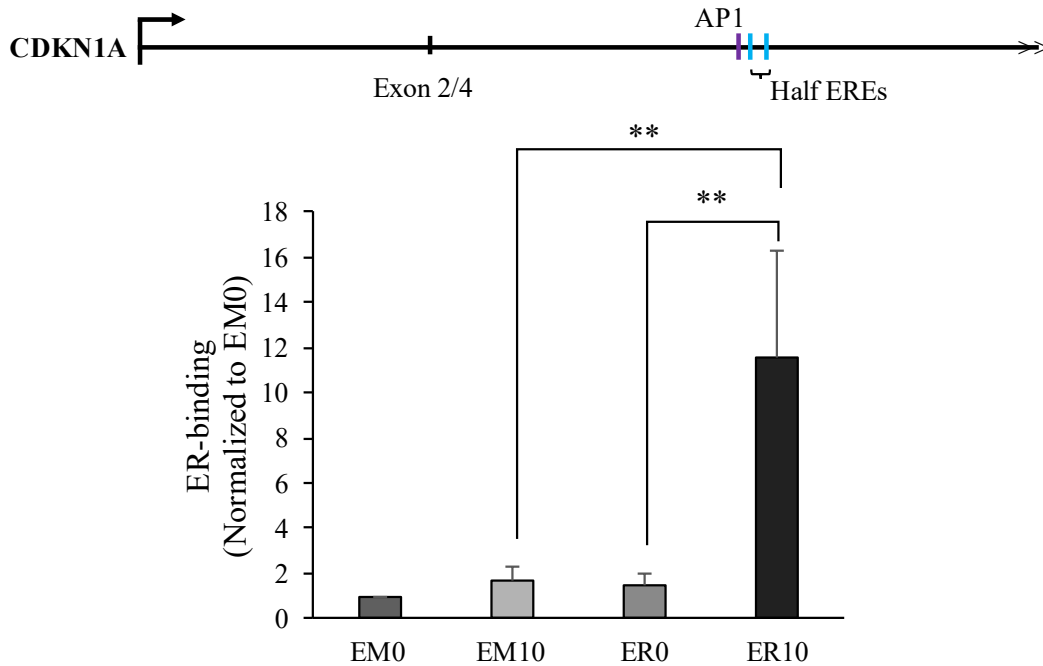


Figure 2.15 ER binding at *CDKN1A* only occurs in MCF7-ER cells treated with E2. Map of the intragenic region of *CDKN1A* with the locations of the AP1 binding site (purple) and two half-ERE motifs (blue). ChIP-String validation of ER binding at an intragenic region of *CDKN1A* with samples normalized to EM0. Data are shown as mean \pm SD. There was a significant increase ER-binding in the MCF7-ER cells after E2 treatment when compared against untreated MCF7-ER cells and E2 treated MCF7-EM cells (Two-way ANOVA followed by Tukey's posthoc analysis, $n=3$, $**P=0.003$).

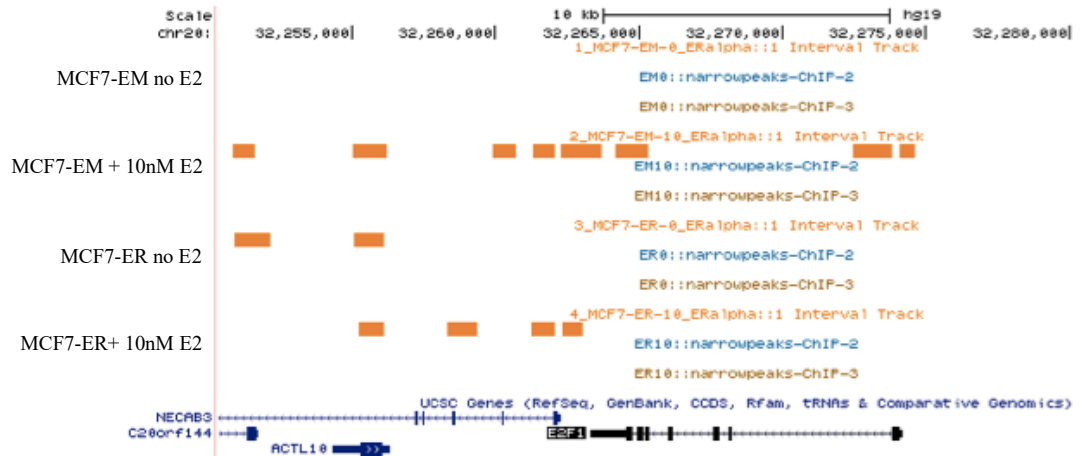


Figure 2.16 ChIP-Seq data from MCF7-EM and MCF7-ER cells at the *E2F1* gene. UCSC genome browser view of the *E2F1* gene showing mapped DNA binding from MCF7-EM and MCF7-ER ChIP-Seq data sets. Orange bars represent ER binding detected in only 1/3 biological replicates and is not considered significant, n=3.

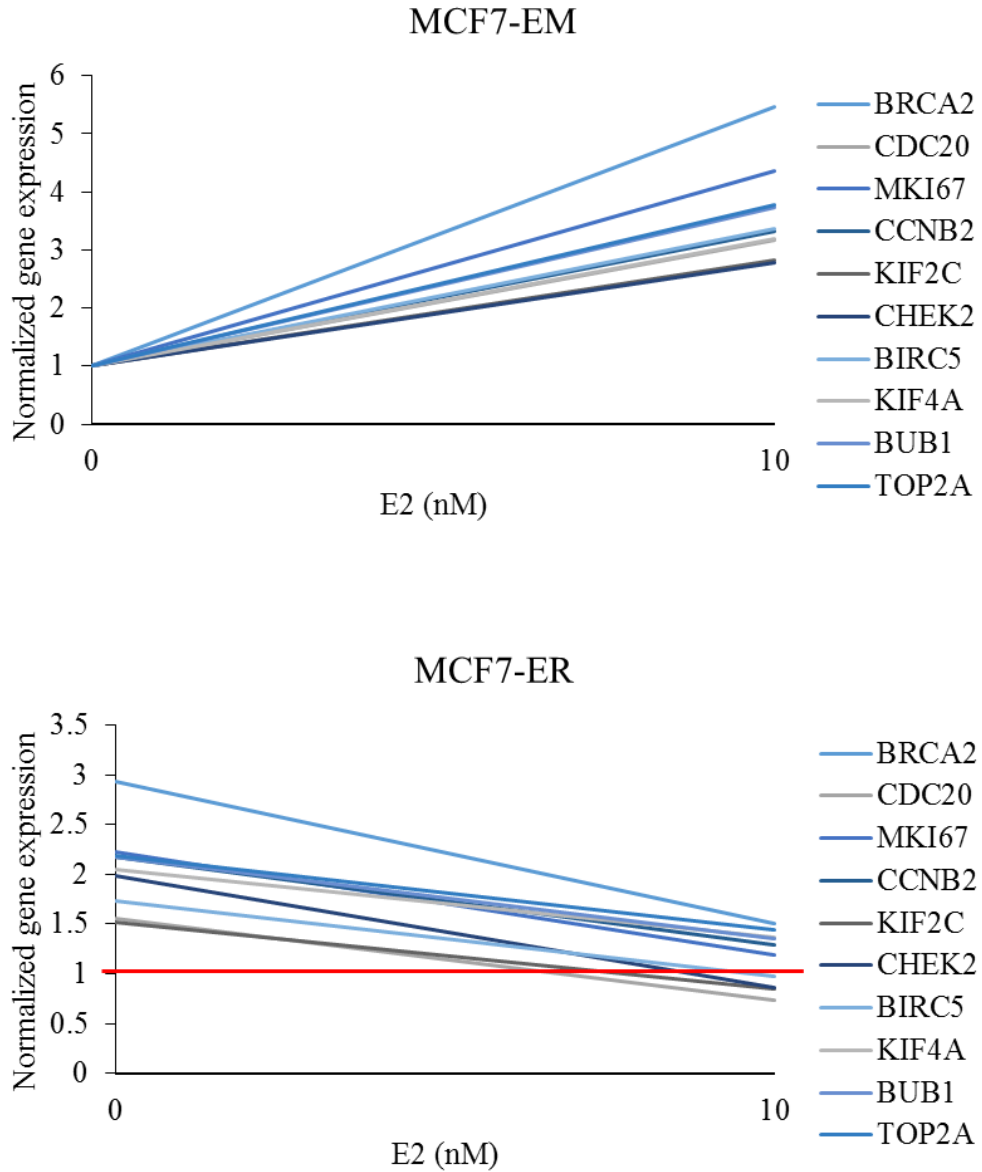


Figure 2.17 E2 induces the differential regulation of 10 cell cycle genes in MCF7-EM and MCF7-ER cells. RNA was extracted from MCF7-EM and MCF7-ER cells treated with 0 or 10 nM E2 for 24 hours and quantified by RT-qPCR. Gene expression was normalized to three house-keeping genes and MCF7-EM 0 E2 control was set to 1. The red line in the MCF7-ER figure marks the value of the MCF7-EM 0 E2 condition. The mean gene expression level is shown, n=3.

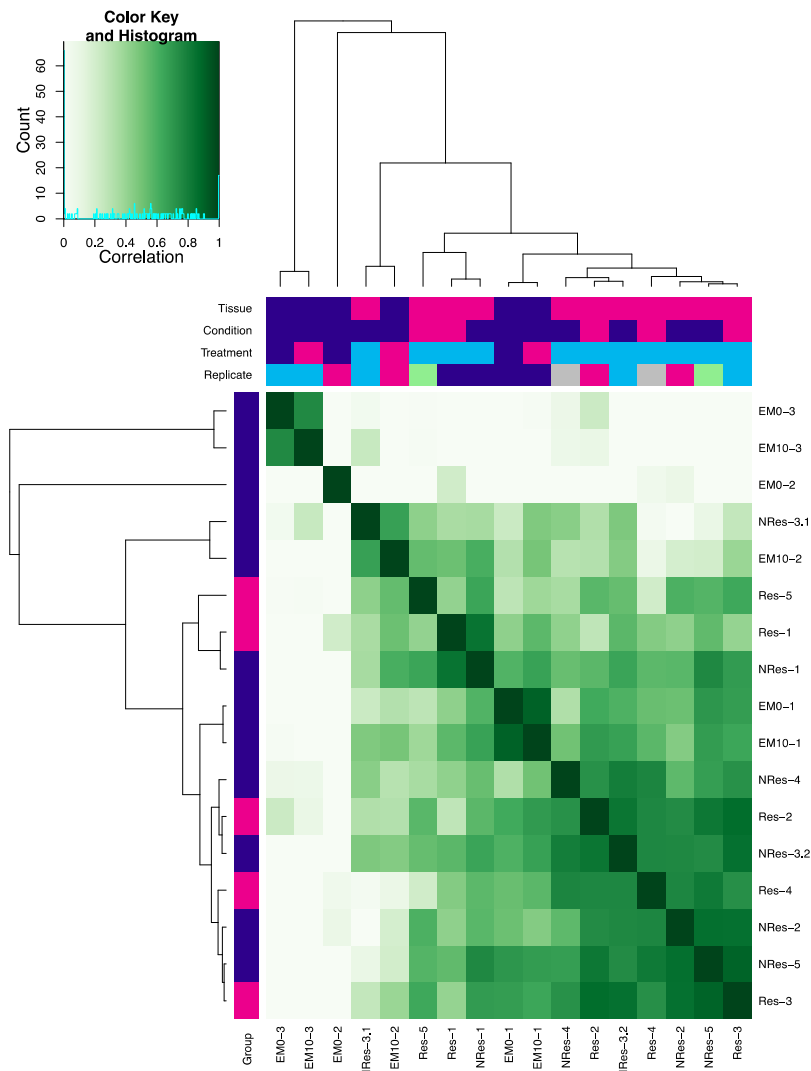


Figure 2.18 ER binding patterns in MCF7-EM cells do not correspond with tamoxifen response. Correlation heat map for ER peaks obtained from MCF7-EM cells treated with vehicle control (EM0; n=3) or 10 nM E2 (EM10; n=3) and tamoxifen responsive (Res; n=5) and tamoxifen nonresponsive (NRes; n=5) patients from (31).

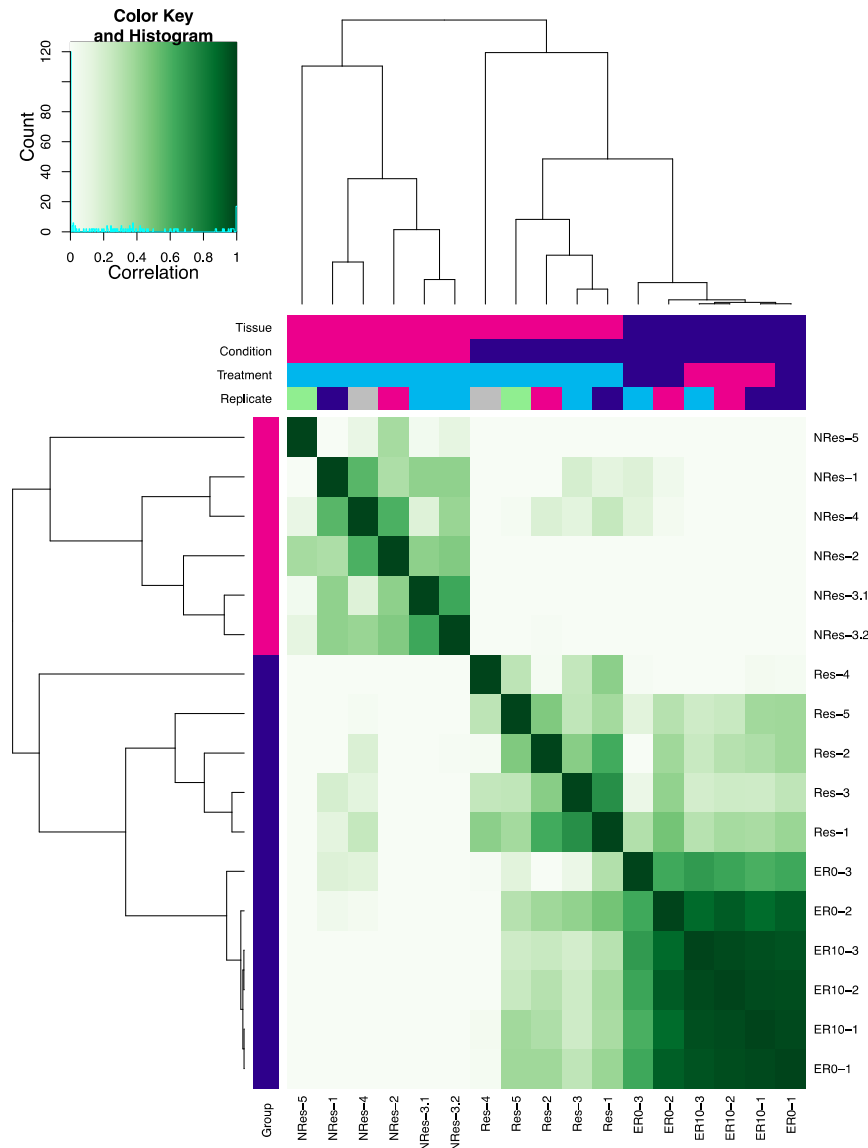


Figure 2.19 ER binding in MCF7-ER cells correlates with ER+ patients that respond to tamoxifen. Correlation heat map for ER peaks obtained from MCF7-ER cells treated with vehicle control (ER0; n=3) or 10 nM E2 (ER10; n=3) and tamoxifen responsive (Res; n=5) and tamoxifen nonresponsive (NRes; n=5) patients from (31).

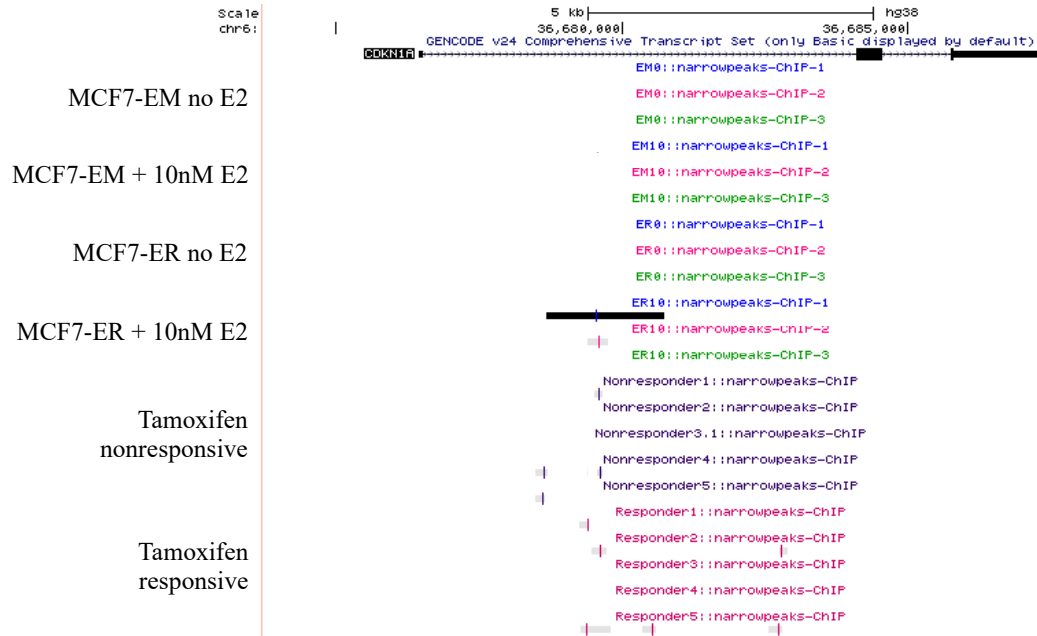


Figure 2.20 The intragenic region of *CDKN1A* is bound by ER in tamoxifen nonresponsive and responsive tumors. UCSC genome browser view of *CDKN1A* showing mapped DNA binding from MCF7-EM (n=3), MCF7-ER (n=3), tamoxifen nonresponsive (n=5) and tamoxifen responsive (n=5) patients from (31). The significant ER peak at an intragenic region of *CDKN1A* is highlighted in light blue. Only the peaks which were present in at least two biological replicates are shown. The three biological replicates for the MCF7-EM and MCF7-ER data are shown by blue, pink and green labels. The five biological replicates for the tamoxifen nonresponsive patients are shown in purple. The five biological replicates for the tamoxifen responsive patients are shown in dark pink.

2.5 References

1. Hugh J, Hanson J, Cheang MCU, Nielsen TO, Perou CM, Dumontet C, et al. Breast Cancer Subtypes and Response to Docetaxel in Node-Positive Breast Cancer: Use of an Immunohistochemical Definition in the BCIRG 001 Trial. *J Clin Oncol.* 2009;27(8):1168-76.
2. Lonning PE. Poor-prognosis estrogen receptorpositive disease: present and future clinical solutions. *Therapeutic Advances in Medical Oncology.* 2012;4(3):127-37.
3. Peethambaram P, Ingle J, Suman V, Hartmann L, Loprinzi C. Randomized trial of diethylstilbestrol vs. tamoxifen in postmenopausal women with metastatic breast cancer. An updated analysis. *Breast Cancer Res Treat.* 1999;54(2):117-22.
4. Ellis MJ, Gao F, Dehdashti F, Jeffe DB, Marcom PK, Carey LA, et al. Lower-dose vs high-dose oral estradiol therapy of hormone receptor-positive, aromatase inhibitor-resistant advanced breast cancer: A phase 2 randomized study. *J Am Med Assoc.* 2009;302(7):774-80.
5. Kedar RP, Bourne TH, Powles TJ, Collins WP, Ashley SE, Cosgrove DO, et al. Effects of Tamoxifen on Uterus and Ovaries of Postmenopausal Women in a Randomized Breast-Cancer Prevention Trial. *Lancet.* 1994;343(8909):1318-21.
6. Love RR, Mazess RB, Barden HS, Epstein S, Newcomb PA, Jordan VC, et al. Effects of Tamoxifen on Bone-Mineral Density in Postmenopausal Women with Breast-Cancer. *N Engl J Med.* 1992;326(13):852-6.
7. Prat A, Karginova O, Parker JS, Fan C, He X, Bixby L, et al. Characterization of cell lines derived from breast cancers and normal mammary tissues for the study of the intrinsic molecular subtypes. *Breast Cancer Res Treat.* 2013;142(2):237-55.

8. Kao J, Salari K, Bocanegra M, Choi Y, Girard L, Gandhi J, et al. Molecular Profiling of Breast Cancer Cell Lines Defines Relevant Tumor Models and Provides a Resource for Cancer Gene Discovery. *Plos One*. 2009;4(7):e6146.
9. Neve RM, Chin K, Fridlyand J, Yeh J, Baehner FL, Fevr T, et al. A collection of breast cancer cell lines for the study of functionally distinct cancer subtypes. *Cancer Cell*. 2006;10(6):515-27.
10. Katzenellenbogen B, Kendra K, Norman M, Berthois Y. Proliferation, Hormonal Responsiveness, and Estrogen-Receptor Content of MCF-7 Human-Breast Cancer-Cells Grown in the Short-Term and Long-Term Absence of Estrogens. *Cancer Res*. 1987;47(16):4355-60.
11. Liao X, Lu D, Wang N, Liu L, Wang Y, Li Y, et al. Estrogen receptor alpha mediates proliferation of breast cancer MCF-7 cells via a p21/PCNA/E2F1-dependent pathway. *Febs Journal*. 2014;281(3):927-42.
12. Foster J, Henley D, Ahamed S, Wimalasena J. Estrogens and cell-cycle regulation in breast cancer. *Trends in Endocrinology and Metabolism*. 2001;12(7):320-7.
13. Grana X, Reddy E. Cell-Cycle Control in Mammalian-Cells - Role of Cyclins, Cyclin-Dependent Kinases (Cdks), Growth Suppressor Genes and Cyclin-Dependent Kinase Inhibitors (Ckis). *Oncogene*. 1995;11(2):211-9.
14. Lodish H, Berk A, Zipursky S, Matsudaira P, Baltimore D, Darnell J. Section 13.7, Checkpoints in Cell-Cycle Regulation. In: *Molecular Cell Biology*. 4th edition ed. W. H. Freeman and Company; 2000.
15. Sherr C, Roberts J. CDK inhibitors: positive and negative regulators of G(1)-phase progression. *Genes Dev*. 1999;13(12):1501-12.

16. Weinberg R. The Retinoblastoma Protein and Cell-Cycle Control. *Cell*. 1995;81(3):323-30.
17. Zheng N, Fraenkel E, Pabo CO, Pavletich NP. Structural basis of DNA recognition by the heterodimeric cell cycle transcription factor E2F-DP. *Genes Dev*. 1999;13(6):666-74.
18. Desdouets C, Sobczak-Thepot J, Murphy M, Brechot C. Cyclin A: function and expression during cell proliferation. *Prog Cell Cycle Res*. 1995;1:115-23.
19. Prall O, Carroll J, Sutherland R. A low abundance pool of nascent p21(WAF1/Cip1) is targeted by estrogen to activate cyclin E-Cdk2. *J Biol Chem*. 2001;276(48):45433-42.
20. Zhao H, Yu J, Peltier CP, Davie JR. Elevated expression of the estrogen receptor prevents the down-regulation of p21(Waf1/Cip1) in hormone dependent breast cancer cells. *J Cell Biochem*. 2004;93(3):619-28.
21. Miller TW. ER α -dependent E2F transcription can mediate resistance to estrogen deprivation in human breast cancer. *ArrayExpress Archive*. 2012 2015-08-27.
22. Stender JD, Frasor J, Komm B, Chang KCN, Kraus WL, Katzenellenbogen BS. Estrogen-regulated gene networks in human breast cancer cells: Involvement of E2F1 in the regulation of cell proliferation. *Molecular Endocrinology*. 2007;21(9):2112-23.
23. Peng J, Jordan VC. Expression of estrogen receptor alpha with a Tet-off adenoviral system induces G0/G1 cell cycle arrest in SKBr3 breast cancer cells. *Int J Oncol*. 2010;36(2):451-8.

24. Sørli T, Perou CM, Tibshirani R, Aas T, Geisler S, Johnsen H, et al. Gene expression patterns of breast carcinomas distinguish tumor subclasses with clinical implications. *Proc Natl Acad Sci U S A*. 2001;98(19):10869-74.
25. Dowsett M, Ebbs SR, Dixon JM, Skene A, Griffith C, Boeddinghaus I, et al. Biomarker changes during neoadjuvant anastrozole, tamoxifen, or the combination: Influence of hormonal status and HER-2 in breast cancer - A study from the IMPACT trialists. *Journal of Clinical Oncology*. 2005;23(11):2477-92.
26. Jenkins EO, Deal AM, Anders CK, Prat A, Perou CM, Carey LA, et al. Age-specific changes in intrinsic breast cancer subtypes: A focus on older women. *Oncologist*. 2014;19(10):1076-83.
27. Verkasalo PK, Thomas HV, Appleby PN, Davey GK, Key TJ. Circulating levels of sex hormones and their relation to risk factors for breast cancer: A cross-sectional study in 1092 pre- and postmenopausal women (United Kingdom). *Cancer Causes Control*. 2001;12(1):47-59.
28. Langmead B, Salzberg SL. Fast gapped-read alignment with Bowtie 2. *Nature Methods*. 2012;9(4):357-U54.
29. Li H, Handsaker B, Wysoker A, Fennell T, Ruan J, Homer N, et al. The Sequence Alignment/Map format and SAMtools. *Bioinformatics*. 2009;25(16):2078-9.
30. Zhang Y, Liu T, Meyer CA, Eeckhoute J, Johnson DS, Bernstein BE, et al. Model-based Analysis of ChIP-Seq (MACS). *Genome Biol*. 2008;9(9):R137.
31. Ross-Innes CS, Stark R, Teschendorff AE, Holmes KA, Ali HR, Dunning MJ, et al. Differential oestrogen receptor binding is associated with clinical outcome in breast cancer. *Nature*. 2012;481(7381):389-U177.

32. DiffBind: differential binding analysis of ChIP-seq peak data [Internet].: Bioconductor; 2011. Available from:
<http://bioconductor.org/packages/release/bioc/html/DiffBind.html>.
33. Leclercq G, Heuson JC. Therapeutic Significance of Sex-Steroid Hormone Receptors in Treatment of Breast-Cancer. *Eur J Cancer*. 1977;13(11):1205-15.
34. Heuson JC, Longeval E, Mattheiem WH, Deboel MC, Sylvester RJ, Leclercq G. Significance of Quantitative Assessment of Estrogen Receptors for Endocrine Therapy in Advanced Breast-Cancer. *Cancer*. 1977;39(5):1971-7.
35. Villalobos M, Olea N, Brotons J, Oleaserrano M, Dealmodovar J, Pedraza V. The E-Screen Assay - a Comparison of Different MCF7 Cell Stocks. *Environ Health Perspect*. 1995;103(9):844-50.
36. Fowler A, Solodin N, Preisler-Mashey M, Zhang P, Lee A, Alarid E. Increases in estrogen receptor-alpha concentration in breast cancer cells promote serine 118/104/106-independent AF-1 transactivation and growth in the absence of estrogen. *Faseb Journal*. 2004;18(1):81-93.
37. Sobell H. Actinomycin and Dna-Transcription. *Proc Natl Acad Sci U S A*. 1985;82(16):5328-31.
38. Schodin D, Zhuang Y, Shapiro D, Katzenellenbogen B. Analysis of mechanisms that determine dominant negative estrogen receptor effectiveness. *J Biol Chem*. 1995;270(52):31163-71.
39. Kushner P, Hort E, Shine J, Baxter J, Greene G. Construction of Cell-Lines that Express High-Levels of the Human Estrogen-Receptor and are Killed by Estrogens. *Molecular Endocrinology*. 1990;4(10):1465-73.

40. Jordan VC. The new biology of estrogen-induced apoptosis applied to treat and prevent breast cancer. *Endocr Relat Cancer*. 2015;22(1):R1-R31.
41. Moggs JG, Murphy TC, Lim FL, Moore DJ, Stuckey R, Antrobus K, et al. Anti-proliferative effect of estrogen in breast cancer cells that re-express ER α is mediated by aberrant regulation of cell cycle genes. *J Mol Endocrinol*. 2005;34(2):535-51.
42. Prall OWJ, Sarcevic B, Musgrove EA, Watts CKW, Sutherland RL. Estrogen-induced activation of Cdk4 and Cdk2 during G(1)-S phase progression is accompanied by increased cyclin D1 expression and decreased cyclin-dependent kinase inhibitor association with cyclin E-Cdk2. *J Biol Chem*. 1997;272(16):10882-94.
43. Dalvai M, Bystricky K. Cell Cycle and Anti-Estrogen Effects Synergize to Regulate Cell Proliferation and ER Target Gene Expression. *Plos One*. 2010;5(6):e11011.
44. Docquier A, Harmand P, Fritsch S, Chanrion M, Darbon J, Cavailles V. The Transcriptional Coregulator RIP140 Represses E2F1 Activity and Discriminates Breast Cancer Subtypes. *Clinical Cancer Research*. 2010;16(11):2959-70.

**Chapter 3: Increased ER expression mediates differential gene regulation by
binding to high and low affinity DNA regions**

3.1 Introduction

The findings from chapter 2 suggest that increased ER expression promotes an anti-proliferative response that involves direct ER-DNA binding. There has been a steady evolution of knowledge regarding ER-DNA interactions. Early ChIP experiments found ER binding within the 5 kb proximal promoter regions of *pS2 (TFF1)* which subsequently is associated with the recruitment of cofactors to regulate gene transcription (1, 2). More recent experiments combining ChIP with genome wide sequencing have shown that 96% of ER binding occurs outside of the gene's proximal promoter (3). With the majority of ER binding within a 50 kb window around the gene's transcription start site (TSS) (3, 4). Surprisingly, ChIP-Seq experiments done in E2-depleted cells have recently shown that unliganded ER can bind DNA and regulate gene expression (5). The transcriptional capacity of unliganded ER may serve as the mechanism that regulates the basal expression of cell cycle genes described in chapter 2.

To date, ChIP-Seq experiments studying the ER-binding patterns that mediate transcriptional regulation in the presence and absence of E2 have been heavily focused on the MCF-7 cell line (3, 5-8). Comparison of MCF-7 cells against ER+ patient samples found that the ER-binding patterns correlate more closely to patients who were nonresponsive to tamoxifen (9). These findings suggest the ER binding signatures obtained from MCF-7 ChIP-Seq datasets are not representative of the ER-mediated transcriptional responses that might occur in luminal A tumors. The results from chapter 2 have shown ER binding in MCF7-ER cells correlates best with tamoxifen responsive patients. This suggests that increased ER expression generates a DNA binding pattern that may be more representative of the hormone response seen in luminal A tumors. The results from chapter

2 and those of others have shown that increased ER expression promotes an anti-proliferative response to E2 that is mediated by the regulation of several proliferation and cell cycle associated genes (10, 11). This anti-proliferative response is mediated via transcriptional regulation that requires an intact DBD. Significantly, one study investigating ER-binding in MDA-MB-231 cells with exogenous ER expression (231-ER) found 44% of ER peaks obtained from these cells do not overlap with those from MCF-7 ChIP-Seq profiles (12). Unlike parental MCF-7 cells, the 231-ER cells have an anti-proliferative response to E2 (11) and the presence of a unique set of ER peaks in the 231-ER cells may enable this growth suppressive response. In this chapter the effects of increased ER expression on gene regulation will be examined using full transcriptome sequencing combined with the ChIP-Seq data from chapter 2. These experiments will test the hypothesis that increased ER expression enables receptor binding to lower affinity sites that regulate a differential transcriptional response to E2.

3.2 Methods

All experiments were designed through equal collaboration between Judith Hugh and Lacey Haddon and were conducted by Lacey Haddon. Additional support for the bioinformatics was provided by Hosna Jabbari and is documented in the appropriate sections.

3.2.1 RNA-Seq

Total RNA was extracted from four biological replicates as described in section 2.2.10. RNA quality was assessed using the Agilent Bioanalyzer 2100 Eukaryote Total RNA Nano chip and all samples had RNA integrity number (RIN) scores from 8.9-10 (see Table B1 and Figure B7 in Appendix B). cDNA libraries were made from 1 μ g total RNA

using the NEBNext Poly(A) mRNA Magnetic Isolation Module (E7490) and NEBNext Ultra Directional RNA Library Prep Kit for Illumina (E7420) and indexed for sequencing using NEBNext Multiplex Oligos for Illumina. Library fragment distribution was measured on the Agilent Bioanalyzer 2100 High Sensitivity DNA chip (see Figure B7 in Appendix B). Libraries were sequenced on Illumina's NextSeq 500 using the NextSeq 500/550 High Output Kit (2x75 cycles) by the MBSU team in the Department of Biological Sciences at the University of Alberta (Edmonton, AB).

3.2.2 Differential gene expression analysis

Fastq reads obtained from the NextSeq500 were analyzed using the FastQC program and all Fastq files had mean sequence quality scores in the 'very good quality' range of 28-36 (see Figure B8 Appendix B). Fastq reads were aligned with UCSC genome sequence indexes and transcript annotation files for the hg38 reference genome using the Tophat algorithm (13). Differential gene expression analysis was done using Cuffdiff from the Cufflinks package (14). To determine genes that were differentially regulated between the different experimental conditions, the gene lists obtained from Cuffdiff were sorted and only the genes with a Log₂ fold change ≥ 1 or ≤ -1 were used for further analysis. Any remaining genes that were not called as significant by the Cuffdiff algorithm were excluded. Significance was determined by the Cuffdiff algorithm for genes that had a P value less than a false discovery rate (FDR) of 0.05 after a Benjamini-Hochberg correction for multiple testing. This analysis helps to minimize the Type I error in the statistical analysis.

3.2.3 ChIP-Seq analysis

The ChIP experiments were described in detail in chapter 2. The Diffbind program was used to generate a Venn diagram showing the overlap of differentially bound sites from each experimental condition and was generated by Dr. Hosna Jabbari. This analysis used BED files containing all the mapped ER peaks from the three biological replicates for each experimental condition which were generated by Lacey Haddon and Hosna Jabbari.

3.2.4 Motif analysis for ChIP-Seq peaks

The BED files containing ChIP-Seq peak sets for the MCF7-EM and MCF7-ER cells treated with and without E2 were uploaded to the online submission form for MEME-ChIP (Version 4.12.0) which conducts motif analysis of large nucleotide datasets (15). The motif analysis was run in normal mode against a set of known vertebrate motifs from the eukaryotic DNA database. This analysis provided the most common motif associated with each experimental condition. The HOMER (version 4.9.1) motif analysis program was used to determine the top ten motifs that were enriched in the peak sets for each experimental condition (16). For this analysis a BED file was generated as described in section 2.2.14 but with all peak sequences for the three biological replicates included. These BED files were input into the Homer program and analyzed for known motifs that were 5, 10, 15 bp in length.

The sequences associated with peaks of interest were further investigated for the presence of full EREs, non-consensus EREs and ERE half sites. To determine if a potential non-consensus ERE was significant the sequence was input into the online TomTom motif comparison tool from the MEME suite (17). TomTom analysis compared the input sequences against a database of known motifs associated with eukaryotic DNA. The output from this analysis shows motifs that have a similar alignment to the input sequences and

provides a P value representing the probability that this match occurred by random chance. Only P values of ≤ 0.05 were considered significant.

3.2.5 ChIP-String analysis

The methods for ChIP-String analysis are described in section 2.2.16.

3.2.6 Statistical analysis

All experiments had a least 3 biological replicates in order to assess statistical significance. Calculations were done as described in section 2.2.17.

3.3 Results

3.3.1 Increased ER expression mediates differential gene expression in response to E2

The mRNA expression levels for the entire transcriptome in the MCF7-EM and MCF7-ER cells treated with or without E2 for 24 hours were obtained by RNA-Seq experiments. These experiments were done in quadruplicate and the Fastq files obtained from each replicate were annotated to the most recent reference genome (hg38) using the Tophat program. The annotated files were input into the Cuffdiff program to perform differential expression (DE) analysis between conditions. Any genes with a Log₂ fold change of ≥ 1 were considered as significantly up-regulated and those genes with a Log₂ fold change ≤ -1 as significantly down-regulated. Using these criteria, the DE analysis of MCF7-EM cells treated with or without E2 (EM10:EM0) showed 691 genes were up-regulated and 435 genes were down-regulated (Table 3.1). Interestingly, the MCF7-ER cells treated with or without E2 (ER10:ER0) had 2,107 up-regulated genes and 1,866 down-regulated genes (Table 3.1). A comparison of the genes that were up-regulated in the MCF7-EM and MCF7-ER cells after E2 treatment showed only 4% overlap between the two MCF-7

transfectants (Figure 3.1). Similar comparisons for the down-regulated genes in the MCF7-EM and MCF7-ER cells treated with E2 showed only 5.4% of genes were overlapped between the two MCF-7 transfectants (Figure 3.1). These results suggest that in the presence of E2 increased ER expression mediates the expression of a large percentage of genes that are not significantly regulated in the MCF7-EM cells after E2 treatment. A DE analysis between the two MCF-7 transfectants in the absence of E2 (ER0:EM0) showed 794 genes were up-regulated and 1,049 genes were down-regulated in the MCF7-ER cells (Table 3.1). This comparison further suggests the presence of increased ER expression can cause major global changes in transcriptional regulation.

The significantly up-regulated genes from the EM10:EM0 (691), ER0:EM0 (794) and ER10:ER0 (2,107) were compared against the PAM50 gene list, which is currently approved as the Prosigna[®] diagnostic assay for the intrinsic subtyping of breast cancers (18, 19). Twenty genes that were up-regulated in the EM10:EM0 were present in the PAM50 gene list (Table 3.2). These 20 genes were heavily associated with proliferation and included proliferation markers *MKI67* and *CCNB1*. These findings are consistent with the luminal B status of the MCF7-EM cells. Seven genes that were up-regulated in the ER10:ER0 comparison were also present in the PAM50 gene list (Table 3.2). These genes included *BCL2* and *FOXA1* which are associated with the luminal A intrinsic subtype (20, 21). This provides further support that increased ER expression in the presence of E2 promotes a gene profile that better matches that of luminal A tumors. There were eight genes up-regulated in the ER0:EM0 analysis that were also present in the PAM50 gene list (Table 3.2). Interestingly, six of these genes were also up-regulated in the EM10:EM0

comparison (Table 3.2). This overlap is consistent with the increased basal proliferation seen in the MCF7-ER cells in the absence of E2 described in chapter 2

In order to investigate the mechanism whereby increased ER can mediate an anti-proliferative response to E2, subsequent experiments were focused on genes that show a differential response to E2 in the MCF7-EM versus MCF7-ER cells. Targeting this subset of genes allowed the examination of potential changes in ER binding near genes that became repressed by E2 when the level of ER was increased. The DE datasets for EM10:EM0 and ER10:ER0 were used to determine which genes show a differential response to E2 in the two MCF-7 transfectants. This analysis found 383 genes that were up-regulated in the ER10:ER0 and down-regulated in the EM10:EM0 datasets (Table 3.3). Conversely, there were 349 genes that were up-regulated in the EM10:EM0 and down-regulated in the ER10:ER0 datasets (Table 3.3).

The protein analysis through evolutionary relationships (PANTHER) classification system (22, 23) was used for functional analysis of these two gene lists. This analysis found the 383 genes that are down-regulated in the EM10:EM0 and up-regulated in the ER10:ER0 datasets were enriched for regulation of cell communication (65%) a functional group that includes genes involved in signal transduction (Figure 3.2). These genes may be involved in pro-maturation or secretory responses involved in differentiation rather than proliferation. The presence of only 11% of genes associated with cell cycle function also suggests there is minimal regulation of cell cycle associated genes consistent with the anti-proliferative response present in the MCF7-ER cells treated with E2 (Figure 3.2). As expected the 349 genes that were up-regulated in the EM10:EM0 and down-regulated in the ER10:ER0 datasets were enriched for genes associated with the cell cycle (40%) as well

as cell communication (27%) and chromosome segregation (13%) consistent with the increased mitotic activity in the MCF7-EM cells upon E2 treatment (Figure 3.3). Since these differentially regulated genes were likely responsible for the differences in proliferative response to E2 further investigations focused on this 349 gene subset.

The results from chapter 2 indicated MCF7-ER cells have a basal increase in proliferation when compared to MCF7-EM cells grown in the absence of E2. Therefore, the assumption that genes in the ER0:EM0 DE dataset would be regulated in the same direction as the EM10:EM0 DE analysis was made. When this comparison was included, the 349 gene list was narrowed to 72 genes that were: (i) significantly increased in MCF7-EM cells treated with E2; (ii) decreased in the MCF7-ER cells with E2; and (iii) increased in the MCF7-ER cells without E2 (Table 3.4, Figure 3.4). When the 72-gene list was analyzed with the PANTHER classification system 20 of the 68 recognized genes were found to be involved in chromosome segregation (4), mitosis (6) and cell cycle (10) processes (FDR<0.05) (Table 3.5).

The ChIP-Seq data was used to further investigate the role of ER-binding in the differential transcriptional response to E2. Increased ER expression was shown to lead to an overall increase in ER binding in the absence of E2 (75,565 in ER0 vs. 56,432 in EM0) (Figure 3.5). A similar number of total ER binding events was found between the MCF7-EM cells treated with E2 (108,380) and the MCF7-ER cells treated with E2 (105,330) (Figure 3.6). Notably, only 35,913 ER peaks were shared between these two conditions. The ChIP-Seq results found thousands of ER peaks that were unique to the MCF7-ER cells indicating that increased ER expression promotes receptor binding to novel regions both in the presence and absence of E2. Motif analysis using the MEME-ChIP program (15)

showed the most common motifs for the MCF7-EM cells in the absence and presence of E2 were a half ERE and the full ERE, respectively (Figure 3.5). For the MCF7-ER cells, the most common motif was a half ERE, irrespective of the absence or presence of E2 (Figure 3.5). Further analysis of the motif enrichment using the HOMER motif analysis software (16) found the MCF7-EM cells treated with E2 show enrichment of essential cofactors for ER-mediated chromatin reconfiguration: CTCF, FOXA1, GATA3 and AP-2 γ (Table 3.6) (24). Importantly, the MCF7-ER cells have a significantly greater enrichment of these motifs in the absence of E2 and maintain the enrichment of FOXA1, GATA3 and AP-2 γ motifs after E2 treatment (Table 3.6). The increase in ER binding with or without E2 suggests that ER may regulate the differential response to E2 through novel binding at genes involved in cell cycle regulation and proliferation in the MCF7-ER cells. The enrichment of the half ERE in the MCF7-ER peak sets suggests that these novel binding sites may harbor lower affinity ER motifs. The enrichment of motifs for factors involved in chromatin reconfiguration suggest that DNA remodeling may be involved in this mechanism.

Using the ChIP-Seq peak sets loaded onto the UCSC genome browser; a search of a 50 kb window around the TSS was done for each of the 72 differentially expressed genes and found 37 genes with ER bound within 50 kb in at least one experimental condition (Figure 3.4). ER peaks were only considered significant if they were present in at least 2/3 biological replicates. The ChIP-String assay was used to confirm the presence of ER binding for 14 genes that had significant ER binding under multiple experimental conditions (Figure 3.6). Three previously mapped ER binding sequences associated with well-known E2-regulated genes (*GREB1*, *BCL2* and *CCND1*) were included as positive

controls (Figure 3.6). The ChIP-String assay uses custom designed fluorescently labelled DNA probes that hybridize DNA sequences that match individual ER peaks. Once hybridized to ChIP DNA samples the fluorescent labelling enables the probes to be counted and quantified. The use of this assay enabled an assessment of the enrichment of multiple ER peaks simultaneously. When ER binding was normalized to the MCF7-EM cells without E2 (EM0) increases in ER binding were detected for the majority of these genes, with the greatest level of binding being present after E2 treatment for both the MCF7-EM and MCF7-ER cells (Figure 3.6).

Five of the genes that had ER binding validated by ChIP-String were selected for RT-qPCR validation of gene expression due to the presence of ER binding at proximal and distal regions in the ChIP-Seq data which were associated with previously mapped DNA loops (Figure 3.4). This binding pattern was required for further experiments that will be described in chapter 4. RT-qPCR analysis confirmed *ADORA1*, *TFF1*, *XBPI*, *AURKB*, and *IGFBP4* were up-regulated in the MCF7-EM cells after E2 treatment, and down-regulated in the MCF7-ER cells after E2 treatment (Figure 3.7). Furthermore, a basal level of transcription was confirmed for these genes in the MCF7-ER cells in the absence of E2 (Figure 3.7).

To determine how ER may be regulating the differential expression of the five genes the UCSC genome browser was used to examine the patterns of ER binding within a 50 kb window of each gene (Table 3.7). Four genes (*ADORA1*, *TFF1*, *XBPI* and *IGFBP4*) had ER binding in the MCF7-EM cells treated with E2 and in the MCF7-ER cells treated with and without E2 (Table 3.7; Figures 3.8-3.11). These regions contained full EREs which were confirmed by the TomTom motif comparison tool (Table 3.7) (17). The ChIP-Seq

data also indicated additional ER binding within a 50 kb window for each of these four genes (Table 3.7; Figures 3.8-3.11). These regions were most commonly found in only the MCF7-ER cells and may be involved in the basal activity and repressive effects of ER seen in these cells. Unlike the first four genes, *AURKB* had ER binding outside of a 100 kb window that was present in the MCF7-ER cells with and without E2 but not in either of the MCF7-EM peak sets (Table 3.7; Figure 3.12). This region did not contain an ERE but did have one ERE half site (TGACC) and binding was confirmed at this region in the MCF7-ER cells treated with E2 (Figure 3.12). There were four additional ER peaks present in the MCF7-ER cells only, and one ER peak that was bound only in the MCF7-EM cells treated with E2. This data suggests that when ER expression is increased the receptor may regulate this gene by binding to completely separate regions on the DNA.

Further investigation into the ER peaks that were unique to the MCF7-ER cells for each of the five differentially regulated genes showed that these regions most often harbor half-EREs rather than the full palindromic sequence. This is in line with the finding that the half ERE was the most enriched sequence in the ChIP-Seq peak sets for the MCF7-ER cells.

3.4 Conclusions

The results from the RNA-Seq experiments have shown that increased ER expression alters the expression of hundreds of genes that were not significantly regulated in the MCF7-EM cells. These experiments have also shown that there is minimal overlap in the genes that are up-regulated or down-regulated by E2 when comparing the two MCF-7 transfectants. This result suggests that a significant portion of genes may have a differential response to E2 depending on the level of ER expression. Investigation into whether increased ER expression could promote differential regulation led to 349 genes that were

up-regulated in the MCF7-EM cells and down-regulated in the MCF7-ER cells after E2 treatment. This list was narrowed further by including genes that were significantly up-regulated in the absence of E2 in the MCF7-ER cells compared to the MCF7-EM cells to account for the basal proliferation seen in the MCF7-ER cells. From this analysis a final list of 72 genes that show a differential response to E2 that is most likely mediated by increased ER expression was obtained. This dataset was enriched for genes involved in chromosomal segregation, mitosis and cell cycle function. This provides further evidence that the differential proliferative response is mediated through the ER regulation of cell cycle genes.

The expression of five genes with significant ER binding within 50-100 kb of the TSS from the 72-gene list was confirmed by RT-qPCR. Four genes had ER bound at the same region in both the MCF7-EM and MCF7-ER cells, indicating ER may regulate gene activation and repression through the same binding site. These ER peaks often contained full EREs which further confirms their function as high affinity ER binding sites. This was also consistent with the finding that the full ERE was the most common motif in the MCF7-EM + E2 peak set. More notably, several regions were found to be bound only in the MCF7-ER cells. Consistent with motif analysis results these regions primarily contained half EREs and not full ERE motifs. These data suggest that increased ER expression enables binding at high affinity ERE sites as well as novel lower affinity regions that can alter the response of nearby gene(s). HOMER analysis of the ChIP-Seq peak sets found enrichment of CTCF, FOXA1, GATA3 and AP-2 γ motifs and these transcription factors are associated with chromatin remodeling (24). A recent study found that interactions with PR could re-direct ER DNA-binding to distal enhancer regions that were associated with long-range DNA

loops (25). When put in the context of the current findings; this could suggest that increased ER expression leads to a differential response to E2 that is mediated by novel ER binding to distal enhancer regions involved in DNA reconfiguration.

Table 3.1 Summary of differential expression (DE) analysis results. The number of genes that were significantly up-regulated and down-regulated in MCF7-EM cells treated with (EM10; n=4) or without E2 (EM0; n=4) and MCF7-ER cells treated with (ER10; n=4) or without E2 (ER0; n=4).

DE comparison	Up-regulated	Down-regulated
EM10:EM0	691	435
ER10:ER0	2107	1866
ER0:EM0	794	1049

Significant genes have log₂ fold change ≥ 1 or ≤ -1

EM0: MCF7-EM no E2

EM10: MCF7-EM + 10 nM E2

ER0: MCF7-ER no E2

ER10: MCF7-ER + 10 nM E2

Table 3.2 Summary of up-regulated genes that overlap with the PAM50 gene list.

PAM50	EM10:EM0	ER0:EM0	ER10:ER0
UBE2C	X		
PTTG1	X	X	
MYBL2	X	X	
BIRC5	X		
CCNB1	X		
TYMS	X		
MELK	X		
CEP55	X		
KNTC2			
UBE2T	X		
RRM2	X	X	
CDC6	X		
ANLN	X		
ORC6L			
KIF2C	X		
EXO1	X		
CDCA1			
CENPF	X		
CCNE1			
MKI67	X		
CDC20	X		
MMP11			X
GRB7			
ERBB2			
TMEM45B			
BAG1			
PGR	X	X	X
MAPT			
NAT1			
GRP160			
FOXA1			X
BLVRA			
CXXC5		X	
ESR1			
SLC39A6			
KRT17			
KRT5		X	

SFRP1			
BCL2			X
KRT14			
MLPH			
MDM2			
FGFR4			X
MYC	X	X	
MIA			
FOXC1	X	X	X
ACTR3B			
PHGDH			
CDH3			
EGFR			X

X indicates a gene that was up-regulated in the RNA-Seq data by differential analysis

EM0: MCF7-EM no E2 (n=4)

EM10: MCF7-EM + 10 nM E2 (n=4)

ER0: MCF7-ER no E2 (n=4)

ER10: MCF7-ER + 10 nM E2 (n=4)

Table 3.3 Two-way comparison of DE datasets.

Down-regulated	Up-regulated	
	EM10:EM0	ER10:ER0
EM10:EM0	--	383
ER10:ER0	349	--

EM0: MCF7-EM no E2 (n=4)
EM10: MCF7-EM + 10 nM E2 (n=4)
ER0: MCF7-ER no E2 (n=4)
ER10: MCF7-ER + 10 nM E2 (n=4)

Table 3.4 72 genes with a differential response to E2.

Gene	EM0:EM10		EM0:ER0		ER0:ER10	
	Log2 fold change	P value	Log2 fold change	P value	Log2 fold change	P value
CD22[†]	2.80	5.00E ⁻⁰⁵	4.42	5.00E ⁻⁰⁵	-1.89	5.00E ⁻⁰⁵
ITIH2[†]	1.27	5.00E ⁻⁰⁵	1.82	5.00E ⁻⁰⁵	-1.76	5.00E ⁻⁰⁵
MYB[†]	2.61	5.00E ⁻⁰⁵	1.97	5.00E ⁻⁰⁵	-2.75	5.00E ⁻⁰⁵
RASGRP1[†]	1.73	5.00E ⁻⁰⁵	2.65	5.00E ⁻⁰⁵	-2.76	5.00E ⁻⁰⁵
SLC17A9[†]	2.68	5.00E ⁻⁰⁵	2.86	5.00E ⁻⁰⁵	-2.97	5.00E ⁻⁰⁵
SLC47A1[†]	1.55	5.00E ⁻⁰⁵	3.19	5.00E ⁻⁰⁵	-1.04	5.00E ⁻⁰⁵
ADORA1^{**†}	3.19	5.00E ⁻⁰⁵	5.14	5.00E ⁻⁰⁵	-1.10	5.00E ⁻⁰⁵
AMZ1[†]	3.30	5.00E ⁻⁰⁵	3.45	5.00E ⁻⁰⁵	-1.72	5.00E ⁻⁰⁵
AURKB^{*†}	1.72	5.00E ⁻⁰⁵	1.04	5.00E ⁻⁰⁵	-1.58	5.00E ⁻⁰⁵
IGFBP4^{*†}	2.34	5.00E ⁻⁰⁵	1.49	5.00E ⁻⁰⁵	-2.18	5.00E ⁻⁰⁵
OSGIN1[†]	1.12	5.00E ⁻⁰⁵	2.60	5.00E ⁻⁰⁵	-1.72	5.00E ⁻⁰⁵
TFF1^{**†}	3.11	5.00E ⁻⁰⁵	2.06	5.00E ⁻⁰⁵	-1.01	5.00E ⁻⁰⁵
XBP1^{*†}	2.78	5.00E ⁻⁰⁵	2.89	5.00E ⁻⁰⁵	-1.68	5.00E ⁻⁰⁵
AREG[†]	2.46	5.00E ⁻⁰⁵	2.16	5.00E ⁻⁰⁵	-2.07	5.00E ⁻⁰⁵
UGT2B15	5.09	5.00E ⁻⁰⁵	5.68	5.00E ⁻⁰⁵	-2.66	5.00E ⁻⁰⁵
RGS22	4.32	5.00E ⁻⁰⁵	3.69	5.00E ⁻⁰⁵	-1.25	5.00E ⁻⁰⁵
PDZK1	4.07	5.00E ⁻⁰⁵	4.02	5.00E ⁻⁰⁵	-1.54	5.00E ⁻⁰⁵
AGR3	3.47	5.00E ⁻⁰⁵	3.54	5.00E ⁻⁰⁵	-3.70	5.00E ⁻⁰⁵
LOC101928841	3.38	5.00E ⁻⁰⁵	3.23	5.00E ⁻⁰⁵	-2.15	5.00E ⁻⁰⁵

SYTL5	3.22	5.00E- 05	3.29	5.00E- 05	-2.00	5.00E- 05
NPR1	2.69	5.00E- 05	1.85	5.00E- 05	-2.37	5.00E- 05
RERG	2.58	5.00E- 05	1.77	5.00E- 05	-1.52	5.00E- 05
SCNN1B	2.58	5.00E- 05	2.04	5.00E- 05	-1.87	5.00E- 05
SLC4A10	2.39	5.00E- 05	1.22	5.00E- 05	-2.41	5.00E- 05
HS3ST3A1	2.32	5.00E- 05	1.29	5.00E- 05	-1.81	5.00E- 05
SPOCK1	2.16	5.00E- 05	2.11	5.00E- 05	-1.53	5.00E- 05
ASCL1	2.07	5.00E- 05	1.23	5.00E- 05	-5.24	5.00E- 05
DSCC1	2.06	5.00E- 05	1.08	5.00E- 05	-1.40	5.00E- 05
C1QTNF6	2.04	5.00E- 05	1.16	5.00E- 05	-1.18	5.00E- 05
PRC1	1.45	5.00E- 05	1.15	5.00E- 05	-1.16	5.00E- 05
PBK	1.97	5.00E- 05	1.00	5.00E- 05	-1.10	5.00E- 05
SPAG5	1.44	5.00E- 05	1.05	5.00E- 05	-1.39	5.00E- 05
KRT16	1.97	5.00E- 05	3.01	5.00E- 05	-1.28	5.00E- 05
RLN2	1.42	5.00E- 05	1.70	5.00E- 05	-1.14	5.00E- 05
TMEM26	1.95	5.00E- 05	2.76	5.00E- 05	-2.57	5.00E- 05
RNF223	1.41	5.00E- 05	1.64	5.00E- 05	-2.30	5.00E- 05
SEMA3B	1.36	5.00E- 05	3.30	5.00E- 05	-1.86	5.00E- 05
MYBL2	1.79	5.00E- 05	1.08	5.00E- 05	-1.62	5.00E- 05
PRR11	1.36	5.00E- 05	1.24	5.00E- 05	-1.37	5.00E- 05
RNF183	1.75	5.00E- 05	2.12	5.00E- 05	-1.43	5.00E- 05
SHCBP1	1.75	5.00E- 05	1.16	5.00E- 05	-1.03	5.00E- 05

KRT6A	1.32	5.00E ⁻⁰⁵	3.85	5.00E ⁻⁰⁵	-1.20	5.00E ⁻⁰⁵
HLA-DRA	1.26	5.00E ⁻⁰⁵	2.22	5.00E ⁻⁰⁵	-2.24	5.00E ⁻⁰⁵
SKA1	1.68	5.00E ⁻⁰⁵	1.06	5.00E ⁻⁰⁵	-1.00	5.00E ⁻⁰⁵
DIRAS2	1.26	5.00E ⁻⁰⁵	1.14	5.00E ⁻⁰⁵	-3.54	5.00E ⁻⁰⁵
WDR62	1.67	5.00E ⁻⁰⁵	1.02	5.00E ⁻⁰⁵	-1.02	5.00E ⁻⁰⁵
UHRF1	1.25	5.00E ⁻⁰⁵	1.09	5.00E ⁻⁰⁵	-1.46	5.00E ⁻⁰⁵
SYTL4	1.67	5.00E ⁻⁰⁵	1.54	5.00E ⁻⁰⁵	-1.24	5.00E ⁻⁰⁵
MAD2L1	1.66	5.00E ⁻⁰⁵	1.03	5.00E ⁻⁰⁵	-1.25	5.00E ⁻⁰⁵
CCNB2	1.20	5.00E ⁻⁰⁵	1.06	5.00E ⁻⁰⁵	-1.55	5.00E ⁻⁰⁵
ORC1	1.64	5.00E ⁻⁰⁵	1.15	5.00E ⁻⁰⁵	-1.65	5.00E ⁻⁰⁵
HMMR	1.20	5.00E ⁻⁰⁵	1.05	5.00E ⁻⁰⁵	-1.00	5.00E ⁻⁰⁵
CKAP2L	1.60	5.00E ⁻⁰⁵	1.21	5.00E ⁻⁰⁵	-1.25	5.00E ⁻⁰⁵
ARHGAP11A	1.50	5.00E ⁻⁰⁵	1.04	5.00E ⁻⁰⁵	-1.21	5.00E ⁻⁰⁵
ARHGAP11B	1.18	5.00E ⁻⁰⁵	1.04	5.00E ⁻⁰⁵	-1.28	5.00E ⁻⁰⁵
NDC80	1.60	5.00E ⁻⁰⁵	1.09	5.00E ⁻⁰⁵	-1.28	5.00E ⁻⁰⁵
ST8SIA6	1.17	5.00E ⁻⁰⁵	1.09	5.00E ⁻⁰⁵	-1.05	5.00E ⁻⁰⁵
COL21A1	1.59	5.00E ⁻⁰⁵	1.87	5.00E ⁻⁰⁵	-1.66	5.00E ⁻⁰⁵
RAD51AP1	1.57	5.00E ⁻⁰⁵	1.17	5.00E ⁻⁰⁵	-1.15	5.00E ⁻⁰⁵
MMP13	1.12	0.00035	3.71	5.00E ⁻⁰⁵	-1.80	5.00E ⁻⁰⁵
OIP5	1.56	5.00E ⁻⁰⁵	1.12	5.00E ⁻⁰⁵	-1.37	5.00E ⁻⁰⁵
COL6A3	1.05	5.00E ⁻⁰⁵	1.57	5.00E ⁻⁰⁵	-2.15	5.00E ⁻⁰⁵
DTL	1.49	5.00E ⁻⁰⁵	1.02	5.00E ⁻⁰⁵	-1.66	5.00E ⁻⁰⁵

KRT13	1.02	5.00E ⁻⁰⁵	2.38	5.00E ⁻⁰⁵	-1.66	5.00E ⁻⁰⁵
CENPU	1.49	5.00E ⁻⁰⁵	1.09	5.00E ⁻⁰⁵	-1.40	5.00E ⁻⁰⁵
SHC4	2.04	0.0068	2.19	0.00355	-2.43	0.03145
CITED1	1.23	0.0018	3.73	5.00E ⁻⁰⁵	-1.15	5.00E ⁻⁰⁵
MSMB	1.06	0.0009	1.10	0.00025	-1.46	0.00025
CDC25C	1.03	0.0163	1.10	0.0088	-1.34	0.0025
VIM-AS1	2.09	5.00E ⁻⁰⁵	1.05	0.01395	-2.40	0.0055
LOC100506860	1.80	0.0004	1.86	0.0005	-1.22	0.00295
LINC00239	1.34	0.02095	2.31	0.0008	-2.31	0.0018

† ER peaks confirmed by ChIP-String

*Genes confirmed by RT-qPCR

EM0: MCF7-EM no E2 (n=4)

EM10: MCF7-EM + 10 nM E2 (n=4)

ER0: MCF7-ER no E2 (n=4)

ER10: MCF7-ER + 10 nM E2 (n=4)

Table 3.5 PANTHER Overrepresentation results.

PANTHER GO-Slim Biological Process	H. sapiens REFLIST (21042)	Input (68)	Input (expected)	Input (over/under)	Input (fold enrichment)	Input (raw P value)	Input (FDR)
Chromosome segregation	96	4	0.31	+	12.89	3.06E ⁻⁰⁴	2.49E ⁻⁰²
Mitosis	231	6	0.75	+	8.04	1.15E ⁻⁰⁴	1.40E ⁻⁰²
Cell cycle	723	10	2.34	+	4.28	1.13E ⁻⁰⁴	2.75E ⁻⁰²

Table 3.6 HOMER motif analysis of ChIP-Seq peaks.

Condition		Motifs				
		ERE	CTCF	FOXA1	GATA3	AP-2 γ
EM0	P value	1E-357	1E-11	1E-361	1E-72	1E-65
	% Target	8.31	1.60	17.52	16.69	17.17
	% Background	2	0.98	7.24	11.57	12.24
	Enrichment	4.16	1.63	2.42	1.44	1.40
EM10	P value	1E-180	1.0	1E-37	1E-08	1E-47
	% Target	5.04	1.2	3.92	5.7	28.08
	% Background	2.54	1.59	2.82	5.06	24.98
	Enrichment	1.98	0.75	1.39	1.13	1.12
ER0	P value	1E-1415	1E-645	1E-893	1E-893	1E-195
	% Target	11.14	5.12	13.08	13.7	20.89
	% Background	2.6	1.18	4.86	8.57	15.3
	Enrichment	4.28	4.34	2.69	1.60	1.37
ER10	P value	1E-3449	1E-63	1E-447	1E-183	1E-149
	% Target	15.02	2.24	7.12	9.59	23.79
	% Background	3.17	1.4	3.43	6.59	19.61
	Enrichment	4.74	1.60	2.08	1.46	1.21

EM0: MCF7-EM no E2 (n=4)

EM10: MCF7-EM + 10 nM E2 (n=4)

ER0: MCF7-ER no E2 (n=4)

ER10: MCF7-ER + 10 nM E2 (n=4)

Table 3.7 Summary of ChIP-Seq ER binding for five genes with a differential response to E2.

Gene	ER peaks [†]			Tom Tom P value	Additional ER peaks
	Conditions bound	Location (relative to TSS)	Motif		
ADORA1	EM10, ER0, ER10	≤ 50 kb	Full ERE	2.57e ⁻⁰⁵	1 peak bound in ER0 and ER10 5 peaks bound in ER10 only
TFF1	EM10, ER0, ER10	TSS	Full ERE	6.63e ⁻⁰⁴	5 peaks bound in ER10 only
	EM10, ER0, ER10	≤10 kb	Full ERE	3.04e ⁻⁰⁴	
XBP1	EM10, ER0, ER10	≤ 20 kb	Full ERE	3.57e ⁻⁰³	1 peak bound in EM10, ER0 and ER10
IGFBP4	EM10, ER0, ER10	Intragenic	Full ERE	2.39e ⁻⁰⁴	3 peaks bound in ER10 only
AURKB	ER0, ER10	≥ 100kb	Half ERE	-	1 peak bound in EM10 only 1 peak bound in ER0 and ER10 5 peaks bound in ER10 only

[†] ER peaks were validated by ChIP-String analysis

EM0: MCF7-EM no E2 (n=3)

EM10: MCF7-EM + 10 nM E2 (n=3)

ER0: MCF7-ER no E2 (n=3)

ER10: MCF7-ER + 10 nM E2 (n=3)

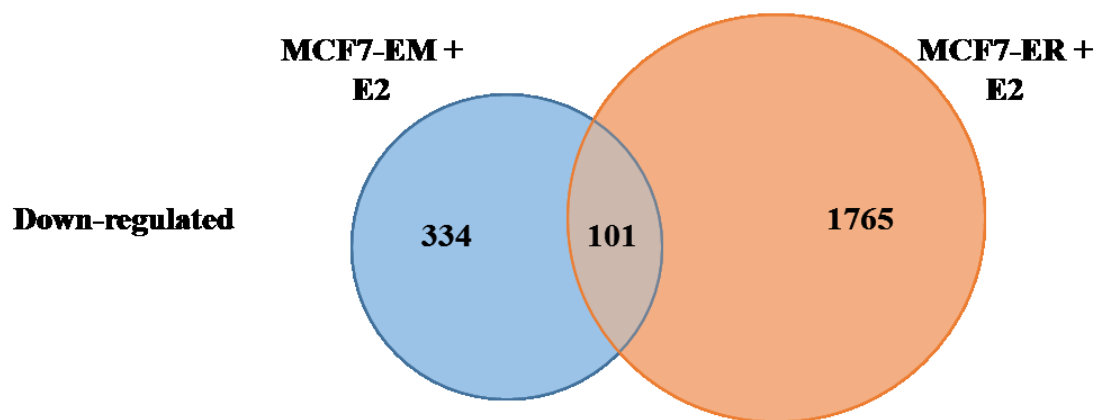
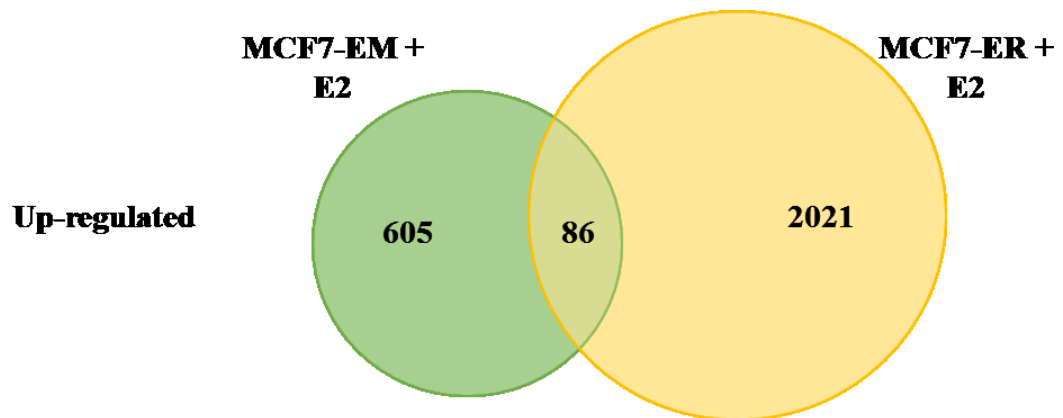


Figure 3.1 Venn diagrams for genes that are up-regulated and down-regulated by E2 in the MCF7-EM and MCF7-ER cells.

EM10:EM0 Down-regulated

ER10:ER0 Up-regulated

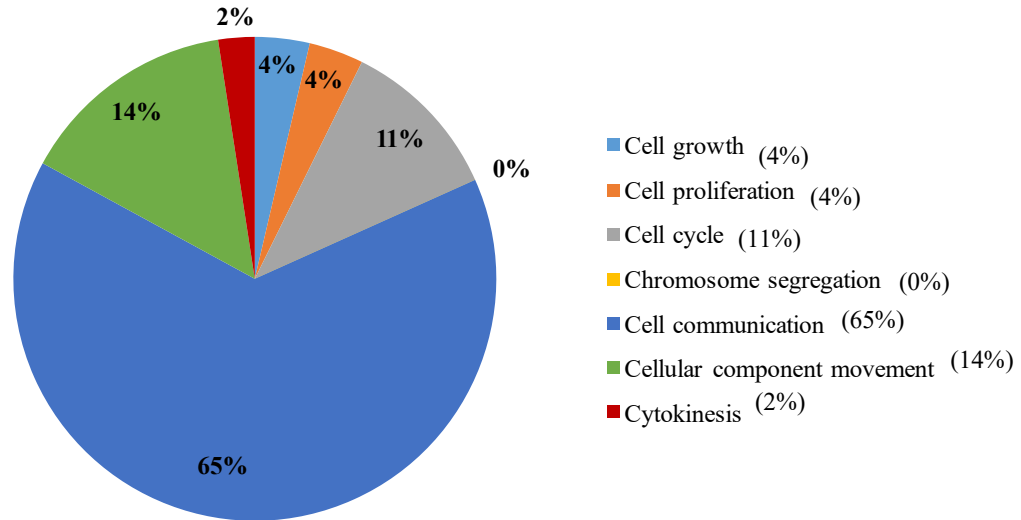


Figure 3.2 Differentially regulated genes that are up-regulated in the MCF7-ER cell line are enriched for cell communication. PANTHER functional analysis showing the major cellular processes for genes that were down-regulated in the MCF7-EM cells after E2 treatment (EM10:EM0) and up-regulated in the MCF7-ER cells after E2 treatment (ER10:ER0).

EM10:EM0 UP-REGULATED

ER10:ER0 DOWN-REGULATED

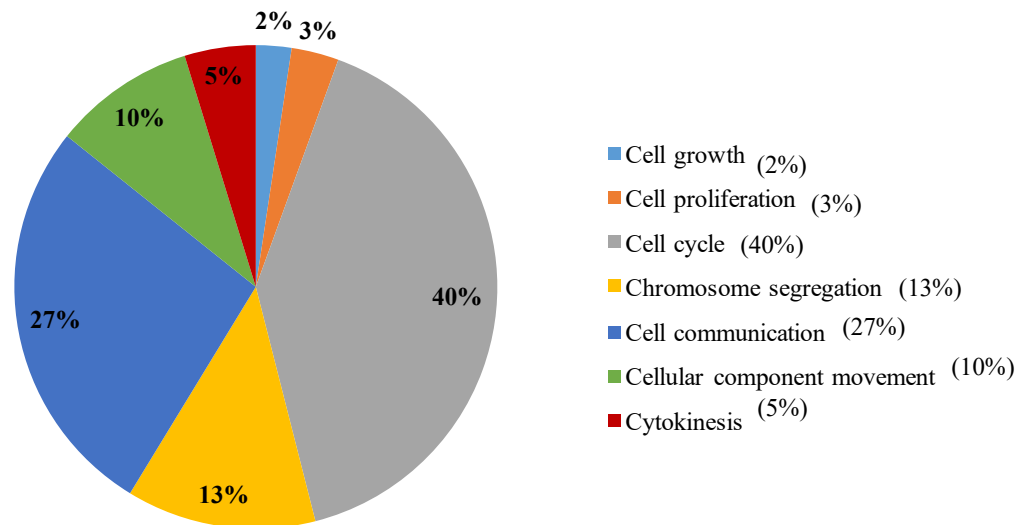


Figure 3.3 Differentially regulated genes that are up-regulated in the MCF7-EM cell line are enriched for cell cycle function. PANTHER functional analysis showing the major cellular processes for genes that were up-regulated in the MCF7-EM cells after E2 treatment (EM10:EM0) and down-regulated in the MCF7-ER cells after E2 treatment (ER10:ER0).

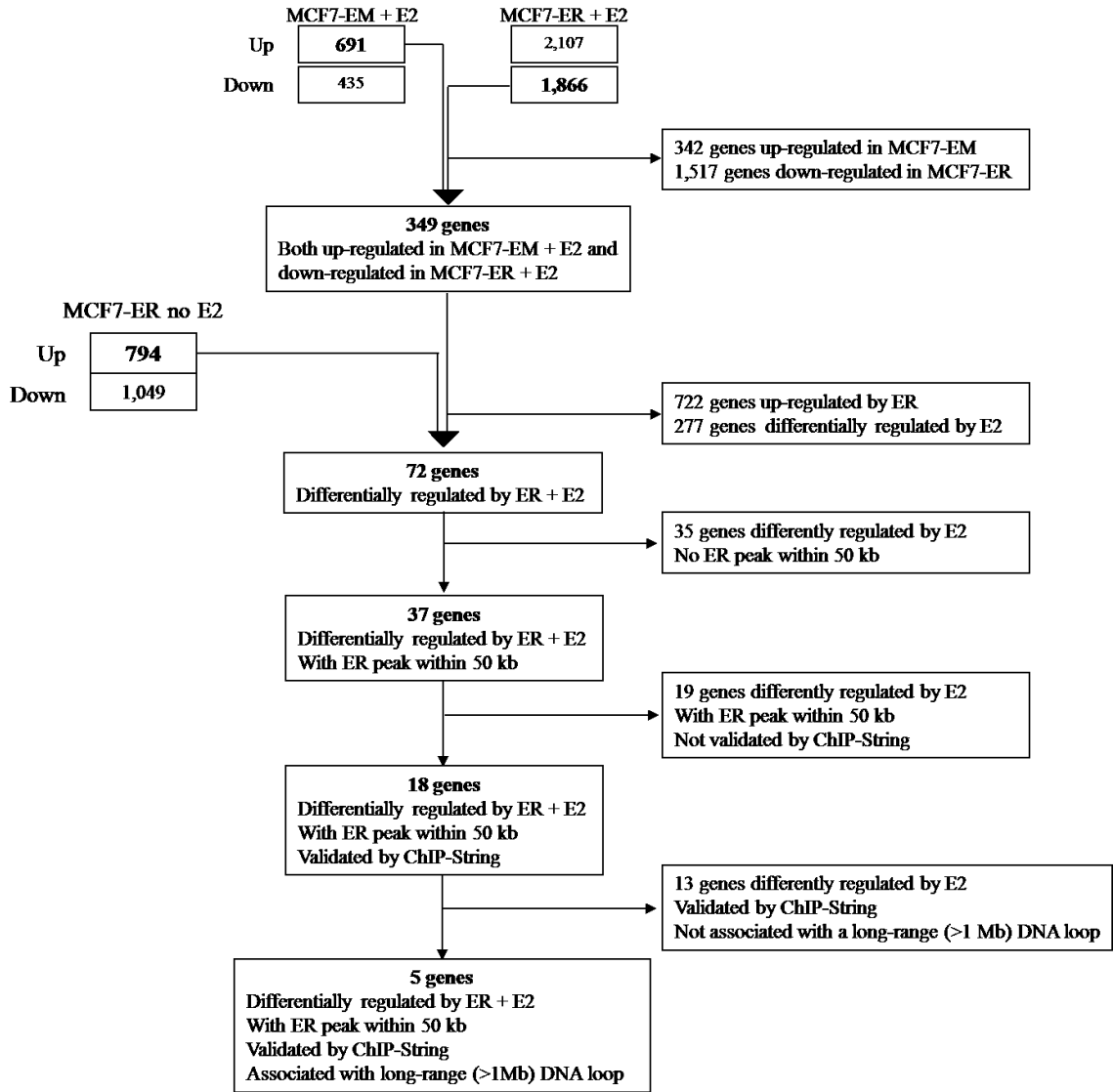


Figure 3.4 Selection process for selecting five differentially regulated genes for validation.

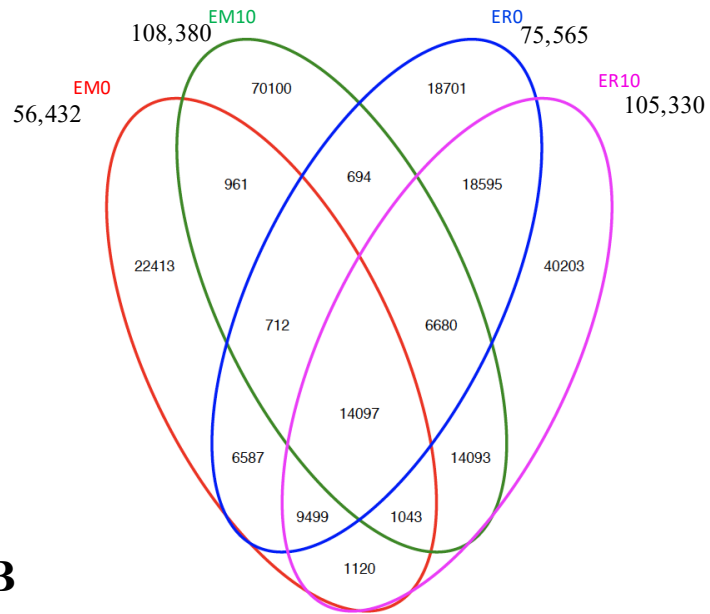
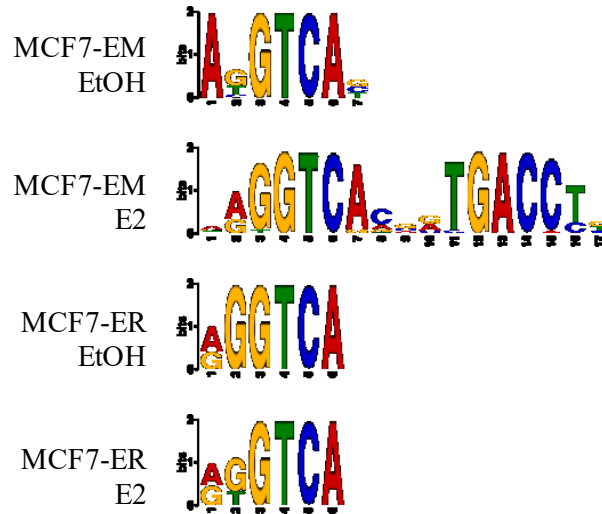
A**B**

Figure 3.5 Increased ER expression leads to novel ER peaks associated with half ERE motifs. **A.** Venn diagram of total ER peaks mapped by ChIP-Seq in MCF7-EM and MCF7-ER cells treated with vehicle control (EM0 and ER0) or 10 nM E2 (EM10 and ER10). Numbers represent the total number of peaks from all three biological replicates. **B.** Top motifs from MEME-ChIP analysis for MCF7-EM and MCF7-ER cells treated with vehicle control (EtOH) or 10 nM E2 (E2).

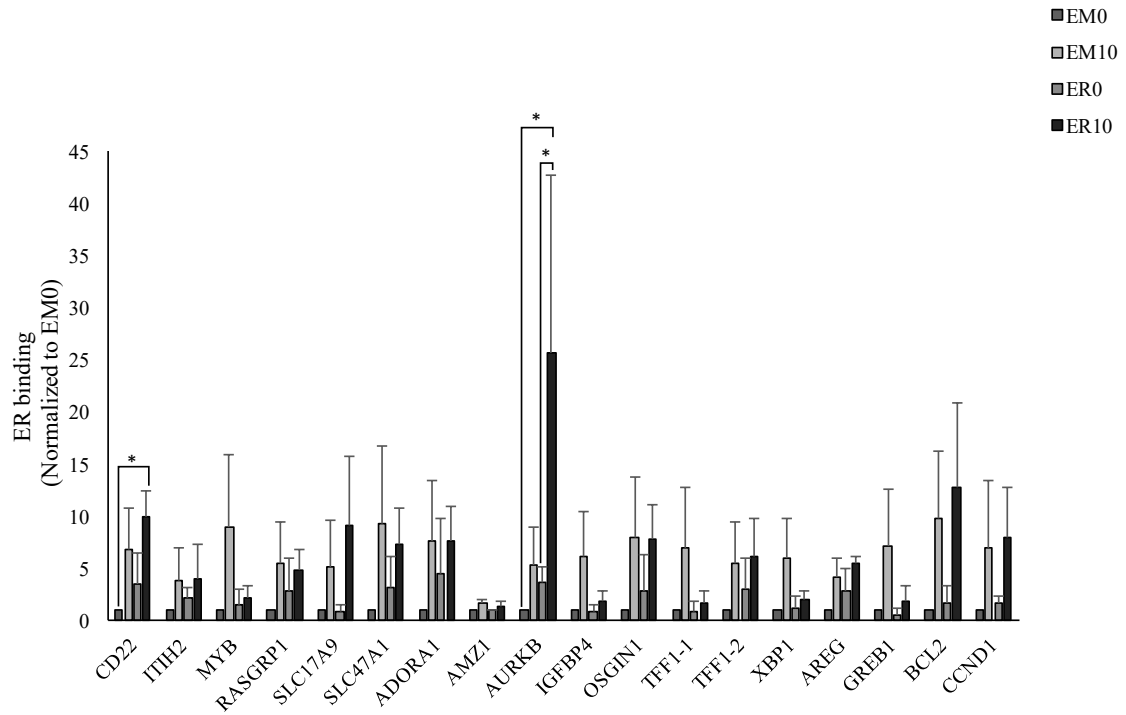


Figure 3.6 ER peaks are located near genes that show a differential response to E2.

ER binding at locations associated with 14 differentially regulated genes. *GREB1*, *BCL2* and *CCND1* were included as positive controls. ChIP DNA was extracted from MCF7-EM and MCF7-ER cells treated with vehicle control (EM0 and ER0) or 10 nM E2 (EM10 and ER10) and analyzed using custom ChIP-String probe sets. ER binding was normalized to EM0. Data are shown as mean \pm SD. There was a significant increase in ER binding at the CD22 and AURKB genes in the MCF7-ER cells after E2 treatment when compared against MCF7-EM cells without E2 treatment. E2 treatment lead to a significant increase in ER binding at the AURKB gene in the MCF7-ER cells (Two-way ANOVA followed by Tukey's posthoc analysis, n=3, * P <0.03).

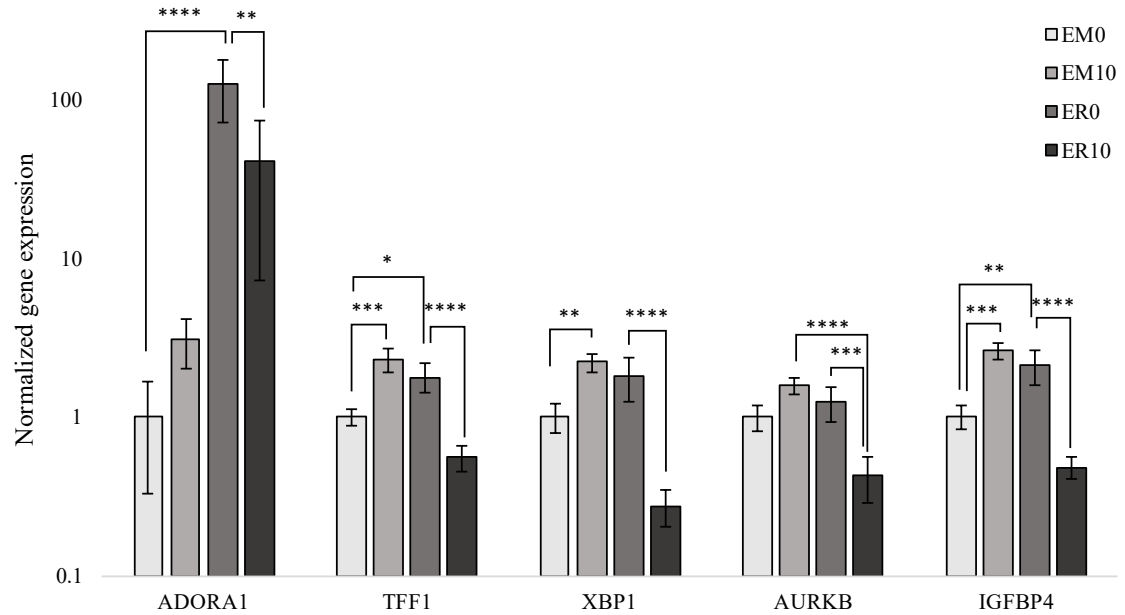


Figure 3.7 Increased ER mediates differential gene expression in response to E2. Relative mRNA expression of the *ADORA1*, *TFF1*, *XBP1*, *AURKB* and *IGFBP4* genes in MCF7-EM and MCF7-ER cells treated with vehicle control (EM0 and ER0) or 10 nM E2 (EM10 and ER10) for 24 hours. mRNA expression was normalized to three housekeeping genes: *PUM1*, *TBP*, and *RPL13A*. Data have been log transformed and are shown as mean \pm SD. Statistical significance was determined using two-way ANOVA followed by Tukey's posthoc analysis, n=3, * $P < 0.02$, ** $P < 0.007$, *** $P < 0.003$, **** $P < 0.0001$

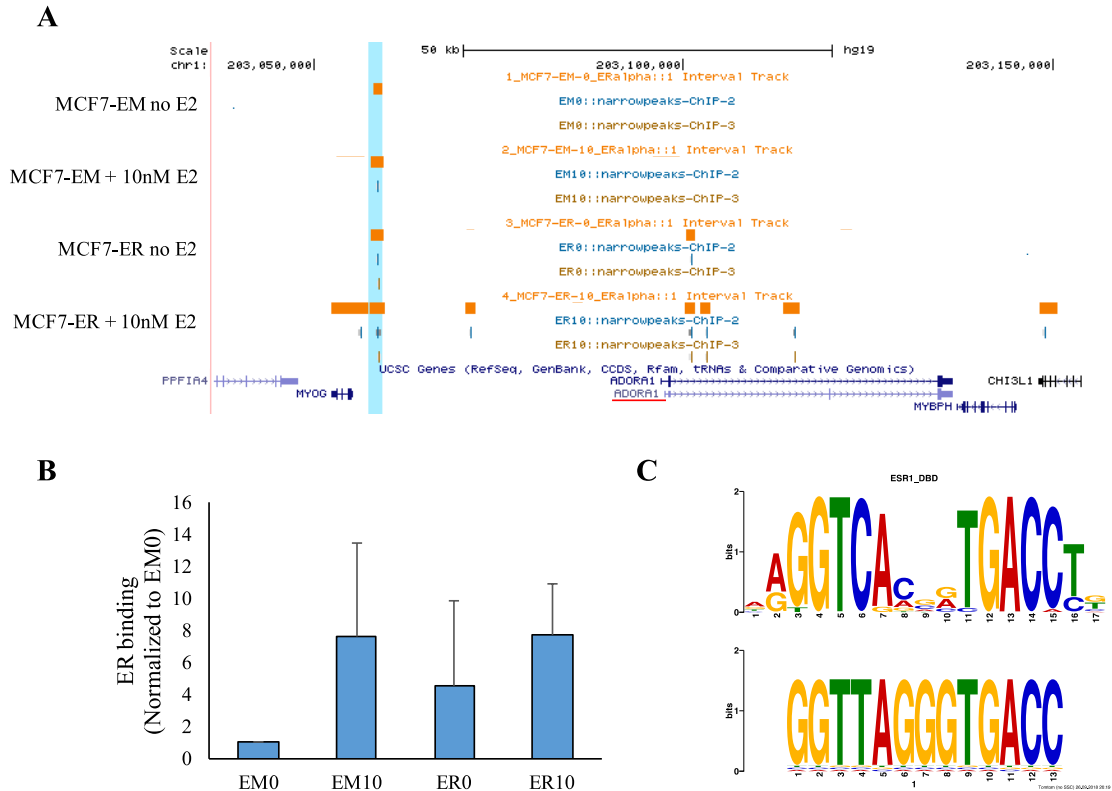


Figure 3.8 ER binds a region upstream of *ADORA1* in the MCF7-EM and MCF7-ER cells. **A. UCSC genome browser images for a > 50 kb window surrounding the *ADORA1* gene (underlined in red). The region that was bound in both the MCF7-EM and MCF7-ER cells is highlighted in blue. ER peaks that occurred in at least 2/3 biological replicates are shown. Replicate 1= orange bars; replicate 2= blue bars; replicate 3= brown bars. **B.** ChIP-String validation experiments for the peak highlighted in A. Bars represent mean \pm SD, $n=3$. There was no significant interaction between ER binding and the treatment conditions by Two-way ANOVA. **C.** TomTom results for a potential ERE motif located in the ER peak confirmed by ChIP-String.**

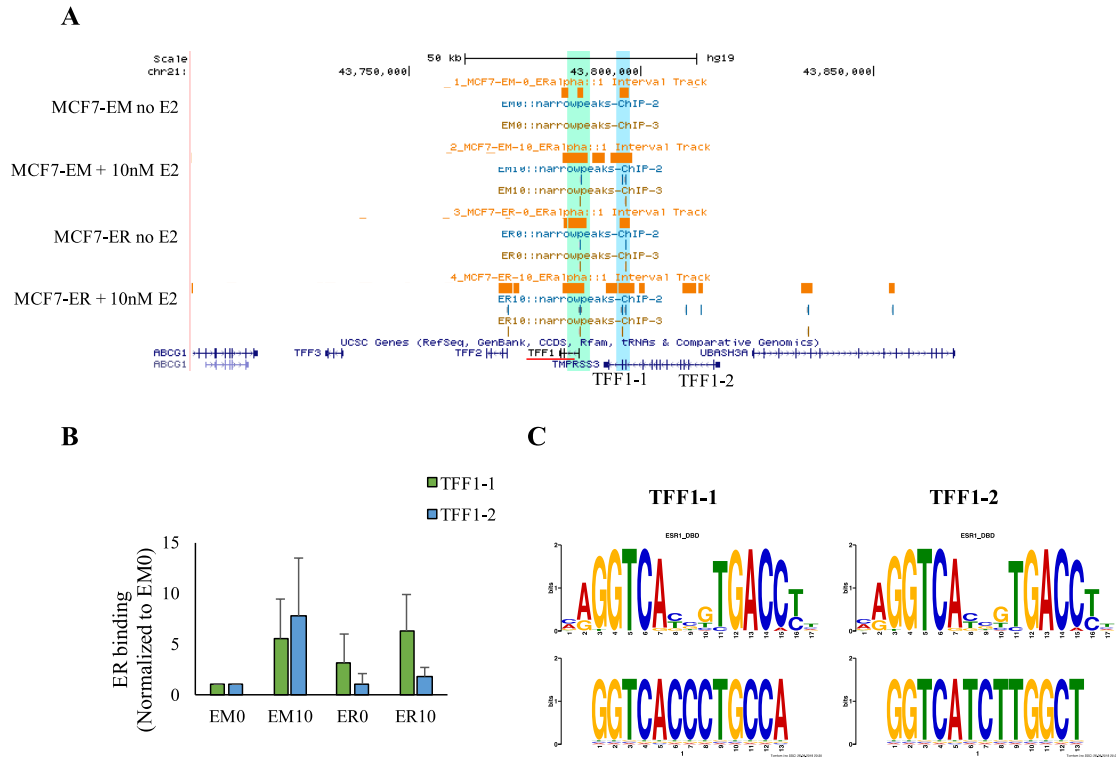


Figure 3.9 ER binds two regions near the *TFF1* TSS in the MCF7-EM and MCF7-ER cells. A. UCSC genome browser images for > 50 kb window surrounding the *TFF1* gene (underlined in red). A region that was bound nearest to the TSS (TFF1-1) in both the MCF7-EM and MCF7-ER cells is highlighted in green. A second region bound near *TFF1* (TFF1-2) in both the MCF7-EM and MCF7-ER cells is highlighted in blue. ER peaks that occurred in at least 2/3 biological replicates are shown. Replicate 1= orange bars; replicate 2= blue bars; replicate 3= brown bars. **B.** ChIP-String validation experiments for the two ER peaks highlighted in A. Bars represent mean \pm SD, n=3. There was no significant interaction between ER binding and the treatment conditions by Two-way ANOVA. **C.** TomTom results for the potential ERE motifs from the TFF1-1 and TFF1-2 peaks confirmed by ChIP-String.

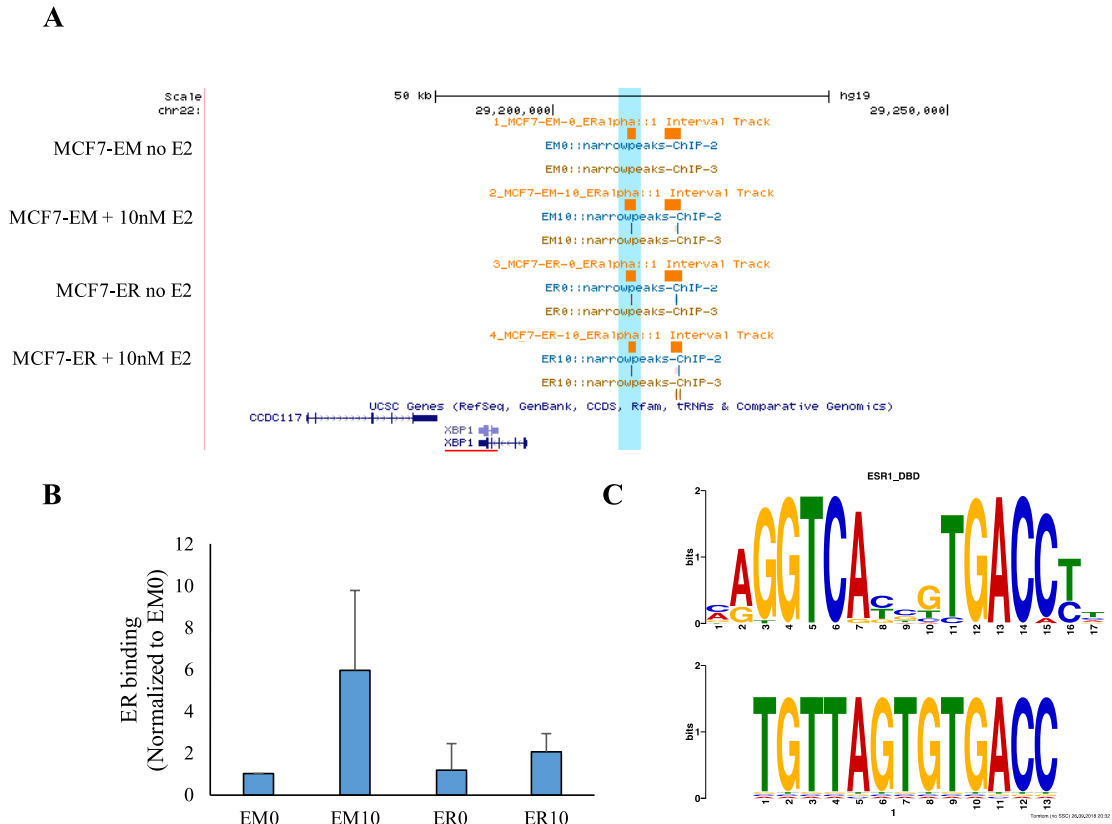


Figure 3.10 ER binds a region downstream from the *XBP1* gene in the MCF7-EM and MCF7-ER cells. A. UCSC genome browser images for a > 50 kb window surrounding the *XBP1* gene (underlined in red). A region that was bound nearest to *XBP1* in both the MCF7-EM and MCF7-ER cells is highlighted in blue. ER peaks that occurred in at least 2/3 biological replicates are shown. Replicate 1= orange bars; replicate 2= blue bars; replicate 3= brown bars. **B.** ChIP-String validation experiments for the ER peak highlighted in A. Bars represent mean \pm SD, n=3. There was no significant interaction between ER binding and the treatment conditions by Two-way ANOVA. **C.** TomTom results for the potential ERE motif located in the ER peak that was confirmed by ChIP-String.

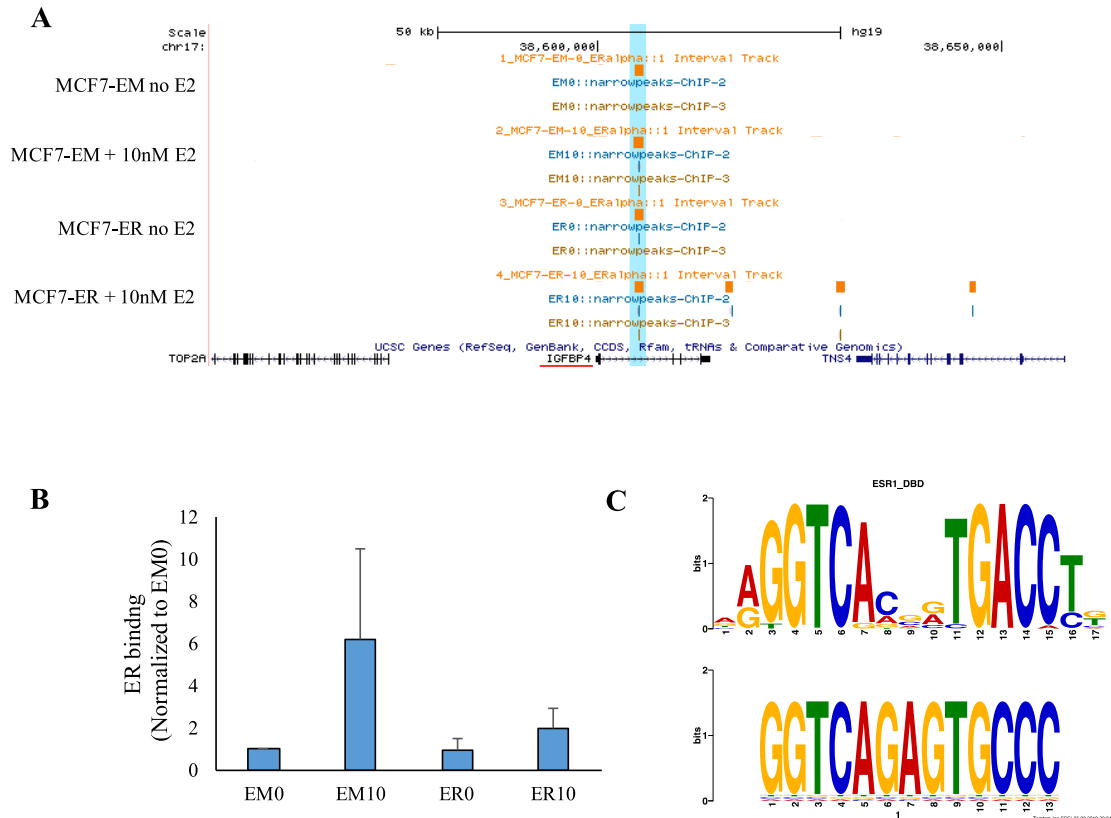
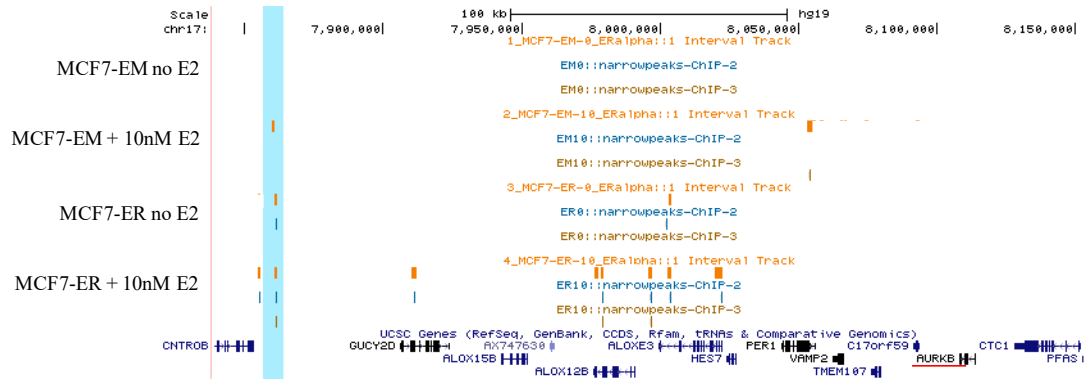


Figure 3.11 ER binds an intragenic region of *IGFBP4* in the MCF7-EM and MCF7-ER cells. **A.** UCSC genome browser images for a > 50 kb window surrounding the *IGFBP4* gene (underlined in red). An intragenic region of *IGFBP4* was bound in both the MCF7-EM and MCF7-ER cells is highlighted in blue. ER peaks that occurred in at least 2/3 biological replicates are shown. Replicate 1= orange bars; replicate 2= blue bars; replicate 3= brown bars. **B.** ChIP-String validation experiments for the ER peak highlighted in A. Bars represent mean \pm SD, n=3. There was no significant interaction between ER binding and the treatment conditions by Two-way ANOVA. **C.** TomTom results for the potential ERE motif located in the ER peak that was confirmed by ChIP-String.

A



B

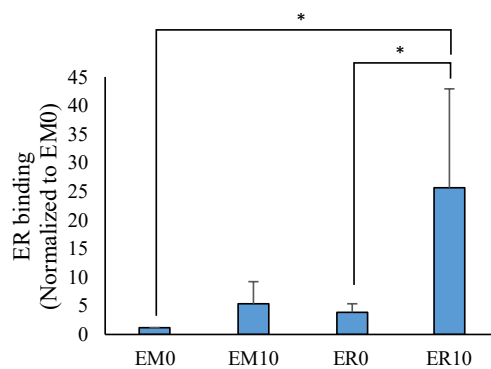


Figure 3.12 ER binds a region > 100 kb away from *AURKB* in only MCF7-ER cells.

A. UCSC genome browser images for a > 100 kb window upstream of the *AURKB* gene (underlined in red). A distal region that was bound in only the MCF7-ER cells is highlighted in blue. ER peaks that occurred in at least 2/3 biological replicates are shown. Replicate 1= orange bars; replicate 2= blue bars; replicate 3= brown bars. **B.** ChIP-String validation experiments for the ER peak highlighted in A. Bars represent mean ± SD. There was a significant increase in ER binding in the MCF7-ER cells after E2 treatment when compared against MCF7-EM cells without E2 treatment and a significant increase when compared to MCF7-ER cells without E2 treatment (Two-way ANOVA followed by Tukey's posthoc analysis, n=3, * $P < 0.03$).

3.5 References

1. Shang Y, Hu X, DiRenzo J, Lazar MA, Brown M. Cofactor dynamics and sufficiency in estrogen receptor-regulated transcription. *Cell*. 2000;103(6):843-52.
2. Metivier R, Penot G, Hubner MR, Reid G, Brand H, Kos M, et al. Estrogen receptor- α directs ordered, cyclical, and combinatorial recruitment of cofactors on a natural target promoter. *Cell*. 2003;115(6):751-63.
3. Carroll JS, Meyer CA, Song J, Li W, Geistlinger TR, Eeckhoute J, et al. Genome-wide analysis of estrogen receptor binding sites. *Nat Genet*. 2006;38(11):1289-97.
4. Chen J, Hu Z, Phatak M, Reichard J, Freudenberg JM, Sivaganesan S, et al. Genome-Wide Signatures of Transcription Factor Activity: Connecting Transcription Factors, Disease, and Small Molecules. *Plos Computational Biology*. 2013;9(9): e1003198.
5. Caizzi L, Ferrero G, Cutrupi S, Cordero F, Ballaré C, Miano V, et al. Genome-wide activity of unliganded estrogen receptor- α in breast cancer cells. *Proc Natl Acad Sci U S A*. 2014;111(13):4892-7.
6. Carroll JS, Liu XS, Brodsky AS, Li W, Meyer CA, Szary AJ, et al. Chromosome-wide mapping of estrogen receptor binding reveals long-range regulation requiring the forkhead protein FoxA1. *Cell*. 2005;122(1):33-43.
7. Lin C, Vega VB, Thomsen JS, Zhang T, Kong SL, Xie M, et al. Whole-genome cartography of estrogen receptor α binding sites. *Plos Genetics*. 2007;3(6):867-85.
8. Welboren W, van Driel MA, Janssen-Megens EM, van Heeringen SJ, Sweep FCGJ, Span PN, et al. ChIP-Seq of ER α and RNA polymerase II defines genes differentially responding to ligands. *EMBO J*. 2009;28(10):1418-28.

9. Ross-Innes CS, Stark R, Teschendorff AE, Holmes KA, Ali HR, Dunning MJ, et al. Differential oestrogen receptor binding is associated with clinical outcome in breast cancer. *Nature*. 2012;481(7381):389-U177.
10. Moggs J, Murphy T, Lim F, Moore D, Stuckey R, Antrobus K, et al. Anti-proliferative effect of estrogen in breast cancer cells that re-express ER alpha is mediated by aberrant regulation of cell cycle genes. *J Mol Endocrinol*. 2005;34(2):535-51.
11. Stender JD, Frasor J, Komm B, Chang KCN, Kraus WL, Katzenellenbogen BS. Estrogen-regulated gene networks in human breast cancer cells: Involvement of E2F1 in the regulation of cell proliferation. *Molecular Endocrinology*. 2007;21(9):2112-23.
12. Stender JD, Kim K, Charn TH, Komm B, Chang KCN, Kraus WL, et al. Genome-Wide Analysis of Estrogen Receptor alpha DNA Binding and Tethering Mechanisms Identifies Runx1 as a Novel Tethering Factor in Receptor-Mediated Transcriptional Activation. *Mol Cell Biol*. 2010;30(16):3943-55.
13. Trapnell C, Pachter L, Salzberg SL. TopHat: discovering splice junctions with RNA-Seq. *Bioinformatics*. 2009;25(9):1105-11.
14. Trapnell C, Roberts A, Goff L, Pertea G, Kim D, Kelley DR, et al. Differential gene and transcript expression analysis of RNA-seq experiments with TopHat and Cufflinks. *Nature Protocols*. 2012;7(3):562-78.
15. Machanick P, Bailey TL. MEME-ChIP: motif analysis of large DNA datasets. *Bioinformatics*. 2011;27(12):1696-7.
16. Heinz S, Benner C, Spann N, Bertolino E, Lin YC, Laslo P, et al. Simple Combinations of Lineage-Determining Transcription Factors Prime cis-Regulatory Elements Required for Macrophage and B Cell Identities. *Mol Cell*. 2010;38(4):576-89.

17. Gupta S, Stamatoyannopoulos JA, Bailey TL, Noble WS. Quantifying similarity between motifs. *Genome Biol.* 2007;8(2): R24.
18. Parker JS, Mullins M, Cheang MCU, Leung S, Voduc D, Vickery T, et al. Supervised Risk Predictor of Breast Cancer Based on Intrinsic Subtypes. *Journal of Clinical Oncology.* 2009;27(8):1160-7.
19. Wallden B, Storhoff J, Nielsen T, Dowidar N, Schaper C, Ferree S, et al. Development and verification of the PAM50-based Prosigna breast cancer gene signature assay. *Bmc Medical Genomics.* 2015; 8:54.
20. Bernhardt SM, Dasari P, Walsh D, Townsend AR, Price TJ, Ingman WV. Hormonal Modulation of Breast Cancer Gene expression: Implications for Intrinsic Subtyping in Premenopausal Women. *Frontiers in Oncology.* 2016; 6:241.
21. Eom YH, Kim HS, Lee A, Song BJ, Chae BJ. BCL2 as a Subtype-Specific Prognostic Marker for Breast Cancer. *Journal of Breast Cancer.* 2016;19(3):252-60.
22. Mi H, Muruganujan A, Casagrande JT, Thomas PD. Large-scale gene function analysis with the PANTHER classification system. *Nature Protocols.* 2013;8(8):1551-66.
23. Mi H, Huang X, Muruganujan A, Tang H, Mills C, Kang D, et al. PANTHER version 11: expanded annotation data from Gene Ontology and Reactome pathways, and data analysis tool enhancements. *Nucleic Acids Res.* 2017;45(D1): D183-9.
24. Liu MH, Cheung E. Estrogen receptor-mediated long-range chromatin interactions and transcription in breast cancer. *Mol Cell Endocrinol.* 2014;382(1):624-32.
25. Singhal H, Greene ME, Tarulli G, Zarnke AL, Bourgo RJ, Laine M, et al. Genomic agonism and phenotypic antagonism between estrogen and progesterone receptors in breast cancer. *Science Advances.* 2016;2(6): e1501924.

Chapter 4: Increased ER expression regulates the formation of long-range DNA loops in the presence and absence of E2

4.1 Introduction

The results from the previous two chapters have shown that increased ER expression leads to an anti-proliferative response to E2 which may be mediated by differential gene regulation. ChIP-Seq experiments found ER can bind novel, low affinity regions when the level of receptor expression is increased. These regions are most frequently bound in the MCF7-ER cells upon E2 treatment suggesting they may be involved in regulating E2-induced repression in a subset of genes that are required for proliferation. ER's transcriptional activity is a dynamic process that is influenced by the surrounding chromatin structure. The classic model for ER-mediated gene repression is through the recruitment of HDAC corepressor complexes which modify the gene promoter region into a tightly packed structure that prevents further recruitment of the transcriptional machinery (1).

Though this effect of ER at promoter regions is well understood, it has been shown that the vast majority of E2-repressed genes have ER bound outside of their proximal promoter regions (2). A role for more distal binding has been recently described for ER+/PR+ breast cancer cells where activated PR was shown to remodel the chromatin and promote ER binding at distal regions (3). The authors of this study found this novel binding pattern was associated with a loss in proliferation (3). These findings provide evidence that ER may bind at distal enhancer regions and promote an anti-proliferative response that is mediated by gene repression.

As described in section 1.4.3.2 chromatin is organized into sub-megabase TADs which contain several small- and large-scale DNA loops (4). The formation of DNA loops enables distal enhancer and proximal promoter regions to directly interact leading to the simultaneous activation of multiple genes through direct association with the

transcriptional machinery (5, 6). In MCF-7 cells, ER has been mapped to the anchor regions of small- and large-scale DNA loops and these anchors are often associated with the promoter regions of E2-activated genes (5). ER binding at these anchor regions in the absence of E2 enables loop formation and poises the promoter for activation upon E2 treatment (7). ER can mediate gene repression through several mechanisms such as (i) loop reconfiguration which sequesters the gene in the non-anchor areas of the looped DNA preventing interactions with the transcriptional machinery, or (ii) isolation from the transcriptional machinery through the dissolution of the previously formed loop (5, 7). This second mechanism may be mediated through ER binding to intra-loop regions which promotes chromatin reconfiguration and leads to an overall loss of loop stability (7). Therefore, the role of loop structure in mediating the E2-induced repression in the MCF7-ER cells will be investigated. The ChIP-Seq data suggest that increased ER expression promotes ER binding in the absence of E2 and enables binding to lower affinity sites after E2 treatment. In this chapter, previously mapped ER anchor regions will be used to determine how increased ER expression correlates with the DNA loops associated with the five differentially regulated genes from chapter 3. The hypothesis that increased ER expression can promote the formation of previously described E2-dependent DNA loops in the absence of E2 will be examined. The additional hypothesis that ER binding at low affinity regions within previously mapped loops in the MCF7-ER cells after E2 treatment may promote the loss of loop formation leading to the down-regulation of the nearby genes will also be assessed.

4.2 Methods

All experiments were designed through equal collaboration between Judith Hugh and Lacey Haddon, and were conducted by Lacey Haddon.

4.2.1 Cross-referencing ER binding with ER anchors from a published ChIA-PET dataset

BED files from the ChIP-Seq analysis were uploaded to the UCSC genome browser along with a chromatin interaction analysis by paired-end tag sequencing (ChIA-PET) dataset for MCF-7 cells treated with 10 nM E2 and immunoprecipitated with an ER α antibody generated by the ENCODE project (GSM970212). These combined datasets were used to locate ER peaks bound near each of the five differentially expressed genes. Peaks that were present in at least 2/3 ChIP-Seq replicates and overlapped with a mapped ChIA-PET anchor point associated with a long-range DNA loop (> 1 Mb) near differentially expressed genes were validated by ChIP-String analysis. The 1 Mb threshold for selecting loop anchors was set in order to facilitate the subsequent validation for the presence of DNA loops in the MCF-7 transfectants using fluorescence *in situ* hybridization (FISH). This 1 Mb distance between distal and proximal anchor sites was previously described as the borderline resolution for the validation of DNA loops by FISH (5 supplemental materials).

4.2.2 ChIP-String validation

The methods for ChIP-String analysis are described in section 2.2.16.

4.2.3 Fluorescence *in situ* hybridization (FISH)

MCF7-EM and MCF7-ER cells were treated with or without 10 nM E2 for 1 hour, trypsinized and resuspended in PBS. Cells were fixed in methanol and glacial acetic acid (3:1) overnight. Fixed cells were resuspended and dropped onto glass slides at 60°C then

air dried for 30 minutes at room temperature. The dried slides were incubated in 2X SSC buffer at 37°C for 30 minutes, then rinsed in ddH₂O and dehydrated through 50%, 70%, 85% and 100% ethanol. FISH probes were designed commercially (Empire Genomics Inc.) using bacterial artificial chromosome (BAC) clones for the genomic sequences associated with each of the anchor regions. For each loop, a BAC probe associated with the proximal anchor region (P1) was labelled with the green fluorescent dye 5-Fluorescein dUTP (FITC). The BAC clone for the distal anchor region (P2) was labelled with the orange fluorescent dye 5-TAMRA dUTP. These probes were considered the positive probe set (P1/P2). A control BAC probe associated with a region located at least 1 Mb away from the DNA loop (P3) was included for each gene and was labeled with the green FITC dye. This BAC probe was paired with the orange distal anchor probe (P2) and served as a negative control (P2/P3). The negative probe set was used to assess the level of background reconfiguration within the chromatin. This method of FISH validation for long-range DNA loops has been previously described (5). The positive and negative probe sets were prepared separately in hybridization buffer and each probe set was added to individual slides containing fixed cells from one of the four experimental conditions. A coverslip was placed over the probe and sealed with rubber cement to avoid drying of the probe during the hybridization step. The probes were denatured at 73°C for 5 minutes then hybridized at 37°C overnight. After hybridization, the coverslips were removed, and the slides were washed in 0.4X SSC buffer (0.4X SSC and 0.3% IGEPAL, pH 7.0-7.5) at 73°C for 2 minutes, followed by 2X SSC wash buffer (2X SSC, 0.1% IGEPAL, pH 7.0 +/-0.2) at room temperature for 1 minute. Slides were rinsed in ddH₂O for 1 minute, then dehydrated through 70%, 85% and 100% ethanol and air dried in a dark drawer for 10 minutes. Dried slides were counterstained with

DAPI I diluted 1:20 in VECTASHIELD mounting medium and stored at -20°C for at least 30 minutes or until ready for confocal imaging. All FISH experiments were designed and performed by Lacey Haddon

4.2.4 Confocal imaging and Imaris image analysis

FISH slides were imaged using the Zeiss LSM 710 laser scanning confocal with a 40x 1.3 oil plan-Apochromat objective and avalanche photodiode detectors (APDs) which have the highest sensitivity and enable detection of a wide spectral range. The use of these APDs enable the detection of weak fluorescent signals from the BAC probes. The Zeiss LSM software (ZEN) was used to set up Z-stacking for 3D imaging and 11 slices were taken from the centre of the slide for each Z-stack image. The acquisition settings were kept constant for all images and were set to a preset scan speed of 9 and averaging of 2 frames. The tile scanning function was used to enable imaging of a large field at high resolution and enabled the generation of 3D images that contained 200-300 nuclei. The orange signals from the TAMRA FISH probes were visualized as red signal on all confocal images. One image file was generated for each experimental condition and probe set and was further analyzed using the IMARIS software (version 9.1.2) loaded with the Imaris Cell and Imaris XT licenses.

For the image analysis individual cells were counted using the DAPI channel and the Imaris Cell function. The settings for the Cell function were kept the same throughout the analysis and included a filter width of 0.5 μM and a split by seed point setting of 10. The split by seed point setting enabled the program to identify the individual nuclei within groups of overlapping cells (See Figure B9 in Appendix B). This generated a 3D mask which shows the individual nuclei that met the threshold settings. The FISH probe signals

were analyzed individually using their respective fluorescent channels for the Imaris Spot function. For this analysis, the FITC (green) or TAMRA (red) channel was selected and probe signals that had an XY diameter of at least 0.5 μM and a fluorescence signal above 0.5 were indicated with a green (for the FITC channel) or red (for the TAMRA channel) spot by the Imaris software. These red and green spots were used to determine the presence of overlapping signals by inputting them into the Imaris colocalized spot function. For this analysis the program was set to call red and green spots that were within a $\leq 0.45 \mu\text{M}$ distance as a colocalized spot which was coloured yellow. Using an automated colocalization function enables accurate detection of signals that are within the 0.45 μM distance within the Z-axis. The 0.45 μM threshold was used as it was shown to detect only those signals that were directly touching in the nuclei. The red, green and yellow spots were input into the 3D mask generated with the Imaris Cell function using the import spots to vesicles function. This generated a final 3D mask that shows the separate (red and green) and colocalized (yellow) spots that are associated with each individual nucleus. The Imaris statistics package was then used to generate an output excel file which contained the number of green, red and colocalized spots associated with each individual cell. Some cells had DAPI staining but no FISH probe signals and were excluded from further analyses. Confocal imaging was done by Lacey Haddon with guidance from Dr. Xuejun Sun. Imaris image analysis was done by Lacey Haddon with guidance from Geraldine Barron.

4.2.5 Calculations and statistics

The excel file generated by Imaris lists each cell individually along with the total number of red, green, and colocalized spots associated with each cell. For these analyses only the green signals that had a corresponding red signal within the same cell were counted

in order to determine the total number of paired signals for each experimental condition and probe set. This means that a cell that had three red spots and four green spots would be counted as having three paired signals in the final analysis (see Figure B10 in Appendix B). The red and green spots that were called as colocalized were also included in this calculation of total number of paired signals. The colocalized spots were also given in a separate sheet of the excel file which enabled us to determine the number of overlapped signals for each experimental condition and probe set. The presence of looping was calculated as described by Fullwood et al. (2009) (5). This analysis calculates the percent overlap for each experimental condition for the positive (P1/P2) and negative control (P2/P3) probes using the following formula:

$$\text{Percent Overlap (PO)} = \left(\frac{\text{Overlapped}}{\text{Total}} \right) * 100$$

The percent overlap for the positive probe set was divided by the percent overlap calculated for the negative probe set to give a final normalized overlap rate:

$$\text{Normalized overlap rate: } \frac{PO(\text{positive})}{PO(\text{negative})}$$

Statistical significance was determined using Fisher's Exact test which compared the number of overlapped signals between the different treatment conditions. A P value of ≤ 0.05 was considered as significant. All calculations were performed by Lacey Haddon.

4.3 Results

4.3.1 Differentially expressed genes are associated with ER-mediated DNA loops

To determine the likelihood of DNA looping in this study the publicly available ChIA-PET dataset derived from MCF-7 cells treated with E2 (GSM 970212) was obtained from

the Gene Expression Omnibus (GEO) website and uploaded to the UCSC genome browser. The DNA used for the ChIA-PET experiment was obtained from parental MCF-7 cells treated with E2 and was immunoprecipitated with the same ER antibody (HC-20) that was used for the ChIP-Seq experiments described in chapter 2. Since the MCF7-EM cells maintain the endogenous ER expression of parental cells the peak sets obtained from the MCF7-EM cells treated with E2 were expected to best match the ChIA-PET data.

The association of ER binding sites with DNA loops for the five differentially expressed genes validated in chapter 3 are summarized in Table 4.1. There were several small- and large-scale DNA loops associated with each of the five genes (Figures 4.1-4.5). The peaks that were bound within 50 kb of these genes (validated in chapter 3) overlapped with an ER anchor associated with several DNA loops that extend upstream and downstream in the ChIA-PET dataset (Figures 4.1-4.5). ER binding was confirmed at the proximal anchor regions in the MCF7-EM cells after E2 treatment for four out of five genes (Table 4.1; Figures 4.1-4.4). *AURKB* was the only gene that did not show significant ER binding at the proximal anchor in the MCF7-EM cells treated with E2 (Table 4.1; Figure 4.5). A more significant finding was the presence of ER binding at the proximal anchor region for all five genes in the MCF7-ER cells in the absence of E2 and this binding was maintained after E2 treatment (Table 4.1; Figures 4.1-4.5).

These proximal anchor sites were used to determine whether distal enhancers may be involved in mediating a differential response to E2. The presence of ER binding at the distal anchors associated with long-range DNA loops (> 1 Mb) was confirmed for each of the five differentially regulated genes as loops of this size can be further validated by FISH. Examination of the distal anchors for the long-range DNA loops in each of the five genes

confirmed the presence of ER binding in the ChIP-Seq peak sets (Table 4.1; Figures 4.1-4.5). Out of the five genes, *TFF1* was the only gene that had ER binding in the MCF7-EM cells treated with E2 as well as the MCF7-ER cells with and without E2 treatment (Table 4.1; Figure 4.1). The other four genes had ER binding at the distal anchor only in the MCF7-ER cells with and without E2 (Table 4.1; Figures 4.2-4.5). The DNA sequences associated with the distal anchor regions were enriched in multiple half EREs rather than full EREs (Table 4.1). ER binding was validated at these distal anchors by ChIP-String and combined the results with the previously validated ChIP-String data for the proximal anchor regions obtained in chapter 3 (Figure 4.6), thus confirming the presence of ER binding at the anchors of long-range DNA loops. This assay was able to detect ER binding at the distal anchor in the MCF7-EM cells treated with E2 for all five genes despite the absence of ER peaks in the ChIP-Seq datasets (Figure 4.6). This discrepancy may be due to the lower sensitivity of full-genome sequencing techniques which need significant enrichment to detect an ER peak compared to the ChIP-String probes which are designed for DNA associated with a specific genomic region. The ChIP-Seq analysis also detected ER binding at several unique regions associated with the looped DNA for each of the five genes. Interestingly, these regions were only bound in the MCF7-ER cells after E2 treatment (Figure 4.1-4.5).

4.3.2 Increased ER expression promotes ER-mediated DNA loops

Fluorescently labelled BAC probes specific for the proximal and distal anchor regions of the long-range loops detected near the *ADORA1* and *TFF1* genes were hybridized to methanol fixed nuclei obtained from both MCF-7 transfectants treated with and without E2. The level of DNA loop formation is described as normalized overlap rate, with the

negative probe set (P2/P3) set as 1X. The results for the probe signals for *ADORA1* are summarized in Table 4.2. The normalized overlap rate for the MCF7-EM cells increased from 1.15X without E2 treatment to 1.32X in cells treated with E2 (Figure 4.7). This increase was not found to be significant by Fisher's exact test ($P=1$). For the MCF7-ER cells the normalized overlap rate was increased to 1.62X in the absence of E2 and decreased to 1.09X in cells treated with E2 (Figure 4.8). This decrease in overlap was not significant by Fisher's exact test ($P=0.1987$). These results indicate the *ADORA1* FISH probe set is unable to detect changes in DNA loops in this chromosomal region.

The results for the *TFF1* probe set are summarized in Table 4.3 and show the MCF7-EM cells had a significant increase in normalized overlap rate to 6.44X after E2 treatment ($P=0.0002$) (Figure 4.9). For the MCF7-ER cells the normalized overlap rate was 4.0X in the absence of E2 (Figure 4.10), and this increase was significant when compared to the MCF7-EM cells without E2 treatment by Fisher's exact test ($P=0$). Interestingly, the normalized overlap rate for MCF7-ER cells treated with E2 was 3.77X and this was significant compared to MCF7-EM cells without E2 treatment ($P=0.0007$). These results are consistent with the presence of ER peaks at the anchor regions of the *TFF1* long-range DNA loop in the MCF7-EM cells treated with E2 and the MCF7-ER cells with and without E2 treatment.

There were obvious differences in the FISH signals obtained for the *ADORA1* and *TFF1* probe sets. Cells hybridized with the *ADORA1* probes showed consistently high numbers of signals compared to those with the *TFF1* probe set (compare Table 4.2 and Table 4.3). The presence of fewer signals in the *TFF1* probe set may be caused by a decreased affinity of the BAC clones selected for DNA associated with the anchor regions of the *TFF1* loop.

Support for this is the observation of several cells without *TFF1* probe signals in all of the experimental conditions. Furthermore, the signal intensity for the *TFF1* probes was much less than that of the *ADORA1* probe, and this reduces the ability for detection on the confocal microscope. The use of a fluorescence threshold of 0.5 for detecting probe signals provides further assurance that the signals obtained for the *TFF1* probe set were valid. With the limitations of the current probe sets the current FISH data can only provide preliminary evidence for chromatin remodeling in MCF7-EM and MCF7-ER cells. This finding should be further validated by using FISH probes that have a stronger fluorescence signal or using a complimentary molecular method such as chromatin conformation capture (3C).

4.4 Conclusions

These results have shown that the ER peaks validated in chapter 3 are located at previously mapped ER anchors from MCF7 cells treated with E2. These ER binding sites may serve as the proximal anchor region for small- and large-scale DNA loops. Consistent with this, ER binding was confirmed at distal anchor regions associated with long-range (<1 Mb) loops for each of the five differentially expressed genes from chapter 3. Validation of the long-range DNA loops associated with the *ADORA1* and *TFF1* genes was done by FISH analysis. There were no significant changes in DNA looping for the *ADORA1* FISH probe set detected in these experiments. This result may suggest that this long-range DNA loop is not involved in the transcriptional regulation of *ADORA1*.

A significant increase in DNA loop formation was detected in the MCF7-EM cells after E2 treatment using the FISH probe set for the long-range loop for *TFF1*. This is consistent with the previously described E2-dependent nature of DNA loops in the MCF-7 parental cell line (5). A significant increase in the *TFF1* long-range loop was present in the MCF7-

ER cells in the absence of E2. These data offer preliminary evidence that increased ER expression may enable loop formation in the absence of E2 and promote the basal gene expression of genes located near these anchors. When compared to the MCF7-EM cells without E2, there was a significant increase in *TFF1* long-range loops in MCF7-ER cells that were treated with E2. This finding is in opposition with previous reports which found that loops are lost near genes that become repressed (7). When taken together, these data suggest that increased ER expression can regulate changes in chromatin configuration and provides preliminary evidence that long-range DNA loops may be involved in the activation and repression of genes with a differential response to E2.

Table 4.1 Summary of ER binding associated with ChIA-PET anchors for five genes with a differential response to E2

Gene	Proximal anchor		Distal anchor	
	Conditions	Motif(s)	Conditions	Motif(s)
ADORA1	EM10, ER0, ER10	Full ERE	ER0, ER10*	2-Half EREs
TFF1	EM10, ER0, ER10	Full ERE	EM10, ER0, ER10	3-Half EREs
XBP1	EM10, ER0, ER10	Full ERE	ER0, ER10*	3-Half EREs
IGFBP4	EM10, ER0, ER10	Full ERE	ER0, ER10*	3-Half EREs
AURKB	ER0, ER10*	Full ERE	ER0, ER10*	7- Half EREs

EM0: MCF7-EM no E2 (n=3)

EM10: MCF7-EM + 10 nM E2 (n=3)

ER0: MCF7-ER no E2 (n=3)

ER10: MCF7-ER + 10 nM E2 (n=3)

* ER peak was later confirmed in EM10 condition by ChIP-String

Table 4.2 FISH validation data for *ADORA1*. Raw counts for paired signals for the negative (NEG) and positive (POS) FISH probe sets in the absence (ETOH) or presence (E2) of estrogen.

MCF7-EM FISH experiment data				
<i>Paired signals</i>	NEG (P2/P3)	POS (P1/P2)	NEG (P2/P3)	POS (P1/P2)
	ETOH	ETOH	E2	E2
<i>Separate*</i>	2023	1478	1754	1063
<i>Overlap[†]</i>	499	434	365	312
<i>Total</i>	2522	1912	2119	1375
<i>% Overlap</i>	19.79	22.70	17.23	22.69
<i>Normalized probe overlap rate (X)</i>	1X	1.15X	1X	1.32X
<i>Total number of cells (n)</i>	432	301	350	281
MCF7-ER FISH experiment data				
<i>Paired signals</i>	NEG (P2/P3)	POS (P1/P2)	NEG (P2/P3)	POS (P1/P2)
	ETOH	ETOH	E2	E2
<i>Separate*</i>	1182	1586	2010	1569
<i>Overlap[†]</i>	195	474	488	425
<i>Total</i>	1377	2060	2498	1994
<i>% Overlap</i>	14.16	23.01	19.54	21.31
<i>Normalized probe overlap rate (X)</i>	1X	1.62X	1X	1.09X
<i>Total number of cells (n)</i>	340	361	373	344

* Red and green probe signals separated by $> 0.45\mu\text{M}$

[†] Red and green probe signals within $\leq 0.45\mu\text{M}$

Table 4.3 FISH validation data for *TFF1*. Raw counts for paired signals for the negative (NEG) and positive (POS) FISH probe sets in the absence (ETOH) or presence (E2) of estrogen.

MCF7-EM FISH experiment data				
<i>Paired Signals</i>	NEG (P2/P3)	POS (P1/P2)	NEG (P2/P3)	POS (P1/P2)
	ETOH	ETOH	E2	E2
<i>Separate*</i>	1300	338	155	975
<i>Overlap</i> [†]	54	20	3	136
<i>Total</i>	1354	358	158	1111
<i>% Overlap</i>	3.99	5.59	1.90	12.24
<i>Normalized probe overlap rate (X)</i>	1X	1.40X	1X	6.44X
<i>Total number of cells (n)</i>	361	196	120	264
MCF7-ER FISH experiment data				
<i>Paired Signals</i>	NEG (P2/P3)	POS (P1/P2)	NEG (P2/P3)	POS (P1/P2)
	ETOH	ETOH	E2	E2
<i>Separate*</i>	238	1568	708	1460
<i>Overlap</i> [†]	8	234	22	187
<i>Total</i>	246	1802	730	1647
<i>% Overlap</i>	3.25	12.99	3.01	11.35
<i>Normalized probe overlap rate (X)</i>	1X	4.0X	1X	3.77X
<i>Total number of cells (n)</i>	127	292	287	268

* Red and green probe signals separated by > 0.45 μ M

[†] Red and green probe signals within \leq 0.45 μ M

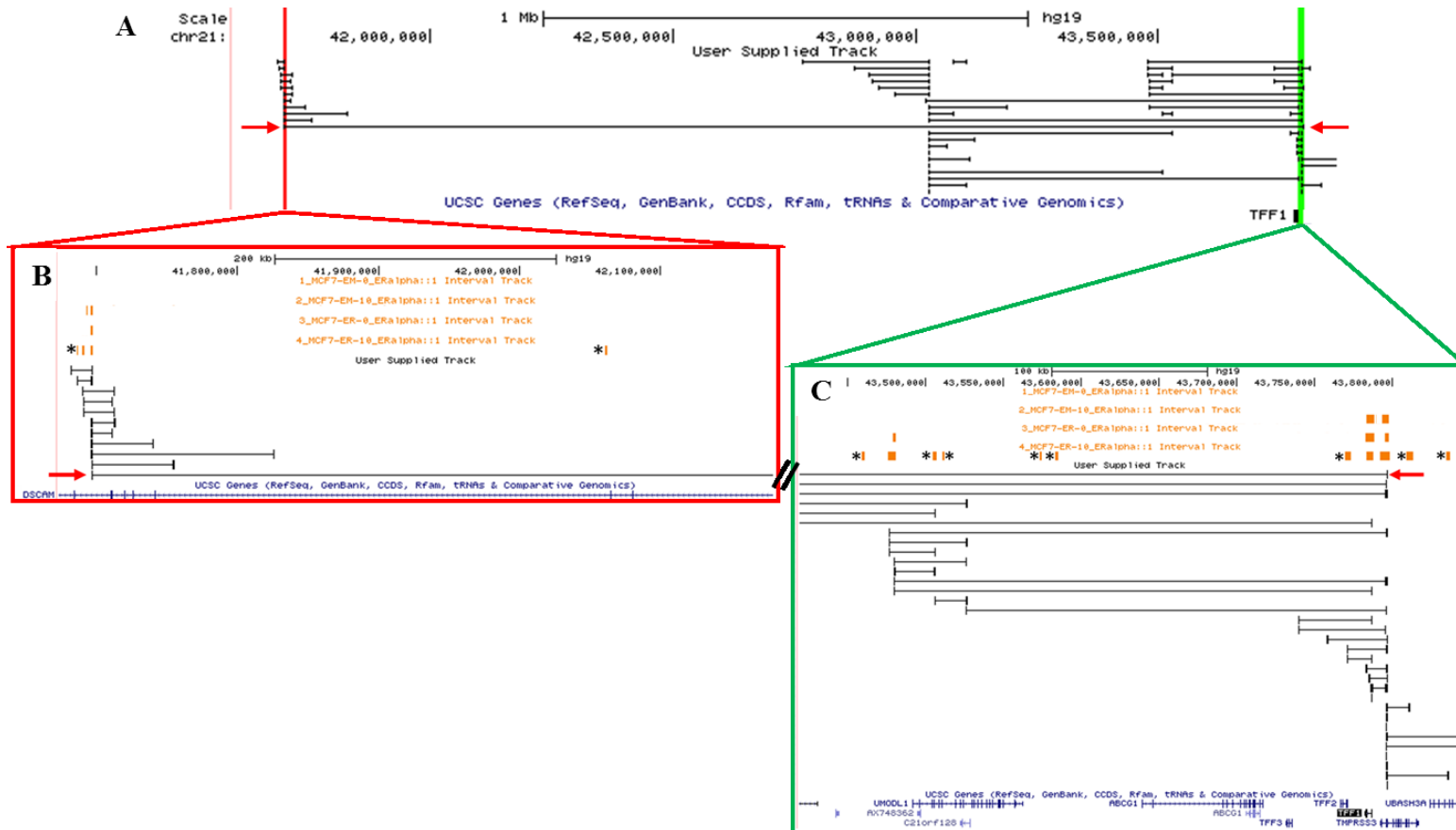


Figure 4.1 ER binding at anchor regions of a long-range DNA loop near *TFF1*. A. UCSC genome browser image for a > 1 Mb window shows small- and large-scale DNA loops associated with the *TFF1* gene. The presence of a long-range DNA loop is indicated

(Figure 4.1 continued) by red arrows. The location of *TFF1* proximal (green) and distal (red) anchor regions are highlighted. Boxes show a > 200 kb window for the distal anchor region (**B**) and a > 100 kb window the proximal anchor region (**C**). ChIA-PET data showing previously mapped ER interactions (DNA loops) from the MCF-7 cells treated with E2 are shown. ER peaks that were present in at least 2/3 replicates are shown (orange boxes). ER peaks that were only present in the MCF7-ER cells after E2 treatment are indicated with an asterisk (*). Black boxes indicate ER-bound anchor regions and the lines indicate the region of looped DNA. The location of the anchors associated with the long-range loop are indicated with a red arrow. ChIP-Seq experiments were done in triplicate.

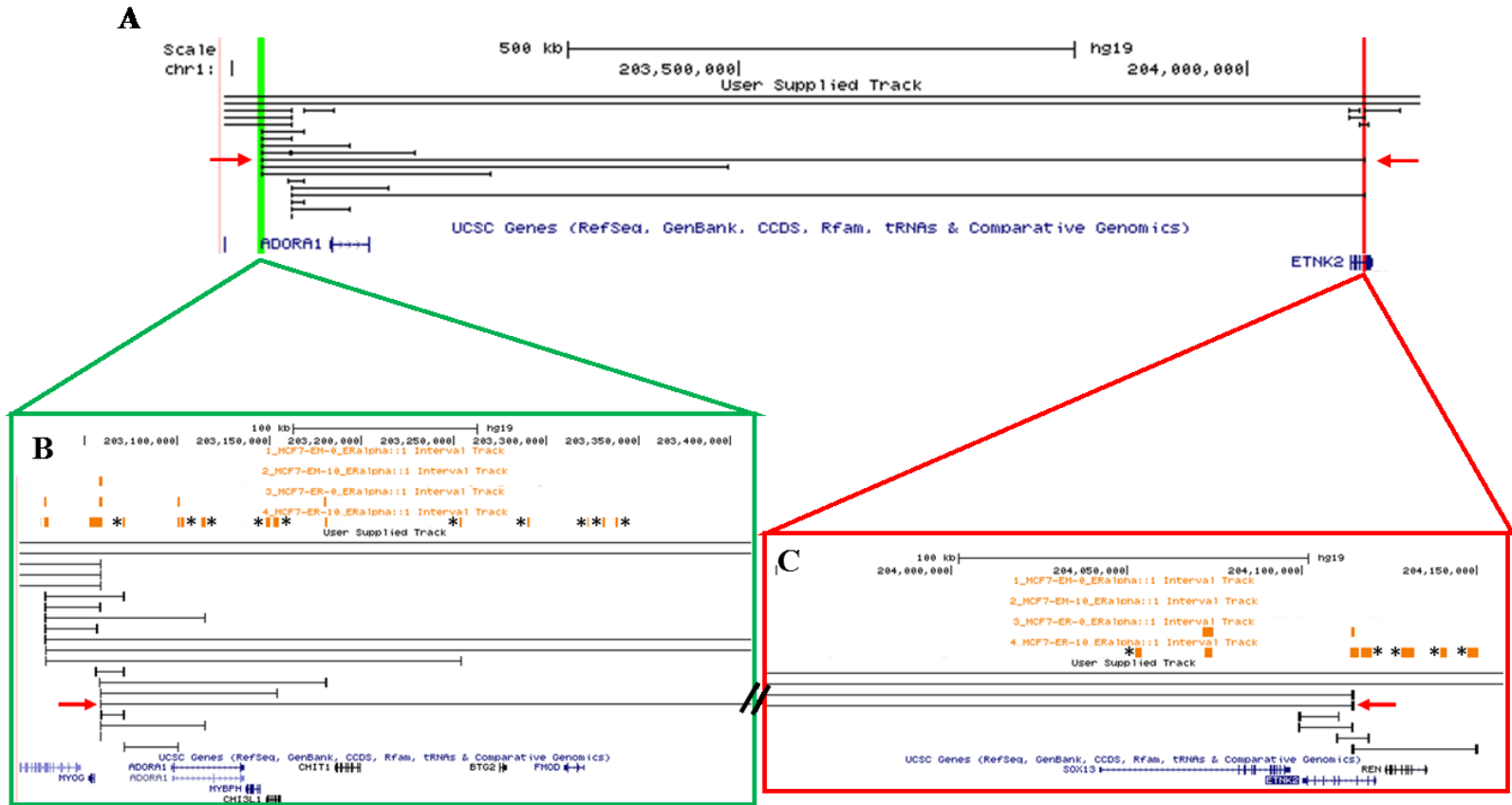


Figure 4.2 ER binding at anchor regions of a long-range DNA loop near *ADORA1*. **A.** UCSC genome browser image for a > 500 kb window shows small- and large-scale DNA loops associated with the *ADORA1* gene. The presence of a long-range DNA loop is indicated by red arrows. The location of the proximal (green) and distal (red) anchor regions are highlighted. Boxes show a > 100 kb

(Figure 4.2 continued) window for the proximal anchor region (**B**) and distal anchor region (**C**). ChIA-PET data showing previously mapped ER interactions (DNA loops) from the MCF-7 cells treated with E2 are shown. ER peaks that were present in at least 2/3 replicates are shown (orange boxes). ER peaks that were only present in the MCF7-ER cells after E2 treatment are indicated with an asterisk (*). Black boxes indicate ER-bound anchor regions and the lines indicate the region of looped DNA. The location of the anchors associated with the long-range loop are indicated with a red arrow. ChIP-Seq experiments were done in triplicate.

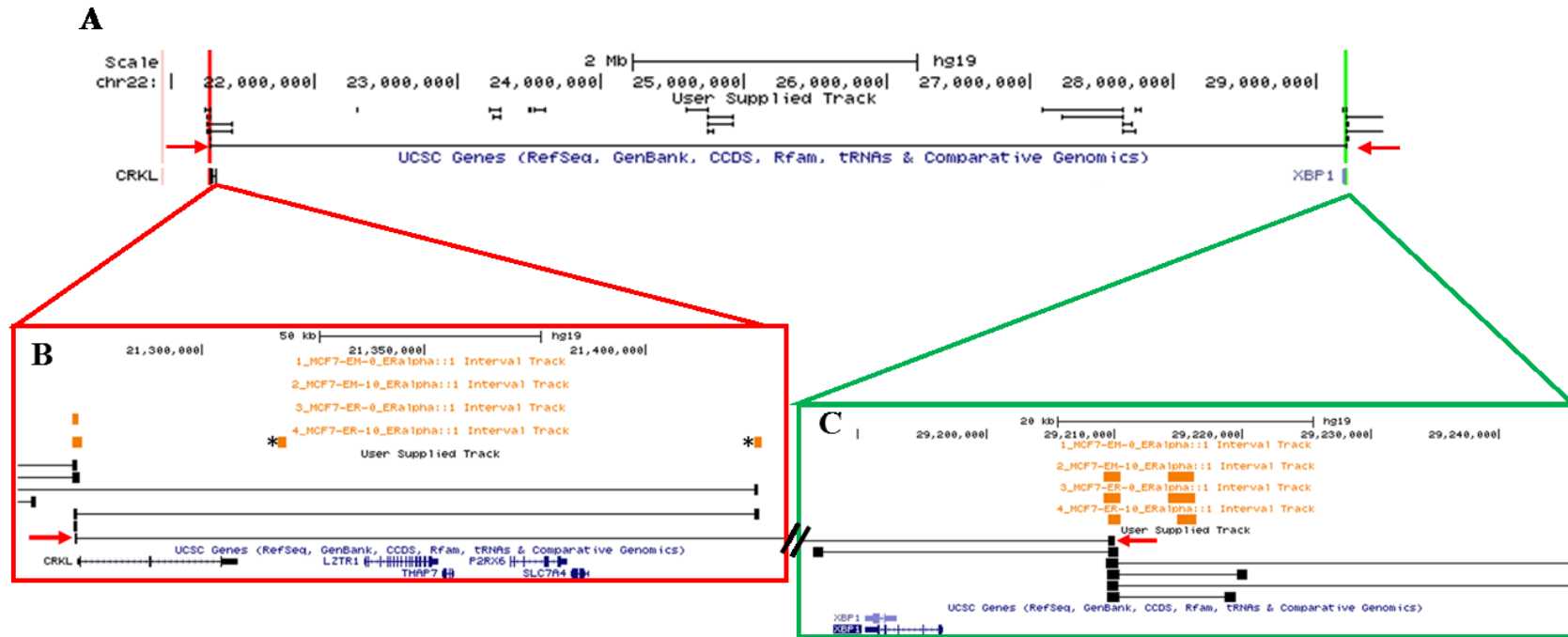


Figure 4.3 ER binding at anchor regions of a long-range DNA loop near *XBP1*. **A.** UCSC genome browser image for a > 2 Mb window shows small- and large-scale DNA loops associated with the *XBP1* gene. The presence of a long-range DNA loop is indicated by red arrows. The location of the proximal (green) and distal (red) anchor regions are highlighted. Boxes show a > 50 kb window for the distal anchor region (**B**) and a > 20 kb window for the proximal anchor region (**C**). ChIA-PET data showing previously mapped ER interactions (DNA loops) from the MCF-7 cells treated with E2 are shown. ER peaks that were present in at least 2/3 replicates are shown (orange boxes). ER peaks that were only present in the MCF7-ER cells after E2 treatment are indicated with an asterisk (*). Black

(Figure 4.3 continued) boxes indicate ER-bound anchor regions and the lines indicate the region of looped DNA. The location of the anchors associated with the long-range loop are indicated with a red arrow. ChIP-Seq experiments were done in triplicate.

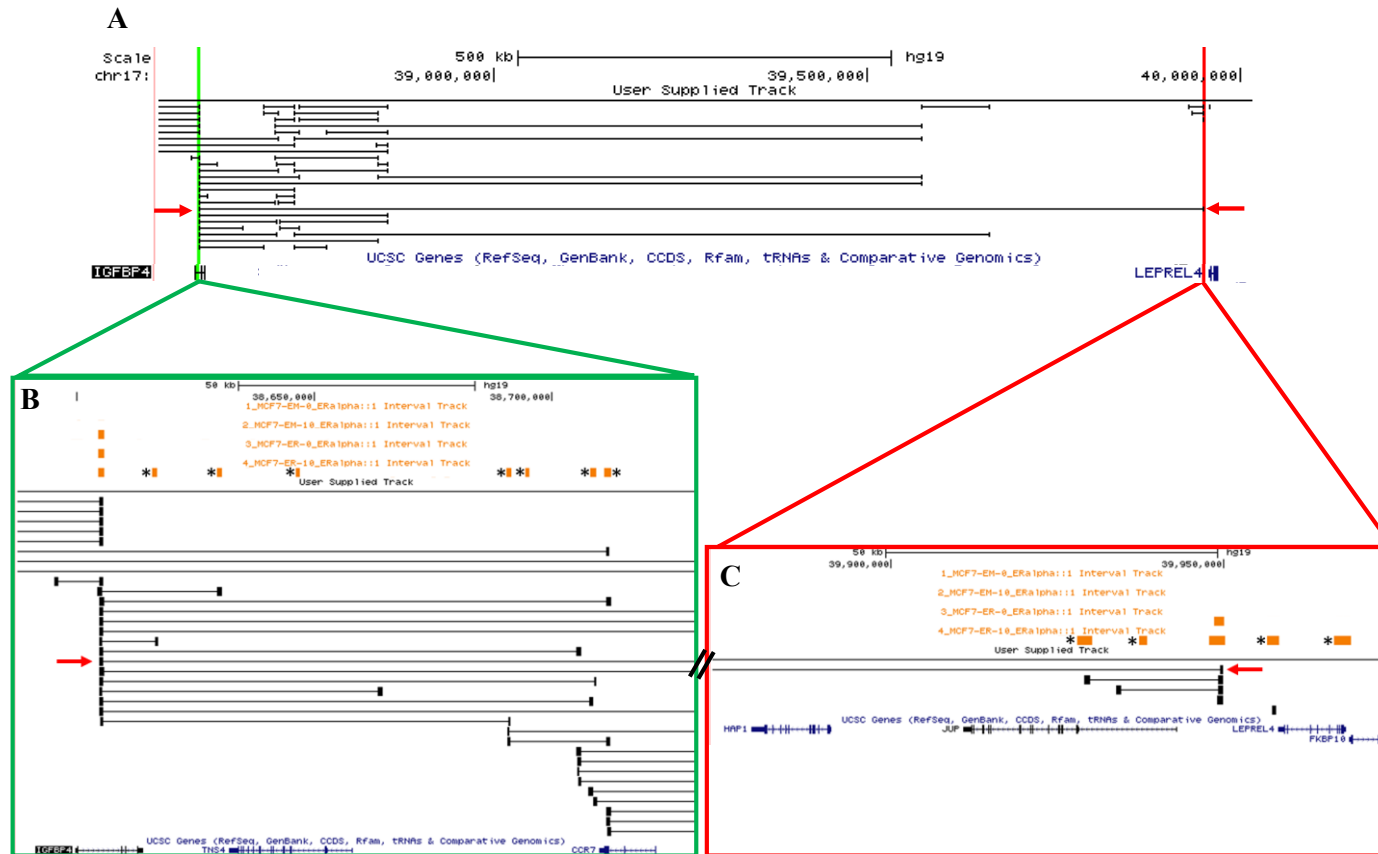


Figure 4.4 ER binding at anchor regions of a long-range DNA loop near *IGFBP4*. A. UCSC genome browser image for a > 500 kb window shows small- and large-scale DNA loops associated with the *IGFBP4* gene. The presence of a long-range DNA loop is indicated by red arrows. The location of the proximal (green) and distal (red) anchor regions are highlighted. Boxes show a > 50 kb window for

(Figure 4.4 continued) the proximal anchor region **(B)** and distal anchor region **(C)**. ChIA-PET data showing previously mapped ER interactions (DNA loops) from the MCF-7 cells treated with E2 are shown. ER peaks that were present in at least 2/3 replicates are shown (orange boxes). ER peaks that were only present in the MCF7-ER cells after E2 treatment are indicated with an asterisk (*). Black boxes indicate ER-bound anchor regions and the lines indicate the region of looped DNA. The location of the anchors associated with the long-range loop are indicated with a red arrow. ChIP-Seq experiments were done in triplicate.

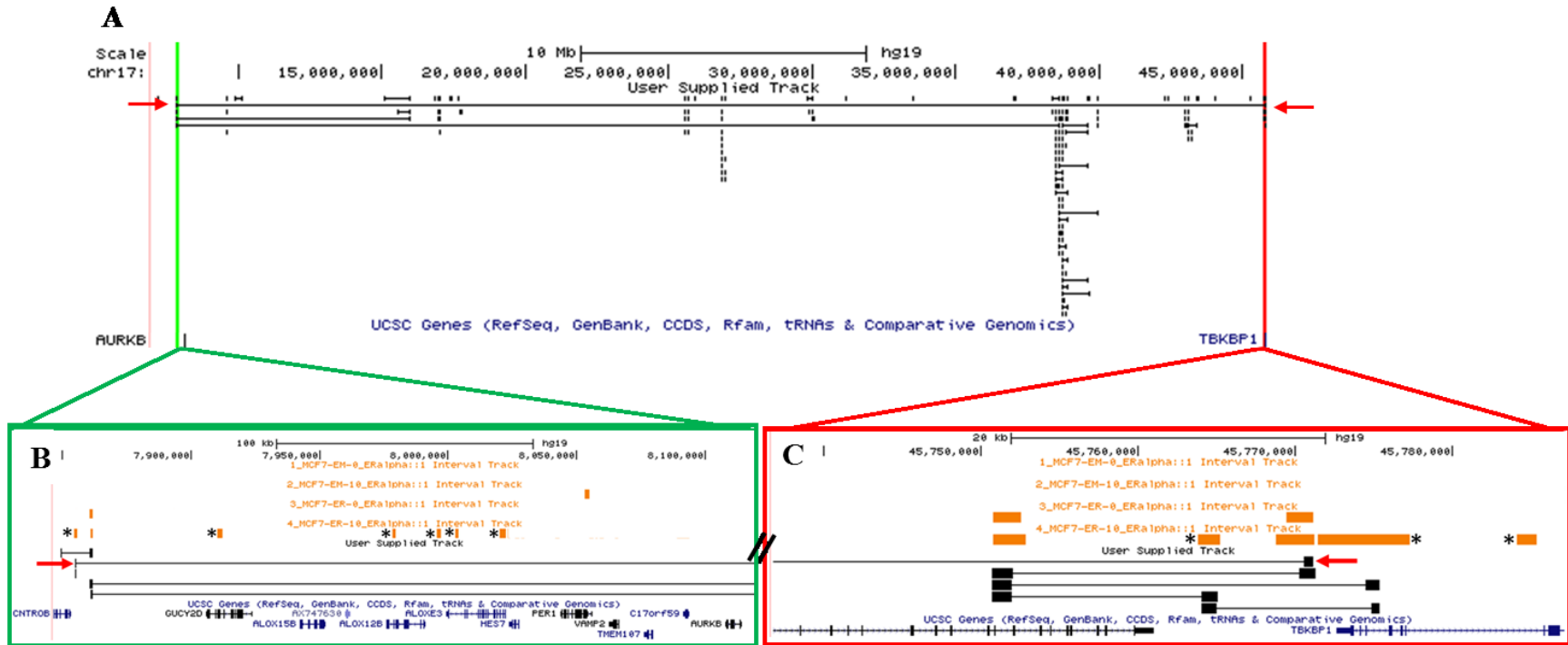


Figure 4.5 ER binding at anchor regions of a long-range DNA loop near *AURKB*. **A.** UCSC genome browser image for a > 10 Mb window shows small- and large-scale DNA loops associated with the *AURKB* gene. The presence of a long-range DNA loop is indicated by red arrows. The location of the proximal (green) and distal (red) anchor regions are highlighted. Boxes show a > 100 kb window for the proximal anchor region (**B**) and a > 20 kb window of the distal anchor region (**C**). ChIA-PET data showing previously mapped ER interactions (DNA loops) from the MCF-7 cells treated with E2 are shown. ER peaks that were present in at least 2/3 replicates are

(Figure 4.5 continued) shown (orange boxes). ER peaks that were only present in the MCF7-ER cells after E2 treatment are indicated with an asterisk (*). Black boxes indicate ER-bound anchor regions and the lines indicate the region of looped DNA. The location of the anchors associated with the long-range loop are indicated with a red arrow. CHIP-Seq experiments were done in triplicate.

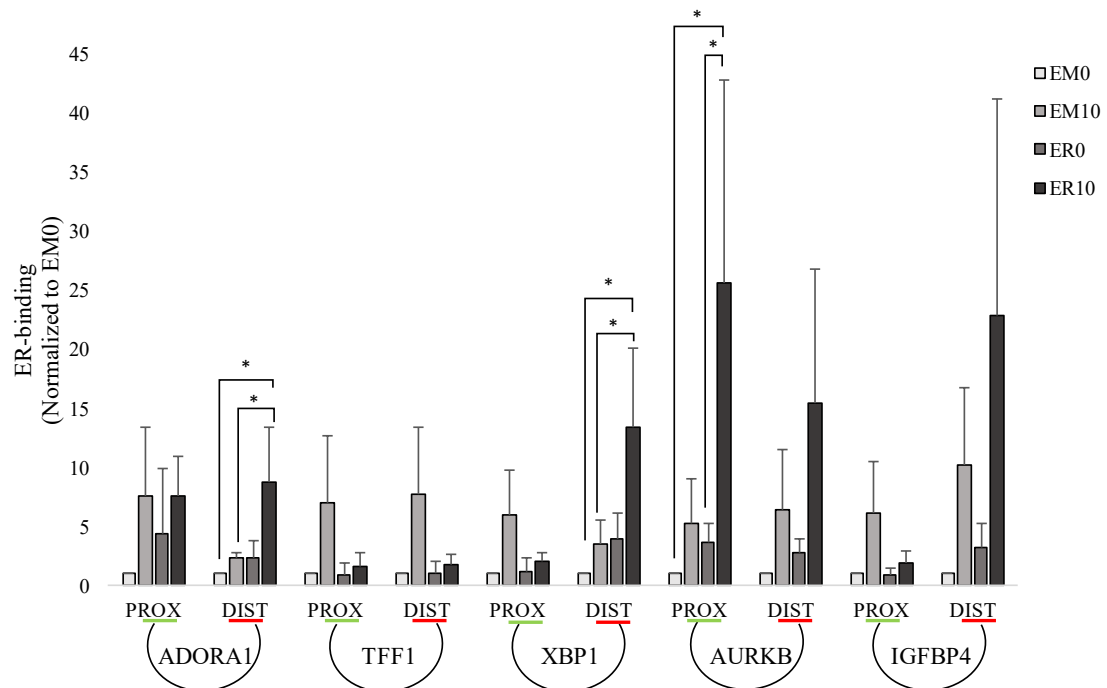


Figure 4.6 ER binding at proximal and distal anchor regions confirmed by ChIP-String. ER binding at locations associated with the proximal (PROX) and distal (DIST) anchor regions for long-range DNA loops associated with five differentially regulated genes. ChIP DNA was extracted from MCF7-EM and MCF7-ER cells treated with vehicle control (EM0 and ER0) or 10 nM E2 (EM10 and ER10) and analyzed using custom ChIP-String probe sets. ER binding was normalized to EM0. Data are shown as mean \pm SD. MCF7-ER cells treated with E2 (ER10) had a significant increase in ER binding at the distal anchors for the ADORA1 and XBP1 DNA loops when compared to MCF7-EM cells treated with (EM10) or without E2 (EM0). (Two-way ANOVA followed by Tukey's posthoc analysis, $n=3$, $*P<0.04$). The significant increase in ER binding at the proximal anchor for the AURKB DNA loop was previously described in chapter 2.

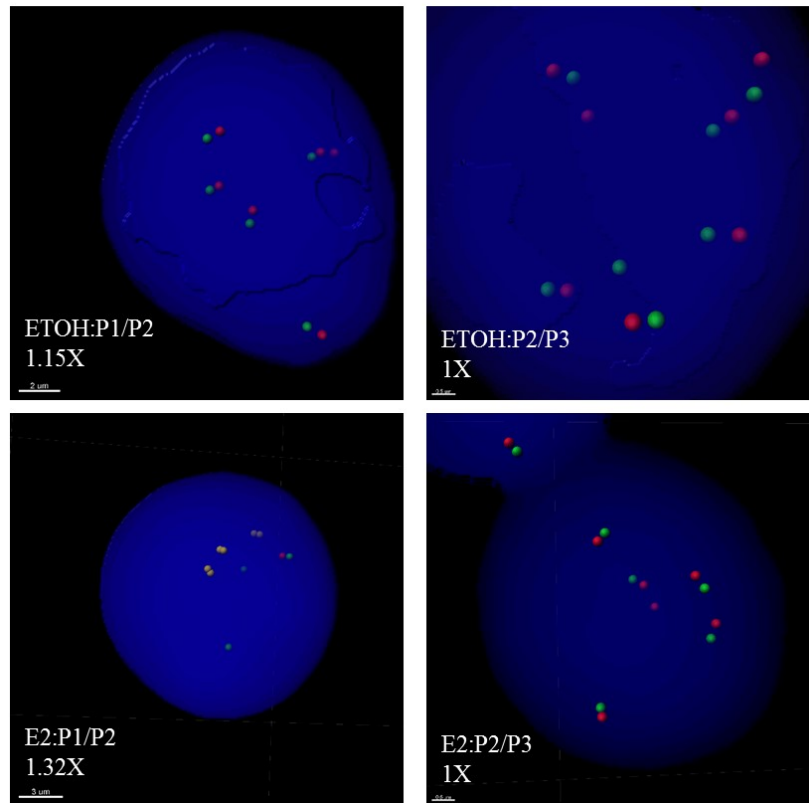
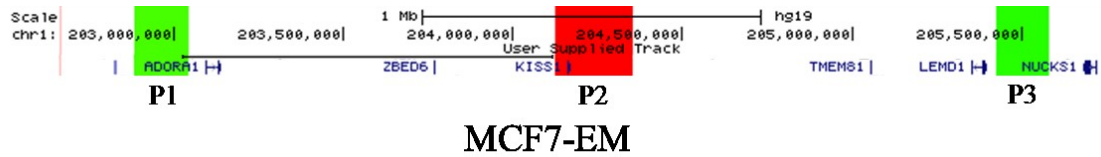


Figure 4.7 FISH analysis of the long-range loop for *ADORA1* in MCF7-EM cells. The location of fluorescently labelled BAC probes for the proximal anchor (P1), distal anchor (P2) and a negative probe (P3). Images shown were obtained by Imaris software and indicate nuclei with individual probe signals shown as red and green spots. Overlapped signals are shown as yellow spots. MCF7-EM cells were treated with ethanol (ETOH) or 10 nM E2 (E2). The P1/P2 represents probes specific for the long-range loop for *ADORA1*. The P2/P3 probe set represents a > 1 Mb region devoid of long-range loops. The normalized overlap rates for each condition are also indicated.

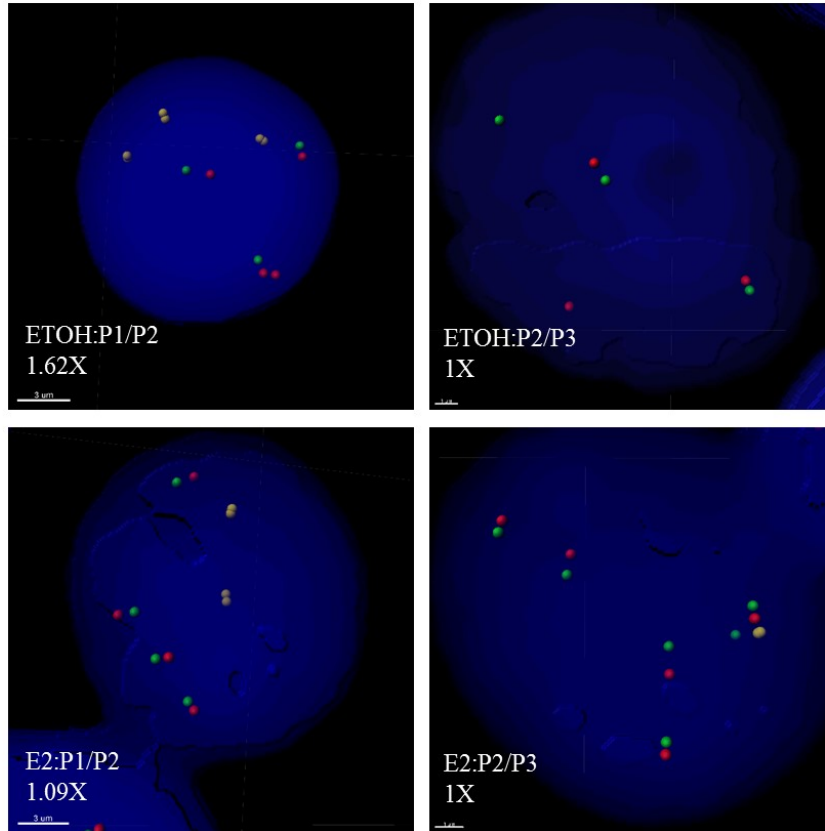
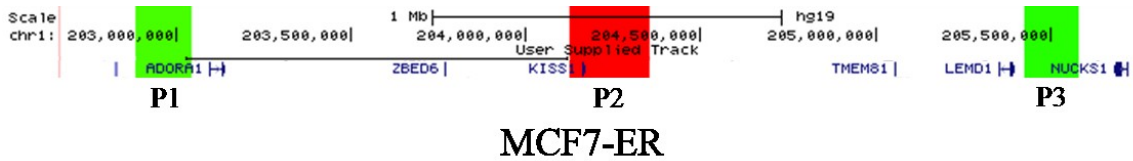


Figure 4.8 FISH analysis of the long-range loop for *ADORA1* in MCF7-ER cells. The location of fluorescently labelled BAC probes for the proximal anchor (P1), distal anchor (P2) and a negative probe (P3). Images shown were obtained by Imaris software and indicate nuclei with individual probe signals shown as red and green spots. Overlapped signals are shown as yellow spots. MCF7-ER cells were treated with ethanol (ETOH) or 10 nM E2 (E2). The P1/P2 represents probes specific for the long-range loop for *ADORA1*. The P2/P3 probe set represents a > 1 Mb region devoid of long-range loops. The normalized overlap rates for each condition are also indicated.



MCF7-EM

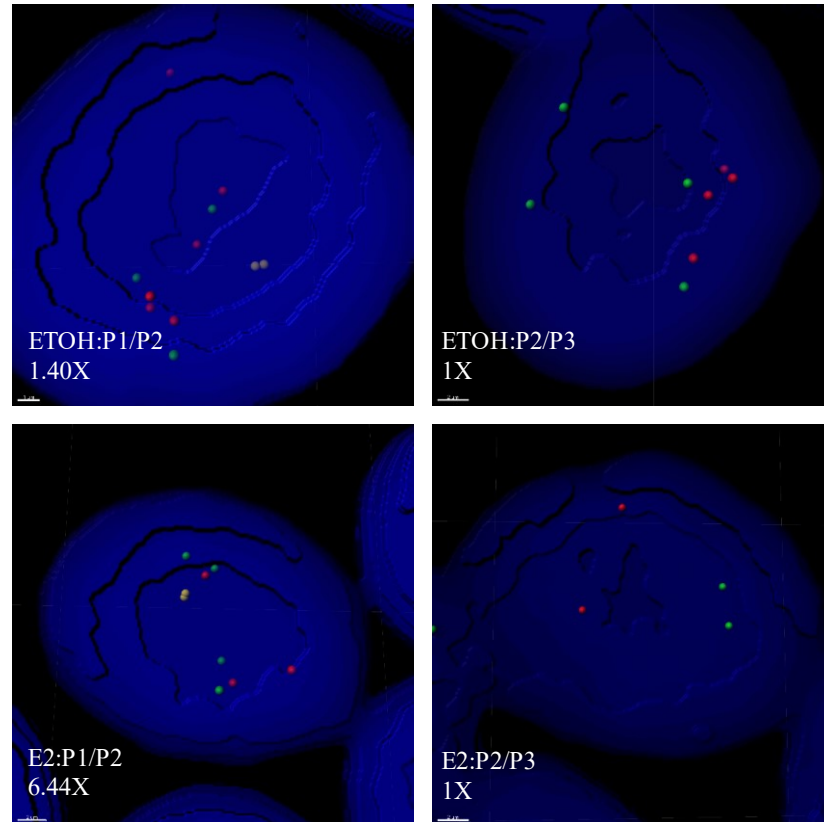


Figure 4.9 FISH analysis of the long-range loop for *TFF1* in MCF7-EM cells. The location of fluorescently labelled BAC probes for the proximal anchor (P1), distal anchor (P2) and a negative probe (P3). Images shown were obtained by Imaris software and indicate nuclei with individual probe signals shown as red and green spots. Overlapped signals are shown as yellow spots. MCF7-EM cells were treated with ethanol (ETOH) or 10 nM E2 (E2). The P1/P2 represents probes specific for the long-range loop for *TFF1*. The P2/P3 probe set represents a > 2 Mb region devoid of long-range loops. The normalized overlap rates for each condition are also indicated.

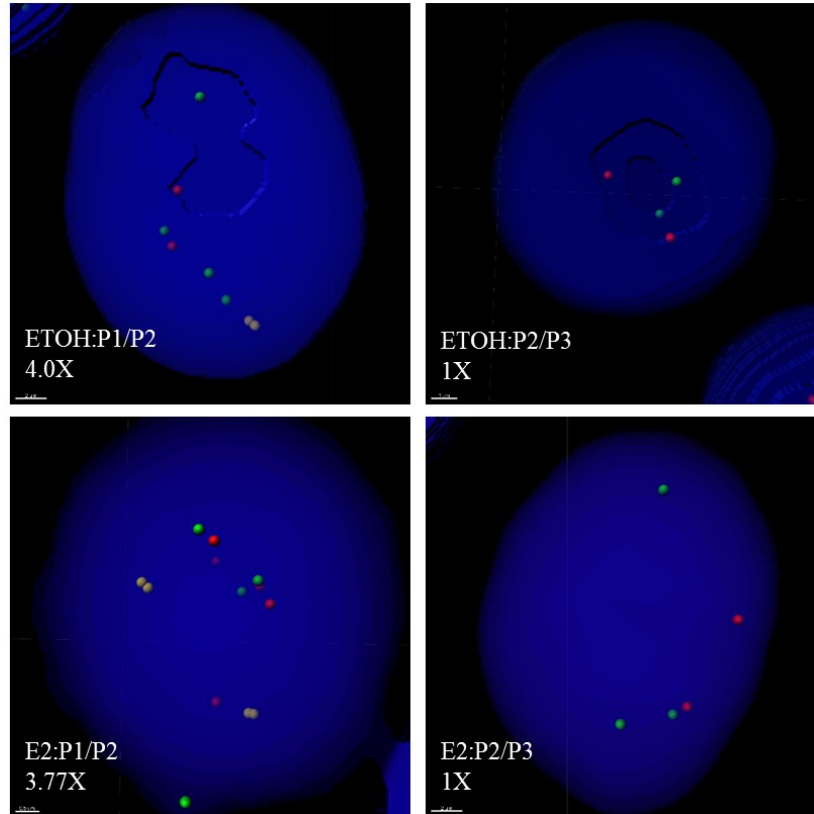
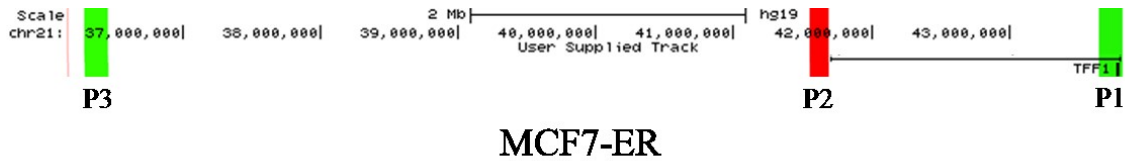


Figure 4.10 FISH analysis of the long-range loop for *TFF1* in MCF7-ER cells. The location of fluorescently labelled BAC probes for the proximal anchor (P1), distal anchor (P2) and a negative probe (P3). Images shown were obtained by Imaris software and indicate nuclei with individual probe signals shown as red and green spots. Overlapped signals are shown as yellow spots. MCF7-ER cells were treated with ethanol (ETOH) or 10 nM E2 (E2). The P1/P2 represents probes specific for the long-range loop for *TFF1*. The P2/P3 probe set represents a > 2 Mb region devoid of long-range loops. The normalized overlap rates for each condition are also indicated.

4.5 References

1. Metivier R, Penot G, Carmouche RP, Hubner MR, Reid G, Denger S, et al. Transcriptional complexes engaged by apo-estrogen receptor-alpha isoforms have divergent outcomes. *EMBO J.* 2004;23(18):3653-66.
2. Carroll JS, Meyer CA, Song J, Li W, Geistlinger TR, Eeckhoute J, et al. Genome-wide analysis of estrogen receptor binding sites. *Nat Genet.* 2006;38(11):1289-97.
3. Singhal H, Greene ME, Tarulli G, Zarnke AL, Bourgo RJ, Laine M, et al. Genomic agonism and phenotypic antagonism between estrogen and progesterone receptors in breast cancer. *Science Advances.* 2016;2(6): e1501924.
4. Le Dily F, Bau D, Pohl A, Vicent GP, Serra F, Soronellas D, et al. Distinct structural transitions of chromatin topological domains correlate with coordinated hormone-induced gene regulation. *Genes Dev.* 2014;28(19):2151-62.
5. Fullwood MJ, Liu MH, Pan YF, Liu J, Xu H, Mohamed YB, et al. An oestrogen-receptor-a-bound human chromatin interactome. *Nature.* 2009;462(7269):58-64.
6. Liu MH, Cheung E. Estrogen receptor-mediated long-range chromatin interactions and transcription in breast cancer. *Mol Cell Endocrinol.* 2014;382(1):624-32.
7. Osmanbeyoglu HU, Lu KN, Oesterreich S, Day RS, Benos PV, Coronello C, et al. Estrogen represses gene expression through reconfiguring chromatin structures. *Nucleic Acids Res.* 2013;41(17):8061-71.

Chapter 5: Discussion and future directions

5.1 Discussion

For ER+ breast cancer patients the diagnosis of luminal subtype has a major impact on the recommended treatment. Luminal A patients have an excellent response to endocrine therapies such as tamoxifen, whereas luminal B patients require additional chemotherapy (1, 2). The growing clinical evidence for the therapeutic effect of E2 (described in section 1.3.2.3.5) and the known estrogenic properties of tamoxifen (3-5) led to the hypothesis that the difference in the response to endocrine therapy in the luminal subtypes is actually a differential response to E2. Early studies of ER+ tumors have shown the response to tamoxifen is regulated by the ER concentration (6, 7). This relationship has been consistently shown in more recent clinical studies where tumors with the highest levels of ER expression have the greatest response to tamoxifen (8, 9). Luminal A tumors have the highest ER expression and there is clinical and *in vitro* evidence that increased ER expression can promote an anti-proliferative response to tamoxifen and E2 (8-13). The aim of this was to confirm the level of ER expression can regulate a differential response to E2. MCF-7 cells with inducible exogenous ER expression were used to determine how ER regulates this response to hormones. The final objective of this work was to use these findings as a basis for developing a diagnostic test that can improve the ability to predict the response of ER+ patients to hormonal treatments.

5.1.1 Increased ER expression leads to an anti-proliferative response to E2

The parental MCF-7 cell line was stably transduced with a doxycycline inducible ER plasmid (MCF7-ER) and obtained a 20-fold increase in ER protein compared to endogenous levels (MCF7-EM). This level of ER expression is consistent with quantitative measurements of ER concentrations that find a sigmoidal response relationship over 100-fold increases in ER (6, 7). The results from section 2.3.1 found that as the level of ER

increases the prototypical proliferative response seen in the MCF-7 parental cells decreases and switches to significant growth-suppression at a standard 0.5 µg/ml dose of doxycycline. Previous reports have shown that MCF-7 cells that were long-term E2 deprived (LTED) have an apoptotic response upon E2 treatment with release of cytochrome C from the mitochondria and increased PARP cleavage (reviewed in (14)). PARP cleavage and cytochrome C in the cytosolic fraction was detected in MCF7-ER cells treated with the apoptotic agent STS, but not after E2 treatment. These results confirmed the apoptotic response is intact in the MCF7-ER cells but was not present upon E2 treatment. Similar to previous reports (13, 15) a G1/S cell cycle block was found in the MCF7-ER cells after E2 treatment. These results suggest that increased ER expression mediates the anti-proliferative response to E2 through initiation of a cell cycle block and not apoptosis.

Cyclin/CDK complexes as well as cyclin dependent kinase inhibitors (p21, p27, p57) tightly regulate several checkpoint transitions of the cell cycle. Previous studies have shown that tamoxifen prevents the proliferation of MCF-7 cells through a G0/G1 arrest regulated by p21 and p27 (16). p21 prevents the phosphorylation of Rb and release of the E2F transcription factors thus preventing cell cycle progression through inhibition of E2F binding at its own promoter as well as the promoters of G1 cell cycle associated genes. Increased p21 expression can also negatively regulate cyclin B2 gene (*CCNB2*) transcription by promoting the recruitment of the repressive RB-like and E2F4 components of the DREAM (DP, RB-like, E2F4 and MuvB) complex to the *CCNB2* gene promoter preventing the requisite increase in cyclin B2 and leading to a G2/M block (17). A previous study implicated a role for ER in the transcriptional regulation of the p21 gene (*CDKN1A*) through interactions with the transcription factors AP1 and Sp1 at the gene promoter (18).

The results from chapter 2 show that MCF7-EM cells treated with E2 for 24 hours have a marked increase in S-phase fraction. This proliferative response was lost in MCF7-ER cells which encounter a G1/S-phase and a G2/M checkpoint arrest after 24 hours of E2 treatment. This cell cycle block was associated with a significant decrease in cyclin B2 and a significant increase in p21 expression. The formaldehyde crosslinking protocol in the ChIP-Seq experiments may have prevented the detection of ER tethering interactions with AP-1 at the previously described promoter region, however a novel ER peak at an intragenic region near the promoter of *CDKN1A* was observed in MCF7-ER cells treated with E2. These results suggest that increased ER expression in these cells enables binding of the *CDKN1A* gene in the presence of E2 and this may promote the up-regulation of p21 leading to the anti-proliferative response to E2. However, when the ChIP-Seq peak sets obtained from the MCF7-EM and MCF7-ER cells were compared against those generated from ER+ patient tumors that were either responsive or nonresponsive to tamoxifen treatment (19) there was significant ER binding at the intragenic region of *CDKN1A* identified in section 2.3.3 for both tamoxifen responsive and nonresponsive patients. This finding indicates that binding of ER at the putative regulatory site for p21 expression may occur in both responsive and nonresponsive patients. Preliminary results from the Hugh lab's PRESTO clinical trial found no significant correlation with p21 expression in patient tumors that had decreased proliferation after two weeks of E2 treatment (See Figure C3 in Appendix C). The role of increased p21 expression in breast cancer is controversial. While some clinical studies have shown that increased p21 expression correlates with high histological grade and short DFS (20, 21), others report high levels of p21 correlate with increased survival (22). There are also reports that p21 expression offers no prognostic value for breast cancer (23). When taken together with the clinical data the findings

reported here suggest that p21 expression alone is not enough to differentiate ER+ patients that will respond to endocrine or E2 therapy.

Further findings from chapter 2 suggest that the E2-induced cell cycle block in the MCF7-ER cells may be due to the down-regulation of the E2F transcriptional pathway as a primary effect of increased ER expression. The E2F pathway is a major driver of proliferation in normal and cancerous breast tissues. Proliferation in the normal breast is highest in the luteal phase of the menstrual cycle (24, 25) and full-transcriptome studies on normal breast tissues have shown an increase in *E2F1* expression during this phase (26). Similarly, E2-independent growth and resistance to aromatase inhibitors in ER+ patients correlate with an E2F gene signature (27). *In vitro* studies of the anti-proliferative response to E2 seen in MDA-MB-231 cells transfected to express high levels of ER (231-ER+) found that E2F1 was the major regulator of the differential response to E2 (11).

An increase in E2F1 expression was detected in the MCF7-ER cells in the absence of E2. Interestingly, this level of E2F1 expression was similar to that found in the MCF7-EM cells after E2 treatment. The increase in E2F1 in the MCF7-ER cells also correlated with a basal increase in the expression of ten cell cycle genes with known E2F motifs in the absence of E2. These findings are consistent with results from the proliferation experiments in section 2.3.1 and other reports (28) of an increased basal proliferation in the MCF7-ER cells in the absence of E2. Another significant finding was a decrease in E2F1 protein and mRNA expression in the MCF7-ER cells after E2 treatment. This decrease in E2F1 expression correlated with the down-regulation of the ten cell cycle genes under this condition. Previous reports have shown an ER/Sp1 complex can bind at the *E2F1* promoter and mediate *E2F1* expression in tamoxifen resistant MCF-7 cells (29). There were no significant ER peaks near the *E2F1* promoter to link increased ER expression to *E2F1*

regulation in the ChIP-Seq data. It is possible that tethering interactions between ER and Sp1 were not maintained during the formaldehyde crosslinking used in the ChIP-Seq protocol. Nevertheless, the gene expression results suggest that increased ER expression may mediate a differential response to E2 through regulation of the E2F1 pathway.

5.1.2 Increased ER expression leads to differential gene regulation upon E2 treatment

The current diagnostic assays used to determine a breast cancer patient's molecular subtype use gene expression signatures which rely heavily on genes associated with proliferation (30, 31). This proliferative score is a major determining factor in the generation of the risk of recurrence (ROR) score and contributes to the differentiation between luminal A and luminal B tumors for the Prosigna[®] (PAM50) breast cancer gene signature assay (31). The results from chapter 3 showed very few genes have a similar response to E2 in the MCF7-EM and MCF7-ER cells. When the genes that were up-regulated by E2 in each MCF-7 transfectant were compared against the PAM50 gene list 20 genes associated with proliferation were found to be up-regulated in the MCF7-EM cells after E2 treatment. Interestingly, six of these genes were also up-regulated in the MCF7-ER cells in the absence of E2 and correlates with the increase in basal proliferation seen in these cells. This result correlates with clinical finding that the incidence of luminal A breast cancers increases after the menopause, when the level of serum E2 becomes undetectable (32, 33). This is a significant finding as it suggests that under certain conditions, such as E2-deprivation, luminal A tumors may show a pattern of gene expression that more closely resembles the luminal B subtype. This may be the mechanism that causes diagnostic gene panels enriched in proliferative markers to incorrectly subtype luminal tumors.

Interestingly, when the MCF7-ER cells were treated with E2 there were seven up-regulated genes that were also included in the PAM50 gene list. Significantly, two of these genes (*FOXA1* and *BCL2*) are associated with the luminal A subtype (34, 35). This result indicates that E2 treatment can shift these cells towards a gene expression pattern that is more representative of the less aggressive luminal A subtype. When taken together, these results highlight the current limitations in the accurate diagnosis of luminal subtypes. Development of a diagnostic assay that can detect the biological mechanism that regulates the differential gene expression patterns may provide a more accurate separation of the luminal subtypes.

ER binding at promoter and distal enhancer regions has been described in the regulation of thousands of genes. The results from chapter 2 suggest that the anti-proliferative response to E2 is mediated through transcriptional regulation that requires an intact ER DBD and found that increased ER expression promotes novel ER binding patterns that are more representative of tamoxifen responsive patients. This led to the hypothesis that changes in ER-DNA binding may enable the differential regulation of a subset of genes in the presence of E2. To investigate the mechanism for ER induced differential gene expression a list of 72 genes that were up-regulated by E2 in the MCF7-EM, down-regulated by E2 in the MCF7-ER cells and had a significant basal increase in expression in the MCF7-ER cells in the absence of E2 was obtained. The differential expression of five genes from this list (*TFF1*, *ADORA1*, *XBPI*, *IGFBP4*, and *AURKB*) that were associated with ER binding at non-consensus ERE motifs within 50-100 kb of TSS in the ChIP-Seq data was confirmed by RT-qPCR. Whereas ER binding was only present after E2 treatment at the promoter regions for four of the five genes in the MCF7-EM cells, ER binding at this region was detected for all five genes in the MCF7-ER cells in the absence of E2.

Furthermore, these ER peaks were maintained after E2 treatment for all five genes. Mobility shift assays have shown that binding of ER to a consensus ERE requires receptor dimerization, whereas a non-consensus ERE can be bound by monomeric ER DBD at low concentrations and then switches to homodimer binding when the concentration of the ER DBD increases (36). Therefore, the finding of unliganded ER binding at non-consensus ERE motifs would suggest that increased ER expression may promote receptor dimerization in the absence of E2. The maintenance of an ER peak at these regions also suggests these homodimers may be further stabilized upon E2 binding. The presence of ER homodimers at these regions would enable the bending of the DNA toward the major groove which has been suggested to promote gene activation by enabling DNA looping (37).

Advances in molecular techniques have highlighted an important role for chromatin reconfiguration into small- and large-scale DNA loops during gene transcription (38, 39). These studies have shown that genes that are activated by E2 are often located near anchor regions where they can interact directly with the transcriptional machinery, whereas down-regulated genes are often located away from the anchor regions and become sequestered in the looped DNA (38). ER-DNA binding in MCF-7 cells in the absence of E2 was shown to correlate with the formation of DNA loops which contain paused Pol II (40). These unliganded ER-mediated loops were thought to serve as a mechanism to promote immediate transcriptional elongation upon E2 treatment (40).

Experiments from chapter 3 found that the ChIP-Seq peaks were enriched with motifs for CTCF, FOXA1, GATA3 and AP-2 γ which are known to mediate DNA loop formation (41). These motifs had the highest level of enrichment in the MCF7-ER cells in the absence of E2. An in-depth investigation into ER-DNA binding in the absence of E2

described transcriptional activity of the unliganded receptor at enhancer regions for genes associated with proliferation and development (42). Interestingly, these enhancer regions were enriched with motifs for two known DNA loop mediators, FOXA1 and AP-2 γ , (42) which may support a role for DNA looping in the basal activation of genes associated with these regions.

Consistent with the presence of DNA-loop cofactors the regions bound within 50-100 kb of the five differentially expressed genes were associated with anchors for previously mapped ER-mediated DNA loops. ER binding was detected at a distal anchor of a long-range (≥ 1 Mb) DNA loop for each of these genes which were enriched with ERE half sites. ChIP-Seq results show these distal regions were bound in the MCF7-ER cells only after E2 treatment, and FISH experiments confirmed a significant increase in the long-range loop associated with the *TFF1* gene under this condition. These findings suggest that the formation of this long-range loop is E2-dependent in cells that express low levels of ER. Additional results from chapter 3 indicate a basal increase in expression for each of the five genes in the MCF7-ER cells in the absence of E2. ER binding was confirmed at both anchor regions of the >1 Mb DNA loop for the five genes. FISH experiments confirmed a significant increase in the long-range loop near *TFF1* in the MCF7-ER cells in the absence of E2. Previous studies have shown unliganded ER is bound at DNA loops that are transcriptionally paused in the absence of E2 (40). This suggests that ER enables loop formation in the absence of E2 as a mechanism to allow immediate activation upon E2 treatment. The findings outlined here suggest that increased ER expression may promote DNA loop formation and activation of the transcriptional machinery in the absence of E2.

Previous studies on E2-induced gene repression suggested that the reconfiguration of DNA loops may be mediated by novel ER binding within the looped region which

destabilizes the surrounding chromatin (40). The down-regulation of the five genes by E2 in the MCF7-ER cells led to the hypothesis that increased ER binding within the loop region may promote the destabilization of the loop leading to loss of ER binding at the anchor regions associated with these genes. Several unique ER binding sites were detected within the looping regions associated with each of the five long-range loops in the MCF7-ER cells after E2 treatment. However, ER binding was also detected at the anchor regions for these long-range loops and maintained in the MCF7-ER cells upon E2 treatment. FISH analysis of the long-range loop for *TFF1* found loop formation was still significantly increased in the MCF7-ER cells after E2 treatment. These findings suggest that rather than disruption of loops being the mechanism of gene regulation this long-range loop may be maintained under repressive conditions. An alternative explanation for this is that a loop can switch from an active to repressive state depending on the receptor conformation. The stability of ER-mediated loops near *TFF1* under repressive conditions was previously shown in MCF-7 cells treated with tamoxifen (43). Further support for repressive loop structures was shown in studies of the glucocorticoid receptor (GR), which found that a constitutively active loop near the *GR* gene could be repressed in the presence of ligand through GR recruitment of corepressors to the promoter region (44).

5.1.3 A theoretical model for ER-mediated gene regulation

When considering these results along with published data a theoretical model for the unliganded transcriptional function of ER can be formulated. Fluorescence resonance energy transfer (FRET) studies have shown that the unliganded ER-LBD can form stable dimers in the absence of E2 (45). There is also evidence that at high concentrations the ER DBD binds to non-consensus EREs as a homodimer rather than a monomer (36). In this

model, increased ER expression may increase the propensity for receptor-receptor interactions which enable spontaneous homodimerization that stabilize the receptors in the absence of ligand. The formation of unliganded ER homodimers could explain the presence of ER binding at the full ERE motifs located in the proximal anchor regions of the five differentially regulated genes in this study (Figure 5.1). Previous studies have shown that multiple, close proximity non-consensus EREs or ERE half sites promote a transcriptional synergism that may be mediated through interactions between multiple ER dimers and/or co-recruitment of coactivators (46). In the experiments outline here, the distal anchor regions were enriched in ERE half sites and may therefore enable simultaneous binding of multiple unliganded ER homodimers which synergize to stabilize receptor binding at lower affinity sites (Figure 5.1). Unliganded ER has been shown to recruit coactivators as well as members of the basal transcriptional machinery to the *TFF1* promoter (47), and studies have found that Pol II is often paused at these promoter regions in MCF-7 cells in the absence of E2 in order to promote rapid transcriptional response upon E2 treatment (40, 48, 49). In the model described here, coactivator recruitment at both anchor regions may promote chromatin remodeling and the formation of DNA loops which may enable enough basal coactivator activity to activate the paused Pol II at the nearby promoter region (Figure 5.1). This would permit a basal level of gene expression in the absence of ligand.

The experimental data show that long-range DNA loops associated with basally expressed genes become repressed upon the E2 treatment in the MCF7-ER cells. In this model, E2 binding may lead to a change in the conformation of the ER dimers previously bound at the anchor regions which promotes the dissociation of the coactivator complexes (Figure 5.2). Gene repression may then be mediated by the recruitment of corepressor complexes to these regions (Figure 5.2). Additional ER binding within and outside of the

anchor regions may further stabilize the formation of these repressed loops (Figure 5.2). It is important to note that none of the proliferation genes that overlapped with the PAM50 gene list were associated with ER-mediated loops in this study. This suggests that the genes included in current diagnostic assays may be secondary targets of ER-mediated transcription which serve as a readout for the overall level of proliferation in a given tumor but may not directly reflect the biological mechanism which enables this response.

5.1.4 Comparison of experimental results against previously published ER+ cell line models

Previous studies have shown E2-induces apoptosis in MCF-7 cells that have been E2 deprived for 6 months up to 2 years (long term estrogen deprived-LTED) (reviewed in (50)). These cells often have increased levels of ER expression and an initial increase in S phase fraction after E2 treatment that switches to an apoptotic response after 96 hours (50). Classic measures of apoptosis such as PARP cleavage and cytochrome C release from the mitochondria were not detected in the MCF7-ER cells after 24 hours of E2 treatment. Whether prolonged treatment of these cells with E2 would eventually lead to an apoptotic response would have to be further tested. Additionally, the three-day adaption period used in this study is unlikely to cause similar overall changes in the MCF-7 phenotype that are seen after prolonged E2 deprivation and thus cannot be directly compared to the results obtained for LTED MCF-7 cell lines.

The proliferative response of MCF-7 cells to E2 has been well-documented and reviewed (51). This pro-proliferative pathway was shown to be mediated by ER through the down-regulation of the p21 protein which promotes the activation of cell cycle proteins such as Cyclin E further allowing the transition from G1 into S phase of the cell cycle (16, 52). These reports are consistent with the increase in S phase fraction and corresponding

decrease in p21 expression obtained in the MCF7-EM cells after E2 treatment in chapter 2, though the decrease in p21 protein did not reach statistical significance. Another study investigating E2-induced proliferation in MCF-7 cells found the level of p21 expression did not significantly decrease after E2 treatment but showed an increased interaction with cyclin D1 which led to increased Cyclin E activity and progression into the S phase of the cell cycle (53). When taken together, the results from the MCF7-EM cell line are consistent with the previously described proliferative ability of parental MCF-7 cells and a regulatory role for p21 and S phase progression.

Several studies have shown that increased ER expression in ER negative or ER positive cell lines leads to an anti-proliferative response to E2 (10-13, 15, 54). A study by Moggs et al (2005) found that an ER negative cell line (MDA-MB-231) transfected for exogenous ER expression had an anti-proliferative response to E2 which was mediated through the down-regulation of several cell cycle associated genes (10). Another study using MDA-MB-231 cells with exogenous ER expression treated with E2 found a similar anti-proliferative response that was mediated by increased expression of p21 (11). This effect has also been reported for the MCF-7 cell line with increased exogenous ER (13). This mechanism of cell cycle regulation is consistent with the results from chapter 2 which show a significant increase in p21 expression in the MCF7-ER cells after E2 treatment. The presence of a G1/S phase block in the MCF7-ER cells after E2 treatment is also consistent with these previous reports.

Interestingly, a study by Liao et al. (2014) found that exogenous expression of wild type ER in the MCF-7 cell line led to an increase in E2-induced proliferation which was mediated through down-regulation of p21 (55). However, the level of ER expression after transfection was not reported in this study and therefore may not have been within the range

to promote an anti-proliferative response to E2. This would be consistent with the doxycycline titration experiments in chapter 2 and previous reports by Zhao et al (2004) which indicate that MCF-7 cells expressing low levels of exogenous ER can maintain their proliferative response to E2 (13). The maintenance of the proliferative response to E2 in MCF-7 cells transfected with exogenous ER on a doxycycline promoter has also been reported by Fowler et al. (2004) (28). These studies found that MCF-7 cells with an ~8-fold increase in ER expression (referred to as ER α HA) had a similar growth response to E2 when compared against cells that did not receive doxycycline (28). The discrepancies between this work and the results reported here may be due to differences in overall transfection efficiency and the use of a stable clone versus the nonclonal stable MCF7-ER transfectants reported here.

The ER α HA cell line reported by Fowler et al (2004) showed a marked increase in the level of basal proliferation in the absence of E2, which was attributed the increased ER expression and transcriptional activation of the AF-1 domain (28). Consistent with this, results from the MCF7-ER cells in chapter 2 found an increase in basal growth and S phase fraction when induced with 0.5 μ g/ml of doxycycline in the absence of E2. Additional investigation into the ER α HA cell line found that high ER expression led to increased basal gene transcription at estrogen-responsive genes, such as *TFF1* (56). Similar results were shown for the MCF7-ER cell line in this report. However, the effect of high ER expression on gene transcription in the presence of E2 was not reported by Fowler et al. (2006)(56) and therefore it is difficult to conclude whether the increased level of ER expression in the ER α HA cells caused a similar decrease in gene transcription when E2 was present that has been reported in the MCF7-ER cell line.

ChIP-Seq experiments on MCF-7 cells that were E2-deprived for 3-12 days showed that unliganded ER binds 585 unique DNA sites associated with differentiation, development and morphogenesis (42). ChIP-Seq results from the MCF7-EM cell line maintained in E2-deprived media for a total of four days in chapter 3 showed 39,619 ER peaks. This is a massive increase in ER binding sites when compared to the results from the previous study. Reasons for this discrepancy may include the reporting of the total number of peaks for all 3 biological replicates in chapter 3. It is likely that the actual number of significant peaks (present in at least 2/3 biological replicates) would be much lower and more representative of the previously published data. Furthermore, the first biological replicate reported in chapter 3 was done commercially by Active Motif and had very high numbers of ER peaks that could not be validated in subsequent replicates.

The most common motif in the MCF7-EM cells in the absence of E2 was a half-ERE, whereas the previous ChIP-Seq experiments reported enrichment of the full ERE in the top 25% of unliganded ER peaks and enrichment of a half-ERE in the bottom 25% of unliganded ER peaks (42). The presence of numerous nonspecific peaks in the data reported in chapter 3 may skew the motif analysis toward the presence of lower affinity ER binding sites. Consequently, significant ER binding was not detected near the *TFF1* gene in the MCF7-EM cells without E2 treatment though it was previously reported by ChIP-qPCR by Caizzi et al. (2014) (42). This discrepancy may be due to the increased sensitivity provided by the additional rounds of DNA amplification steps in ChIP-qPCR experiments compared to the ChIP-Seq and ChIP-String experiments in this report.

The ChIP-Seq experiments on the MCF7-ER cells with and without E2 treatment reported here are the first studies to investigate the effect of increased ER expression on DNA binding and subsequent gene regulation in an ER positive breast cancer cell line. One

previous report investigated the changes in ER binding using ChIP-Seq in MDA-MB-231 cells expressing exogenous levels of ER (231-ER) (57). Comparison of the ChIP-Seq peak sets from 231-ER cells against those obtained from MCF-7 cells showed 44% of ER peaks obtained from the 231-ER cells do not overlap with the MCF-7 ChIP-Seq profiles. However, it was unclear whether these peaks were obtained after E2-treatment or before (57). ChIP-Seq results from the MCF7-ER cells reported here are consistent with the presence of unique ER binding sites when the level of ER is increased. A strength for ChIP-Seq experiments obtained from the MCF7-ER cells rather than the 231-ER cells is that these studies allow the assessment of the effects of increased ER expression in the same cell line. Thus, differences in ER binding patterns are more likely to be caused by the increased level of ER expression rather than differences in the expression of specific cofactors or pioneer factors in ER-negative versus ER-positive cell lines.

When taken together, there are several previous reports that support the anti-proliferative response to E2 in cells that have high levels of ER expression reported here. Differences in cell culture protocols, the cell lines used, ER-transfection efficiencies, the number of days for E2-deprivation, as well as the overall heterogeneity of the MCF-7 cell line (see section 5.2) could all contribute to the discrepancies between the previous results and those reported here. Despite this, there is a strong body of evidence that increased ER expression can alter the proliferative response to E2 through regulation of the cell cycle. The ability to detect this anti-proliferative response in multiple cell lines and in different research laboratories indicate that the role for ER in the regulation of proliferation is a robust and critical function. Further investigations into this effect may shed new light on the underlying mechanisms that regulate hormone responsiveness in ER+ breast cancers.

5.1.5 Clinical significance

This work aimed to uncover how increased ER expression may mediate the anti-proliferative response to E2 that has been reported in normal breast tissue and some ER+ breast cancer patients (58-62). To accomplish this, a stable MCF-7 transfectant with increased ER expression and an anti-proliferative response to E2 was generated. This is the first study to suggest that breast cancer cells with increased ER expression can serve as an *in vitro* model which better represents the response to hormones in luminal A tumors. Results from the MCF7-ER cells combined with preliminary evidence from the Hugh lab's ongoing PRESTO clinical trial suggest that patients with increased ER expression have an anti-proliferative response to E2. Furthermore, the increase in basal proliferation detected in the MCF7-ER cells in the absence of E2 highlights a potential mechanism that enables luminal A tumors to develop in post-menopausal women with low or undetectable serum E2.

The results of ChIP-Seq experiments indicate increased ER expression can generate a subset of unique DNA-binding sites which correlate more closely to those obtained from patients with a good response to tamoxifen. Preliminary FISH experiments indicated increased ER expression alone may be enough to reconfigure chromatin into large-scale loops that become repressed upon E2 treatment. The detection of DNA loops that are poised for an anti-proliferative response in patient tumors may offer a novel predictive assay that can determine a patient's response to endocrine therapy.

5.2 Limitations

I appreciate that there are limitations to this work. The major limitation remains the absence of a cell line that has a validated luminal A molecular profile. Despite the finding that the ER binding patterns of the MCF7-ER cells correlate well with those for tamoxifen

responsive patients, it cannot be assumed that increased ER expression alone is enough to generate a luminal A subtype. The MCF-7 cell line was obtained from a pleural effusion and therefore represents an inherently aggressive phenotype (63). This cell line consistently shows the molecular profile of luminal B tumors which are associated with increased DNA amplification near proliferation genes, increased TP53 mutations, and increased expression of *FOXMI* which all contribute to transcriptional hyperactivity (64, 65). Luminal A tumors have the fewest overall mutations and “simplex” copy number alterations with the gain of the long arm of chromosome 1 and the loss of the long arm of chromosome 16 (1q/16) (64). This simplex 1q/16 pattern has not been detected in any of the ER+ breast cancer cell lines (66) and how this phenotype contributes to ER binding and DNA reconfiguration cannot be easily assessed. It is possible that the DNA looping patterns in luminal A tumors have a completely novel configuration that cannot be obtained in the MCF-7 cell line. These studies were meant as a proof of principle for the role of increased ER expression in regulating chromatin reconfiguration and gene transcription. Further validation of the FISH probes using tissues obtained from luminal A and luminal B patients would be needed to confirm whether these findings are representative of the ER+ subtypes. Patient material is difficult to obtain and has been formalin-fixed making confocal imaging difficult, therefore these validation experiments were not feasible for this study.

Breast cancer is a heterogeneous disease with differences occurring both between patients as well as within an individual tumor (67). Genetic heterogeneity between breast cancer patients diagnosed as the same intrinsic molecular subtype could lead to differences in the response to the same therapies due to underlying differences in gene expression and somatic mutations (67). In the context of ER expression, the presence of intratumoral heterogeneity could lead to differences in the level of ER expression throughout the tumor

mass, with some cells having high ER and others having low to no ER expression. Thus, in the presence of E2, certain cells within the tumor would be growth inhibited (high ER cells) while others would be growth promoted (low ER cells). This heterogeneity of ER expression could lead to the development of an E2-resistant tumor. In the case of intertumoral heterogeneity, multiple patients who are subtyped as luminal A may have differing levels of ER expression which could lead to differences in the overall therapeutic response to hormone therapies or E2.

The marked genetic heterogeneity of the MCF-7 cell line has been well described (68-70). A recent study has shown that vials from the same lot of MCF-7 cells obtained from ATCC already contain subpopulations with differing genetic backgrounds (71). The presence of these subpopulations may be the cause of the differences in cell growth rates, DNA synthesis, ER, PR and EGFR expression and E2-sensitivity seen in MCF-7 cells from different laboratories (71). These differences in phenotypic heterogeneity cannot be assessed by common cell line authentication practices, such as the short tandem repeat (STR) genotyping experiments that are widely used (71). This hinders the comparisons of MCF-7 data obtained from different research laboratories and limits the integrity of cross-validations of previous studies. Thus, caution must be taken when comparing the data obtained in this study against previously published data using the MCF-7 cell line.

Another limitation of this work was the use of previously mapped ER-loops obtained from the MCF-7 cell line. The high correlation between the ChIP data and this published ChIA-PET dataset indicates that the chromatin structure in the MCF-7 cell line is relatively stable. There was strong preliminary evidence in this study that loops that are formed in cells with low endogenous ER expression are maintained with increased ER expression. It is not possible to determine whether the novel ER binding sites associated with increased

ER expression had any impact on the overall chromatin configuration without performing similar high-throughput ChIA-PET or chromosome conformation capture techniques combined with sequencing such as 4C and Hi-C on the MCF7-ER cells. These protocols are technically difficult and costly to perform and therefore were not within the scope of this study.

The genomic integration site for the ER-mEmerald retroviral plasmid has not been mapped for the MCF-7 transfectants used in this study. Without this information it is unclear where the plasmid was integrated into the genomic DNA and whether this would have an impact on gene transcription or chromatin structures. The genomic integration site of DNA vectors previously used to transfect ER have not been reported. However, studies have shown that HIV retroviral DNA vectors favour regions of high gene activity, as these regions are rich in GC content and have a more open conformation that promotes DNA integration (reviewed in (72)). pLVX is a HIV-1 based vector, thus the p-LVX-ER-mEmerald plasmid was likely integrated into a region of high gene activity which would further promote the expression of the ER-mEmerald transcript.

The use of RNA-Seq to detect changes in transcription may present a limitation as these experiments measure the overall level of a transcript at the time of the experiment. In this way, though cells have been E2-deprived for three days it is possible that certain mRNA transcripts were maintained over the three-day adaptation period leading to a false measurement of basal increase in the absence of E2. Techniques such as global run-on sequencing (GRO-Seq) would have provided a more accurate measure of active transcription as these methods enable the assessment of newly synthesized transcripts. The MCF7-EM and MCF7-ER cells were both adapted for three days prior to being induced with doxycycline, and therefore both of the transfectants would maintain the endogenous

low levels of ER during this time. The lack of basal gene expression in the MCF7-EM cells provides support that it was the increase in ER expression induced by the doxycycline treatment that enabled the increase in basal transcription.

The use of FISH as a validation for the presence of DNA loops also has limitations. A major limitation for FISH is the lower resolution for loops obtained by FISH compared to assays such as ChIA-PET, 4C and Hi-C. While ChIA-PET, 4C and Hi-C can detect small- and large-scale DNA loops, the confocal imaging of fluorescent FISH signals requires large distances between the probes in order to accurately distinguish colocalized signals (73, 74). Studies have also shown the contact frequency detected by ChIA-PET and 4C does not directly correlate into spatial distances obtained by FISH (75). The FISH validation experiments conducted by Fullwood et al. (2009) indicated a detection limit of 1 Mb for accurate assessment of DNA loops (38). This published criterion was followed when designing the FISH probe sets and the negative probes showed that in regions where mapped looping was minimal there was distinct separation of the probe signals. Another limitation for the detection of DNA loops by FISH is the transient nature of these structures which may only be detected in 18% of cells in a given experiment (76). Furthermore, ChIA-PET and 4C techniques require an input of millions of cells which enables detection of infrequent loops, such as the long-range loops that can be detected by FISH (75). Thus, though a loop may be present under specific experimental condition, it may be difficult to assess a significant enrichment by FISH due to the limited number of cells counted. The use of a confocal microscope enabled the acquisition of images which contained 300-400 cells generating a relatively large sample size when compared to what could be done by visual counting.

The design of the negative FISH probe set also has limitations. The current design of these probes is to assess the level of background looping in the region being studied. Therefore, these probes often share one probe for an anchor region and then extend at least 1 Mb away from the loop. For certain genes, there may be additional loops which extend beyond the 5' and/or 3' anchor regions, making it difficult to find a region that is devoid of looping to use as a negative control. Using a negative probe in a region with a significant amount of looping may lead to an increase in the collocated signals obtained for the negative probe sets. When the positive probe set is normalized against this larger number it will lead to an overall lower level of overlap rate. The negative probes designed for the *TFF1* FISH experiments were located in areas devoid of long-range loops and should not have this issue. The negative probe sets are also measured on a separate set of slides, and though the cells are prepared at the same time, they do not reflect the actual background looping seen in the cells measured for the positive probes. This could be overcome by adding a negative probe with a different fluorophore that can be hybridized on the same slide. However, this experimental set-up is limited by the overlap in the spectra of the available fluorescent dyes for commercial FISH probes as well as the filters and lasers available on confocal microscope being used.

5.3 Future directions

The findings from this study suggest that increased ER expression enables a DNA configuration which promotes transcriptional regulation in the absence of E2. These results provided an important proof of principle which can be further tested to determine whether the increased ER expression in luminal A tumors generates a unique 3D DNA configuration that can be detected by FISH. This work was focused on the conformational changes

associated with genes that have a differential response to E2. However, these genes are predominately associated with proliferation and had overlapping expression profiles in the MCF7-ER cells in the absence of E2. This highlights the need for a diagnostic method that will not be influenced by serum E2 levels of ER+ patients at the time of diagnosis. With this in mind, the next steps are to utilize 4C-Seq to investigate whether the peaks that are unique to the MCF7-ER cells are associated with novel DNA loops. The presence of a long-range loop in only the MCF7-ER cells could serve as a target for the development of a set of FISH probes that could be validated on patient samples. The current results have shown that loops which were formed in the MCF7-ER cells in the absence of E2 were maintained after E2 treatment. This would suggest that a loop that is unique to a breast tumor with increased ER expression could be detected regardless of the level of serum E2 that patient may have. Further comparison of these ER peaks against those mapped in the tamoxifen responsive and nonresponsive ChIP-Seq dataset (19) may indicate the DNA loops that are most likely associated with a response to hormone therapy. This could overcome the limitations of the current diagnostic gene expression assays. These loops may also serve a prognostic value, as they would indicate a biological mechanism that is poised for an anti-proliferative response to E2 or tamoxifen.

Previous reports indicate that DNA loops are only present in 18% of cells in a given experiment (76). This would make detecting loops in patient samples difficult as FISH procedures commonly count only 50 interphase nuclei (77). To overcome this, multiple FISH probes associated with different DNA loop targets will be developed to generate a more robust FISH signal and to increase the likelihood of detecting a significant portion of DNA loops in the limited number of nuclei. If the 4C-Seq experiments from the MCF7-ER cells are unable to detect significant differences in the DNA loops compared to the MCF7-

EM cell line, then tissue samples from ER+ patients to will need to be obtained in order to conduct additional 4C experiments. Patients for these experiments would be chosen based on their molecular profile (luminal A and luminal B) and response to hormone therapy. The feasibility of these experiments may be limited by the requirement for large amounts of archived frozen tissues which will be difficult and costly to retrieve. Validation of the FISH probes on a large number of patient samples will be an important step in the development of the diagnostic tool as it will allow the effect of tumor heterogeneity to be assessed. Patient tissues are formalin-fixed paraffin-embedded which can generate significant background autofluorescence (78), therefore multiple FISH probes will be required for each anchor region to ensure a robust fluorescent signal. These probes will have to be designed carefully to ensure the regions bound by the probes for each loop anchor are not close enough to cause overlap of the red and green probe signals in the absence of DNA loops. If the 4C and FISH studies are unsuccessful then further investigation of the genes that were up-regulated by high ER expression may provide potential biomarkers which could be further validated by qPCR on material obtained from patient tissues.

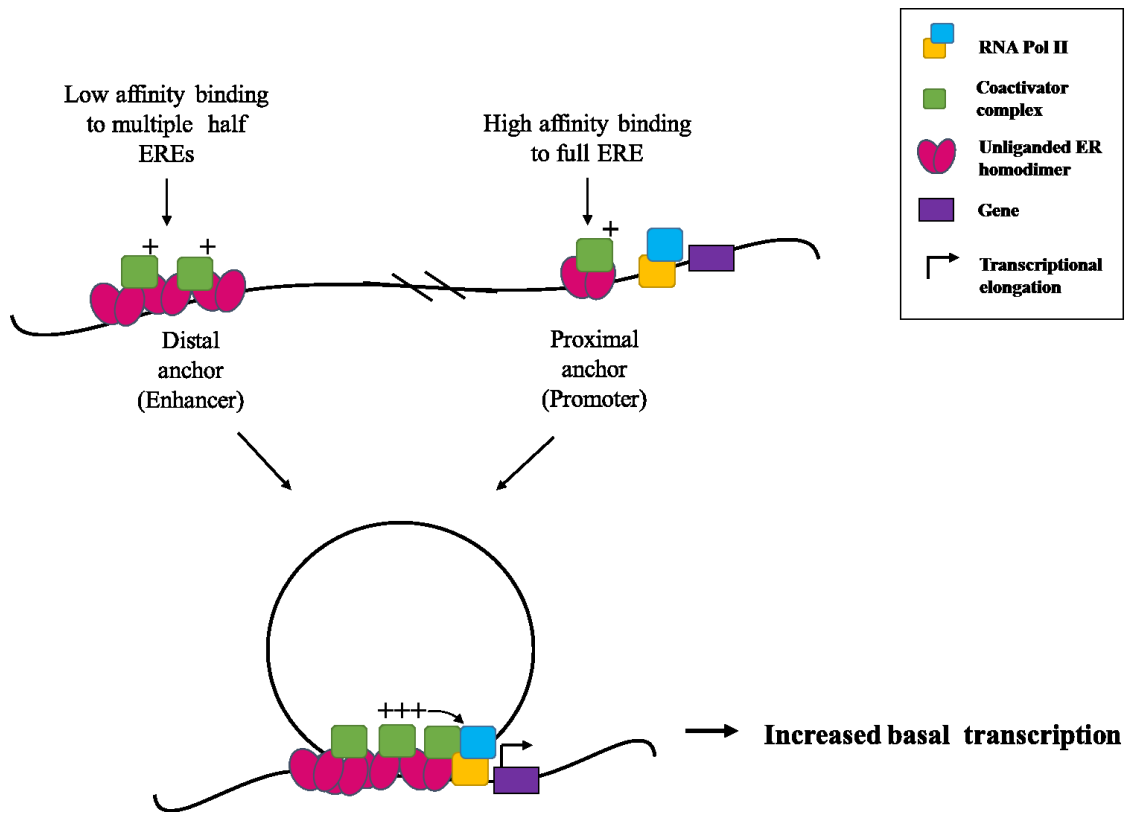


Figure 5.1 Theoretical mechanism for unliganded ER mediated DNA loop formation. Increased ER expression promotes the binding of unliganded ER homodimers to proximal (promoter) anchor regions containing full ERE motifs and paused RNA Pol II and distal anchors (enhancers) enriched in ERE half sites. Unliganded homodimer configuration enables recruitment of coactivator complexes which promote DNA reconfiguration and the stabilization of DNA loops. Loop formation enables association between the enhancer and promoter regions and enables a basal activation of RNA Pol II to initiate transcriptional elongation at near by gene.

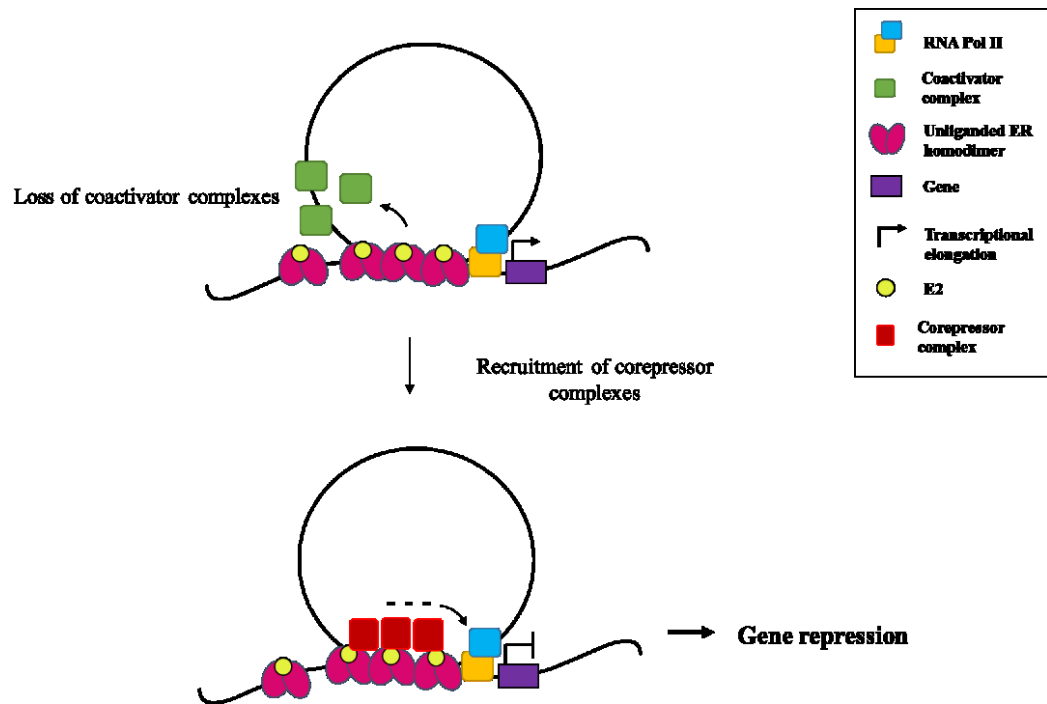


Figure 5.2 Theoretical mechanism for ER mediated repression at DNA loops. Upon E2 ligation, the structure of the ER homodimers changes leading to dissociation of the coactivator complexes. Additional ER binding at the distal anchor region stabilizes the DNA loop. ER recruitment of corepressors to the loop further prevents RNA Pol II function leading to down-regulation of the nearby gene.

5.4 References

1. Hugh J, Hanson J, Cheang MCU, Nielsen TO, Perou CM, Dumontet C, et al. Breast Cancer Subtypes and Response to Docetaxel in Node-Positive Breast Cancer: Use of an Immunohistochemical Definition in the BCIRG 001 Trial. *J Clin Oncol.* 2009;27(8):1168-76.
2. Lonning PE. Poor-prognosis estrogen receptorpositive disease: present and future clinical solutions. *Therapeutic Advances in Medical Oncology.* 2012;4(3):127-37.
3. Fisher B, Costantino J, Redmond C, Fisher E, Wickerham D, Cronin W, et al. Endometrial Cancer in Tamoxifen-Treated Breast-Cancer Patients - Findings from the National Surgical Adjuvant Breast and Bowel Project (Nsbap) B-14. *J Natl Cancer Inst.* 1994;86(7):527-37.
4. Kedar RP, Bourne TH, Powles TJ, Collins WP, Ashley SE, Cosgrove DO, et al. Effects of Tamoxifen on Uterus and Ovaries of Postmenopausal Women in a Randomized Breast-Cancer Prevention Trial. *Lancet.* 1994;343(8909):1318-21.
5. Love RR, Mazess RB, Barden HS, Epstein S, Newcomb PA, Jordan VC, et al. Effects of Tamoxifen on Bone-Mineral Density in Postmenopausal Women with Breast-Cancer. *N Engl J Med.* 1992;326(13):852-6.
6. Leclercq G, Heuson JC. Therapeutic Significance of Sex-Steroid Hormone Receptors in Treatment of Breast-Cancer. *Eur J Cancer.* 1977;13(11):1205-15.
7. Heuson JC, Longeval E, Mattheiem WH, Deboel MC, Sylvester RJ, Leclercq G. Significance of Quantitative Assessment of Estrogen Receptors for Endocrine Therapy in Advanced Breast-Cancer. *Cancer.* 1977;39(5):1971-7.

8. Dowsett M, Smith IE, Ebbs SR, Dixon JM, Skene A, A'Hern R, et al. Prognostic value of Ki67 expression after short-term presurgical endocrine therapy for primary breast cancer. *J Natl Cancer Inst.* 2007;99(2):167-70.
9. Kim C, Tang G, Pogue-Geile KL, Costantino JP, Baehner FL, Baker J, et al. Estrogen Receptor (ESR1) mRNA Expression and Benefit From Tamoxifen in the Treatment and Prevention of Estrogen Receptor-Positive Breast Cancer. *Journal of Clinical Oncology.* 2011;29(31):4160-7.
10. Moggs JG, Murphy TC, Lim FL, Moore DJ, Stuckey R, Antrobus K, et al. Anti-proliferative effect of estrogen in breast cancer cells that re-express ER α is mediated by aberrant regulation of cell cycle genes. *J Mol Endocrinol.* 2005;34(2):535-51.
11. Stender JD, Frasor J, Komm B, Chang KCN, Kraus WL, Katzenellenbogen BS. Estrogen-regulated gene networks in human breast cancer cells: Involvement of E2F1 in the regulation of cell proliferation. *Molecular Endocrinology.* 2007;21(9):2112-23.
12. Zajchowski DA, Sager R, Webster L. Estrogen Inhibits the Growth of Estrogen Receptor-Negative, but Not Estrogen Receptor-Positive, Human Mammary Epithelial-Cells Expressing a Recombinant Estrogen-Receptor. *Cancer Res.* 1993;53(20):5004-11.
13. Zhao H, Yu J, Peltier CP, Davie JR. Elevated expression of the estrogen receptor prevents the down-regulation of p21(Waf1/Cip1) in hormone dependent breast cancer cells. *J Cell Biochem.* 2004;93(3):619-28.
14. Lewis-Wambi JS, Jordan VC. Estrogen regulation of apoptosis: how can one hormone stimulate and inhibit? *Breast Cancer Research.* 2009;11(3):206.

15. Peng J, Jordan VC. Expression of estrogen receptor alpha with a Tet-off adenoviral system induces G0/G1 cell cycle arrest in SKBr3 breast cancer cells. *Int J Oncol.* 2010;36(2):451-8.
16. Cariou S, Donovan J, Flanagan W, Milic A, Bhattacharya N, Slingerland J. Down-regulation of p21(WAF1/CIP1) or p27(Kip1) abrogates antiestrogen-mediated cell cycle arrest in human breast cancer cells. *Proc Natl Acad Sci U S A.* 2000;97(16):9042-6.
17. Fischer M, Quaas M, Steiner L, Engeland K. The p53-p21-DREAM-CDE/CHR pathway regulates G(2)/M cell cycle genes. *Nucleic Acids Res.* 2016;44(1):164-74.
18. Mandal S, Davie JR. Estrogen Regulated Expression of the p21(Waf1/Cip1) Gene in Estrogen Receptor Positive Human Breast Cancer Cells. *J Cell Physiol.* 2010;224(1):28-32.
19. Ross-Innes CS, Stark R, Teschendorff AE, Holmes KA, Ali HR, Dunning MJ, et al. Differential oestrogen receptor binding is associated with clinical outcome in breast cancer. *Nature.* 2012;481(7381):389-93.
20. Barbareschi M, Caffo O, Doglioni C, Fina P, Marchetti A, Buttitta F, et al. p21(WAF1) immunohistochemical expression in breast carcinoma: Correlations with clinicopathological data, oestrogen receptor status, MIB1 expression, p53 gene and protein alterations and relapse-free survival. *Br J Cancer.* 1996;74(2):208-15.
21. Caffo O, Doglioni C, Veronese S, Bonzanini M, Marchetti A, Buttitta F, et al. Prognostic value of p21(WAF1) and p53 expression in breast carcinoma: An immunohistochemical study in 261 patients with long-term follow-up. *Clinical Cancer Research.* 1996;2(9):1591-9.

22. Jiang M, Shao Z, Wu J, Lu J, Yu L, Yuan J, et al. P21/waf1/cip1 and Mdm-2 Expression in Breast Carcinoma Patients as Related to Prognosis. *International Journal of Cancer*. 1997;74(5):529-34.
23. Pellikainen MJ, Pekola TT, Ropponen KM, Kataia VV, Kellokoski JK, Eskelinen MJ, et al. p21(WAF1) expression in invasive breast cancer and its association with p53, AP-2, cell proliferation, and prognosis. *J Clin Pathol*. 2003;56(3):214-20.
24. Anderson T, Battersby S, King R, McPherson K, Going J. Oral-Contraceptive use Influences Resting Breast Proliferation. *Hum Pathol*. 1989;20(12):1139-44.
25. McCarty K. Proliferative Stimuli in the Normal Breast - Estrogens Or Progestins. *Hum Pathol*. 1989;20(12):1137-8.
26. Pardo I, Lillemoe HA, Blosser RJ, Choi M, Sauder CAM, Doxey DK, et al. Next-generation transcriptome sequencing of the premenopausal breast epithelium using specimens from a normal human breast tissue bank. *Breast Cancer Research*. 2014;16(2):R26.
27. Miller TW, Balko JM, Fox EM, Ghazoui Z, Dunbier A, Anderson H, et al. ER α -dependent E2F transcription can mediate resistance to estrogen deprivation in human breast cancer. *Cancer Discov*. 2011;1(4):338-51.
28. Fowler A, Solodin N, Preisler-Mashey M, Zhang P, Lee A, Alarid E. Increases in estrogen receptor-alpha concentration in breast cancer cells promote serine 118/104/106-independent AF-1 transactivation and growth in the absence of estrogen. *Faseb Journal*. 2004;18(1):81-93.
29. Louie MC, McClellan A, Siewit C, Kawabata L. Estrogen Receptor Regulates E2F1 Expression to Mediate Tamoxifen Resistance. *Molecular Cancer Research*. 2010;8(3):343-52.

30. Paik S, Shak S, Tang G, Kim C, Baker J, Cronin M, et al. A multigene assay to predict recurrence of tamoxifen-treated, node-negative breast cancer. *New Engl J Med.* 2004;351(27):2817-26.
31. Wallden B, Storhoff J, Nielsen T, Dowidar N, Schaper C, Ferree S, et al. Development and verification of the PAM50-based Prosigna breast cancer gene signature assay. *Bmc Medical Genomics.* 2015;8:54.
32. Jenkins EO, Deal AM, Anders CK, Prat A, Perou CM, Carey LA, et al. Age-specific changes in intrinsic breast cancer subtypes: A focus on older women. *Oncologist.* 2014;19(10):1076-83.
33. Verkasalo PK, Thomas HV, Appleby PN, Davey GK, Key TJ. Circulating levels of sex hormones and their relation to risk factors for breast cancer: A cross-sectional study in 1092 pre- and postmenopausal women (United Kingdom). *Cancer Causes Control.* 2001;12(1):47-59.
34. Bernhardt SM, Dasari P, Walsh D, Townsend AR, Price TJ, Ingman WV. Hormonal Modulation of Breast Cancer Gene expression: Implications for Intrinsic Subtyping in Premenopausal Women. *Frontiers in Oncology.* 2016;6:241.
35. Eom YH, Kim HS, Lee A, Song BJ, Chae BJ. BCL2 as a Subtype-Specific Prognostic Marker for Breast Cancer. *Journal of Breast Cancer.* 2016;19(3):252-60.
36. Wood J, Greene G, Nardulli A. Estrogen response elements function as allosteric modulators of estrogen receptor conformation. *Mol Cell Biol.* 1998;18(4):1927-34.
37. Kim J, deHaan G, Nardulli AM, Shapiro DJ. Prebending the estrogen response element destabilizes binding of the estrogen receptor DNA binding domain. *Mol Cell Biol.* 1997;17(6):3173-80.

38. Fullwood MJ, Liu MH, Pan YF, Liu J, Xu H, Bin Mohamed Y, et al. An oestrogen-receptor-alpha-bound human chromatin interactome. *Nature*. 2009;462(7269):58-64.
39. Li G, Ruan X, Auerbach RK, Sandhu KS, Zheng M, Wang P, et al. Extensive Promoter-Centered Chromatin Interactions Provide a Topological Basis for Transcription Regulation. *Cell*. 2012;148(1-2):84-98.
40. Osmanbeyoglu HU, Lu KN, Oesterreich S, Day RS, Benos PV, Coronello C, et al. Estrogen represses gene expression through reconfiguring chromatin structures. *Nucleic Acids Res*. 2013;41(17):8061-71.
41. Liu MH, Cheung E. Estrogen receptor-mediated long-range chromatin interactions and transcription in breast cancer. *Mol Cell Endocrinol*. 2014;382(1):624-32.
42. Caizzi L, Ferrero G, Cutrupi S, Cordero F, Ballare C, Miano V, et al. Genome-wide activity of unliganded estrogen receptor-alpha in breast cancer cells. *Proc Natl Acad Sci U S A*. 2014;111(13):4892-7.
43. Pan YF, Wansa KDSA, Liu MH, Zhao B, Hong SZ, Tan PY, et al. Regulation of Estrogen Receptor-mediated Long Range Transcription via Evolutionarily Conserved Distal Response Elements. *J Biol Chem*. 2008;283(47):32977-88.
44. Ramamoorthy S, Cidlowski JA. Ligand-Induced Repression of the Glucocorticoid Receptor Gene Is Mediated by an NCoR1 Repression Complex Formed by Long-Range Chromatin Interactions with Intragenic Glucocorticoid Response Elements. *Mol Cell Biol*. 2013;33(9):1711-22.
45. Tamrazi A, Carlson K, Daniels J, Hurth K, Katzenellenbogen J. Estrogen receptor dimerization: Ligand binding regulates dimer affinity and dimer dissociation rate. *Molecular Endocrinology*. 2002;16(12):2706-19.

46. Gruber CJ, Gruber DM, Gruber IML, Wieser F, Huber JC. Anatomy of the estrogen response element. *Trends in Endocrinology and Metabolism*. 2004;15(2):73-8.
47. Metivier R, Penot G, Carmouche RP, Hubner MR, Reid G, Denger S, et al. Transcriptional complexes engaged by apo-estrogen receptor-alpha isoforms have divergent outcomes. *EMBO J*. 2004;23(18):3653-66.
48. Kininis M, Chen BS, Diehl AG, Isaacs GD, Zhang T, Siepel AC, et al. Genomic analyses of transcription factor binding, histone acetylation, and gene expression reveal mechanistically distinct classes of estrogen-regulated promoters. *Mol Cell Biol*. 2007;27(14):5090-104.
49. Kininis M, Isaacs GD, Core LJ, Hah N, Kraus WL. Postrecruitment Regulation of RNA Polymerase II Directs Rapid Signaling Responses at the Promoters of Estrogen Target Genes. *Mol Cell Biol*. 2009;29(5):1123-33.
50. Obiorah IE, Fan P, Sengupta S, Jordan VC. Selective estrogen-induced apoptosis in breast cancer. *Steroids*. 2014;90:60-70.
51. Comsa S, Cimpean AM, Raica M. The Story of MCF-7 Breast Cancer Cell Line: 40 years of Experience in Research. *Anticancer Res*. 2015;35(6):3147-54.
52. Prall OWJ, Sarcevic B, Musgrove EA, Watts CKW, Sutherland RL. Estrogen-induced activation of Cdk4 and Cdk2 during G(1)-S phase progression is accompanied by increased cyclin D1 expression and decreased cyclin-dependent kinase inhibitor association with cyclin E-Cdk2. *J Biol Chem*. 1997;272(16):10882-94.
53. Planas-Silva M, Weinberg R. Estrogen-dependent cyclin E-cdk2 activation through p21 redistribution. *Mol Cell Biol*. 1997;17(7):4059-69.

54. Jiang S, Jordan V. Growth-Regulation of Estrogen Receptor-Negative Breast-Cancer Cells Transfected with Complementary Dnas for Estrogen-Receptor. *J Natl Cancer Inst.* 1992;84(8):580-91.
55. Liao X, Lu D, Wang N, Liu L, Wang Y, Li Y, et al. Estrogen receptor alpha mediates proliferation of breast cancer MCF-7 cells via a p21/PCNA/E2F1-dependent pathway. *Febs Journal.* 2014;281(3):927-42.
56. Fowler A, Solodin N, Valley C, Alarid E. Altered target gene regulation controlled by estrogen receptor-alpha concentration. *Molecular Endocrinology.* 2006;20(2):291-301.
57. Stender JD, Kim K, Charn TH, Komm B, Chang KCN, Kraus WL, et al. Genome-Wide Analysis of Estrogen Receptor alpha DNA Binding and Tethering Mechanisms Identifies Runx1 as a Novel Tethering Factor in Receptor-Mediated Transcriptional Activation. *Mol Cell Biol.* 2010;30(16):3943-55.
58. Peethambaram P, Ingle J, Suman V, Hartmann L, Loprinzi C. Randomized trial of diethylstilbestrol vs. tamoxifen in postmenopausal women with metastatic breast cancer. An updated analysis. *Breast Cancer Res Treat.* 1999;54(2):117-22.
59. Ellis MJ, Gao F, Dehdashti F, Jeffe DB, Marcom PK, Carey LA, et al. Lower-dose vs high-dose oral estradiol therapy of hormone receptor-positive, aromatase inhibitor-resistant advanced breast cancer: A phase 2 randomized study. *J Am Med Assoc.* 2009;302(7):774-80.
60. LaCroix AZ, Chlebowski RT, Manson JE, Aragaki AK, Johnson KC, Martin L, et al. Health Outcomes After Stopping Conjugated Equine Estrogens Among Postmenopausal Women With Prior Hysterectomy A Randomized Controlled Trial. *Jama-Journal of the American Medical Association.* 2011;305(13):1305-14.

61. Anderson GL, Chlebowski RT, Aragaki AK, Kuller LH, Manson JE, Gass M, et al. Conjugated equine oestrogen and breast cancer incidence and mortality in postmenopausal women with hysterectomy: extended follow-up of the Women's Health Initiative randomised placebo-controlled trial. *Lancet Oncology*. 2012;13(5):476-86.
62. Manson JE, Chlebowski RT, Stefanick ML, Aragaki AK, Rossouw JE, Prentice RL, et al. Menopausal Hormone Therapy and Health Outcomes During the Intervention and Extended Poststopping Phases of the Women's Health Initiative Randomized Trials. *Obstet Gynecol Surv*. 2014;69(2):83-5.
63. Soule H, Vazquez J, Long A, Albert S, Brennan M. Human Cell Line from a Pleural Effusion Derived from a Breast Carcinoma. *J Natl Cancer Inst*. 1973;51(5):1409-16.
64. Koboldt DC, Fulton RS, McLellan MD, Schmidt H, Kalicki-Veizer J, McMichael JF, et al. Comprehensive molecular portraits of human breast tumours. *Nature*. 2012;490(7418):61-70.
65. Vargas-Rondón N, Villegas VE, Rondón-Lagos M. The role of chromosomal instability in cancer and therapeutic responses. *Cancers*. 2018;10(1).
66. Kao J, Salari K, Bocanegra M, Choi Y, Girard L, Gandhi J, et al. Molecular Profiling of Breast Cancer Cell Lines Defines Relevant Tumor Models and Provides a Resource for Cancer Gene Discovery. *Plos One*. 2009;4(7):e6146.
67. Turashvili G, Brogi E. Tumor Heterogeneity in Breast Cancer. *Frontiers in Medicine*. 2017;4:227.
68. Resnicoff M, Medrano E, Podhajcer O, Bravo A, Bover L, Mordoh J. Subpopulations of MCF7 Cells Separated by Percoll Gradient Centrifugation - a Model to Analyze the

- Heterogeneity of Human-Breast Cancer. *Proc Natl Acad Sci U S A*. 1987;84(20):7295-9.
69. Nugoli M, Chuchana P, Vendrell J, Orsetti B, Ursule L, Nguyen C, et al. Genetic variability in MCF-7 sublines: evidence of rapid genomic and RNA expression profile modifications. *BMC Cancer*. 2003;3:13.
70. Jones C, Payne J, Wells D, Delhanty J, Lakhani S, Kortenkamp A. Comparative genomic hybridization reveals extensive variation among different MCF-7 cell stocks. *Cancer Genet Cytogenet*. 2000;117(2):153-8.
71. Kleensang A, Vantangoli MM, Odwin-DaCosta S, Andersen ME, Boekelheide K, Bouhifd M, et al. Genetic variability in a frozen batch of MCF-7 cells invisible in routine authentication affecting cell function. *Scientific Reports*. 2016;6:28994.
72. Bushman F, Lewinski M, Ciuffi A, Barr S, Leipzig J, Hannenhalli S, et al. Genome wide analysis of retroviral DNA integration. *Nature Reviews Microbiology*. 2005;3(11):848-58.
73. Kadauke S, Blobel GA. Chromatin loops in gene regulation. *Biochimica Et Biophysica Acta-Gene Regulatory Mechanisms*. 2009;1789(1):17-25.
74. Giorgetti L, Heard E. Closing the loop: 3C versus DNA FISH. *Genome Biol*. 2016;17:215.
75. Fudenberg G, Imakaev M. FISHing for captured contacts: towards reconciling FISH and 3C. *Nature Methods*. 2017;14(7):673.
76. Amano T, Sagai T, Tanabe H, Mizushina Y, Nakazawa H, Shiroishi T. Chromosomal Dynamics at the Shh Locus: Limb Bud-Specific Differential Regulation of Competence and Active Transcription. *Developmental Cell*. 2009;16(1):47-57.

77. Mascarello JT, Hirsch B, Kearney HM, Ketterling RP, Olson SB, Quigley DI, et al. Section E9 of the American College of Medical Genetics technical standards and guidelines: Fluorescence in situ hybridization. *Genetics in Medicine*. 2011;13(7):667-75.
78. Schurter M, LeBrun D, Harrison K. Improved technique for fluorescence in situ hybridisation analysis of isolated nuclei from archival, B5 or formalin fixed, paraffin wax embedded tissue. *Journal of Clinical Pathology-Molecular Pathology*. 2002;55(2):121-4.

Bibliography

Ades F, Zardavas D, Bozovic-Spasojevic I, Pugliano L, Fumagalli D, de Azambuja E, et al. Luminal B Breast Cancer: Molecular Characterization, Clinical Management, and Future Perspectives. *Journal of Clinical Oncology*. 2014;32(25):2794.

Ahmed ARH, Griffiths AB, Tilby MT, Westley BR, May FEB. TFF3 is a normal breast epithelial protein and is associated with differentiated phenotype in early breast cancer but predisposes to invasion and metastasis in advanced disease. *Am J Pathol*. 2012;180(3):904-16.

Alberta Health Services. Adjuvant Systemic Therapy for Early Stage (Lymph Node Negative and Lymph Node Positive) Breast Cancer. Alberta Health Services; 2016.

Albrechtsen R, Nielsen M, Wewer U, Engvall E, Ruoslahti E. Basement-Membrane Changes in Breast-Cancer Detected by Immunohistochemical Staining for Laminin. *Cancer Res*. 1981;41(12):5076-81.

Allred DC. Ductal carcinoma in situ: terminology, classification, and natural history. *J Natl Cancer Inst Monogr*. 2010;2010(41):134-8.

Amano T, Sagai T, Tanabe H, Mizushima Y, Nakazawa H, Shiroishi T. Chromosomal Dynamics at the Shh Locus: Limb Bud-Specific Differential Regulation of Competence and Active Transcription. *Developmental Cell*. 2009;16(1):47-57.

Anderson GL, Chlebowski RT, Aragaki AK, Kuller LH, Manson JE, Gass M, et al. Conjugated equine oestrogen and breast cancer incidence and mortality in postmenopausal

women with hysterectomy: extended follow-up of the Women's Health Initiative randomised placebo-controlled trial. *Lancet Oncology*. 2012;13(5):476-86.

Anderson T, Battersby S, King R, McPherson K, GOING J. Oral-Contraceptive Use Influences Resting Breast Proliferation. *Hum Pathol*. 1989;20(12):1139-44.

Anderson WF, Chatterjee N, Ershler WB, Brawley OW. Estrogen receptor breast cancer phenotypes in the surveillance, epidemiology, and end results database. *Breast Cancer Res Treat*. 2002;76(1):27-36.

Arendt LM, Kuperwasser C. Form and Function: how Estrogen and Progesterone Regulate the Mammary Epithelial Hierarchy. *J Mammary Gland Biol Neoplasia*. 2015;20(1-2):9-25.

Barbareschi M, Caffo O, Doglioni C, Fina P, Marchetti A, Buttitta F, et al. p21(WAF1) immunohistochemical expression in breast carcinoma: Correlations with clinicopathological data, oestrogen receptor status, MIB1 expression, p53 gene and protein alterations and relapse-free survival. *Br J Cancer*. 1996;74(2):208-15.

Bernardo GM, Lozada KL, Miedler JD, Harburg G, Hewitt SC, Mosley JD, et al. FOXA1 is an essential determinant of ER alpha expression and mammary ductal morphogenesis. *Development*. 2010;137(12):2045-54.

Bernhardt SM, Dasari P, Walsh D, Townsend AR, Price TJ, Ingman WV. Hormonal Modulation of Breast Cancer Gene expression: Implications for Intrinsic Subtyping in Premenopausal Women. *Frontiers in Oncology*. 2016; 6:241.

Berry NB, Fan M, Nephew KP. Estrogen receptor-alpha hinge-region lysines 302 and 303 regulate receptor degradation by the proteasome. *Molecular Endocrinology*. 2008;22(7):1535-51.

Bjornstrom L, Sjoberg M. Mechanisms of estrogen receptor signaling: Convergence of genomic and nongenomic actions on target genes. *Molecular Endocrinology*. 2005;19(4):833-42.

Boccardo F, Rubagotti A, Amoroso D, Mesiti M, Romeo D, Sismondi P, et al. Cyclophosphamide, methotrexate, and fluorouracil versus Tamoxifen plus ovarian suppression as adjuvant treatment of estrogen receptor-positive pre-/perimenopausal breast cancer patients: Results of the Italian Breast Cancer Adjuvant Study Group 02 Randomized Trial. *Journal of Clinical Oncology*. 2000;18(14):2718-27.

Bombonati A, Sgroi DC. The molecular pathology of breast cancer progression. *J Pathol*. 2011;223(2):307-17.

Bondesson M, Hao R, Lin C, Williams C, Gustafsson J. Estrogen receptor signaling during vertebrate development. *Biochimica Et Biophysica Acta-Gene Regulatory Mechanisms*. 2015;1849(2):142-51.

Breast anatomy and how breast cancer starts [Internet]. Available from:

<https://nbcf.org.au/about-national-breast-cancer-foundation/about-breast-cancer/what-you-need-to-know/breast-anatomy-cancer-starts/>.

Brisken C. Hormonal control of alveolar development and its implications for breast carcinogenesis. *J Mammary Gland Biol Neoplasia*. 2002;7(1):39-48.

Brzozowski AM, Pike ACW, Dauter Z, Hubbard RE, Bonn T, Engstrom O, et al. Molecular basis of agonism and antagonism in the oestrogen receptor. *Nature*. 1997;389(6652):753-8.

Bushman F, Lewinski M, Ciuffi A, Barr S, Leipzig J, Hannenhalli S, et al. Genome wide analysis of retroviral DNA integration. *Nature Reviews Microbiology*. 2005;3(11):848-58.

Caffo O, Doglioni C, Veronese S, Bonzanini M, Marchetti A, Buttitta F, et al. Prognostic value of p21(WAF1) and p53 expression in breast carcinoma: An immunohistochemical study in 261 patients with long-term follow-up. *Clinical Cancer Research*. 1996;2(9):1591-9.

Caizzi L, Ferrero G, Cutrupi S, Cordero F, Ballaré C, Miano V, et al. Genome-wide activity of unliganded estrogen receptor- α in breast cancer cells. *Proc Natl Acad Sci U S A*. 2014;111(13):4892-7.

Canadian Cancer Statistics 2017. Toronto, ON: Canadian Cancer Society: Canadian Cancer Society's Advisory Committee on Cancer Statistics; 2017.

Cancer Genetics [Internet]: MIT; 2016. Available from:

<http://www.cubocube.com/dashboard.php?a=1643&c=1>.

Carey LA, Perou CM, Livasy CA, Dressler LG, Cowan D, Conway K, et al. Race, breast cancer subtypes, and survival in the Carolina Breast Cancer Study. *J Am Med Assoc*. 2006;295(21):2492-502.

Cariou S, Donovan J, Flanagan W, Milic A, Bhattacharya N, Slingerland J. Down-regulation of p21(WAF1/CIP1) or p27(Kip1) abrogates antiestrogen-mediated cell cycle arrest in human breast cancer cells. *Proc Natl Acad Sci U S A*. 2000;97(16):9042-6.

Carroll JS, Liu XS, Brodsky AS, Li W, Meyer CA, Szary AJ, et al. Chromosome-wide mapping of estrogen receptor binding reveals long-range regulation requiring the forkhead protein FoxA1. *Cell*. 2005;122(1):33-43.

Carroll JS, Meyer CA, Song J, Li W, Geistlinger TR, Eeckhoute J, et al. Genome-wide analysis of estrogen receptor binding sites. *Nat Genet*. 2006;38(11):1289-97.

Chang MC, Souter LH, Kamel-Reid S, Rutherford M, Bedard P, Trudeau M, et al. Clinical utility of multigene profiling assays in early-stage breast cancer. *Current Oncology*. 2017;24(5): E403-

Cheang MCU, Chia SK, Voduc D, Gao D, Leung S, Snider J, et al. Ki67 Index, HER2 Status, and Prognosis of Patients with Luminal B Breast Cancer. *Jnci-Journal of the National Cancer Institute*. 2009;101(10):736-50.

Chen DS, Pace PE, Coombes RC, Ali S. Phosphorylation of human estrogen receptor alpha by protein kinase A regulates dimerization. *Mol Cell Biol*. 1999;19(2):1002-15.

Chen J, Hu Z, Phatak M, Reichard J, Freudenberg JM, Sivaganesan S, et al. Genome-Wide Signatures of Transcription Factor Activity: Connecting Transcription Factors, Disease, and Small Molecules. *Plos Computational Biology*. 2013;9(9): e1003198.

Chinnadurai G. CtBP, an unconventional transcriptional corepressor in development and oncogenesis. *Mol Cell*. 2002;9(2):213-24.

Chlebowski RT, Hendrix SL, Langer RD, Stefanick ML, Gass M, Lane D, et al. Influence of estrogen plus progestin on breast, cancer and mammography in healthy postmenopausal women - The Women's Health Initiative Randomized trial. *Jama-Journal of the American Medical Association*. 2003;289(24):3243-53.

Ciriello G, Sinha R, Hoadley KA, Jacobsen AS, Reva B, Perou CM, et al. The molecular diversity of Luminal A breast tumors. *Breast Cancer Res Treat*. 2013;141(3):409-20.

Clarke R. Human breast cell proliferation and its relationship to steroid receptor expression. *Climacteric*. 2004;7(2):129-37.

Comsa S, Cimpean AM, Raica M. The Story of MCF-7 Breast Cancer Cell Line: 40 years of Experience in Research. *Anticancer Res*. 2015;35(6):3147-54

Cserni G, Chmielik E, Cserni B, Tot T. The new TNM-based staging of breast cancer. *Virchows Archiv: an international journal of pathology*. 2018.

Dalvai M, Bystricky K. Cell Cycle and Anti-Estrogen Effects Synergize to Regulate Cell Proliferation and ER Target Gene Expression. *Plos One*. 2010;5(6): e11011.

Deisenroth C, Thorner AR, Enomoto T, Perou CM, Zhang Y. Mitochondrial HEP27 Is a c-Myb Target Gene That Inhibits Mdm2 and Stabilizes p53. *Mol Cell Biol*. 2010;30(16):3981-93.

Desdouets C, Sobczak-Thepot J, Murphy M, Brechot C. Cyclin A: function and expression during cell proliferation. *Prog Cell Cycle Res*. 1995; 1:115-23.

DiffBind: differential binding analysis of ChIP-seq peak data [Internet].: Bioconductor; 2011. Available from:

<http://bioconductor.org/packages/release/bioc/html/DiffBind.html>.

Dixon JR, Selvaraj S, Yue F, Kim A, Li Y, Shen Y, et al. Topological domains in mammalian genomes identified by analysis of chromatin interactions. *Nature*. 2012;485(7398):376-80.

Docquier A, Harmand P, Fritsch S, Chanrion M, Darbon J, Cavailles V. The Transcriptional Coregulator RIP140 Represses E2F1 Activity and Discriminates Breast Cancer Subtypes. *Clinical Cancer Research*. 2010;16(11):2959-70.

Dowsett M, Ebbs SR, Dixon JM, Skene A, Griffith C, Boeddinghaus I, et al. Biomarker changes during neoadjuvant Anastrozole, Tamoxifen, or the combination: Influence of hormonal status and HER-2 in breast cancer - A study from the IMPACT trialists. *Journal of Clinical Oncology*. 2005;23(11):2477-92.

Dowsett M, Smith IE, Ebbs SR, Dixon JM, Skene A, A'Hern R, et al. Prognostic value of Ki67 expression after short-term presurgical endocrine therapy for primary breast cancer. *J Natl Cancer Inst*. 2007;99(2):167-70.

Dutertre M, Smith CL. Ligand-independent interactions of p160/steroid receptor coactivators and CREB-binding protein (CBP) with estrogen receptor-alpha: Regulation by phosphorylation sites in the A/B region depends on other receptor domains. *Molecular Endocrinology*. 2003;17(7):1296-314.

Eberharter A, Becker PB. Histone acetylation: A switch between repressive and permissive chromatin. Second in review on chromatin dynamics. *EMBO Rep.* 2002;3(3):224-9.

Ellis MJ, Ding L, Shen D, Luo J, Suman VJ, Wallis JW, et al. Whole-genome analysis informs breast cancer response to aromatase inhibition. *Nature.* 2012;486(7403):353-60.

Ellis MJ, Gao F, Dehdashti F, Jeffe DB, Marcom PK, Carey LA, et al. Lower-dose vs high-dose oral estradiol therapy of hormone receptor-positive, aromatase inhibitor-resistant advanced breast cancer: A phase 2 randomized study. *J Am Med Assoc.* 2009;302(7):774-80.

Elston C, Ellis I. Pathological Prognostic Factors in Breast-Cancer .1. the Value of Histological Grade in Breast-Cancer - Experience from a Large Study with Long-Term Follow-Up. *Histopathology.* 1991;19(5):403-10.

Eom M, Oh SS, Lkhagvadorj S, Han A, Park KH. HDAC1 Expression in Invasive Ductal Carcinoma of the Breast and Its Value as a Good Prognostic Factor. *Korean Journal of Pathology.* 2012;46(4):311-7.

Eom YH, Kim HS, Lee A, Song BJ, Chae BJ. BCL2 as a Subtype-Specific Prognostic Marker for Breast Cancer. *Journal of Breast Cancer.* 2016;19(3):252-60.

Erbas B, Provenzan E, Armes J, Gertig D. The natural history of ductal carcinoma in situ of the breast: a review. *Breast Cancer Res Treat.* 2006;97(2):135-44.

ESR1 [Internet].; 2017. Available from: <https://www.proteinatlas.org/ENSG00000091831-ESR1/tissue/breast#img>.

Ferlay J, Soerjomataram I, Dikshit R, Eser S, Mathers C, Rebelo M, et al. Cancer incidence and mortality worldwide: Sources, methods and major patterns in GLOBOCAN 2012. *International Journal of Cancer*. 2015;136(5): E359-86.

Fernandes I, Bastien Y, Wai T, Nygard K, Lin R, Cormier O, et al. Ligand-dependent nuclear receptor corepressor LCoR functions by histone deacetylase-dependent and -independent mechanisms. *Mol Cell*. 2003;11(1):139-50.

Filardo EJ, Thomas P. Minireview: G Protein-Coupled Estrogen Receptor-1, GPER-1: Its Mechanism of Action and Role in Female Reproductive Cancer, Renal and Vascular Physiology. *Endocrinology*. 2012;153(7):2953-62.

Fischer M, Quaas M, Steiner L, Engeland K. The p53-p21-DREAM-CDE/CHR pathway regulates G (2)/M cell cycle genes. *Nucleic Acids Res*. 2016;44(1):164-74.

Fisher B, Costantino J, Redmond C, Fisher E, Wickerham D, Cronin W, et al. Endometrial Cancer in Tamoxifen-Treated Breast-Cancer Patients - Findings from the National Surgical Adjuvant Breast and Bowel Project (Nsbp) B-14. *J Natl Cancer Inst*. 1994;86(7):527-37.

Folkerd E, Dowsett M. Sex hormones and breast cancer risk and prognosis. *Breast*. 2013;22(Suppl 2): S38-43.

Foulds CE, Feng Q, Ding C, Bailey S, Hunsaker TL, Malovannaya A, et al. Proteomic Analysis of Coregulators Bound to ER alpha on DNA and Nucleosomes Reveals Coregulator Dynamics. *Mol Cell*. 2013;51(2):185-99.

Foster J, Henley D, Ahamed S, Wimalasena J. Estrogens and cell-cycle regulation in breast cancer. *Trends in Endocrinology and Metabolism*. 2001;12(7):320-7.

Fowler A, Solodin N, Valley C, Alarid E. Altered target gene regulation controlled by estrogen receptor-alpha concentration. *Molecular Endocrinology*. 2006;20(2):291-301.

Fowler AM, Solodin N, Preisler-Mashek MT, Zhang P, Lee AV, Alarid ET. Increases in estrogen receptor-a concentration in breast cancer cells promote serine 118/104/106-independent AF-1 transactivation and growth in the absence of estrogen. *FASEB J*. 2004;18(1):81-93.

Fudenberg G, Imakaev M. FISHing for captured contacts: towards reconciling FISH and 3C. *Nature Methods*. 2017;14(7):673.

Fullwood MJ, Liu MH, Pan YF, Liu J, Xu H, Mohamed YB, et al. An oestrogen-receptor-a-bound human chromatin interactome. *Nature*. 2009;462(7269):58-64.

Gewirtz D. A critical evaluation of the mechanisms of action proposed for the antitumor effects of the anthracycline antibiotics Adriamycin and daunorubicin. *Biochem Pharmacol*. 1999;57(7):727-Geyer FC, Rodrigues DN, Weigelt B, Reis-Filho JS. Molecular Classification of Estrogen Receptor-positive/Luminal Breast Cancers. *Adv Anat Pathol*. 2012;19(1):39-53.

Giorgetti L, Heard E. Closing the loop: 3C versus DNA FISH. *Genome Biol*. 2016; 17:215.

Girault I, Lerebours F, Amarir S, Tozlu S, Tubiana-Hulin M, Lidereau R, et al. Expression analysis of estrogen receptor alpha coregulators in breast carcinoma: Evidence that NCOR1 expression is predictive of the response to Tamoxifen. *Clinical Cancer Research*. 2003;9(4):1259-66.

Glass CK, Rosenfeld MG. The coregulator exchange in transcriptional functions of nuclear receptors. *Genes Dev.* 2000;14(2):121-41.

Goncalves R, Ma C, Luo J, Suman V, Ellis MJ. Use of neoadjuvant data to design adjuvant endocrine therapy trials for breast cancer. *Nature Reviews Clinical Oncology.* 2012;9(4):223-9.

Goss PE, Ingle JN, Pritchard KI, Robert NJ, Muss H, Gralow J, et al. Extending Aromatase-Inhibitor Adjuvant Therapy to 10 Years. *N Engl J Med.* 2016;375(3):209-19.

Grana X, Reddy E. Cell-Cycle Control in Mammalian-Cells - Role of Cyclins, Cyclin-Dependent Kinases (Gdks), Growth Suppressor Genes and Cyclin-Dependent Kinase Inhibitors (Ckis). *Oncogene.* 1995;11(2):211-9.

Green S, Kumar V, Theulaz I, Wahli W, Chambon P. The N-terminal DNA-binding 'zinc finger' of the oestrogen and glucocorticoid receptors determines target gene specificity. *EMBO J.* 1988;7(10):3037-44.

Gruber CJ, Gruber DM, Gruber IML, Wieser F, Huber JC. Anatomy of the estrogen response element. *Trends in Endocrinology and Metabolism.* 2004;15(2):73-8.

Gudjonsson T, Adriance MC, Sternlicht MD, Petersen OW, Bissell MJ. Myoepithelial cells: Their origin and function in breast morphogenesis and neoplasia. *J Mammary Gland Biol Neoplasia.* 2005;10(3):261-72.

Gupta S, Stamatoyannopoulos JA, Bailey TL, Noble WS. Quantifying similarity between motifs. *Genome Biol.* 2007;8(2): R24.

Hall J.M MDP. The Estrogen Receptor β -Isoform (ER β) of the Human Estrogen Receptor Modulates ER α Transcriptional Activity and Is a Key Regulator of the Cellular Response to Estrogens and Antiestrogens. *Endocrinology*. 1999; 140:5566-5578.

Hansen AS, Cattoglio C, Darzacq X, Tjian R. Recent evidence that TADs and chromatin loops are dynamic structures. *Nucleus*. 2018;9(1):20-32.

Hasegawa D, Calvo V, Avivar-Valderas A, Lade A, Chou H, Lee YA, et al. Epithelial Xbp1 Is Required for Cellular Proliferation and Differentiation during Mammary Gland Development. *Mol Cell Biol*. 2015;35(9):1543-56.

Heinz S, Benner C, Spann N, Bertolino E, Lin YC, Laslo P, et al. Simple Combinations of Lineage-Determining Transcription Factors Prime cis-Regulatory Elements Required for Macrophage and B Cell Identities. *Mol Cell*. 2010;38(4):576-89.

Heldring N, Pike A, Andersson S, Matthews J, Cheng G, Hartman J, et al. Estrogen receptors: How do they signal and what are their targets. *Physiol Rev*. 2007;87(3):905-31.

Herschkowitz JI, He X, Fan C, Perou CM. The functional loss of the retinoblastoma tumour suppressor is a common event in basal-like and luminal B breast carcinomas. *Breast Cancer Research*. 2008;10(5): R75.

Heuson JC, Longeval E, Mattheiem WH, Deboel MC, Sylvester RJ, Leclercq G. Significance of Quantitative Assessment of Estrogen Receptors for Endocrine Therapy in Advanced Breast-Cancer. *Cancer*. 1977;39(5):1971-7.

Hodges-Gallagher L, Valentine CD, El Bader S, Kushner PJ. Inhibition of histone deacetylase enhances the anti-proliferative action of antiestrogens on breast cancer cells

and blocks Tamoxifen-induced proliferation of uterine cells. *Breast Cancer Res Treat.* 2007;105(3):297-309.

Hovey R, Trott J, Vonderhaar B. Establishing a framework for the functional mammary gland: From endocrinology to morphology. *J Mammary Gland Biol Neoplasia.* 2002;7(1):17-38.

Howard B, Gusterson B. Human breast development. *J Mammary Gland Biol Neoplasia.* 2000;5(2):119-37.

Howell A. Pure oestrogen antagonists for the treatment of advanced breast cancer. *Endocr Relat Cancer.* 2006;13(3):689-706.

Htun H, Holth LT, Walker D, Davie JR, Hager GL. Direct visualization of the human estrogen receptor alpha reveals a role for ligand in the nuclear distribution of the receptor. *Mol Biol Cell.* 1999;10(2):471-86.

Hu X, Lazar MA. The CoRNR motif controls the recruitment of corepressors by nuclear hormone receptors. *Nature.* 1999;402(6757):93-6.

Hu Z, Fan C, Oh DS, Marron JS, He X, Qaqish BF, et al. The molecular portraits of breast tumors are conserved across microarray platforms. *BMC Genomics.* 2006; 7:96.

Hudis CA. Drug therapy: Trastuzumab - Mechanism of action and use in clinical practice. *N Engl J Med.* 2007;357(1):39-51

Hugh J, Hanson J, Cheang MCU, Nielsen TO, Perou CM, Dumontet C, et al. Breast Cancer Subtypes and Response to Docetaxel in Node-Positive Breast Cancer: Use of an

Immunohistochemical Definition in the BCIRG 001 Trial. *J Clin Oncol.* 2009;27(8):1168-76.

Ingle JN, Ahmann DL, Green SJ, Edmonson JH, Bisel HF, Kvols LK, et al. Randomized Clinical-Trial of Diethylstilbestrol Versus Tamoxifen in Post-Menopausal Women with Advanced Breast-Cancer. *N Engl J Med.* 1981;304(1):16-21.

Inman JL, Robertson C, Mott JD, Bissell MJ. Mammary gland development: cell fate specification, stem cells and the microenvironment. *Development.* 2015;142(6):1028-42.

Iorga A, Cunningham CM, Moazeni S, Ruffenach G, Umar S, Eghbali M. The protective role of estrogen and estrogen receptors in cardiovascular disease and the controversial use of estrogen therapy. *Biology of Sex Differences.* 2017; 8:33.

Iwase H, Zhang ZH, Omoto Y, Sugiura H, Yamashita H, Toyama T, et al. Clinical significance of the expression of estrogen receptors alpha and beta for endocrine therapy of breast cancer. *Cancer Chemother Pharmacol.* 2003;52: S34-8.

Javed A, Lteif A. Development of the Human Breast. *Seminars in Plastic Surgery.* 2013;27(1):5-

Jenkins EO, Deal AM, Anders CK, Prat A, Perou CM, Carey LA, et al. Age-specific changes in intrinsic breast cancer subtypes: A focus on older women. *Oncologist.* 2014;19(10):1076-83.

Jiang M, Shao Z, Wu J, Lu J, Yu L, Yuan J, et al. P21/waf1/cip1 and Mdm-2 Expression in Breast Carcinoma Patients as Related to Prognosis. *International Journal of Cancer.* 1997;74(5):529-34.

Jiang S, Jordan V. Growth-Regulation of Estrogen Receptor-Negative Breast-Cancer Cells Transfected with Complementary Dnas for Estrogen-Receptor. *J Natl Cancer Inst.* 1992;84(8):580-91.

Jones C, Payne J, Wells D, Delhanty J, Lakhani S, Kortenkamp A. Comparative genomic hybridization reveals extensive variation among different MCF-7 cell stocks. *Cancer Genet Cytogenet.* 2000;117(2):153-8.

Jordan V. Antiestrogens and selective estrogen receptor modulators as multifunctional medicines. 1. Receptor interactions. *J Med Chem.* 2003;46(6):883-908.

Jordan VC. The new biology of estrogen-induced apoptosis applied to treat and prevent breast cancer. *Endocr Relat Cancer.* 2015;22(1): R1-R31.

Jordan VC. The Role of Tamoxifen in the Treatment and Prevention of Breast-Cancer. *Curr Probl Cancer.* 1992;16(3):134-76.

Joshi SR, Ghattamaneni RB, Scovell WM. Expanding the Paradigm for Estrogen Receptor Binding and Transcriptional Activation. *Molecular Endocrinology.* 2011;25(6):980-94.

Kadauke S, Blobel GA. Chromatin loops in gene regulation. *Biochimica Et Biophysica Acta-Gene Regulatory Mechanisms.* 2009;1789(1):17-25.

Kalaitzidis D, Gilmore TD. Transcription factor cross-talk: the estrogen receptor and NF-kappa B. *Trends in Endocrinology and Metabolism.* 2005;16(2):46-52.

Kao J, Salari K, Bocanegra M, Choi Y, Girard L, Gandhi J, et al. Molecular Profiling of Breast Cancer Cell Lines Defines Relevant Tumor Models and Provides a Resource for Cancer Gene Discovery. *Plos One*. 2009;4(7): e6146.

Kato S, Endoh H, Masuhiro Y, Kitamoto T, Uchiyama S, Sasaki H, et al. Activation of the Estrogen-Receptor through Phosphorylation by Mitogen-Activated Protein-Kinase. *Science*. 1995;270(5241):1491-4.

Katzenellenbogen B, Kendra K, Norman M, Berthois Y. Proliferation, Hormonal Responsiveness, and Estrogen-Receptor Content of MCF-7 Human-Breast Cancer-Cells Grown in the Short-Term and Long-Term Absence of Estrogens. *Cancer Res*. 1987;47(16):4355-60.

Kawai H, Li H, Avraham S, Jiang S, Avraham H. Overexpression of histone deacetylase HDAC1 modulates breast cancer progression by negative regulation of estrogen receptor alpha. *International Journal of Cancer*. 2003;107(3):353-8.

Kedar RP, Bourne TH, Powles TJ, Collins WP, Ashley SE, Cosgrove DO, et al. Effects of Tamoxifen on Uterus and Ovaries of Postmenopausal Women in a Randomized Breast-Cancer Prevention Trial. *Lancet*. 1994;343(8909):1318-21.

Khalid AB, Krum SA. Estrogen receptors alpha and beta in bone. *Bone*. 2016; 87:130-5.

Kim C, Tang G, Pogue-Geile KL, Costantino JP, Baehner FL, Baker J, et al. Estrogen Receptor (ESR1) mRNA Expression and Benefit from Tamoxifen in the Treatment and Prevention of Estrogen Receptor-Positive Breast Cancer. *Journal of Clinical Oncology*. 2011;29(31):4160-7.

Kim J, deHaan G, Nardulli AM, Shapiro DJ. Prebending the estrogen response element destabilizes binding of the estrogen receptor DNA binding domain. *Mol Cell Biol.* 1997;17(6):3173-80.

King WJ, Greene GL. Monoclonal-Antibodies Localize Estrogen-Receptor in the Nuclei of Target-Cells. *Nature.* 1984;307(5953):745-7.

Kininis M, Chen BS, Diehl AG, Isaacs GD, Zhang T, Siepel AC, et al. Genomic analyses of transcription factor binding, histone acetylation, and gene expression reveal mechanistically distinct classes of estrogen-regulated promoters. *Mol Cell Biol.* 2007;27(14):5090-104.

Kininis M, Isaacs GD, Core LJ, Hah N, Kraus WL. Postrecruitment Regulation of RNA Polymerase II Directs Rapid Signaling Responses at the Promoters of Estrogen Target Genes. *Mol Cell Biol.* 2009;29(5):1123-33.

Kleensang A, Vantangoli MM, Odwin-DaCosta S, Andersen ME, Boekelheide K, Bouhifd M, et al. Genetic variability in a frozen batch of MCF-7 cells invisible in routine authentication affecting cell function. *Scientific Reports.* 2016;6:28994.

Klinge CM. Estrogen receptor interaction with co-activators and co-repressors. *Steroids.* 2000;65(5):227-51.

Knoblauch R, Garabedian MJ. Role for Hsp90-associated cochaperone p23 in estrogen receptor signal transduction. *Mol Cell Biol.* 1999;19(5):3748-59.

Koboldt DC, Fulton RS, McLellan MD, Schmidt H, Kalicki-Veizer J, McMichael JF, et al. Comprehensive molecular portraits of human breast tumours. *Nature*. 2012;490(7418):61-70.

Koide A, Zhao C, Naganuma M, Abrams J, Deighton-Collins S, Skafar DF, et al. Identification of regions within the F domain of the human estrogen receptor alpha that are important for modulating transactivation and protein-protein interactions. *Molecular Endocrinology*. 2007;21(4):829-42.

Kouros-Mehr H, Slorach EM, Sternlicht MD, Werb Z. GATA-3 maintains the differentiation of the luminal cell fate in the mammary gland. *Cell*. 2006;127(5):1041-55.

Kraus WL, McInerney EM, Katzenellenbogen BS. Ligand-dependent, transcriptionally productive association of the amino- and carboxyl-terminal regions of a steroid hormone nuclear receptor. *Proc Natl Acad Sci U S A*. 1995;92(26):12314-8.

Krusche C, Wulfing P, Kersting C, Vloet A, Bocker W, Kiesel L, et al. Histone deacetylase-1 and-3 protein expression in human breast cancer: a tissue microarray analysis. *Breast Cancer Res Treat*. 2005;90(1):15-23.

Kumar P, Wu Q, Chambliss KL, Yuhanna IS, Mumby SM, Mineo C, et al. Direct interactions with G alpha i and G beta gamma mediate nongenomic signaling by estrogen receptor alpha. *Molecular Endocrinology*. 2007;21(6):1370-80.

Kumar R, Zakharov MN, Khan SH, Miki R, Jang H, Toraldo G, et al. The dynamic structure of the estrogen receptor. *Journal of amino acids*. 2011; 2011:812540.

Kumar V, Chambon P. The estrogen receptor binds tightly to its responsive element as a ligand-induced homodimer. *Cell*. 1988;55(1):145-56.

Kurtev V, Margueron R, Kroboth K, Ogris E, Cavailles V, Seiser C. Transcriptional regulation by the repressor of estrogen receptor activity via recruitment of histone deacetylases. *J Biol Chem*. 2004;279(23):24834-43.

Kushner P, Hort E, Shine J, Baxter J, Greene G. Construction of Cell-Lines that Express High-Levels of the Human Estrogen-Receptor and are Killed by Estrogens. *Molecular Endocrinology*. 1990;4(10):1465-73.

LaCroix AZ, Chlebowski RT, Manson JE, Aragaki AK, Johnson KC, Martin L, et al. Health Outcomes After Stopping Conjugated Equine Estrogens Among Postmenopausal Women with Prior Hysterectomy a Randomized Controlled Trial. *Jama-Journal of the American Medical Association*. 2011;305(13):1305-14.

Langmead B, Salzberg SL. Fast gapped-read alignment with Bowtie 2. *Nature Methods*. 2012;9(4):357-U54.

Lavinsky RM, Jepsen K, Heinzel T, Torchia J, Mullen TM, Schiff R, et al. Diverse signaling pathways modulate nuclear receptor recruitment of N-CoR and SMRT complexes. *Proc Natl Acad Sci U S A*. 1998;95(6):2920-5.

Leclercq G, Heuson JC. Therapeutic Significance of Sex-Steroid Hormone Receptors in Treatment of Breast-Cancer. *Eur J Cancer*. 1977;13(11):1205-15.

Leclercq G, Lacroix M, Laios L, Laurent G. Estrogen receptor alpha: Impact of ligands on intracellular shuttling and turnover rate in breast cancer cells. *Current Cancer Drug Targets*. 2006;6(1):39-64.

Le Dily F, Bau D, Pohl A, Vicent GP, Serra F, Soronellas D, et al. Distinct structural transitions of chromatin topological domains correlate with coordinated hormone-induced gene regulation. *Genes Dev*. 2014;28(19):2151-62.

Lester J. Local Treatment of Breast Cancer. *Semin Oncol Nurs*. 2015;31(2):122-33.

Lewis J, Jordan V. Selective estrogen receptor modulators (SERMs): Mechanisms of anticarcinogenesis and drug resistance. *Mutat Res -Fundam Mol Mech Mutag*. 2005;591(1-2):247-63.

Lewis-Wambi JS, Jordan VC. Estrogen regulation of apoptosis: how can one hormone stimulate and inhibit? *Breast Cancer Research*. 2009;11(3):206.

Li G, Ruan X, Auerbach RK, Sandhu KS, Zheng M, Wang P, et al. Extensive Promoter-Centered Chromatin Interactions Provide a Topological Basis for Transcription Regulation. *Cell*. 2012;148(1-2):84-98.

Li H, Handsaker B, Wysoker A, Fennell T, Ruan J, Homer N, et al. The Sequence Alignment/Map format and SAMtools. *Bioinformatics*. 2009;25(16):2078-9.

Li S, Rong M, Grieu F, Iacopetta B. PIK3CA mutations in breast cancer are associated with poor outcome. *Breast Cancer Res Treat*. 2006;96(1):91-5.

Li XM, Onishi Y, Kuwabara K, Rho JY, Wada-Kiyama Y, Sakuma Y, et al. Ligand-dependent transcriptional enhancement by DNA curvature between two half motifs of the estrogen response element in the human estrogen receptor alpha gene. *Gene*. 2002;294(1-2):279-90.

Liao X-, Lu D, Wang N, Liu L, Wang Y, Li Y, et al. Estrogen receptor a mediates proliferation of breast cancer MCF-7 cells via a p21/PCNA/E2F1-dependent pathway. *FEBS J*. 2014;281(3):927-42.

Lin C, Vega VB, Thomsen JS, Zhang T, Kong SL, Xie M, et al. Whole-genome cartography of estrogen receptor alpha binding sites. *Plos Genetics*. 2007;3(6):867-85.

Liu MH, Cheung E. Estrogen receptor-mediated long-range chromatin interactions and transcription in breast cancer. *Mol Cell Endocrinol*. 2014;382(1):624-32.

Liu Z, Merkurjev D, Yang F, Li W, Oh S, Friedman MJ, et al. Enhancer Activation Requires trans-Recruitment of a Mega Transcription Factor Complex. *Cell*. 2014;159(2):358-73.

Lodish H, Berk A, Zipursky S, Matsudaira P, Baltimore D, Darnell J. Section 13.7, Checkpoints in Cell-Cycle Regulation. In: *Molecular Cell Biology*. 4th edition ed. W. H. Freeman and Company; 2000.

Lonard D, Nawaz Z, Smith C, O'Malley B. The 26S proteasome is required for estrogen receptor-alpha and coactivator turnover and for efficient estrogen receptor-alpha transactivation. *Mol Cell*. 2000;5(6):939-48.

Longacre TA, Bartow SA. A Correlative Morphological-Study of Human-Breast and Endometrium in the Menstrual-Cycle. *Am J Surg Pathol*. 1986;10(6):382-93.

Lonning PE. Poor-prognosis estrogen receptor positive disease: present and future clinical solutions. *Therapeutic Advances in Medical Oncology*. 2012;4(3):127-37.

Louie MC, McClellan A, Siewit C, Kawabata L. Estrogen Receptor Regulates E2F1 Expression to Mediate Tamoxifen Resistance. *Molecular Cancer Research*. 2010;8(3):343-52.

Love RR, Mazess RB, Barden HS, Epstein S, Newcomb PA, Jordan VC, et al. Effects of Tamoxifen on Bone-Mineral Density in Postmenopausal Women with Breast-Cancer. *N Engl J Med*. 1992;326(13):852-6.

Lum S, Woltering E, Fletcher W, Pommier R. Changes in serum estrogen levels in women during Tamoxifen therapy. *Am J Surg*. 1997;173(5):399-402.

Machanick P, Bailey TL. MEME-ChIP: motif analysis of large DNA datasets. *Bioinformatics*. 2011;27(12):1696-7.

Mak HY, Hoare S, Henttu PMA, Parker MG. Molecular determinants of the estrogen receptor-coactivator interface. *Mol Cell Biol*. 1999;19(5):3895-903.

Mallepell S, Krust A, Chambon P, Briskin C. Paracrine signaling through the epithelial estrogen receptor alpha is required for proliferation and morphogenesis in the mammary gland. *Proc Natl Acad Sci U S A*. 2006;103(7):2196-201.

Mandal S, Davie JR. Estrogen Regulated Expression of the p21(Waf1/Cip1) Gene in Estrogen Receptor Positive Human Breast Cancer Cells. *J Cell Physiol.* 2010;224(1):28-32.

Mangelsdorf DJ, Thummel C, Beato M, Herrlich P, Schutz G, Umesono K, et al. The Nuclear Receptor Superfamily - the 2nd Decade. *Cell.* 1995;83(6):835-9.

Manson JE, Chlebowski RT, Stefanick ML, Aragaki AK, Rossouw JE, Prentice RL, et al. Menopausal Hormone Therapy and Health Outcomes During the Intervention and Extended Poststopping Phases of the Women's Health Initiative Randomized Trials. *Obstet Gynecol Surv.* 2014;69(2):83-5.

Mascarello JT, Hirsch B, Kearney HM, Ketterling RP, Olson SB, Quigley DI, et al. Section E9 of the American College of Medical Genetics technical standards and guidelines: Fluorescence in situ hybridization. *Genetics in Medicine.* 2011;13(7):667-75.

McCarty K. Proliferative Stimuli in the Normal Breast - Estrogens or Progestins. *Hum Pathol.* 1989;20(12):1137-8.

Metivier R, Penot G, Carmouche RP, Hubner MR, Reid G, Denger S, et al. Transcriptional complexes engaged by apo-estrogen receptor-alpha isoforms have divergent outcomes. *EMBO J.* 2004;23(18):3653-66.

Metivier R, Penot G, Flouriot G, Pakdel F. Synergism between ER alpha transactivation function 1 (AF-1) and AF-2 mediated by steroid receptor coactivator protein-1: Requirement for the AF-1 alpha-helical core and for a direct interaction between the N- and C-terminal domains. *Molecular Endocrinology.* 2001;15(11):1953-70.

Metivier R, Penot G, Hubner MR, Reid G, Brand H, Kos M, et al. Estrogen receptor-alpha directs ordered, cyclical, and combinatorial recruitment of cofactors on a natural target promoter. *Cell*. 2003;115(6):751-63.

Metzger D, Ali S, Bornert JM, Chambon P. Characterization of the Amino-Terminal Transcriptional Activation Function of the Human Estrogen-Receptor in Animal and Yeast-Cells. *J Biol Chem*. 1995;270(16):9535-42.

Mi H, Huang X, Muruganujan A, Tang H, Mills C, Kang D, et al. PANTHER version 11: expanded annotation data from Gene Ontology and Reactome pathways, and data analysis tool enhancements. *Nucleic Acids Res*. 2017;45(D1): D183-9.

Mi H, Muruganujan A, Casagrande JT, Thomas PD. Large-scale gene function analysis with the PANTHER classification system. *Nature Protocols*. 2013;8(8):1551-66.

Miller TW, Balko JM, Fox EM, Ghazoui Z, Dunbier A, Anderson H, et al. ERa-dependent E2F transcription can mediate resistance to estrogen deprivation in human breast cancer. *Cancer Discov*. 2011;1(4):338-51.

Millour J, Lam EW. FOXM1 is a transcriptional target of ERa and has a critical role in breast cancer endocrine sensitivity and resistance. *Breast Cancer Research*. 2010;12: S3-.

Moggs J, Murphy T, Lim F, Moore D, Stuckey R, Antrobus K, et al. Anti-proliferative effect of estrogen in breast cancer cells that re-express ER alpha is mediated by aberrant regulation of cell cycle genes. *J Mol Endocrinol*. 2005;34(2):535-51.

Montano MM, Ekena K, Delage-Mourroux R, Chang WR, Martini P, Katzenellenbogen BS. An estrogen receptor-selective coregulator that potentiates the effectiveness of

antiestrogens and represses the activity of estrogens. *Proc Natl Acad Sci U S A*. 1999;96(12):6947-52.

Montano MM, Muller V, Trobaugh A, Katzenellenbogen BS. The Carboxy-Terminal F-Domain of the Human Estrogen-Receptor - Role in the Transcriptional Activity of the Receptor and the Effectiveness of Antiestrogens as Estrogen Antagonists. *Molecular Endocrinology*. 1995;9(7):814-25.

Mueller BM, Jana L, Kasajima A, Lehmann A, Prinzler J, Budczies J, et al. Differential expression of histone deacetylases HDAC1, 2 and 3 in human breast cancer - overexpression of HDAC2 and HDAC3 is associated with clinicopathological indicators of disease progression. *BMC Cancer*. 2013; 13:215.

Munster PN, Thurn KT, Thomas S, Raha P, Lacevic M, Miller A, et al. A phase II study of the histone deacetylase inhibitor Vorinostat combined with Tamoxifen for the treatment of patients with hormone therapy-resistant breast cancer. *Br J Cancer*. 2011;104(12):1828-35.

Muschler J, Streuli CH. Cell-Matrix Interactions in Mammary Gland Development and Breast Cancer. *Cold Spring Harbor Perspectives in Biology*. 2010;2(10): a003202.

Nardulli AM, Grobner C, Cotter D. Estrogen Receptor-Induced DNA Bending - Orientation of the Bend and Replacement of an Estrogen Response Element with an Intrinsic Dna Bending Sequence. *Molecular Endocrinology*. 1995;9(8):1064-76.

Narod SA, Iqbal J, Giannakeas V, Sopik V, Sun P. Breast Cancer Mortality After a Diagnosis of Ductal Carcinoma in Situ. *Jama Oncology*. 2015;1(7):888-96.

National Breast and Ovarian Cancer Centre. Recommendations for use of chemotherapy for the treatment of advanced breast cancer. Surry Hills, NSW, National Breast and Ovarian Cancer Centre; 2010.

National Breast and Ovarian Cancer Centre. Recommendations for use of endocrine therapy for the treatment of hormone receptor-positive advanced breast cancer. Surry Hills, NSW: National Breast and Ovarian Cancer Centre; 2010.

National Breast and Ovarian Cancer Centre. Recommendations for use of Trastuzumab (Herceptin®) for the treatment of HER2 positive breast cancer. Camperdown, NSW: National Breast and Ovarian Cancer Centre; 2011.

National Center for Biotechnology Information [Internet]. 8600 Rockville Pike, Bethesda MD, 20894 USA: U.S. National Library of Medicine; 2018. Available from: <https://www.ncbi.nlm.nih.gov/>.

National Comprehensive Cancer Network. NCCN Clinical Practice Guidelines in Oncology: Breast Cancer. National Comprehensive Cancer Network; 2016.

Natrajan R, Lambros MBK, Geyer FC, Marchio C, Tan DSP, Vatcheva R, et al. Loss of 16q in High Grade Breast Cancer is Associated with Estrogen Receptor Status: Evidence for Progression in Tumors with a Luminal Phenotype? *Genes Chromosomes & Cancer*. 2009;48(4):351-65.

Nawaz Z, Lonard D, Dennis A, Smith C, O'Malley B. Proteasome-dependent degradation of the human estrogen receptor. *Proc Natl Acad Sci U S A*. 1999;96(5):1858-62.

Neve RM, Chin K, Fridlyand J, Yeh J, Baehner FL, Fevr T, et al. A collection of breast cancer cell lines for the study of functionally distinct cancer subtypes. *Cancer Cell*. 2006;10(6):515-27.

Neville M, McFadden T, Forsyth I. Hormonal regulation of mammary differentiation and milk secretion. *J Mammary Gland Biol Neoplasia*. 2002;7(1):49-66.

Neville MC, Daniel CW. *The Mammary gland: development, regulation, and function*. New York: Plenum Press; 1987.

Nordgard SH, Johansen FE, Alnæs GIG, Bucher E, Syvänen A-, Naume B, et al. Genome-wide analysis identifies 16q deletion associated with survival, molecular subtypes, mRNA expression, and germline haplotypes in breast cancer patients. *Genes Chromosomes Cancer*. 2008;47(8):680-96.

Normal Histology [Internet]. Available from: <http://www.ezpath.org/gallery/#/new-gallery-50/>.

Nugoli M, Chuchana P, Vendrell J, Orsetti B, Ursule L, Nguyen C, et al. Genetic variability in MCF-7 sublines: evidence of rapid genomic and RNA expression profile modifications. *BMC Cancer*. 2003;3:13.

Oakes SR, Hilton HN, Ormandy CJ. Key stages in mammary gland development: The alveolar switch: Coordinating the proliferative cues and cell fate decisions that drive the formation of lobuloalveoli from ductal epithelium. *Breast Cancer Res*. 2006;8(2).

Obiorah IE, Fan P, Sengupta S, Jordan VC. Selective estrogen-induced apoptosis in breast cancer. *Steroids*. 2014;90:60-70.

Oesterreich S, Deng W, Jiang S, Cui X, Ivanova M, Schiff R, et al. Estrogen-mediated down-regulation of E-cadherin in breast cancer cells. *Cancer Res.* 2003;63(17):5203-8.

Ogawa S, Inoue S, Watanabe T, Hiroi H, Orimo A, Hosoi T, et al. The complete primary structure of human estrogen receptor β (hER β) and its heterodimerization with ER α in vivo and in vitro. *Biochem Biophys Res Commun.* 1998;243(1):122-6.

Ogryzko VV, Schiltz RL, Russanova V, Howard BH, Nakatani Y. The transcriptional coactivators p300 and CBP are histone acetyltransferases. *Cell.* 1996;87(5):953-9.

Osmanbeyoglu HU, Lu KN, Oesterreich S, Day RS, Benos PV, Coronello C, et al. Estrogen represses gene expression through reconfiguring chromatin structures. *Nucleic Acids Res.* 2013;41(17):8061-71.

Paik S, Shak S, Tang G, Kim C, Baker J, Cronin M, et al. A multigene assay to predict recurrence of Tamoxifen-treated, node-negative breast cancer. *New Engl J Med.* 2004;351(27):2817-26.

Paine IS, Lewis MT. The Terminal End Bud: The Little Engine that Could. *J Mammary Gland Biol Neoplasia.* 2017;22(2):93-108.

Pan YF, Wansa KDSA, Liu MH, Zhao B, Hong SZ, Tan PY, et al. Regulation of Estrogen Receptor-mediated Long Range Transcription via Evolutionarily Conserved Distal Response Elements. *J Biol Chem.* 2008;283(47):32977-88.

Pardo I, Lillemoe HA, Blosser RJ, Choi M, Sauder CAM, Doxey DK, et al. Next-generation transcriptome sequencing of the premenopausal breast epithelium using specimens from a normal human breast tissue bank. *Breast Cancer Research.* 2014;16(2): R26.

Parker JS, Mullins M, Cheang MCU, Leung S, Voduc D, Vickery T, et al. Supervised Risk Predictor of Breast Cancer Based on Intrinsic Subtypes. *Journal of Clinical Oncology*. 2009;27(8):1160-7.

Pearce S, Jordan V. The biological role of estrogen receptors alpha and beta in cancer. *Critical Reviews in Oncology Hematology*. 2004;50(1):3-22.

Pedram A, Razandi M, Lewis M, Hammes S, Levin ER. Membrane-Localized Estrogen Receptor Alpha Is Required for Normal Organ Development and Function. *Developmental Cell*. 2014;29(4):482-90.

Peethambaram P, Ingle J, Suman V, Hartmann L, Loprinzi C. Randomized trial of diethylstilbestrol vs. Tamoxifen in postmenopausal women with metastatic breast cancer. An updated analysis. *Breast Cancer Res Treat*. 1999;54(2):117-22.

Pellikainen MJ, Pekola TT, Ropponen KM, Kataia VV, Kellokoski JK, Eskelinen MJ, et al. p21(WAF1) expression in invasive breast cancer and its association with p53, AP-2, cell proliferation, and prognosis. *J Clin Pathol*. 2003;56(3):214-20.

Peng J, Jordan VC. Expression of estrogen receptor alpha with a Tet-off adenoviral system induces G0/G1 cell cycle arrest in SKBr3 breast cancer cells. *Int J Oncol*. 2010;36(2):451-8.

Perou CM, Sørlie T, Eisen MB, Van De Rijn M, Jeffrey SS, Renshaw CA, et al. Molecular portraits of human breast tumours. *Nature*. 2000;406(6797):747-52.

Peters GA, Khan SA. Estrogen receptor domains E and F: Role in dimerization and interaction with coactivator RIP-140. *Mol Endocrinol*. 1999;13(2):286-96.

Picard D, Kumar V, Chambon P, Yamamoto KR. Signal transduction by steroid hormones: Nuclear localization is differentially regulated in estrogen and glucocorticoid receptors. *Mol Biol Cell*. 1990;1(3):291-9.

Planas-Silva M, Weinberg R. Estrogen-dependent cyclin E-cdk2 activation through p21 redistribution. *Mol Cell Biol*. 1997;17(7):4059-69.

Prall O, Carroll J, Sutherland R. A low abundance pool of nascent p21(WAF1/Cip1) is targeted by estrogen to activate cyclin E-Cdk2. *J Biol Chem*. 2001;276(48):45433-42.

Prall OWJ, Sarcevic B, Musgrove EA, Watts CKW, Sutherland RL. Estrogen-induced activation of Cdk4 and Cdk2 during G (1)-S phase progression is accompanied by increased cyclin D1 expression and decreased cyclin-dependent kinase inhibitor association with cyclin E-Cdk2. *J Biol Chem*. 1997;272(16):10882-94.

Prat A, Karginova O, Parker JS, Fan C, He X, Bixby L, et al. Characterization of cell lines derived from breast cancers and normal mammary tissues for the study of the intrinsic molecular subtypes. *Breast Cancer Res Treat*. 2013;142(2):237-55.

Prat A, Parker JS, Fan C, Cheang MCU, Miller LD, Bergh J, et al. Concordance among gene expression-based predictors for ER-positive breast cancer treated with adjuvant Tamoxifen. *Ann Oncol*. 2012;23(11):2866-73.

Pratt W. The hsp90-based chaperone system: Involvement in signal transduction from a variety of hormone and growth factor receptors. *Proceedings of the Society for Experimental Biology and Medicine*. 1998;217(4):420-34.

Raha P, Thomas S, Thurn KT, Park J, Munster PN. Combined histone deacetylase inhibition and Tamoxifen induces apoptosis in Tamoxifen-resistant breast cancer models, by reversing Bcl-2 overexpression. *Breast Cancer Research*. 2015; 17:26.

Rakha EA, Reis-Filho JS, Baehner F, Dabbs DJ, Decker T, Eusebi V, et al. Breast cancer prognostic classification in the molecular era: The role of histological grade. *Breast Cancer Res*. 2010;12(4).

Ramamoorthy S, Cidlowski JA. Ligand-Induced Repression of the Glucocorticoid Receptor Gene Is Mediated by an NCoR1 Repression Complex Formed by Long-Range Chromatin Interactions with Intragenic Glucocorticoid Response Elements. *Mol Cell Biol*. 2013;33(9):1711-22.

Resnicoff M, Medrano E, Podhajcer O, Bravo A, Bover L, Mordoh J. Subpopulations of Mcf7 Cells Separated by Percoll Gradient Centrifugation - a Model to Analyze the Heterogeneity of Human-Breast Cancer. *Proc Natl Acad Sci U S A*. 1987;84(20):7295-9.

Restall C, Doherty J, Bin Liu H, Genovese R, Paiman L, Byron KA, et al. A novel histone deacetylase inhibitor augments Tamoxifen-mediated attenuation of breast carcinoma growth. *International Journal of Cancer*. 2009;125(2):483-7.

Rogatsky I, Trowbridge JM, Garabedian MJ. Potentiation of human estrogen receptor alpha transcriptional activation through phosphorylation of serines 104 and 106 by the cyclin A-CDK2 complex. *J Biol Chem*. 1999;274(32):22296-302.

Ross-Innes CS, Brown GD, Carroll JS. A coordinated interaction between CTCF and ER in breast cancer cells. *BMC Genomics*. 2011;12.

Ross-Innes CS, Stark R, Teschendorff AE, Holmes KA, Ali HR, Dunning MJ, et al. Differential oestrogen receptor binding is associated with clinical outcome in breast cancer. *Nature*. 2012;481(7381):389-93.

Rowinsky E. The development and clinical utility of the taxane class of antimicrotubule chemotherapy agents. *Annu Rev Med*. 1997; 48:353-74.

Ruff M, Gangloff M, Wurtz JM, Moras D. Estrogen receptor transcription and transactivation Structure-function relationship in DNA- and ligand-binding domains of estrogen receptors. *Breast Cancer Research*. 2000;2(5):353-9.

Russo J, Russo IH. Development of the human breast. *Maturitas*. 2004;49(1):2-15.

Rye IH, Lundin P, Månér S, Fjellidal R, Naume B, Wigler M, et al. Quantitative multigene FISH on breast carcinomas identifies der (1;16) (q10; p10) as an early event in luminal A tumors. *Genes Chromosomes Cancer*. 2015;54(4):235-48.

Safe S, Kim K. Non-classical genomic estrogen receptor (ER)/specificity protein and ER/activating protein-1 signaling pathways. *J Mol Endocrinol*. 2008;41(5-6):263-75.

Schodin D, Zhuang Y, Shapiro D, Katzenellenbogen B. Analysis of mechanisms that determine dominant negative estrogen receptor effectiveness. *J Biol Chem*. 1995;270(52):31163-71.

Schurter M, LeBrun D, Harrison K. Improved technique for fluorescence in situ hybridisation analysis of isolated nuclei from archival, B5 or formalin fixed, paraffin wax embedded tissue. *Journal of Clinical Pathology-Molecular Pathology*. 2002;55(2):121.

Schwabe J, Chapman L, Finch J, Rhodes D. The Crystal-Structure of the Estrogen-Receptor Dna-Binding Domain Bound to Dna - how Receptors Discriminate between their Response Elements. *Cell*. 1993;75(3):567-78.

Schwabe JWR, Chapman L, Rhodes D. The Estrogen-Receptor Recognizes an Imperfectly Palindromic Response Element through an Alternative Side-Chain Conformation. *Structure*. 1995;3(2):201-13.

Schwartz JA, Zhong L, Deighton-Collins S, Zhao CQ, Skafar DF. Mutations targeted to a predicted helix in the extreme carboxyl-terminal region of the human estrogen receptor- α alter its response to estradiol and 4-hydroxytamoxifen. *J Biol Chem*. 2002;277(15):13202-9.

Sentis S, Le Romancer M, Bianchin C, Rostan M-, Corbo L. Sumoylation of the estrogen receptor β hinge region regulates its transcriptional activity. *Mol Endocrinol*. 2005;19(11):2671-84.

Seo J, Min SK, Park H, Kim DH, Kwon MJ, Kim LS, et al. Expression of Histone Deacetylases HDAC1, HDAC2, HDAC3, and HDAC6 in Invasive Ductal Carcinomas of the Breast. *Journal of Breast Cancer*. 2014;17(4):323-31.

Shang Y, Hu X, DiRenzo J, Lazar MA, Brown M. Cofactor dynamics and sufficiency in estrogen receptor-regulated transcription. *Cell*. 2000;103(6):843-52.

Sharma D, Saxena N, Davidson N, Vertino P. Restoration of Tamoxifen sensitivity in estrogen receptor-negative breast cancer cells: Tamoxifen-bound reactivated ER recruits distinctive corepressor complexes. *Cancer Res*. 2006;66(12):6370-8.

Sherr C, Roberts J. CDK inhibitors: positive and negative regulators of G (1)-phase progression. *Genes Dev.* 1999;13(12):1501-12.

Shiau AK, Barstad D, Loria PM, Cheng L, Kushner PJ, Agard DA, et al. The structural basis of estrogen receptor/coactivator recognition and the antagonism of this interaction by Tamoxifen. *Cell.* 1998;95(7):927-37.

Silvestrini R, Veneroni S, Daidone MG, Benini E, Boracchi P, Mezzetti M, et al. The Bcl-2 protein: A prognostic indicator strongly related to p53 protein in lymph node-negative breast cancer patients. *J Natl Cancer Inst.* 1994;86(7):499-504.

Singhal H, Greene ME, Tarulli G, Zarnke AL, Bourgo RJ, Laine M, et al. Genomic agonism and phenotypic antagonism between estrogen and progesterone receptors in breast cancer. *Science Advances.* 2016;2(6): e1501924.

Smalley M, Ashworth A. Stem cells and breast cancer: A field in transit. *Nat Rev Cancer.* 2003;3(11):832-44.

Smith CL, Nawaz Z, O'Malley BW. Coactivator and corepressor regulation of the agonist/antagonist activity of the mixed antiestrogen, 4-hydroxytamoxifen. *Mol Endocrinol.* 1997;11(6):657-66.

Smith GH. Experimental mammary epithelial morphogenesis in an in vivo model: Evidence for distinct cellular progenitors of the ductal and lobular phenotype. *Breast Cancer Res Treat.* 1996;39(1):21-31.

Smith IE, Dowsett M. Aromatase inhibitors in breast cancer. *New Engl J Med.* 2003;348(24):2431-42.

Sobell H. Actinomycin and Dna-Transcription. Proc Natl Acad Sci U S A. 1985;82(16):5328-31.

Sørli T, Perou CM, Tibshirani R, Aas T, Geisler S, Johnsen H, et al. Gene expression patterns of breast carcinomas distinguish tumor subclasses with clinical implications. Proc Natl Acad Sci U S A. 2001;98(19):10869-74.

Soule H, Vazquez J, Long A, Albert S, Brennan M. Human Cell Line from a Pleural Effusion Derived from a Breast Carcinoma. J Natl Cancer Inst. 1973;51(5):1409-16.

Stender JD, Frasor J, Komm B, Chang KCN, Kraus WL, Katzenellenbogen BS. Estrogen-regulated gene networks in human breast cancer cells: Involvement of E2F1 in the regulation of cell proliferation. Mol Endocrinol. 2007;21(9):2112-23.

Stender JD, Kim K, Charn TH, Komm B, Chang KCN, Kraus WL, et al. Genome-Wide Analysis of Estrogen Receptor alpha DNA Binding and Tethering Mechanisms Identifies Runx1 as a Novel Tethering Factor in Receptor-Mediated Transcriptional Activation. Mol Cell Biol. 2010;30(16):3943-55.

Subramanian K, Jia D, Kapoor-Vazirani P, Powell DR, Collins RE, Sharma D, et al. Regulation of Estrogen Receptor a by the SET7 Lysine Methyltransferase. Mol Cell. 2008;30(3):336-47.

Tamrazi A, Carlson K, Daniels J, Hurth K, Katzenellenbogen J. Estrogen receptor dimerization: Ligand binding regulates dimer affinity and dimer dissociation rate. Molecular Endocrinology. 2002;16(12):2706-19.

Tan W, Li Q, Chen K, Su F, Song E, Gong C. Estrogen receptor beta as a prognostic factor in breast cancer patients: A systematic review and meta-analysis. *Oncotarget*. 2016;7(9):10373-85.

Trapnell C, Pachter L, Salzberg SL. TopHat: discovering splice junctions with RNA-Seq. *Bioinformatics*. 2009;25(9):1105-11.

Trapnell C, Roberts A, Goff L, Pertea G, Kim D, Kelley DR, et al. Differential gene and transcript expression analysis of RNA-seq experiments with TopHat and Cufflinks. *Nature Protocols*. 2012;7(3):562-78.

Tsarouha H, Pandis N, Bardi G, Teixeira M, Andersen J, Heim S. Karyotypic evolution in breast carcinomas with i (1) (q10) and der (1;16) (q10; p10) as the primary chromosome abnormality. *Cancer Genet Cytogenet*. 1999;113(2):156-61.

Turashvili G, Brogi E. Tumor Heterogeneity in Breast Cancer. *Frontiers in Medicine*. 2017;4:227.

Vargas-Rondón N, Villegas VE, Rondón-Lagos M. The role of chromosomal instability in cancer and therapeutic responses. *Cancers*. 2018;10(1).

Varlakhanova N, Snyder C, Jose S, Hahm JB, Privalsky ML. Estrogen receptors recruit SMRT and N-CoR corepressors through newly recognized contacts between the corepressor N terminus and the receptor DNA binding domain. *Mol Cell Biol*. 2010;30(6):1434-45.

Venet D, Dumont JE, Detours V. Most Random Gene Expression Signatures Are Significantly Associated with Breast Cancer Outcome. *Plos Computational Biology*. 2011;7(10): e1002240.

Verkasalo PK, Thomas HV, Appleby PN, Davey GK, Key TJ. Circulating levels of sex hormones and their relation to risk factors for breast cancer: A cross-sectional study in 1092 pre- and postmenopausal women (United Kingdom). *Cancer Causes Control*. 2001;12(1):47-59.

Villalobos M, Olea N, Brotons J, Oleaserrano M, Dealmodovar J, Pedraza V. The E-Screen Assay - a Comparison of Different Mcf7 Cell Stocks. *Environ Health Perspect*. 1995;103(9):844-50.

Vo N, Fjeld C, Goodman RH. Acetylation of nuclear hormone receptor-interacting protein RIP140 regulates binding of the transcriptional corepressor CtBP. *Mol Cell Biol*. 2001;21(18):6181-8.

Vogel VG, Costantino JP, Wickerham DL, Cronin WM, Cecchini RS, Atkins JN, et al. Effects of Tamoxifen vs Raloxifene on the Risk of Developing Invasive Breast Cancer and Other Disease Outcomes The NSABP Study of Tamoxifen and Raloxifene (STAR) P-2 Trial. *JAMA*. 2006;295(23):2727-2741.

Wakeling A, Dukes M, Bowler J. A Potent Specific Pure Antiestrogen with Clinical Potential. *Cancer Res*. 1991;51(15):3867-73.

Wallden B, Storhoff J, Nielsen T, Dowidar N, Schaper C, Ferree S, et al. Development and verification of the PAM50-based Prosigna breast cancer gene signature assay. *BMC Med Genomics*. 2015;8(1).

Wang C, Fu M, Angeletti RH, Siconolfi-Baez L, Reutens AT, Albanese C, et al. Direct Acetylation of the Estrogen Receptor a Hinge Region by p300 Regulates Transactivation and Hormone Sensitivity. *J Biol Chem*. 2001;276(21):18375-83.

Warnmark A, Treuter E, Wright A, Gustafsson J. Activation functions 1 and 2 of nuclear receptors: Molecular strategies for transcriptional activation. *Molecular Endocrinology*. 2003;17(10):1901-9.

Weigelt B, Peterse JL, Van't Veer LJ. Breast cancer metastasis: Markers and models. *Nat Rev Cancer*. 2005;5(8):591-602.

Weinberg R. The Retinoblastoma Protein and Cell-Cycle Control. *Cell*. 1995;81(3):323-30.

Welboren W, van Driel MA, Janssen-Megens EM, van Heeringen SJ, Sweep FCGJ, Span PN, et al. ChIP-Seq of ER alpha and RNA polymerase II defines genes differentially responding to ligands. *EMBO J*. 2009;28(10):1418-28.

Welshons WV, Lieberman ME, Gorski J. Nuclear localization of unoccupied oestrogen receptors. *Nature*. 1984;307(5953):747-9.

Wood J, Greene G, Nardulli A. Estrogen response elements function as allosteric modulators of estrogen receptor conformation. *Mol Cell Biol*. 1998;18(4):1927-34.

Wu X, Chen G, Qiu J, Lu J, Zhu W, Chen J, et al. Visualization of basement membranes in normal breast and breast cancer tissues using multiphoton microscopy. *Oncology Letters*. 2016;11(6):3785-9.

Xu J, Wu R-, O'Malley BW. Normal and cancer-related functions of the p160 steroid receptor co-activator (SRC) family. *Nat Rev Cancer*. 2009;9(9):615-30.

Yang X, Ferguson A, Nass S, Phillips D, Butash K, Wang S, et al. Transcriptional activation of estrogen receptor alpha in human breast cancer cells by histone deacetylase inhibition. *Cancer Res*. 2000;60(24):6890-4.

Yersal O, Barutca S. Biological subtypes of breast cancer: Prognostic and therapeutic implications. *World J Clin Oncol*. 2014;5(3):412-24.

Yi P, Wang Z, Feng Q, Pintilie GD, Foulds CE, Lanz RB, et al. Structure of a Biologically Active Estrogen Receptor-Coactivator Complex on DNA. *Mol Cell*. 2015;57(6):1047-58.

Ylikomi T, Bocquel MT, Berry M, Gronemeyer H, Chambon P. Cooperation of proto-signals for nuclear accumulation of estrogen and progesterone receptors. *EMBO J*. 1992;11(10):3681-94.

Zajchowski D, Sager R, Webster L. Estrogen Inhibits the Growth of Estrogen Receptor-Negative, but Not Estrogen Receptor-Positive, Human Mammary Epithelial-Cells Expressing a Recombinant Estrogen-Receptor. *Cancer Res*. 1993;53(20):5004-11.

Zhang Y, Liu T, Meyer CA, Eeckhoutte J, Johnson DS, Bernstein BE, et al. Model-based Analysis of ChIP-Seq (MACS). *Genome Biol*. 2008;9(9): R137.

Zhao H, Yu J, Peltier CP, Davie JR. Elevated expression of the estrogen receptor prevents the down-regulation of p21(Waf1/Cip1) in hormone dependent breast cancer cells. *J Cell Biochem.* 2004;93(3):619-28.

Zheng N, Fraenkel E, Pabo CO, Pavletich NP. Structural basis of DNA recognition by the heterodimeric cell cycle transcription factor E2F-DP. *Genes Dev.* 1999;13(6):666-74.

Zwart W, De Leeuw R, Rondaij M, Neefjes J, Mancini MA, Michalides R. The hinge region of the human estrogen receptor determines functional synergy between AF-1 and AF-2 in the quantitative response to estradiol and Tamoxifen. *J Cell Sci.* 2010;123(8):1253-61.

Appendix A

***ESRI* Plasmids**

The *ESRI* human cDNA open reading frame (ORF) clone was purchased from OriGene, (Rockville, MD). The pmEmerald-Dectin1A-N-10 vector was a generous gift Dr. Nicolas Touret (Department of Biochemistry, University of Alberta). The pLVX-Tight-Puro vector, LVX-Tet-on advanced vector were purchased from Clontech Laboratories, Inc (Mountain View, CA). The pLVX-tet-on-tight-IRES-mcherry-*ESRI*-E203G, G204S, A207V-His plasmid was purchased from Creative Biogene (Shirley, NY).

***ESRI* lentiviral constructs**

ESRI was amplified from the *ESRI* (NM 000125) human cDNA ORF clone by PCR using primers listed in Table 2.2. The human *ESRI* ORF was substituted for Dectin 1 into the NheI and SacI sites of pmEmerald-Dectin1A-N-10 to generate the p*ESRI*-Emerald (EM) construct. The *ESRI*-EM was obtained by PCR from this plasmid using primers listed in Table 2.2. In the forward primer, one Kozak consensus sequence was added to enhance expression. The PCR product was directly cloned into XbaI and EcoRI sites of the pLVX-Tight-Puro vector. An *ESRI* mutant containing three point mutations at E203G, G204S, A207V (ER-mDBD) was PCR amplified from pLVX-tet-on-tight-IRES-mcherry-*ESRI*-E203G, G204S, A207V-His using the primers listed in Table 2.2 and cloned into the pLVX-Tight-Puro-*ESRI*-EM using the BamHI restriction sites. DNA sequence orientations and fidelities of the constructs were verified by both restriction enzyme digestion and full insert sequencing.

Stable MCF-7 transfectant generation

Lenti-X 293T cells were resuspended at 1×10^6 cells/ml in DMEM + 10% FBS then seeded in 6 cm tissue culture plates and incubated overnight at 37°C and 5% CO₂. Cells

were 80–90% confluent at the time of transfection. The plasmid DNA was prepared for transfection by combining: 557 μl Xfect reaction buffer, 36 μl Lenti-X HTX packaging mix and 7 μl Lenti-X vector DNA (1 $\mu\text{g}/\mu\text{l}$) in a clean 1.5 ml microcentrifuge tube. The Xfect polymer was prepared by combining: 592.5 μl Xfect reaction buffer and 7.5 μl Xfect polymer in a clean 1.5 ml microcentrifuge tube. The polymer solution was added to the plasmid DNA mixture, mixed for 10 seconds and then incubated for 10 minutes at room temperature to allow nanoparticle complexes to form. The 1200 μl of DNA-Xfect solution was added drop wise to the Lenti-X 293T culture medium and the cells were incubated at 37°C and 5% CO₂ overnight. After 24 hours the transfection medium was replaced with fresh complete growth medium (containing Tet System Approved FBS) and the cells were incubated at 37°C and 5% CO₂ for an additional 24–48 hours. Virus stocks were collected for up to 48 hours after the start of transfection, filtered at 0.45 μm and then stored at -80°C until needed. Virus production was confirmed using a Lenti-X GoStix.

For viral transduction MCF-7 parental cells were plated at 50% confluency in 25 cm² flasks in 5 ml of complete growth medium (containing Tet System Approved FBS) and incubated at 37°C and 5% CO₂ overnight. For transduction 6 $\mu\text{g}/\text{ml}$ polybrene was added to the thawed viral stock and MCF-7 cells were co-transduced with 1 ml of virus stock and 1 ml of the plasmid transfection virus. Cells were incubated for 4-5 hours at 37°C and 5% CO₂ and then the flasks were topped up with 3ml of culture medium. The transduced cells were incubated at 37°C and 5% CO₂ for 48 hours. After this 2 day incubation the cells were rinsed with PBS and selection media containing 500 $\mu\text{g}/\text{ml}$ G418 and 1 $\mu\text{g}/\text{ml}$ puromycin was added to stably select for cells successfully transduced with the lentiviral plasmid. After one week cells showed stable selection and were grown at

increased numbers to generate frozen cell stocks stored in liquid nitrogen. This protocol was used to obtain MCF-7 cells transduced with the pLVX-Tight-Puro-EM (MCF7-EM), pLVX-Tight-Puro-*ESR1*-EM (MCF7-ER) and pLVX-Tight-Puro-*ESR1*-mDBD-EM (MCF7-ERmDBD) vectors (Figure A1).

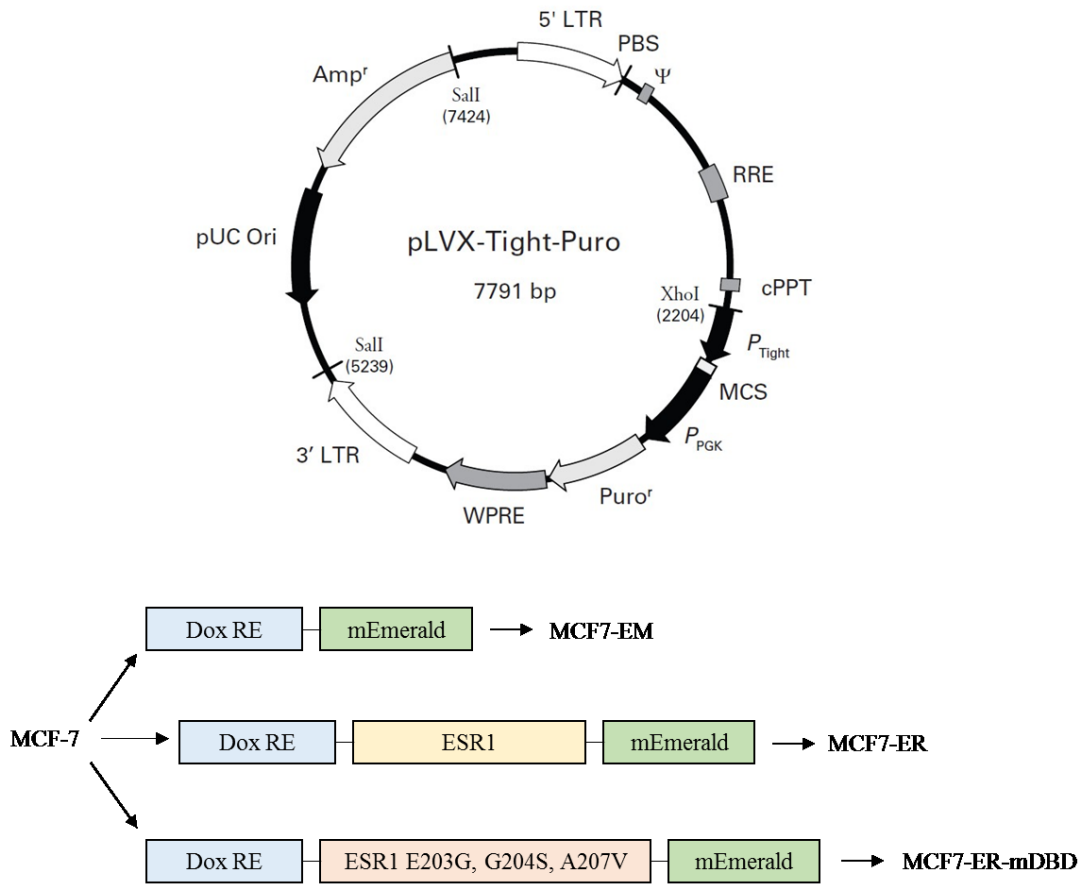


Figure A1 ER lentiviral doxycycline inducible constructs. MCF-7 cells were stably transduced with either the lentiviral mEmerald backbone (MCF7-EM), the lentiviral vector with *ESR1* gene fused with the mEmerald tag (MCF7-ER) or the *ESR1* gene containing three point mutations in the DNA binding domain (MCF7-ER-mDBD).

Appendix B

Table B1 RIN scores for RNA-Seq libraries.

Experimental condition	RIN score
EM0-1	10
EM0-2	10
EM0-3	9.8
EM0-4	9.8
EM10-1	10
EM10-2	10
EM10-3	10
EM10-4	9.7
ER0-1	10
ER0-2	10
ER0-3	9.9
ER0-4	9.8
ER10-1	8.9
ER10-2	10
ER10-3	9.9
ER10-4	9.8

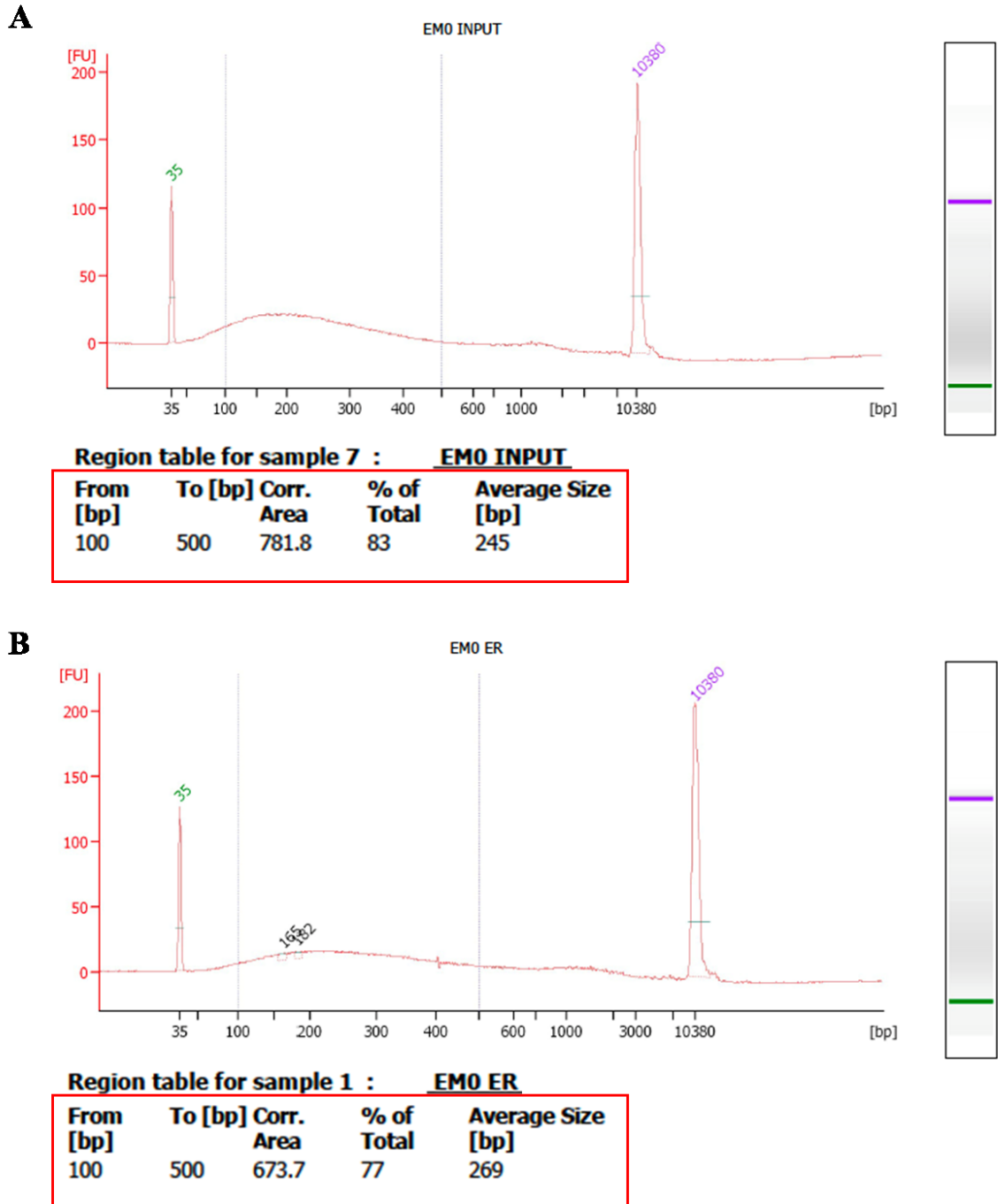


Figure B1 Representative Bioanalyzer trace for DNA shearing. ChIP DNA was obtained from MCF7-EM cells treated for 1 hour with ethanol control (EM0). ChIP DNA from 1% input (A) and ER-immunoprecipitation (B) was analyzed using the Agilent Bioanalyzer 2100 High Sensitivity DNA chip. The percent of total fragments within a 100-500 bp range are shown in the region table below each graph.

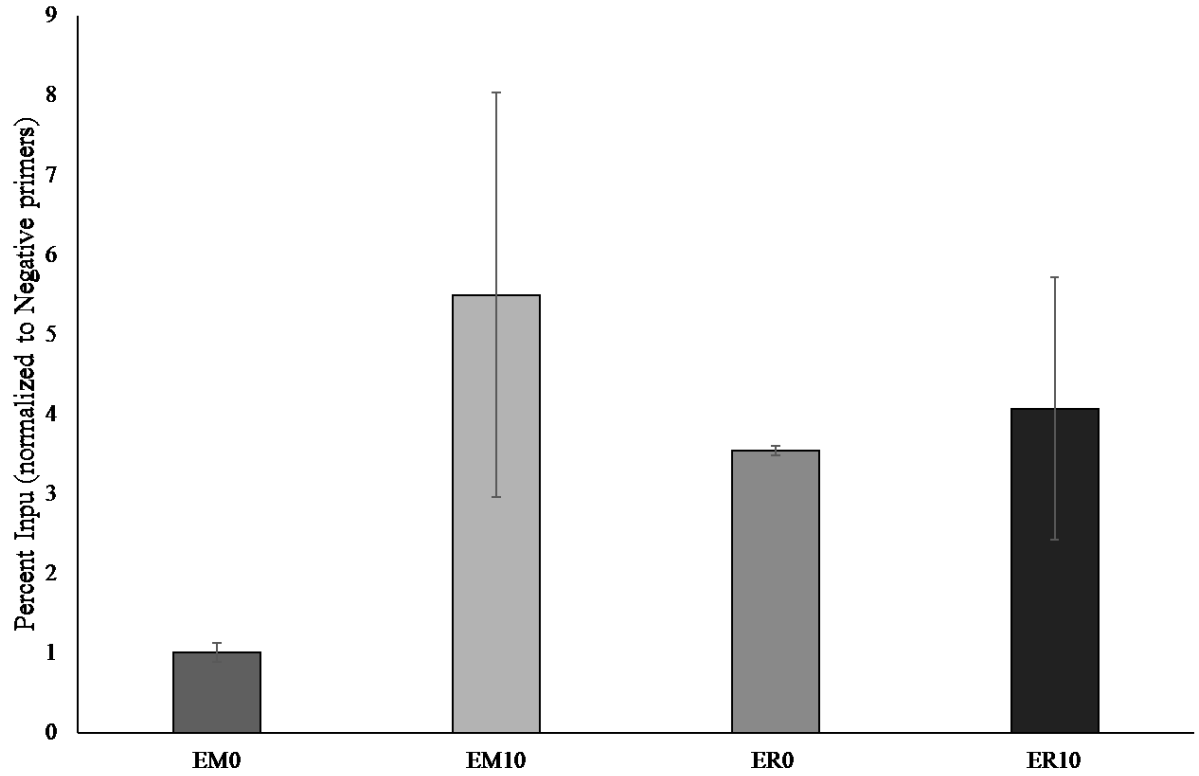


Figure B2 Quality check confirming the presence of ER binding at the *pS2* promoter region. ChIP DNA was measured by qPCR using primers for a known ER binding motif in the promoter region of the *pS2* gene. The results from the *pS2* qPCR were normalized to those obtained for a negative primer set for a gene desert on chromosome 12.

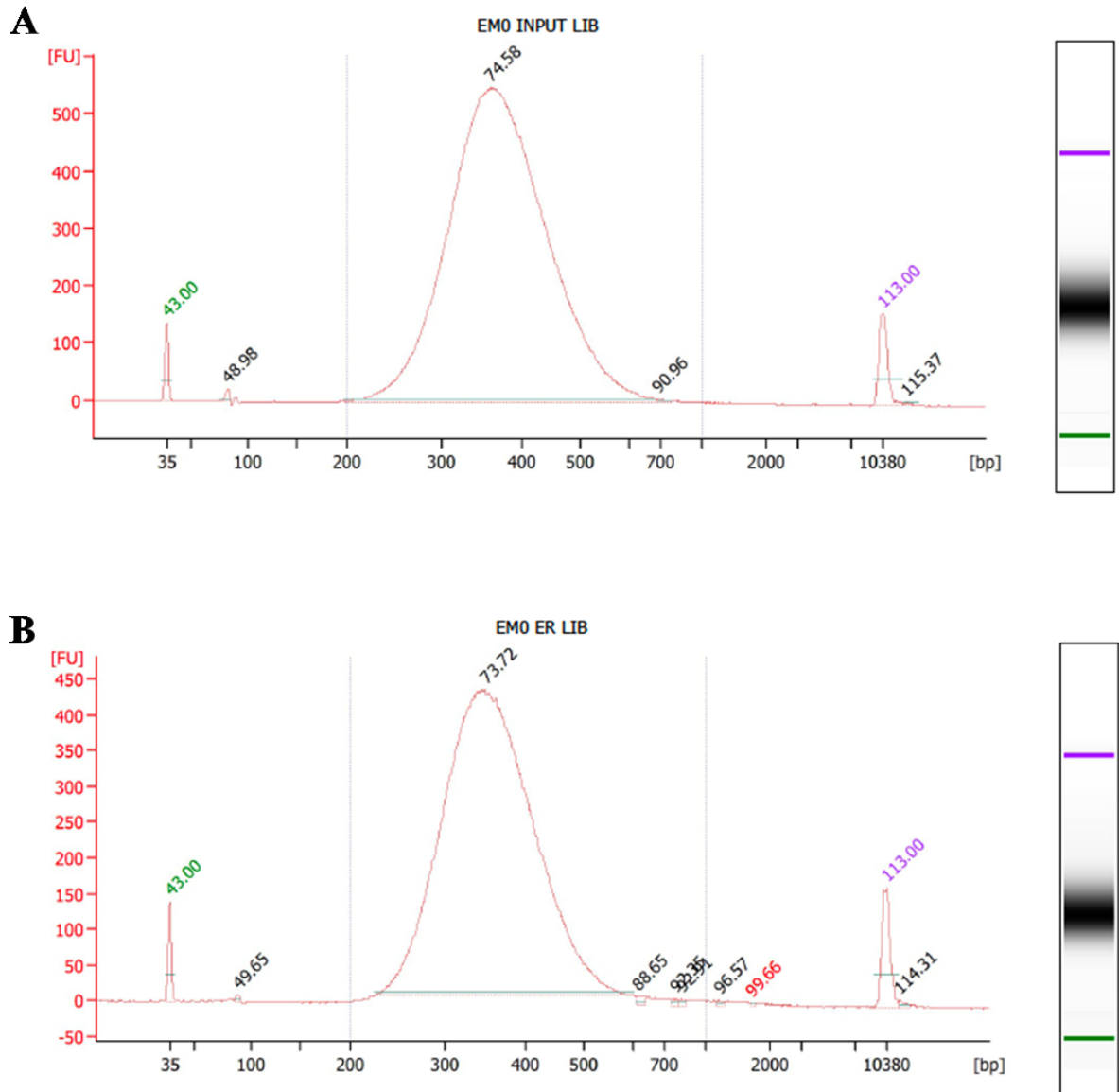


Figure B3 Representative Bioanalyzer trace for ChIP-Seq library. ChIP-Seq library was made using ChIP DNA from MCF7-EM cells treated for 1 hour with ethanol control (EM0). ChIP-Seq library made from 1% input (**A**) and ER-immunoprecipitation (**B**) was analyzed using the Agilent Bioanalyzer 2100 High Sensitivity DNA chip.

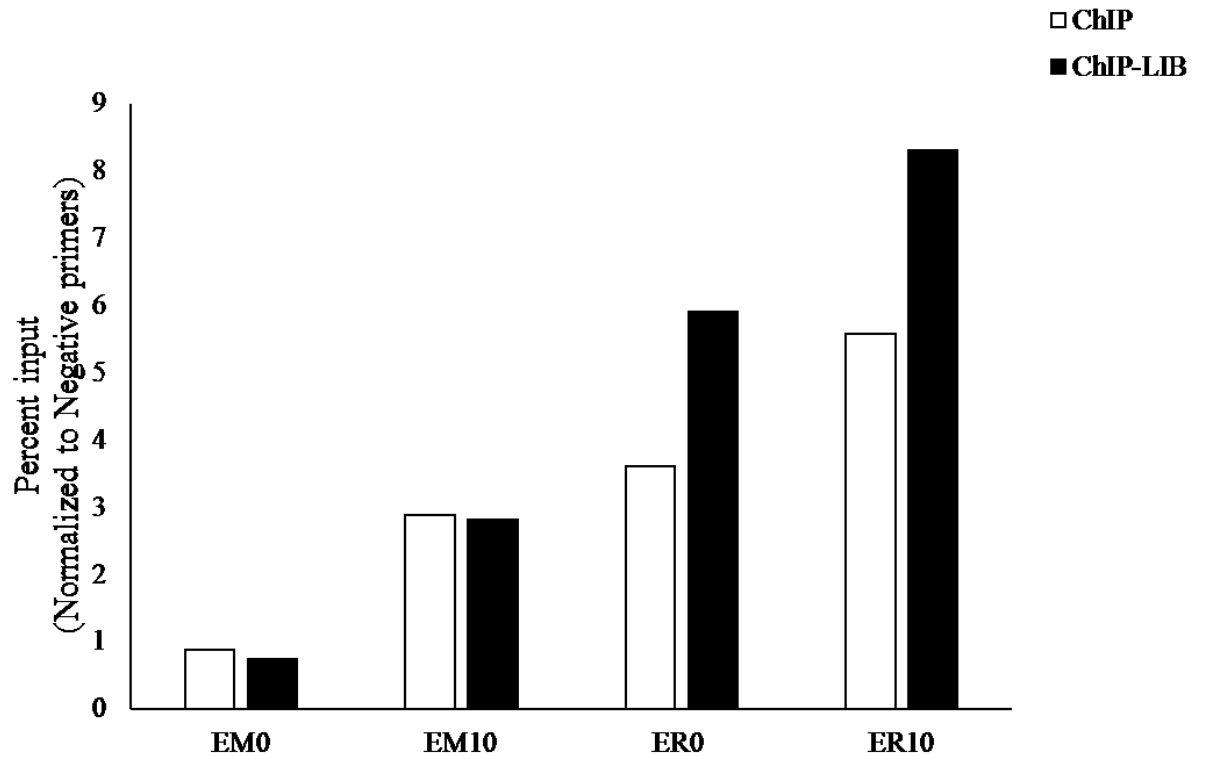


Figure B4 Quality check confirming pattern of ER binding at the *pS2* promoter region in a ChIP-Seq library. ChIP DNA from one biological replicate was measured by qPCR using *pS2* primers before (ChIP) and after building the ChIP-Seq library (ChIP-LIB). The results from the *pS2* qPCR were normalized to those obtained for a negative primer set for a gene desert on chromosome 12.

EMO

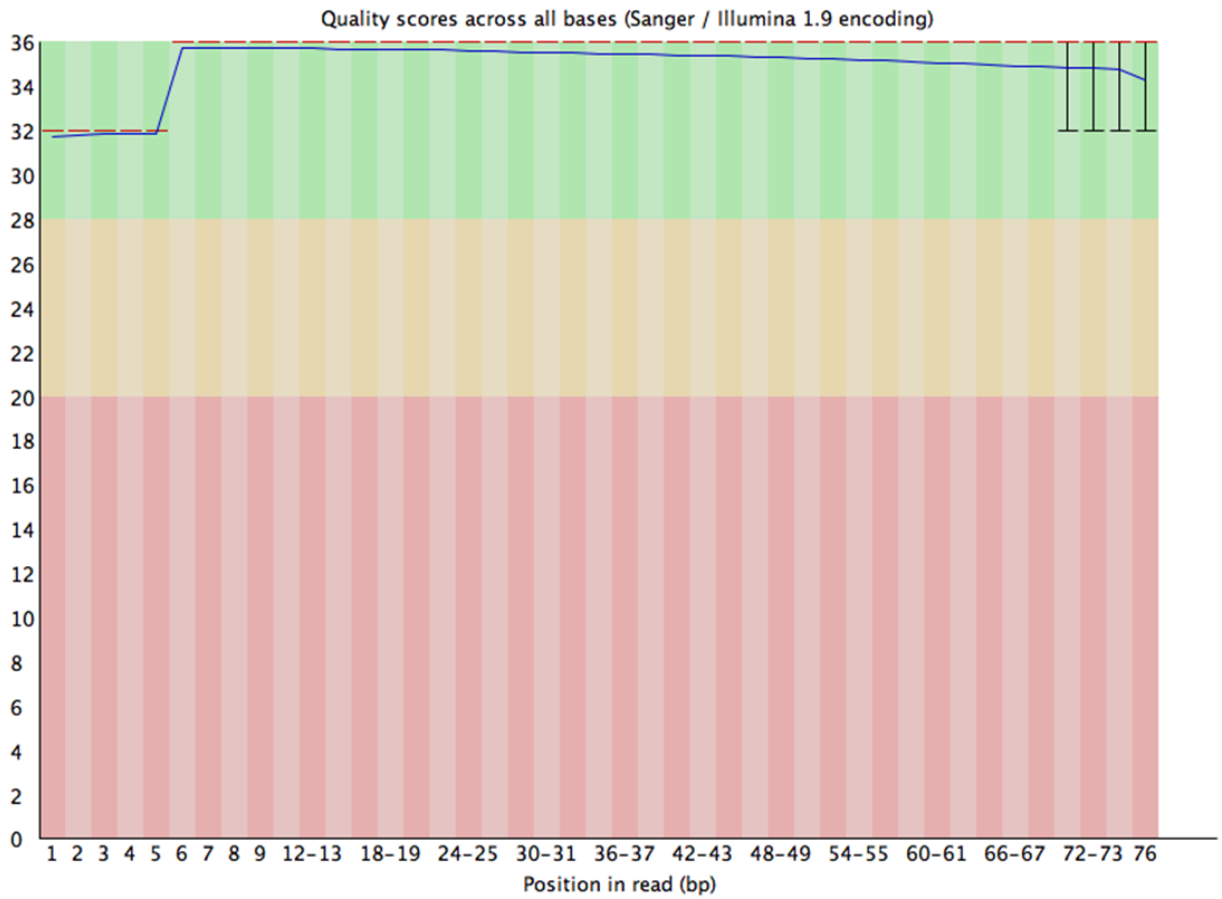


Figure B5 Representative FastQC result obtained from the sequencing of ChIP-Seq library. Graph shows the per base sequence quality across the 76 bp read. The blue line represents the mean quality score. The green region indicates calls of very good quality, orange indicates reasonable quality and red indicates poor quality.

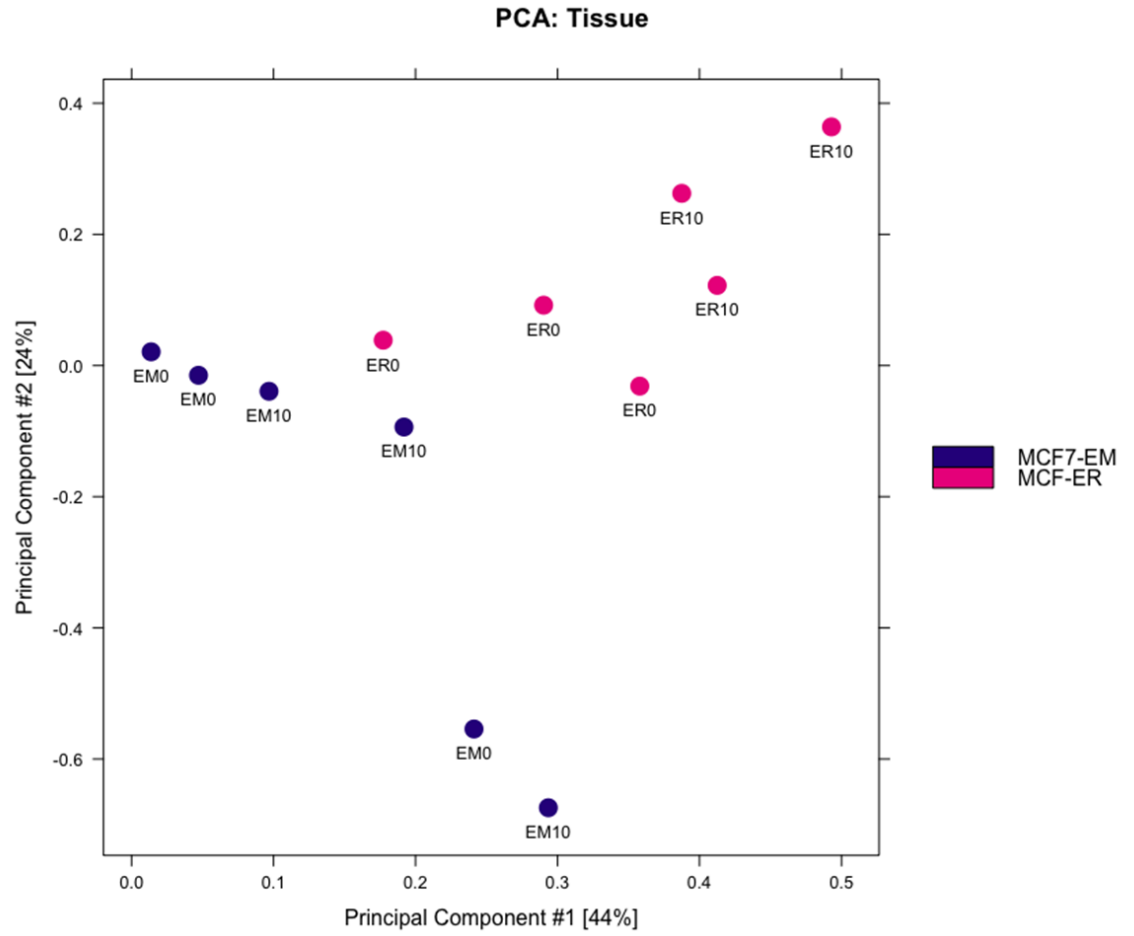


Figure B6 Principle component analysis (PCA) plot for ChIP peak sets. Plot shows the distribution of the 3 biological replicates for each experimental condition.

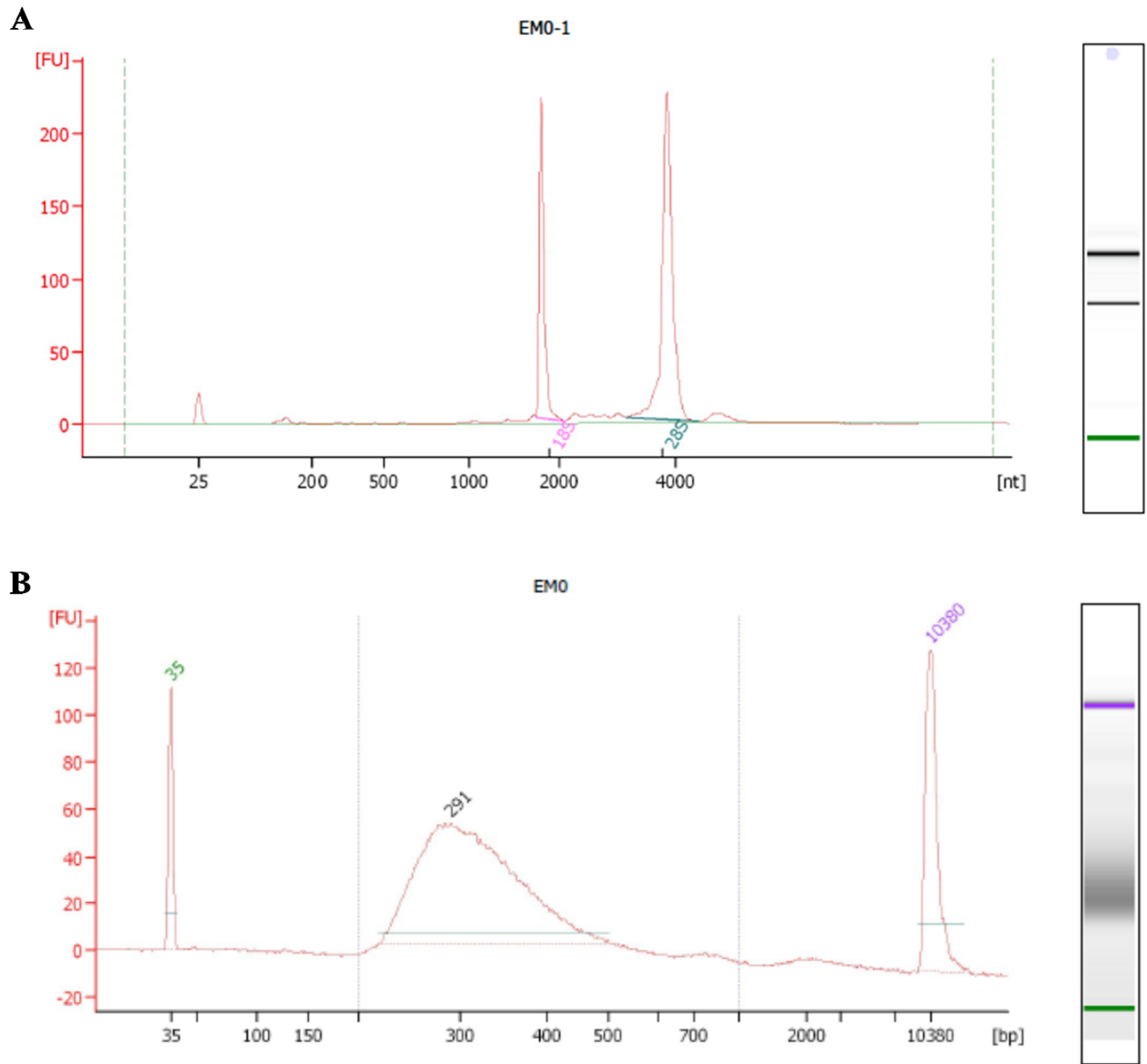
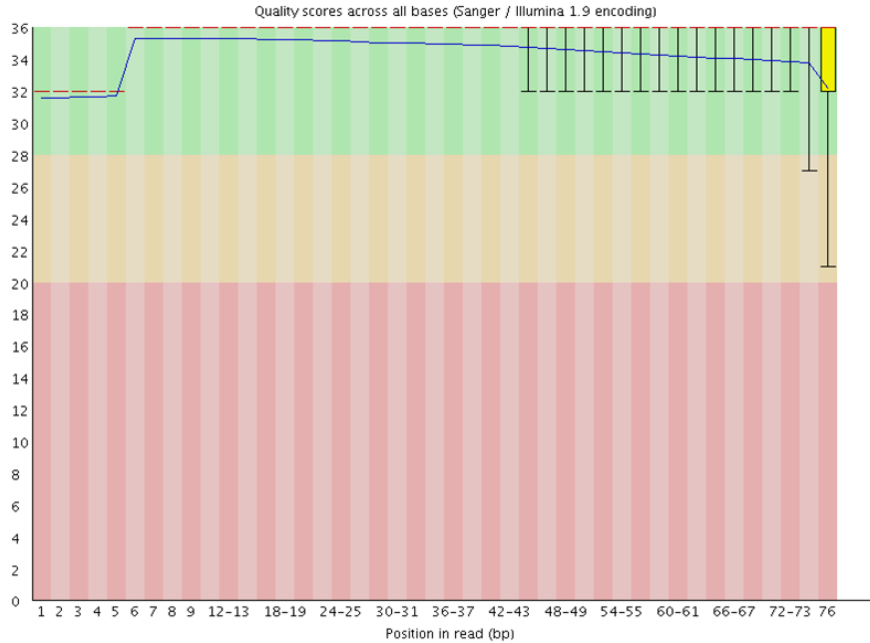


Figure B7 Representative Bioanalyzer traces for RNA-Seq experiments. (A) Bioanalyzer trace for the original RNA sample and **(B)** RNA-Seq library.

EM0

R1



R2

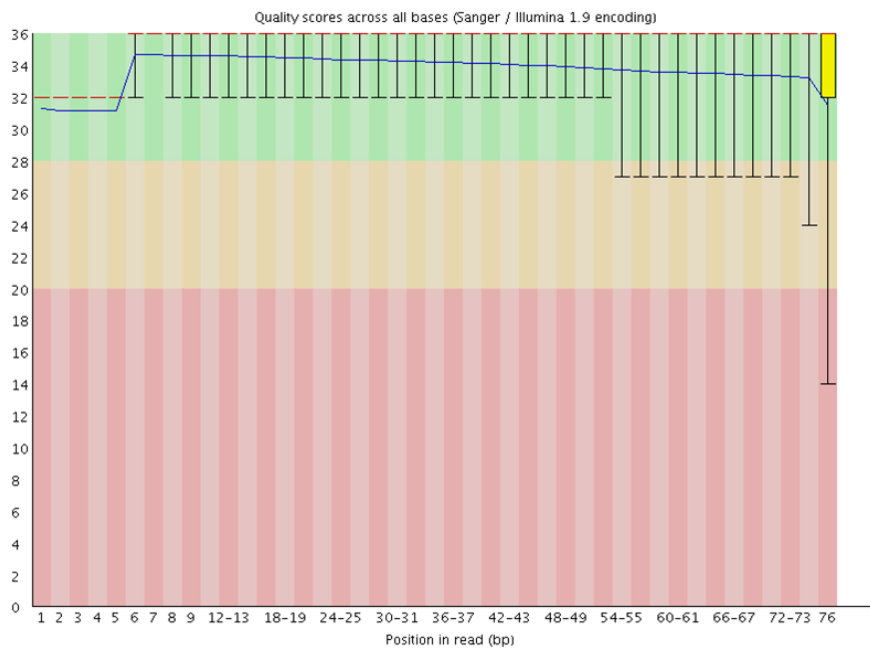
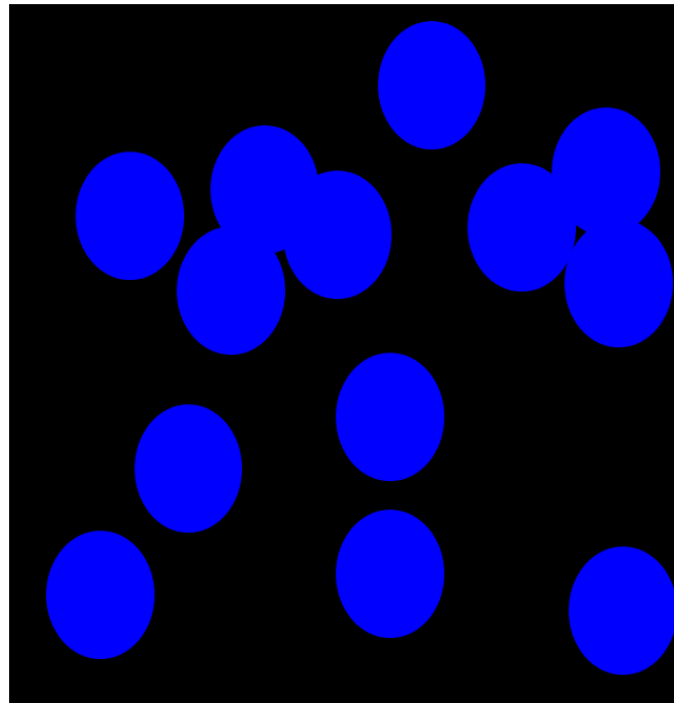


Figure B8 Representative FastQC result obtained from the sequencing of RNA-Seq library. Graphs showing the per base sequence quality across the 76 bp paired-end reads. Read 1 (R1) and Read 2(R2). The blue line represents the mean quality score. The green region indicates calls of very good quality, orange indicates reasonable quality and red indicates poor quality.



↓ Split by seed points

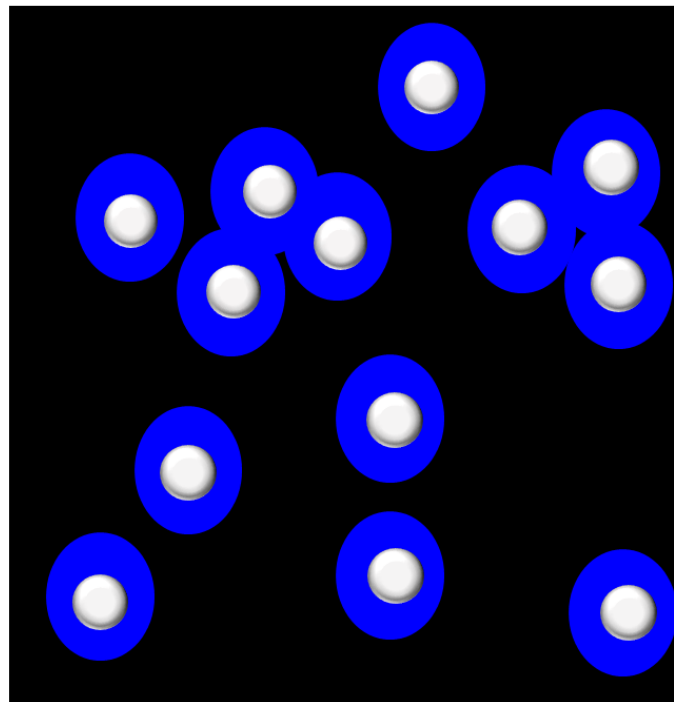


Figure B9 Illustration of the Imaris split by seed points function. Detection of individual nuclei was done by setting the split by seed points to 10.

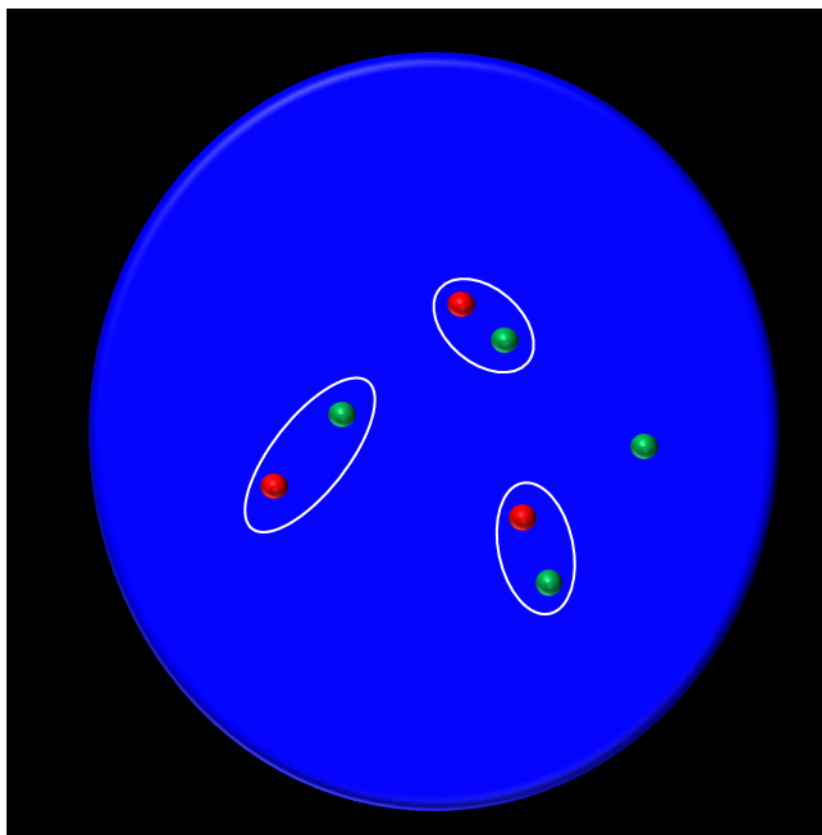


Figure B10 Illustration of paired FISH signals included for analysis.

Appendix C

Interim Report: PRESTO (PRE-operative ESTradiOl Window of Opportunity Study in Post-Menopausal Women with Newly Diagnosed ER Positive Breast Cancer) May 8, 2017
 PI. J. Hugh
 Qualified PI: J. Mackey.

Background:

Hypothesis: Breast cancers with high levels of the estrogen receptor (ER) characteristic of luminal A breast cancers will show an anti-proliferative response to estrogen (E2).

Design of the PRESTO trial with Interim Analysis: Twenty newly diagnosed breast cancer patients at least 55 years old, with presumptive luminal A tumours (grade 1/3 or 2/3, high ER, HER2 negative) will be treated for one to two weeks with 6mg/day of E2 immediately prior to surgery. The primary endpoint is a change in the Ki67 proliferative index of the tumour from the core needle biopsy (CNB) to the surgical specimen (SS). There is a protocol mandated interim analysis after accrual of 10 patients with discontinuation of the trial if at least 3 patients do not show a decrease in the Ki67 index.

Interim Analysis:

Design: Ki67 was performed on the 10 paired CNB and SS by Dr. Gilbert Bigras using his lab developed image analysis test (Ki67Vv) (1). Statistics were performed by Mr. John Hanson. These included: a geometric mean percentage change for each case, a significance value of the changes in the 10 cases as well as the proportion of cases showing a decrease from CNB to SS. Subsequently, the same statistics were calculated on the subset of cases with ≥ 40 day interval between CNB and SS.

Results: The absolute values for Ki67 are plotted in Figure a. This shows that 8 of 10 cases had a decrease in Ki67 from the CNB to the SS. The mean geometric change was -35.4% with a p-value of 0.086. This is lower than the published change of -59.5% at two weeks for Tamoxifen (2). Since the literature suggests that short intervals between the CNB and SS (Surgical Time Interval or STI) may show an increase in Ki67 in untreated patients (3-5) the patients were subdivided based on the median interval (minimum STI of 40 days). The difference in median change in Ki67Vv for the two groups is shown in **Figure b**. Considering those with STI of ≥ 40 days, all 5 patients showed a decrease in Ki67 values with a geometric mean percentage change of -56.8% which is marginally significant ($p=0.056$) and almost identical to the published data for Tamoxifen (**Table 1**).

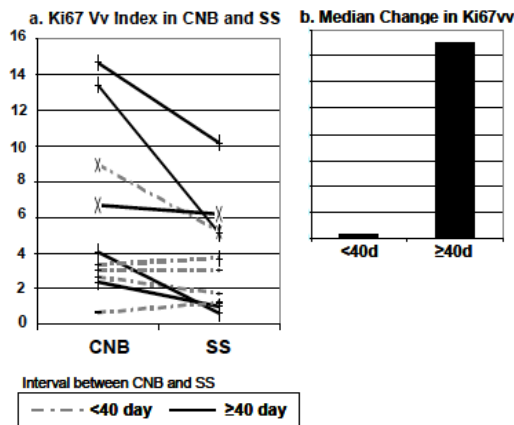


Figure C1. Ki67Vv Index in CNB and SS.

Ki67Vv values from an Image Analysis protocol that calculates the ratio of Ki67 stained area to the total tumour area, with the latter demarcated by the AE1/AE3 cytokeratin stain. Although this method is sensitive to the nuclear to cytoplasmic ratio, when comparing samples of a single tumour it will have unparalleled precision in calculating changes in Ki67.

Figure C2. Median Change in Ki67Vv.

The median difference ($\log \text{Ki67}_{\text{CNB}}$ minus $\log \text{Ki67}_{\text{SS}}$) is compared between the 5 patients with the shortest interval between CNB and SS and those 5 patients with the longest interval.

Table C1. Mean Geometric % Change by Group

	All	<40d STI	≥40d STI	TAM
Mean % Change	-35.4%	-3.4%	-56.8%	-59.5%
p value	0.0856	0.886	0.0561	
Decreased Ki67 (n/total)	8/10	3/5	5/5	48/56

Table 1: The Mean geometric % Change by Group.

Difference in mean geometric change in all 10 patients, as well as the subsets of 5 patients with a STI of <40 days and ≥ 40 days. The comparable value 2 weeks of Tamoxifen (Table 2, ref. 2) is also given. P value represents a t test on the logarithm of the observations. The number of patients showing a decrease in Ki67 is also indicated.

Discussion: Regarding the concordance between CNB and SS in untreated patients with Ki67 ≤20% on CNB: Unlike the excellent reproducibility for ER, PR and HER2, the concordance of Ki67 measurements between CNB and SS is only moderate (6-8). This variation may be due to technical factors such as the well described non-reproducibility of Ki67 measurements (9) or intratumoural heterogeneity which is accentuated by the limited sampling in a core biopsy (10). The non-reproducibility of measurements is unlikely to be a factor in this study since the use of Dr. Bigras' image analysis technique yielded unparalleled precision particularly between pairs of specimens. The issue of intratumoural heterogeneity is also unlikely to be a major factor since this would be expected to yield a random pattern of discordance. However, with the exception of two studies with methodological issues (7,11 - see footnote*), the majority of studies on the concordance of Ki67 between CNB and SS find that there is an increase in Ki67 in untreated patients in patients with initially low Ki67 indices (3-5, 12). This increase may be attributable to the wound-healing pro-proliferative microenvironment (4) since it is lacking when the SS is acquired immediately after the CNB (3). Significantly Morrogh et al. (4) found that several of the genes upregulated by wound healing in untreated patients are included in the Oncotype Dx™ profile.

The effect of wound-healing on the change in Ki67 between CNB and SS: Since a wound healing microenvironment would be most significant with shorter time intervals, we subdivided our data by the median time interval of 40 days and compared the change in Ki67 in the two groups (Figure b). We found that all 5 patients who had ≥ 40 day interval between CNB and SS displayed a decrease in their Ki67 index with a geometric mean percentage change of -56.8% which is almost identical to the published data using Tamoxifen (2). Interestingly, of the 5 patients who had < 40 day interval between CNB and SS, three showed a decrease in Ki67 and two (40%) showed a minor increase (Figure a, grey dotted lines), neither of which would have occasioned a categorical change from Luminal A to B using 14% as a criterion. In untreated patients 24 to 35% of patients will show a category upgrade from Luminal A to B (6,8,10) suggesting that estrogen therapy reduced the pro-proliferative effect of the wound healing microenvironment, which is consistent with the known anti-inflammatory effects of estrogen (13).

However, the most relevant comparator for the 5 patients with < 40 day interval is a pilot Window of Opportunity study which looked at the change in Ki67 after Anastrozole with a median time interval of 31 days (4). Their figure 3 shows that in patients with an initially low Ki67 value on CNB, the administration of 10 days of Anastrozole was associated with a decrease in the number of patients who showed an increase in Ki67 from 63% (5/8 - untreated) to 50% (4/8 - Anastrozole treated). Although small numbers, only 2/5 (40%) of the E2 treated patients showed a very small increase in Ki67.

Interim Report: PRESTO (PRE-operative ESTradiOl Window of Opportunity Study in Post-Menopausal Women with Newly Diagnosed ER Positive Breast Cancer) May 8, 2017

Pl. J. Hugh

Qualified PI: J. Mackey.

Conclusion: These preliminary results suggest that low-dose estrogen therapy may be as effective in decreasing Ki67 (or preventing an increase in Ki67 in the early wound healing phase) as Tamoxifen or an Aromatase Inhibitor in high ER, HER2 negative, post-menopausal patients with an initially low Ki67 index on CNB.

Next Steps and Implications:

1. The PRESTO trial should continue to accrue to the planned 20 patients.
2. There is planned analysis of the data from the 20 PRESTO patients, 40 control untreated patients (20 PRESTO eligible and 20 PRESTO ineligible due to low ER or HER2+) and 20 clinical trial patients treated with aromatase inhibitors acquired through a collaboration with Dr. Arnaout.
3. These findings warrant further study because of their implications for:
 - a. Re-interpretation of the Window-of-Opportunity studies looking at proliferation changes between the CNB and SS.
 - b. Consideration of the effect of the time interval between CNB and surgery for molecular testing on the surgical specimen.

References:

1. Bigras, Applied Immunohistochem & Molec Morphol. 2016 May 20. [Epub ahead of print]
2. Dowsett, Clin Ca Res 2005;11(Suppl):951-958).
3. Iqbal et al. The Breast 2002;11:252-256
4. Morrogh et al. J Surg Res 2012;176:121-132
5. Chen et al. BMC Cancer 2015;15:822
6. Chen et al. BMC Cancer 2013;13:390
7. Greer et al. J Am Coll surg 2013;216:239
8. Kim et al. PLOS ONE 2016;11(3):e0151054
9. Dowsett et al. J Natl Cancer Inst. 2011;103(22):1656-64
10. Knutsvik et al. PLOS ONE 2014;9(11):e112121
11. Romero et al. BMC Cancer 2011;11:341
12. Gandini et al. Ann Oncol 2014;25:618-623
13. Gilliver et al. Clinics in Dermatol 2007;25:56-62

***Footnote:**

Greer et al (7) found that the Ki67 index decreased between the CNB and SS. However, the evaluation of Ki67 on the 2 specimens was performed by 2 different observers using 2 different methods. The CNB was analyzed using image analysis with computer generated percentages based on the 3 highest areas. This hot-spot counting is known to yield higher values for Ki67 particularly when image analysis is used. The SS were analyzed by a single pathologist that obviously "binned" the Ki67 results in steps of 5% (Figure 2). The use of 2 different counting strategies and observers is unlikely to produce comparable statistics.

Romero et al (11) found that core biopsies on average to be 3.9% higher than the Ki67 on surgical specimens with a median of 28 days of STI (range 8-77days). However, their method of quantitation (which is focussed on hot spot) is unusual. Further, their Table 2 indicates that in 33 cases classified on CNB as <20%, four (12%) of these increased their Ki67 index on the surgical specimen to >20%, supporting the findings in the other series noted above.

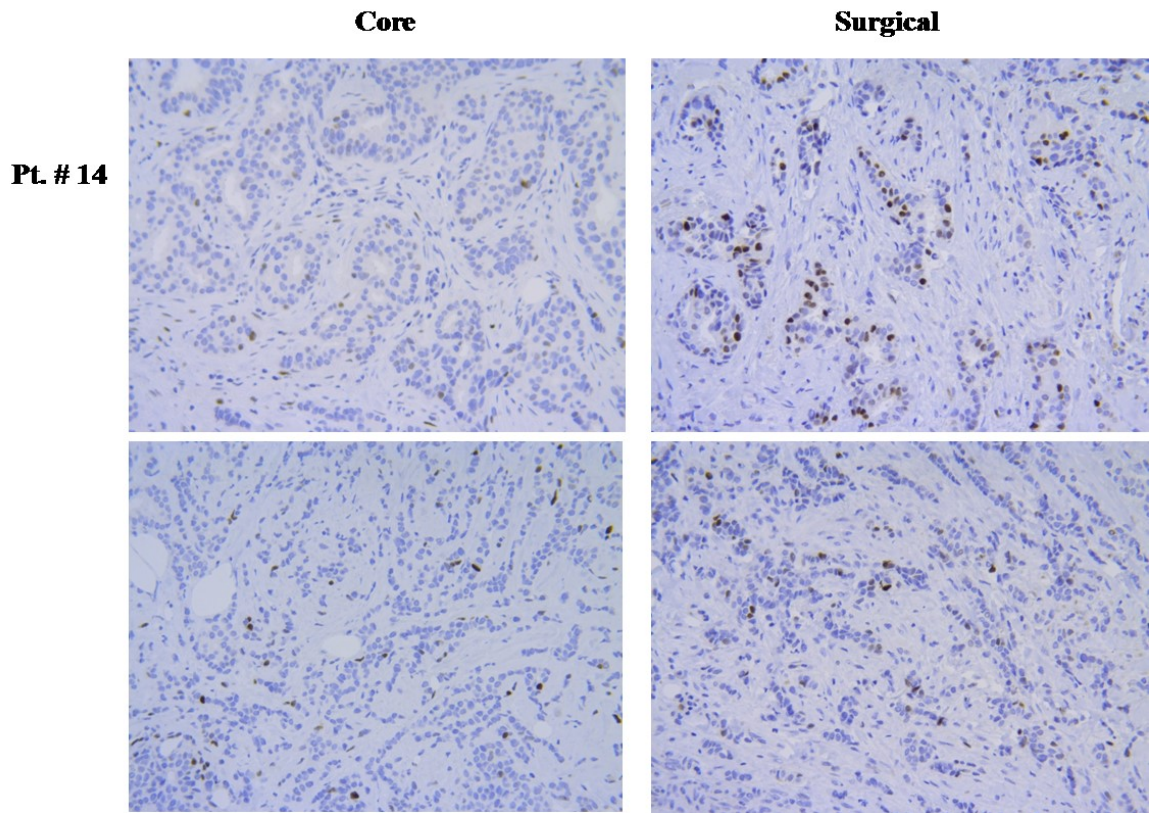


Figure C3 Staining for p21 on the core and surgical tissues from a patient from PRESTO clinical trial.